Assessing Human Exposure to Contaminants in House Dust

by Marco Kaltofen, MS, PE, (Civil, MA) C. NSE

A Dissertation

Submitted to the Faculty of the

WORCESTER POLYTECHNIC INSTITUTE

in partial fulfillment of the requirements for the

Degree of Doctor of Philosophy in Civil Engineering

April 5, 2015

Approved:

John A. Bergendahl, PE (Civil), Ph D.
Primary advisor
Assoc. Professor, Civil &
Environmental Engineering

Paul Mathisen, PE (Civil), Ph D.
Assoc. Professor, Civil &
Environmental Engineering

Germano Iannacchione, Ph D.
Dept. Head, Physics

David Medich, CHP, Ph D.
Assist. Professor, Physics

Abstract

Airborne dusts can transport radioactive materials in the form of isolated individual radioactively-hot particles containing high concentrations of radioisotopes. These airborne particles may be inhaled or ingested, becoming a source of internal radiation exposure. After the March 11, 2011, nuclear reactor accidents at Fukushima Daiichi, in northern Japan; eighty-five Japanese environmental samples and 234 US and Canadian samples were collected and analyzed by gamma spectrometry, autoradiography, scanning electron microscopy with energy dispersive X-ray analysis (SEM/EDS), and total alpha and beta counts. Social media and volunteer organizations were an important part of the sample collection effort. The combination of autoradiography and SEM/EDS allowed individual radioactively-hot particles to be isolated and analyzed. Detectable levels of ^{134}Cs and ^{137}Cs were found in 62 of 85 Japanese particulate matter samples. The median dust specific activity for Japanese samples was 2.5 Bq g^{-1} +/- 1.6 Bq g^{-1}, while the mean dust specific activity was 71 Bq g^{-1} (RSD = 335 %). The mean was skewed high due to five dust samples with sharply higher specific activities. These five samples had specific activities ranging from 167 kBq g^{-1} to 5.2 PBq kg^{-1}. Only four of 234 US and Canadian environmental samples had detectable levels of both ^{134}Cs and ^{137}Cs.

Gross gamma spectroscopy of Japanese samples also detected ^{131}I and ^{60}Co. US and Canadian dust samples showed primarily naturally-occurring nuclides. More than 300 individual hot particles were identified in Japanese samples. The Japanese particles analyzed by SEM/EDS were found to contain cesium, americium, radium, polonium, tellurium, rubidium and other necessarily or potentially radioactive elements. No cesium-containing hot particles were found in the US, however some dust particles were found that contained uranium, thorium and plutonium. These US particles were all related to identified uranium mines or nuclear materials storage and processing sites.

Some of the hot particles detected in this study could cause significant radiation exposures to individuals if inhaled. Where hot particles are present in the environment, radiation dose models must include this exposure component to remain accurate.

Conflicts of Interest and Sources of Funding

The author discloses no financial conflicts of interest. Funding for this study was received from Jeff Ubois and the John D. and Catherine T. MacArthur Foundation, The Lambert Firm, PLC, of New Orleans, LA; Hanford Challenge, the Fairewinds Energy Education Foundation, the Bullitt Foundation of Seattle, WA; Smith Stag, LLC of New Orleans, LA; and the George and Ellen Mitchell Foundation of Austin, TX.

Acknowledgments

My wife Christine Schell has earned my everlasting thanks for her patience, persistence, her editing skills, and for telling me, "Don't you dare quit." My daughters Beryl and Savannah Kaltofen inspired me with their curiosity, by accompanying me to Hanford and Los Alamos, and by saying I could be Sheldon Cooper. I owe a debt to my primary advisor John A. Bergendahl, PE (Civil), Ph D, for his years-worth of good advice and forbearance, and also to the rest of my dissertation committee; Dr. Paul Mathisen, PE (Civil); Physics Dept. Chairman Germano Iannacchione, Ph D, and David Medich, CHP, Ph D. The author gratefully acknowledges the individuals and organizations that donated their time, equipment or environmental samples to this research effort. These donors are: Seth Marvit, Adam Erdossy, Yoshihiko Wada, Ph D; Safecast, and in particular Azby Brown, Alex Malins, Joe Moross, and Pieter Franken; Confederated Tribes and Bands of the Yakama Nation, Tom Carpenter, Esq. and Liz Mattson, of Hanford Challenge; John Apsley, MD (E), ND, DC; Arnie Gundersen (RPI 1971) and Maggie Gundersen (Skidmore College), Spokane Tribe Indians Tribal Council of Wellpinit, WA, Crew members of CVN 76, the USS Ronald Reagan; Mr. Jun Ohnishi, who provided the Namie sample for this research; Pueblo de San Ildefonso, special thanks to Dir. Azby Brown (Future Design Inst.) for samples from Iitate and Minamisoma, Dr. Sergey Pashenko for assistance with Siberian sample collection, Worcester Polytechnic Institute Dept. of Civil Engineering for their constant support, and to Worcester Polytechnic Institute Dept. of Physics for their unwavering enthusiasm. My special thanks to the residents of Los Alamos, NM; Richland, WA; Chelyabinsk, and other exotic locales, who hosted me during sample collecting trips.

Dissertation Advisory Committee

John A. Bergendahl, PE (Civil), Ph D.
Assoc. Professor, WPI Dept. of Civil and Environmental Engineering
Primary advisor

Paul Mathisen, PE (Civil), Ph D.
Assoc. Professor, WPI Dept. of Civil and Environmental Engineering

Germano Iannacchione, Ph D.
Chair, WPI Department of Physics

David Medich, CHP, Ph D.
Assist. Professor, WPI Department of Physics

Abstract

Preface

Funding disclosures
Acknowledgments
Dissertation Advisory Committee

Section 1: Introduction

1.0 Hypothesis

1.1 House dusts

Indoor air and human exposure
Trapping of outdoor pollutants and dusts
Adsorption
Particle size effects
Why is this important - measuring Human exposure

1.2 Pollutants in house dusts

Radiation as hot particles
Low vs. high dose radiation
Hot particle measurement
Source identification and fingerprinting
Fluorinated and chlorinated pesticides & Dioxins

1.3 Dust Forming Processes

Sources of dusts
Macroscopic objects in a dusts and safety issues
Industrial and radioactive dust sources
Examples of hot particles from dust sources

1.4 The importance of size

Dry deposition and soil resuspension
Surface area and adsorption of contaminants
Surface area to size ratio
Respirable particulate matter

1.5 Fingerprinting and dust sources

Morphology: Particle shape vs. source
Elemental composition
Isotopes vs. source

Section 2: Analyses of Japanese surface soils and dusts after the Fukushima accident

Section 1: Introduction to Contaminants in House Dusts

1.0 Hypothesis

Fine matter in dusts convey radioactive material over large distances in a form that results in human exposure to radioactivity.

1.1 House dusts

Dusts consist of small solid particles that are capable of being suspended in the atmosphere. They are typically formed by the breakdown of solid or liquid materials, but may include biological materials, blowing topsoil and sediment particles, and condensates from a gas phase. Condensates may solidify directly from gases, as is the case with the solid-phase radioactive decay products of radon gas. (1, George) Gases may also condense or adsorb on the surface of existing solid particles. Gas condensates may be the products of combustion or pyrolysis. They are often smaller than native dusts, and may form aggregates. Aerosols are solids suspended in gas, including mists, smokes, fumes, dusts, and condensates. (2, Friedlander)

Airborne dusts can transport radioactive materials in the form of isolated individual particles containing high concentrations of radioisotopes. The specific activity of an individual particle can be significantly higher than that of the surrounding particles in a dust sample. These high activity particles, called hot particles (HP) were isolated and analyzed for this research.

Environmental dusts can accumulate indoors and on air filters, potentially causing contaminant exposures to humans via inhalation, dermal contact, and ingestion. Outdoor dusts consist primarily of soil materials. (20, Dordevic) Indoor house dusts are also derived from processes within the home, such as combustion, second hand tobacco smoke, and consumer products. Indoor house dusts also consist of biological, such as human skin cells, insect matter, or pet hair and dander. (2, Friedlander; 3, Cizdziel)

House dusts can harbor more contaminants than the same mass of outdoor soils, in part because house dusts are generally much finer than soil particles. The fineness of the dusts allow these particles to retain a greater amount of adsorbed contaminants than an equivalent amount of more coarsely-grained soils. (4, Lewis) House dusts may also contain contaminants from second hand tobacco smoke, radon infiltration or household combustion sources. (5, US EPA IAQ)

One can measure the average concentration of contaminants in dust on a mass basis, or they can be measured as an average concentration for a given size fraction. The latter method results in a distribution of chemical composition with respect to particle size. (2, Friedlander) Some analytical techniques can also measure the chemical composition of individual dust particles. One such technique is scanning electron microscopy coupled with energy dispersive X-ray analysis., SEM/EDS. This research focuses on measuring contamination in dusts by all three methods, with emphasis on measuring the elemental composition of individual dust particles.

1.1.2 Importance of this research

The sixteenth century Swiss physician Paracelsus is quoted as saying, “The dose makes the poison.” For chemical and radiological poisons in or on dust particles, the size, chemical composition, activity, and concentration of contaminants will all affect the actual dose absorbed by a receptor. For homogeneous chemical contamination in dusts, simple techniques such as gas chromatography coupled with electron capture detection can determine potential dose. For cases where a limited number of particles have substantial amounts of radioactivity compared to bulks dusts requires additional testing. The purpose of this research was to determine the size, morphology, chemical state, and total activity of individual radioactive dust particles.

Knowing the size of particles, the potential for internal vs. external radiation dose may be calculated. Small particles are more readily inhaled and retained, potentially increasing body or possibly just lung doses.

Knowing the morphology of particles can identify their probable source, giving important clues about which potential toxicants may be present.

The chemical form of dust particles may enhance or decrease solubility in body fluids, or affect their rate of excretion. This can yield dose calculations based on short term exposure, or larger, long term, committed doses.

Identifying the actual activity of an individual particle, allows calculation of the actual dose to an individual, and identifies the potential risk of biological effects. This actual dose to an individual may be very different from the mean dose to members of a population. In fact it must be, unless all radioactively-hot particles are identical. Since the processes that form hot particles are not identical, then the particles will be dissimilar.

In the case where the dust from a home is sampled and tested to determine the distribution of hot particles present, a better dose calculation can be made for its occupants. The average data for a population based on a central value for environmental exposure would be replaced by a more accurate actual analysis and a specific dose calculation. The specific home may produce doses very different from the average value. This is critical since a set of homes may be in an area with an average “acceptable” level of radioactive dust contamination, but if the dose comes from a sufficiently limited number of hot particles, then some households must experience doses much higher or lower than the average.

The average acceptable level assumes a uniformity of exposure that may not be present. This would make the level unproductive for those with hot particles present in their house

dust. If excess cancers were detected within this same group, without considering that a small number among that group have high doses due to hot particles, one may incorrectly assign an excessive slope value to the curve of low level radiation exposure vs. biological effect.

The microdosimetry required to accurately predict hot particle exposures is hardly new technology. Brachytherapy, also called internal radiotherapy, call for exactly this type of dose assessment. Researchers have been cataloguing the size and activity of hot particles since the late 1950s and early 1960s, when environmental physicists studied fallout particles. (9, Shleien) Papers in the 1970s and 1980s detailed the mathematics and probability distributions of hot particle sources embedded in living tissues. (27, Roesch; 28, Zaider) Knowing the size distribution, activity distribution and abundance of radioactive particles in environmental samples may also allow calculation of risks to populations, based on using these properties as inputs to a population dose model.

1.1.3 What can you do with this research?

One can measure the actual or probable radiation dose to an individual, and calculate their potential excess cancer risk. The drawback is that one has to measure the actual intake or calculate the probability of exposure to hot particles. This requires knowing the data on hot particle intake at a site, or at least the distribution data for hot particles in the environment. In the sample set used in this study, where there is some skewness, the mean activity is significantly higher than the median activity. In practical terms, this means that a few individuals experience a higher dose than average data would suggest.

1.2 Pollutants in house dusts

Radioactively-hot particles are particles of dust, soil, metals or wastes that have significantly more activity than surrounding radioactively-inert matter. Microscopic nuclear fuel particles, sometimes called fuel fleas, particles of pure isotopes such as ^{239}Pu

particles, nuclear fallout particles, or high activity natural mineral dusts are all examples of hot particles. Sometimes the term hot particle is used exclusively to indicate a particle of nuclear fuel or core material.

Hot particles are formed by multiple processes, including operations of nuclear power reactors, weapons manufacturing programs, test nuclear detonations, and weathering of naturally occurring radioactive materials. As with nonradioactive particles, hot particles have distinguishing characteristics including particle sizes, sphericity, mineralogy, heterogeneity, activity, and nuclide content. The specific conditions associated with each hot particle-forming process affect the properties of the resulting hot particles. The purpose of this research is to investigate HPs and their properties at environmental locations impacted by a known source of HPs. These data will come from two field locations and will be supplemented by relevant peer-reviewed literature. A statistical analysis of the properties of HPs detected in environments dominated by singular known sources of radioactive particles will be performed. The purpose of the analysis is to identify specific property value distributions which are related to specific HP sources. By comparing property statistics for sets of particles from unknown sources to these known distributions, the source of HPs in environmental samples can be determined. A particular mine, processor, or enrichment facility may be distinguished as the source of a given hot particle, based on the nature of the set of detected HPs. Alternatively, if the source of HPs is known, then judgments can be made about the likely properties of the resulting HPs.

This research has application in monitoring the release of radiation from nuclear facilities during both normal and upset conditions, as well as in detailing human exposure to radioactive releases. The physical properties of HPs determine the ultimate environmental fate and the transport mechanisms of hot particles. Quantitation of the physical and chemical nature of hot particles produces more accurate inputs to plume and particle tracking models. Risks to human health from exposure to particulate-bound radiation are

affected by changes in the transport, bioavailability, particle to cell radiation flux, and cellular shielding of hot particles.

Knowing the physical properties of particles that contain radionuclides allows one to make calculations about the probability of exposing humans to HPs by specific vectors. Better knowledge of the vector of radioactive contamination results in a more accurate determination of human exposures to radiation. Knowledge of the transport vectors that result in human exposure may lead to changes in the methods for environmental assessment and remediation of radioactive contamination.

Environmental radiation is normally detected by gross analytical methods that look for the presence of radionuclides at a given confidence limit over the average or site specific background level. The concentration of HPs in environmental samples may be small, so that gross radiochemical analyses may fail to detect excess radioactivity even when such particles are present. Microanalytical methods quantify radiation from individual hot particles. Notably, environmental samples that contain hot particles may or may not be above background levels. Microanalytical methods include serial size fractionation, autoradiography, cadmium telluride gamma spectrometry and Scanning Electron Microscopy / Energy Dispersive X-ray analysis (SEM/EDS).

Using microanalytical tools to quantify the properties of HPs makes it possible to detect the presence of anthropogenic radiation at levels which are at or below background. This is useful tool for nuclides, such as uranium and thorium, which have both natural and anthropogenic sources, and for plutonium, whose toxicity is highly significant, even at barely detectable levels. Samples at the environmental radiation gross background level are, in essence, “nondetects.” Conversely, a reliable quantitative separation, microanalysis, and statistical analysis of HPs in otherwise-background environmental samples provides data on the source, transport, and fate of particulate-bound radioactive material.

This research studied radioactively-hot particles associated with the special nuclear materials processing facility at Hanford, WA, and dusts associated with the Fukushima reactor accidents of March 2011. The goal was to show that analyses of individual particles could help distinguish the source, fate and risks related to hot particles in the environment.

1.3 Dust Forming Processes

While there are many potential sources of house dusts, particles from soils immediately surrounding a home typically make up 50 percent of house dusts by mass. (ATSDR Toxicological Profile for Lead, http://www.atsdr.cdc.gov/toxprofiles/tp13.pdf) The remainder can be expected to be sourced from outdoor airborne particulate matter, biological materials such as pet hair and skin cells, insects and insect parts, diatoms, soot, and plant, fungal, or textile fibers.

For the studies reported in sections 2 and 3, this author also reports detecting the following macroscopic objects in vacuum cleaner bags including bullets and cartridges, various medical and pharmaceutical products, coins, pet Kibbles®, nails, tacks, safety pins, saw dust, concrete and cement dusts, plastic nurdles, metal burs, and paint or paint pigments. Some of these items represent a potential health and safety hazard, requiring that vacuum cleaner bag samples always be handled with care.

These samples should always be treated as potentially toxic, and should only be manipulated in a fume hood, using gloves and eye protection. In addition to the physical hazards of needles, nails, and pins, dusts may also contain crystalline silica (21, Castronova), Hanta virus, asbestos fibers, biocides, as well as the chemical and radiological materials that were the target of this study.

1.3.2 Sources of hot particles in dusts

Radioactively-hot particles have been produced by nuclear test detonations, wastes from nuclear metals processing, accidental fires at nuclear processing and reprocessing facilities, resuspension of radioactively-contaminated sediments, naturally-occurring radioactive isotopes in crustal material, uranium and thorium mining operations, condensation of radon gas progeny, losses from nuclear waste sites, and both minor and catastrophic releases from operating nuclear reactors. Examples of these hot particle-forming processes and events are listed in Table 1.1. Some of these examples listed in Table 1.1 are sources of anthropogenic hot particles, such as the UK Atomic Energy Agency fast breeder reactor at Dounreay, Scotland, that lost fuel particles via its ocean effluent discharge. (38, UK SEPA) By contrast, naturally-occurring monazite sands in India produce radioactive thoriated mineral dusts in Ganges River sediments. (35, Kaltofen)

Nuclear test detonations were a significant source of dust particles containing radioactive contaminants. The peak years for the production and global distribution of HPs from nuclear test detonations was 1962 and 1963. These particles are part of the widely-distributed global radioactive background. Notably for this study, shorter lived isotopes such as ^{134}Cs are absent from these particles, as they have decayed to levels that are essentially undetectable. (9, Schleien) The ^{235}U-fueled nuclear reactors producing weapons grade plutonium created radioactively-hot particles that were released into the atmosphere beginning in the 1940s and continuing until the 1980s. These dusts carried uranium, thorium, plutonium, and rutherfordium into the atmosphere. These particles were released during the chemical processing of burned nuclear fuel to extract plutonium for weapons. (22, Gerber)

Table 1.1, Below, Examples of hot particle releases or sources

Test detonations	1963 Pacific nuclear testing (aerosolized fission products: ^{137}Cs, ^{90}Sr)
Processing plant fires	1969 Rocky Flats, CO (^{239}Pu and ^{241}Am from fire)
Reprocessing plant accidents/fires	1957 Mayak explosion/fires (^{137}Cs and ^{60}Co thermal waste explosion)
Sediment resuspension	Los Alamos - Acid Canyon (^{137}Cs, ^{239}Pu and ^{241}Am in dusts)
Naturally-occurring	India - monazite sands/dusts (Th/U-rare earth mineral sediments)
Mining	Midnight Mine, Washington (Uranium ore tailings)
Radon condensation	Cigarette smoking (^{210}Po and other Rn progeny)
Waste site losses	Hanford, WA (^{239}Pu, ^{137}Cs, ^{90}Sr from weapons production)
Minor reactor releases	Dounreay, Scotland Fast Breeder Reactor (^{239}Pu from waste water discharge)
Major reactor releases	Fukushima Daiichi (^{131}I, ^{134}Cs, and ^{137}Cs containment failure)

Refs. 9, Schleien; 35, Kaltofen; 36, US NIH; 37, US EPA; 38, UK SEPA; 39, US CIA; also see Hanford and Mayak sampling photographs in Appendix G

Figures 1.1 and 1.2 show the SEM/EDS spectra of uranium-plutonium containing dust particles collected from an HVAC air filter, HLW worker clothing change out room, Hanford Nuclear Reservation. All spectral data in this section is by the author with SEM/ EDS data by Microvision of N. Billerica, MA. (32, Kaltofen)

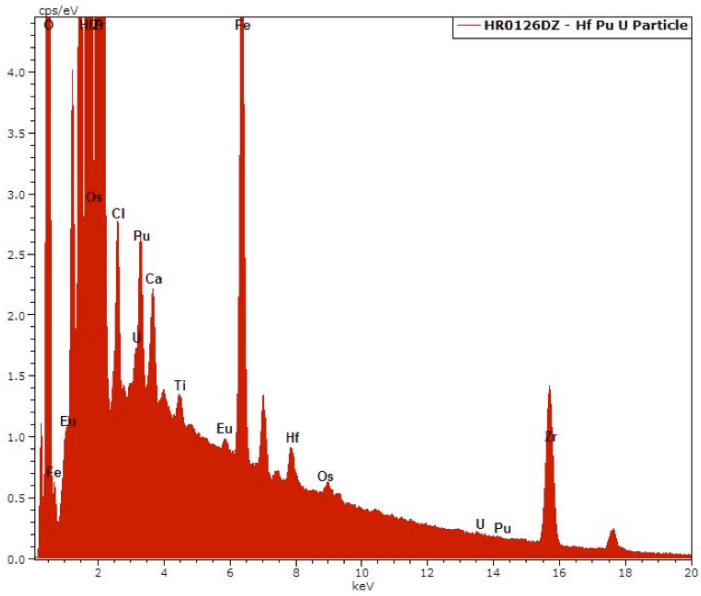

Fig. 1.1 Above, SEM/EDS spectrum of plutonium-bearing hot particle

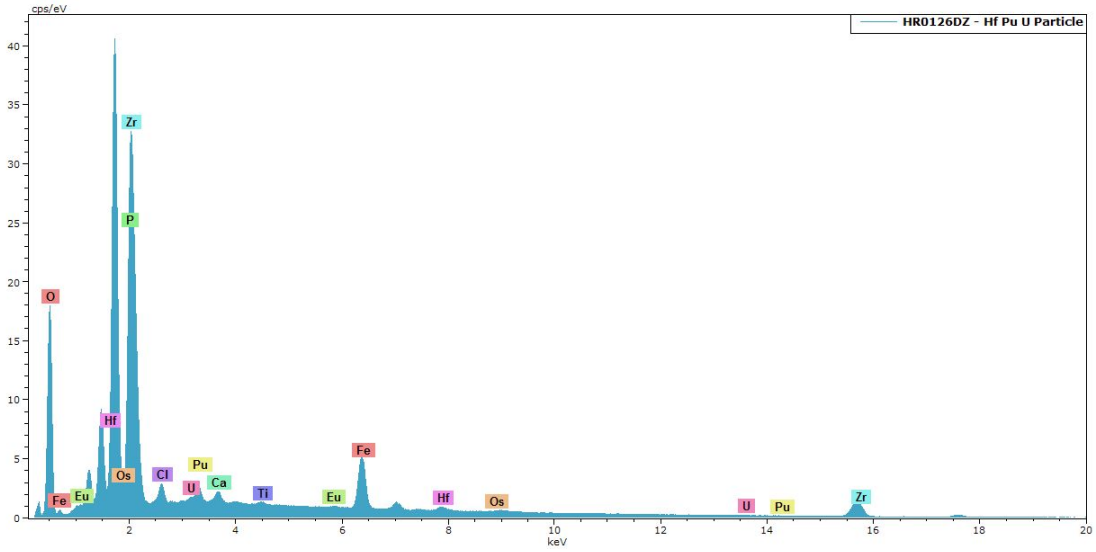

Fig 1.2 Above, SEM/EDS spectrum of uranium/plutonium-bearing hot particle

Figures 1.3 and 1.4 show a thoriated hot particle found in dust from the metal working shop in the 300 Area at Hanford, WA. The sample material was collected from an HVAC system in one of Hanford's waste handling areas. The purity of thorium in the hot particles leaves little doubt that the sample is anthropogenic. (32, Kaltofen; cps to mass data in Appendix E)

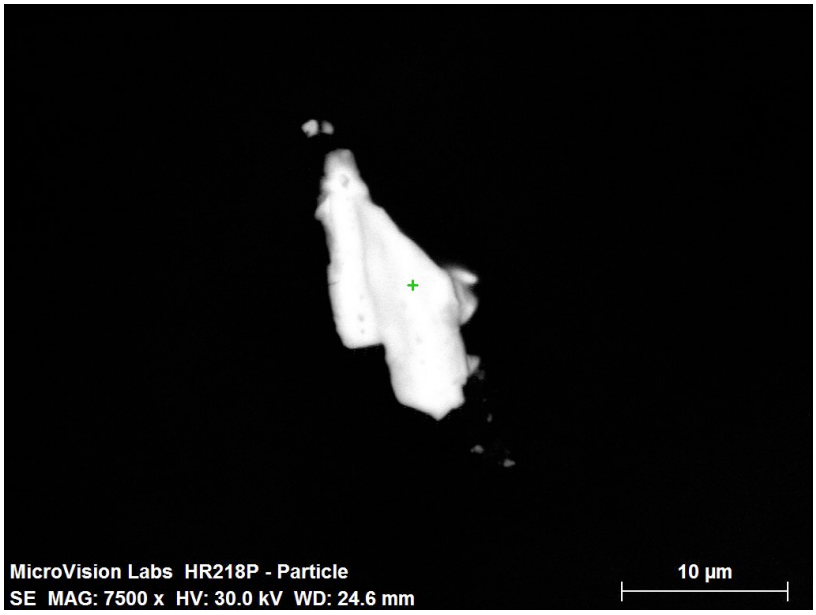

Fig. 1.3 Hanford Nuclear Reservation hot particle composed primarily of thorium.

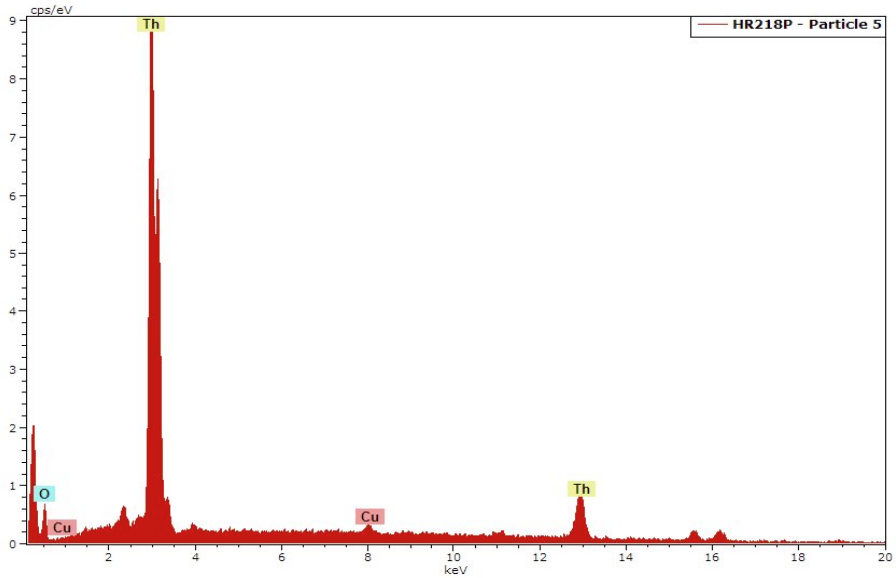

Fig. 1.4 SEM/EDS spectrum for particle in Fig. 1.3

Nuclear fuel and nuclear weapons manufacturing facilities released radioactively hot particles into the atmosphere. For example, fires in 1955 and 1969 at the Rocky Flats, CO, nuclear fuel reprocessing plant sent particulate matter containing plutonium into the atmosphere. (37, EPA) Some of these hot particles were later found in indoor house dusts at nearby homes. For this study, dust samples were collected from crawl spaces in a home built before the opening of the Rocky Flats Arsenal. Figures 1.5 and 1.6 show data for one of the plutonium and americium-bearing dust particles collected from this home near the Rocky Flats nuclear reservation. The data show that house dust can be a source of human exposure to plutonium near Rocky Flats.

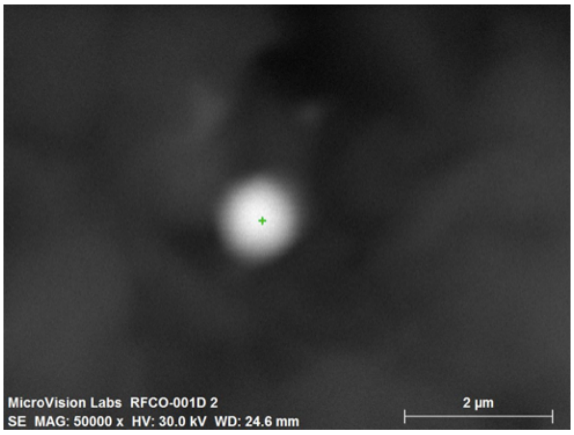

Fig. 1.5 Above, SEM photomicrograph of Rocky Flats dust particle

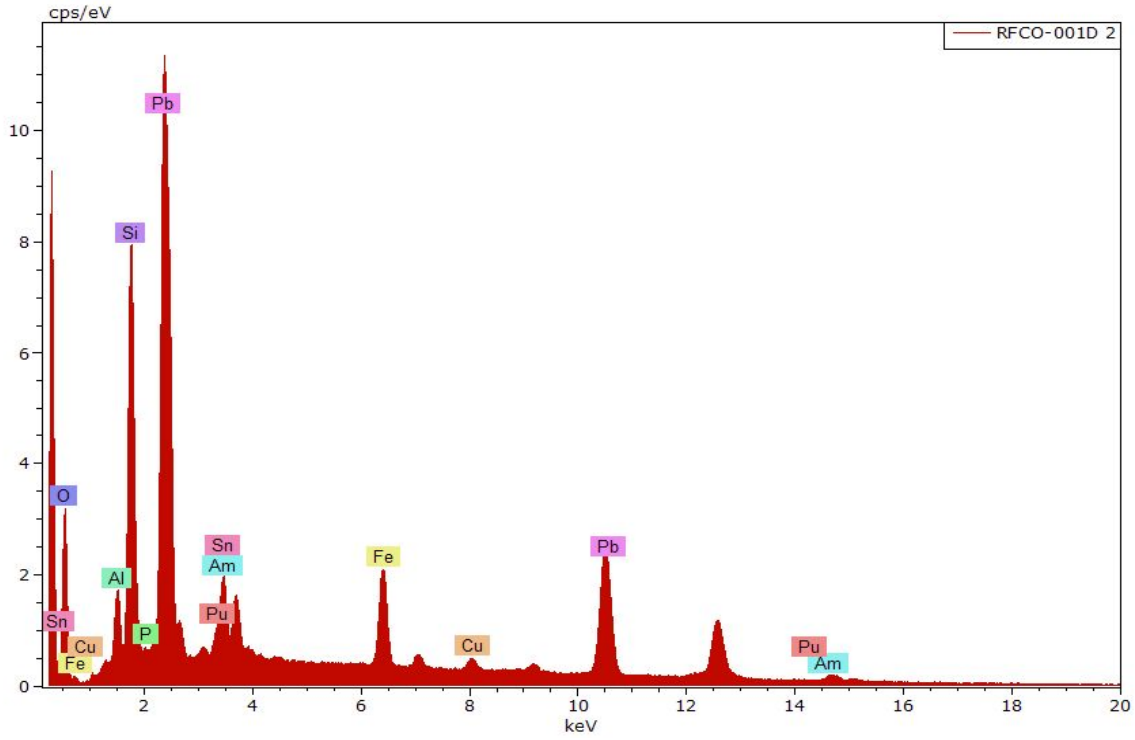

Fig. 1.6 Above, SEM/EDS spectrum of inhalable dust particle w/ Pu & Am

Fig 1.7 Above: Muslymovo a village in Chelyabinsk Oblast, Russia, author photo

Likewise, a 1957 fire and a series of explosions at the former Soviet Union's only nuclear fuel reprocessing plant at the Mayak Chemical Nuclear complex at Kyshtym in Chelyabinsk Oblast, released a torrent of airborne and waterborne radioactively-hot dust particles containing cesium, ^{60}Co, and other radioactive isotopes. Grasses collected at Muslyumovo, Russia, downstream of the accident site and on the bank of the Techa River, contained ^{60}Co 0.17 Bq g^{-1}, ^{137}Cs 154 Bq g^{-1}, and ^{90}Sr 0.33 Bq g^{-1}. A 1986 explosion and fire at the Chernobyl Nuclear Power Station in Ukraine released even larger quantities of radioactively-hot particles than the Kyshtym disaster at Mayak. These particles contained ^{137}Cs, ^{134}Cs, ^{239}Pu and other isotopes, and were detected globally. Radiocesium from this release exists only as ^{137}Cs, as the ^{134}Cs has almost completely decayed away. (23, IAEA) Analysts must determine if ^{137}Cs in environmental samples is from Chernobyl, Kyshtym, nuclear test detonations, or other industrial releases. The 2011 Fukushima Daiichi reactor accidents are recent enough that both ^{134}Cs (half life 2.06 yrs.) and ^{137}Cs are still measurable in these younger hot particles from Japan.

Fig. 1.8 Above, Techa River, author photo

The original 1940's era waste water treatment plant at the Los Alamos National Laboratory discharged Pu, Am and radioactive Cs directly to Acid Canyon, an ephemerally-wet area below the Los Alamos Mesa. As these sediments dry, they can be resuspended, creating radioactively-contaminated dusts. The hot particle (Fig. 1.9) at right and in the SEM/EDS spectrum below contains percent levels of uranium, plutonium, thorium, and rare earths and transition metals. The sample came from dried soils and sediments in Acid Canyon which received effluent from the Los Alamos Laboratory during its early years of operation. Note that although uranium, thorium and plutonium have only radioactive isotopes, the remaining metals in the spectrum may be either stable or radioactive. Given that SEM relies on orbital electron behavior, SEM/EDS does not distinguish between isotopes of the same Z number.

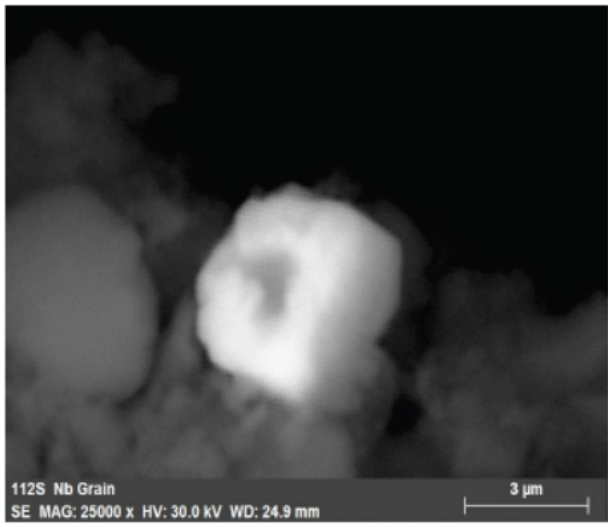

Fig. 1.9 Above, photomicrograph of Los Alamos sediment particle

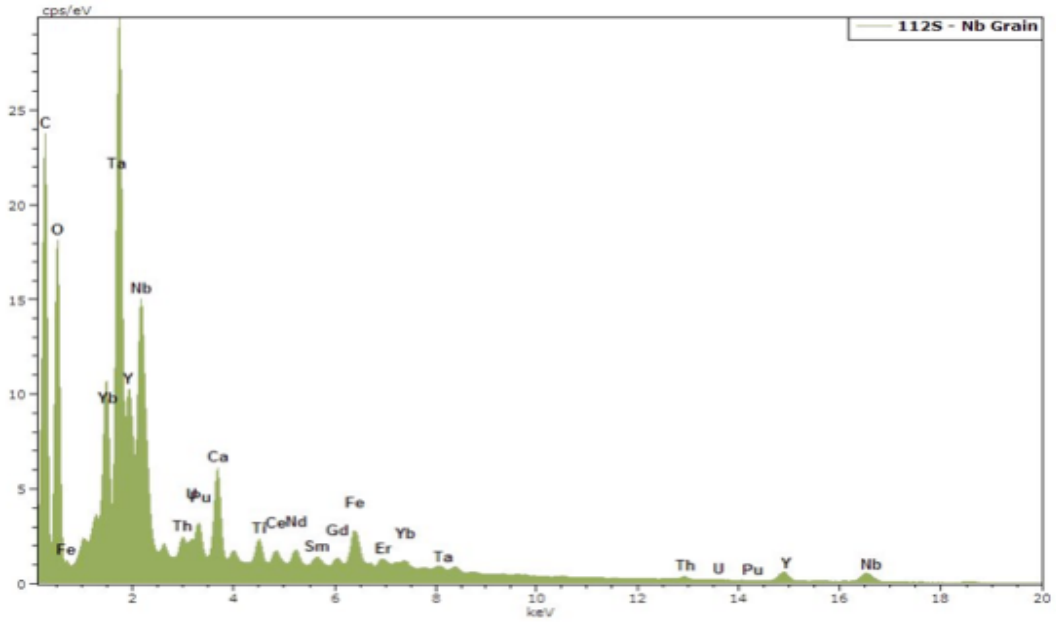

Fig. 1.10 Above, SEM/EDS spectrum of Los Alamos particle, author sample

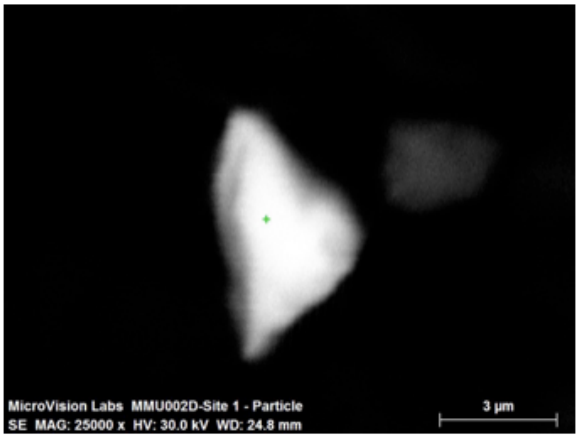

Fig. 1.11 Above, photomicrograph of uranium mine dust particle

Naturally occurring radioactive materials and mining wastes may contain uranium, thorium, or ^{40}K, the primordial radioactive isotope of potassium. Dusts from these crustal radioactive isotopes may be essentially identical to some industrial hot particles. For a given dose and quality of radiation exposure, these natural hot particles may also be as biologically effective as industrial hot particles. The photomicrograph and spectrum on this page are from dusts collected in and around the Midnight uranium mine in Wellpinit, WA. The hot particle shown is less than five microns in size. This size of dust particle may be inhaled and retained in the respiratory system. (4, Lewis; 2010 author sample)

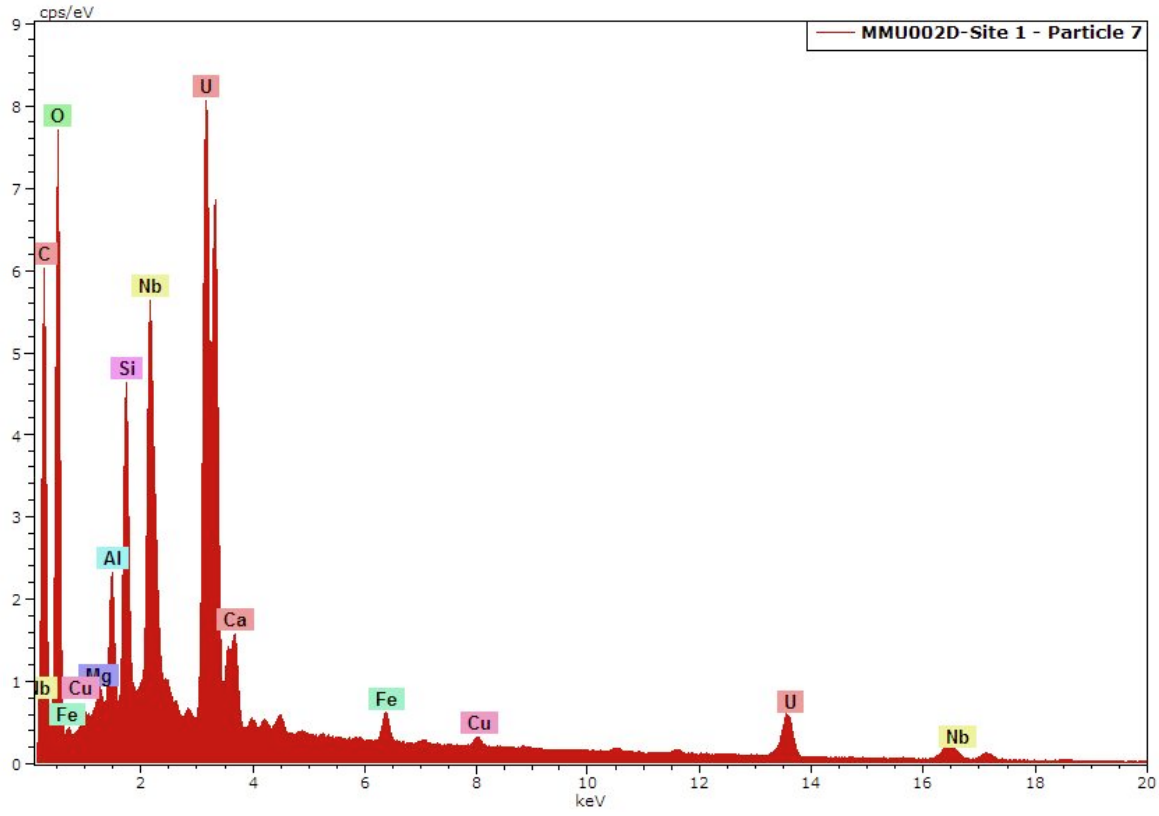

Fig. 1.12 Above, uranium mine dust SEM/EDS spectrum, cps to mass data in Appendix E

Nuclear materials processing produces wastes with hot particles that may escape into the environment. The photomicrograph at right shows processed spherical uranium oxide particles from the Hanford Nuclear Reservation. The original sample was archived by a former plant scientist. (2009 author sample and spectrum)

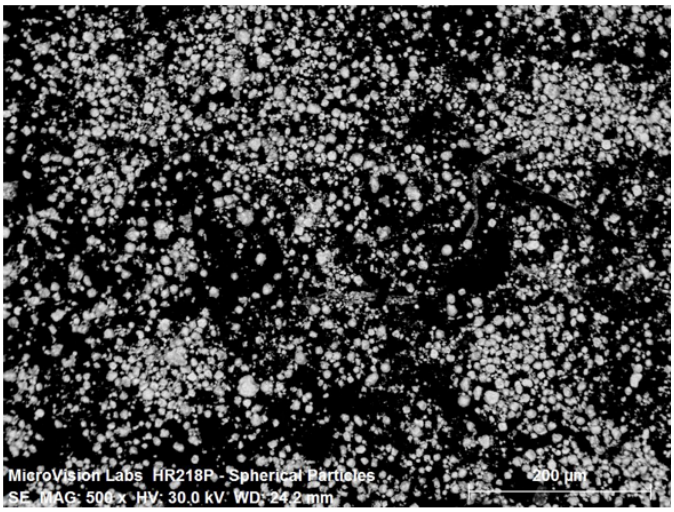

Fig. 1.13 Above, photomicrograph of processed uranium particles

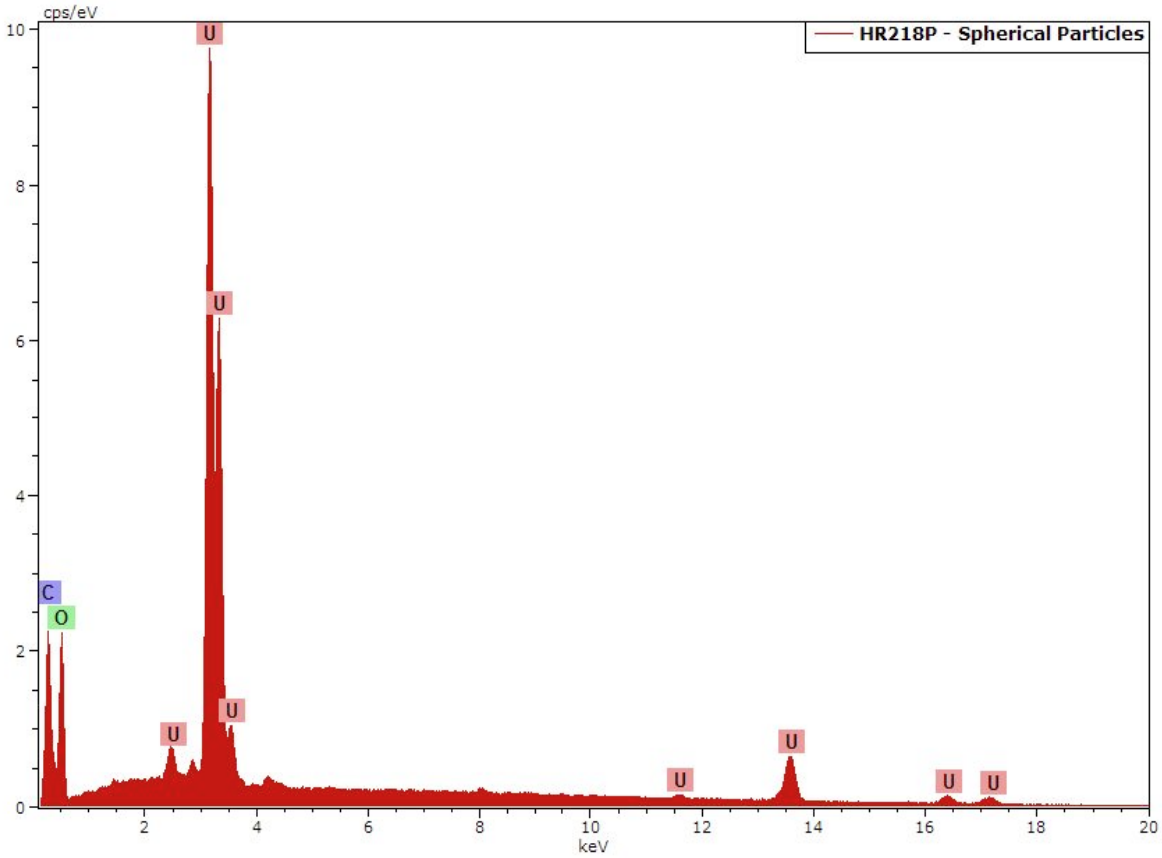

Fig. 1.14 Above, processed uranium particles, Hanford, WA, SEM/EDS spectrum

1.4 The importance of size

Very small particles, those with diameters less than 1.0 microns, tend to have dry deposition settling velocities of 0.1 to 1.0 mm/sec. Depositional velocity is the activity flux to soil surface / activity concentration of air above soil. (12, Evans, citing Chamberlain) For this size range, dry deposition atmospheric removal rates are very slow. (2, Friedlander; 12, Evans) Air turbulence effects dominate over gravitational effects, maintaining these particles in suspension. In general, with decreasing size, frictional forces dominate compared to gravitational forces, and the settling velocity of a particle becomes less dependent on its specific gravity. The approximate size where friction forces give way to gravitational forces is about 1 micron. (8, Sehmel cited by Zannetti) These estimates are true only for dry deposition. Wet deposition would be expected to remove fine and ultra fine materials from the atmosphere that might otherwise have persisted in the atmosphere.

Larger particles may gravitationally settle onto surfaces, such as soils, but will tend to be resuspended when wind velocities increase, bringing larger friction forces into play. The resuspension is the fraction of airborne activity vs. unit soil activity. (12, Evans citing Stewart) Resuspension allows larger particles up to 20 microns in size to be transported by air over significant distances. These would be subject to standard gaussian plume transport models. (11, NZME) The end result is that 20 micron-sized particles or smaller, typical of radioactively-contaminated dusts, may travel thousands of kilometers. Agricultural soil dusts, for example, may be stripped from bare soils and transported. In 2008 W. Birmili used satellite and meteorological observations to show that >1 micron soil particles eroded soils are suspended by strong winds and transported thousands of kilometers. (13, Birmili) The Birmili study and data from Dordevic (20, Dordevic) showed that greater than 65 percent of terrestrial atmospheric dusts were PM10 of crustal origin.

Soon after the peak of atmospheric nuclear weapons testing, Schleien (9, Schleien) measured the particle size of radionuclide-containing dusts presumed to be related to nuclear detonations. Eighty-eight percent of particles containing ^{137}Cs, ^{144}Ce, and ^{106}Ru related to nuclear detonations ranged in size from < 0.25 microns to 1.75 microns. These dusts had travelled on the order of thousands of miles to a Massachusetts collection site, from origins in Nevada and the Pacific Basin, finally settling from the stratosphere. The bulk of radioactive dusts in Schleien's air samples had size distributions indistinguishable from inert nonradioactive dusts. Schleien showed that radioactively-hot particles in this size range could travel globally and settle at large distances from their point of origin. The methodology employed in Schleien's study did break up larger aggregates prior to sample collection, so his size distribution may be biased at the low end. His finding is important to the study of radioactive dusts because particle size can affect the toxicity of dusts. Dusts that lie between 5 and 0.5 microns in size are considered, "respirable particulate matter." These particles may become trapped in the lungs, where they expose lung or other tissues to radiation energy. (4, Lewis; 5, US EPA)

The size of the particle can also impact the rate at which it is cleared from the lung. Fine particles less than 1 to 2.5 microns in size may be removed from alveolar tissue and transported into the lymphatic circulation system. For this reason, particles which might otherwise be insoluble in pulmonary fluids can be cleared from the lungs in a matter of days to months, and moved to other body tissues or be ultimately eliminated by excretion. (25, Chan) Clearance of fine inhaled particles by the lymphatic system will tend to reduce the effective half life of inhaled hot particles. (The effective half life of an isotope is a function of the combined radiological and biological half lives of radioactive materials, US NRC, http://www.nrc.gov/reading-rm/basic-ref/glossary/effective-half-life.html.

Surface area to size ratio: We typically measure human exposure to toxicants using concentration, meaning the mass per unit volume or mass per unit mass. One example is

measuring exposure to air contamination in micrograms per cubic meter times the respired air intake. Another is measuring the mass of contaminant in a given mass of food consumed.

Another way to measure exposure is by measuring the surface area of inhaled or ingested toxicants. Smaller particles have more surface area than larger ones for a given mass. Nanoparticles have vast surface areas with respect to their mass, compared to macroscopic particles. For example, consider air with a particle loading of 10 ug/cm^3. Achieving this concentration in air would require 153 uniform particles having a diameter of 500 microns and a total surface area of 120 um^2/cm^3. If instead the particles had a uniform diameter of 0.5 microns, to achieve the same mass would require a set of 1.53 E11 particles, having a total surface area of 120,000 um^2/cm^3. (10, Shatkin citing Oberdorrster) Exposure to smaller particles increases the potential for exposure to radiation by two mechanisms. A given mass of particles is more numerous if the particles are smaller. Secondly, a given mass of particles has a greater surface area, allowing for more particle to cell surface interactions.

The size of the particle, or more correctly, the surface area to mass ratio of a particle, affects the rate at which a radioactive particle may dissolve in the body. Smaller particles may have faster dissolution rates, especially for less soluble materials. (10, Shatkin) This may reduce the biological lifetime of inhaled particles in the body, while potentially increasing the rate of excretion. This also moves an exposure from an organ exposure, to a whole body exposure. (Author's note: The full biological implications of various dust exposure scenarios were beyond the scope of this work.)

In an organ such as the human lung, which has a working surface area of about 30 square meters for an adult, smaller sized particles are more likely to attack the lung's alveolar surfaces in more locations than would a set of large particles of similar mass. This assumes that particles could even get to the deeper lung surface, given that human

respiratory systems reject large inspired dust particles of diameter greater than 5 to 10 microns. (5, US EPA)

For particles that are close to the size of cells in the lung lining, smaller particle sizes will mean that the same inhaled and retained mass of radioactive material will be in contact with a larger number of cells. This is more critical for alpha emitters that have relatively short penetration ranges in tissue. Alpha radiation is dissipated by about a mm of tissue, depending on the alpha particle's energy. Doubling the mass of an alpha emitting dust particle in the lung tissue would not necessarily double the number of cells impacted by the alpha energy. On the other hand, doubling the number of alpha emitting dust particles in the lung tissue could approximately double the number of tissue cells impacted by the alpha energy. The physical situation is similar for any form of High LET (Linear Energy Transfer) radiation from particles in physical contact with living cells. High LET radiation will irradiate primarily adjacent tissues, because this energy will be fully absorbed before penetrating something on the order of a mm of tissue. (24, NIST)

Gamma emitters, along with neutrons and other lower linear energy transfer forms of radiation, would behave differently. Since these low LET radiations can act at greater distances, doubling the mass of low LET emitters would be expected to approximately double the potential energy absorption by tissues. On the other hand, doubling the number of low LET emitters for the same mass would probably not double the number of cells exposed.

Beta particles, typically having LET rates between those of alpha and gamma radiations, would behave in an intermediate fashion. The number of cells impacted by beta particles generated by inhaled dusts would be a function of both total mass and total number of distributed radioactive dusts.

Self-absorption: An example of this critical means of measuring human exposure comes from radioactive materials that contain isotopes that emit alpha particles. Alpha particles can only penetrate short distances in solid matter, on the order of 10 microns for a 4.0 MeV alpha particle in a sand grain. (24, NIST) For 200 micron diameter sands containing alpha emitting isotopes, most of the alpha particles would be self-absorbed by the sand matrix. Mass would therefore be a poor predictor of exposure to alpha particles for macroscopic sand grains. The total surface area of particles would be a better predictor of potential exposure to alpha particles, as self-absorption is minimal at the surface of the particles. In the interior of larger particles, the mass of the particle itself will self-shield a predictable percentage of the alpha particles.

To sum up, the size of the dust particle carrying radioactive energy into the body can be an important determinant of the biological effectiveness of a given mass of radioactive material. This is distinct from the effective dose for an isotope. Effective dose is measured as the Sieverts per Becquerel for a given isotope. Coefficients have been calculated for each isotope. (26, ICRP) These are expressed as Sv/Bq. For example, highly radiotoxic ^{210}Po has an inhalation effective dose coefficient of 4.3 EE-6 Sv/Bq. (Ibid) What must be ignored by this coefficient is that inhalation exposure to particles of distinct sizes will result in different actual exposures and different degrees of biological hazard. Some of this distinction is encompassed by employing different coefficients for different intake routes (ingestion vs. inhalation) or different body clearance times for various isotopes. Were the data available, one could likewise develop different effective dose coefficients for various size distributions of inhaled radioactive dust particles.

1.5 Fingerprinting and dust sources

Particle morphology vs. particle source: The physical shape of a particle can give important information about how it was formed. In turn, this gives information about the potential source of the particle. For example, many fine (< 10 um diameter) radioactive fallout particles produced by nuclear detonations are spherical. The high temperatures related to nuclear detonations produce these spheres as vapors condense into solid particles upon cooling. (7, Eisenbud) This is not a unique property of nuclear detonations. Any process sufficiently hot to vaporize or melt nuclear materials can produce similar spherical particles. For example, fly ashes produced by the combustion of coal are also spherical. These ash spheres form as molten droplets are suspended in hot combustion gases. (27, UK)

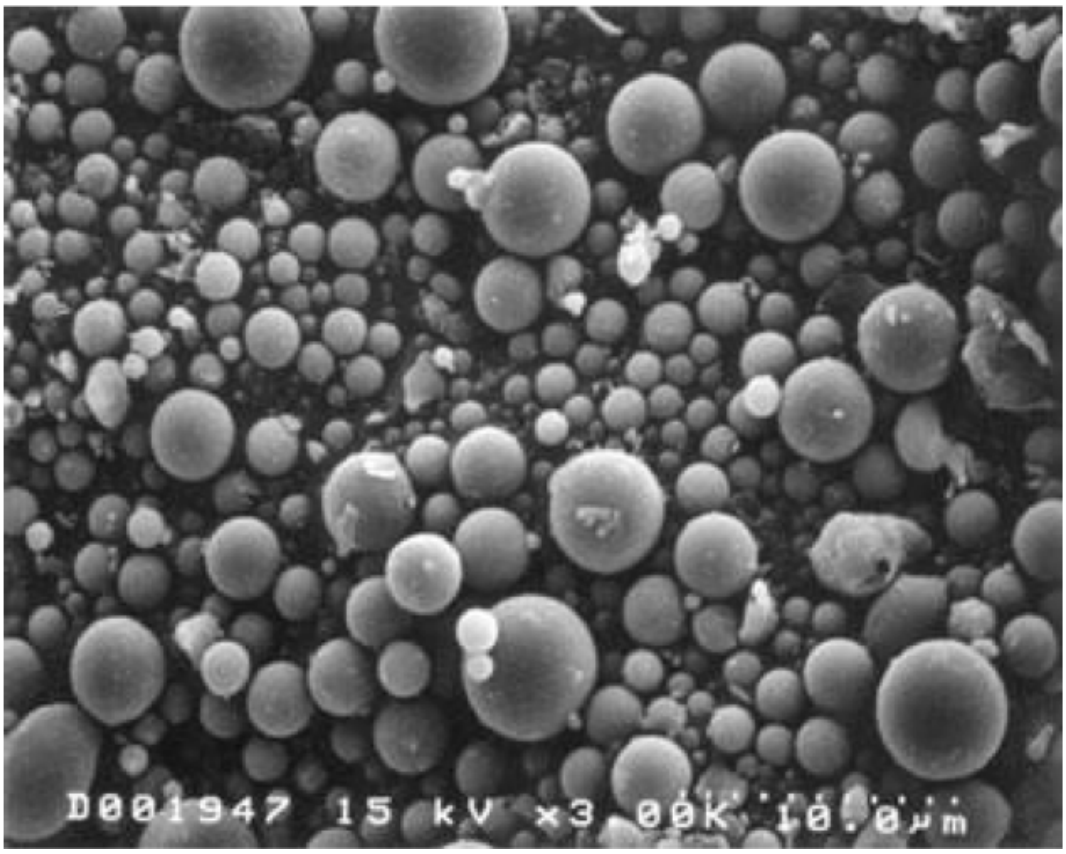

Fig. 1.15 Above, fly ash, US DOT Federal Highway Administration (34, FHWA)

The two SEM/EDS photomicrographs below (Figs. 1.16A and 1.16B) are of thorium-rare earth particles found in house dusts near the Hanford Nuclear Reservation. Thorium rare-earths include the natural mineral, monazite. Monazites contains thorium and/or uranium, along with cerium, samarium, and other rare-earth elements. The thorium in monazite is naturally radioactive. The two photomicrographs are shown in similar scale. The sphericity of these particles suggests exposure to high temperatures. Monazites are an important source of thorium. (33, MIT) Fertile ^{232}Th can absorb a fast neutron then beta decay to form fissionable ^{233}U. (author samples, 2011)

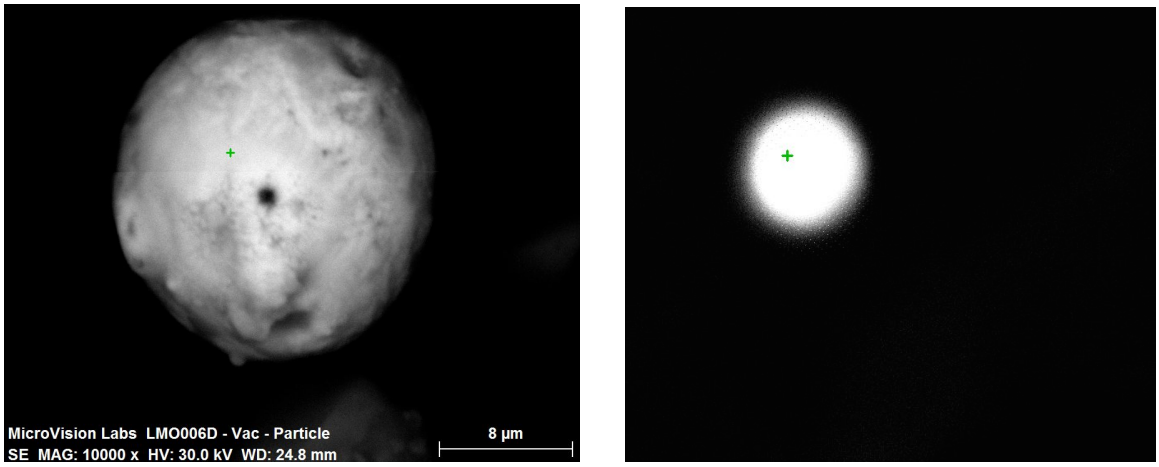

Figures 1.16A Above left and 1.16B above right:

The spherical thorium-containing particles above are from the house dust of a high level nuclear waste worker at Hanford, WA. The particle of Hanford Tank Farm dust on the following page (Fig. 1.17) has a composition identical to the two particles above. Nevertheless, the crystalline morphology of the particle below suggests a somewhat different original source for this Hanford radioactive dust particle. It is notable that similar crystalline morphologies were also found for thorium monazite particles in the worker's house dust. The particle in Figure 1.17 is similar in morphology and identical in composition to natural thorium monazite crystals. The three particles in Figs. 1.16A, 1.16B and 1.17 are likely Hanford-related monazites. Nevertheless, their morphologies suggest that their processing histories are different.

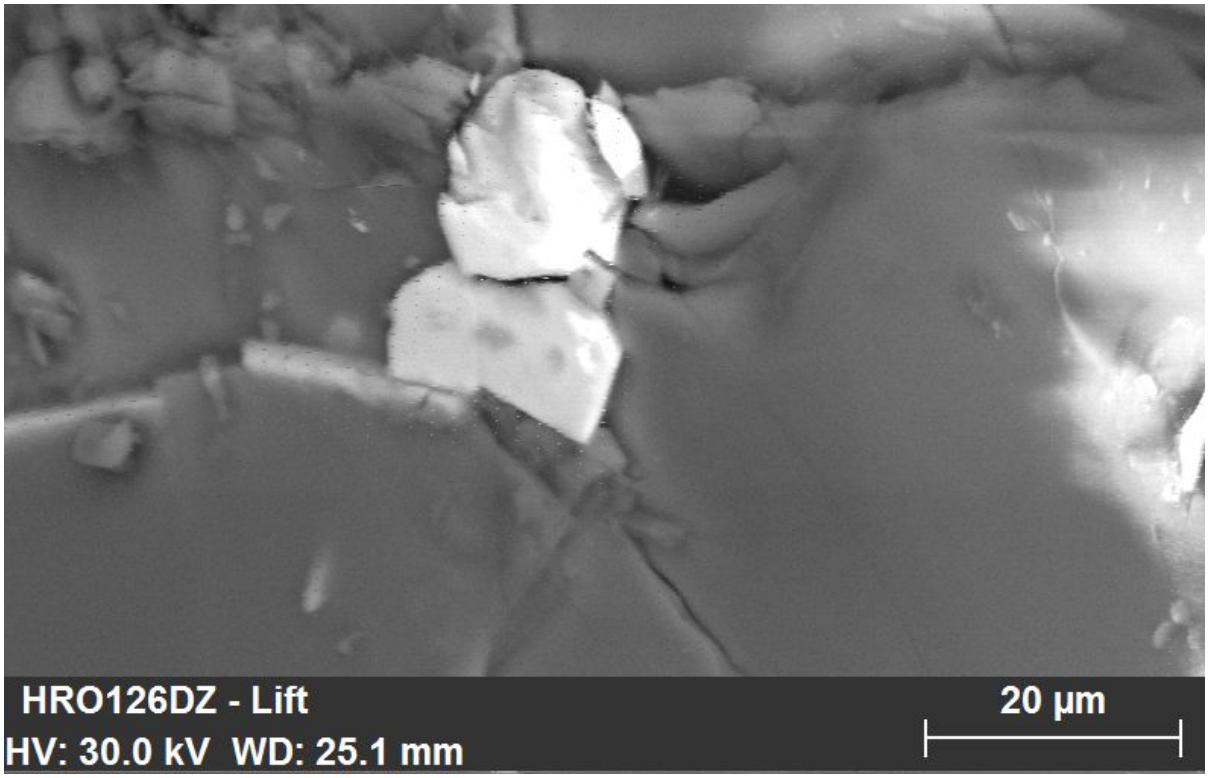

Fig. 1.17 Above, Th-monazite crystal in Hanford high level nuclear waste tank farm dust.

Elemental composition and source fingerprinting: The elemental composition of individual dust particles can provide data regarding the source of radioactive materials in dusts. For example, the first radioactive particle depicted on the following page (Figs. 1.18A and 1.18B) is composed primarily of the element thorium. This radioactive particle was found in HVAC system dust at a worker clothing change area just outside of a high level nuclear waste storage area at Hanford. Figure 1.19 shows the SEM/EDS spectrum for a particle with similar elemental composition. The second particle is from a Hanford nuclear waste tank farm worker's house dust sample. The presence of similar thorium compositions in dust particles from both sites suggests a common source. The evidence suggests that the thoriated hot particle found in the home is likely the result of accidental transport from the Hanford employee's workplace.

Fig. 1.18A Above: photomicrograph of thorium metal particle

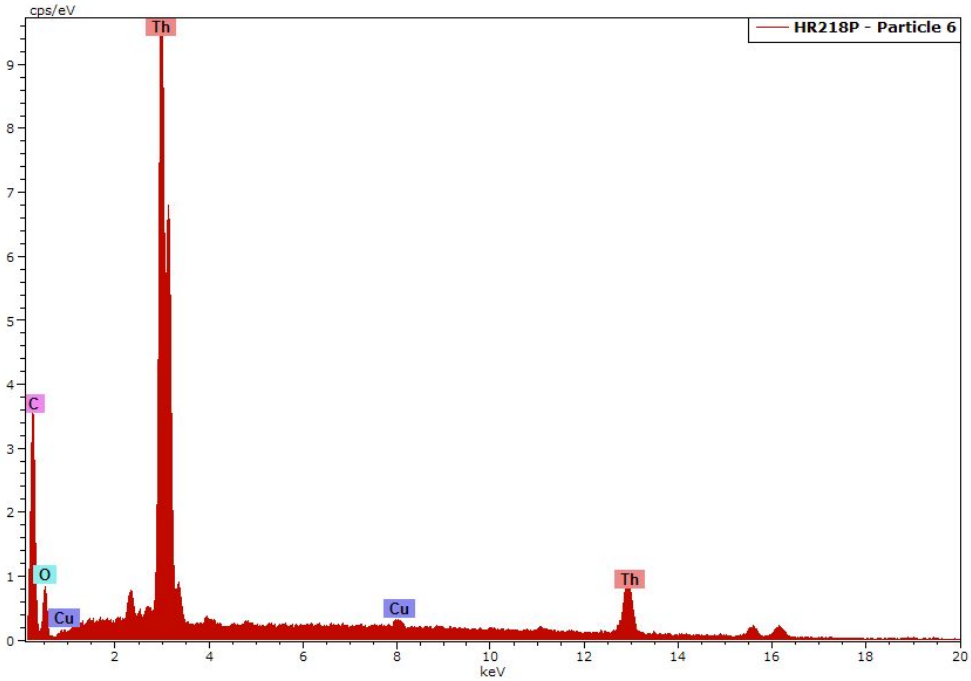

Fig. 1.18B Above: SEM/EDS data for the particle from the Hanford waste tank farm clothing change area

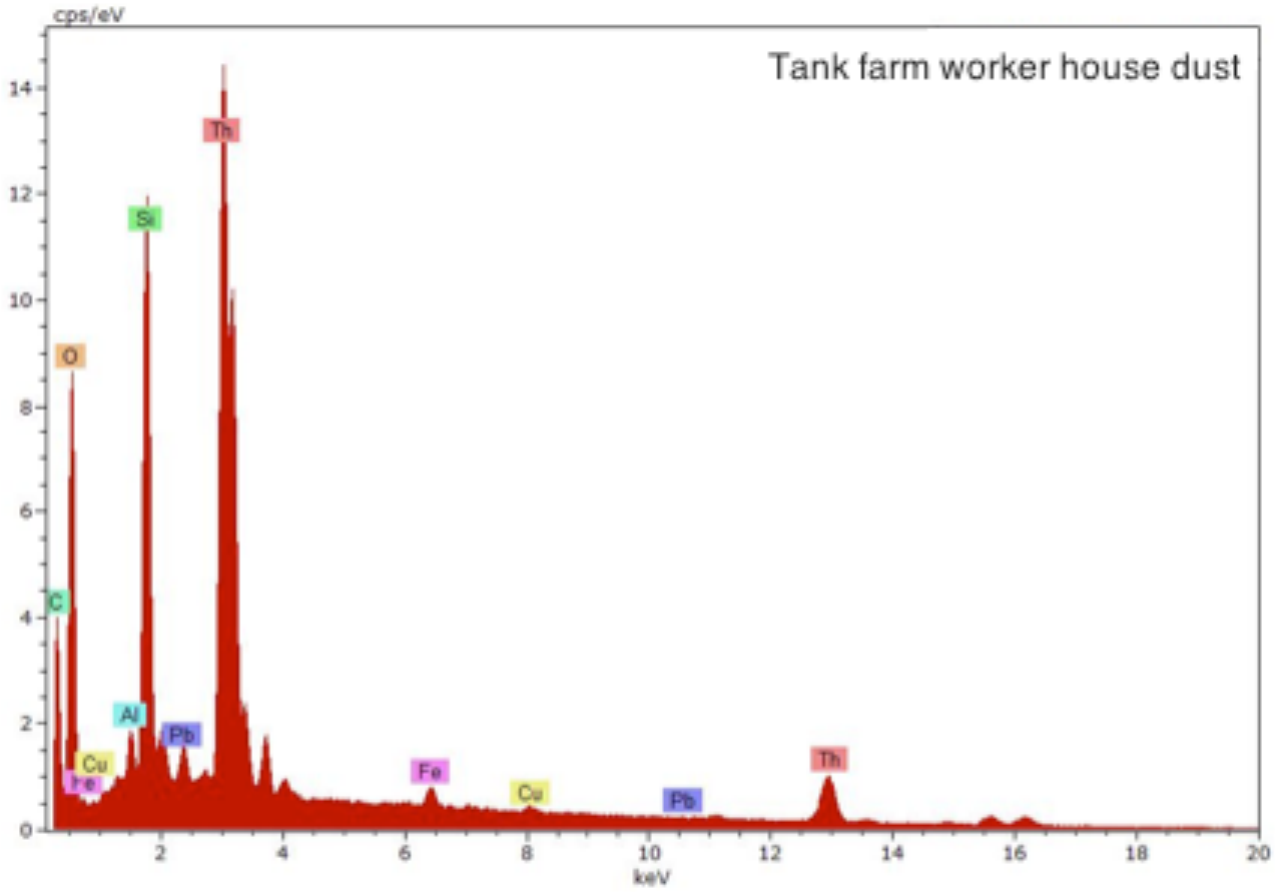

Fig. 1.19 Above: SEM/EDS data for a particle found in a Hanford tank farm worker's house dust.

This particle's SEM/EDS spectrum is very similar to the one found for particles from dusts at the high level waste tank farm in Fig. 1.18B. Given that the employee worked or resided at these two locations, workplace exposure and transport on clothing or belongings is a likely means of hot particle transport. If the transport were by air movement, one would expect to find similar particles in area soils. No such particles were detected in outdoor offsite (compared to Hanford) soils in this study. (Mass data in Appendix E)

The elemental composition of the particles in the tank farm dust vs. the tank farm worker house dust have some minor differences. The additional elements in the house dust sample are typical alumino-silicate elements commonly found in soil material.

Contrast the previous particles with the thorium-containing dust particle below. It is from a uranium mine assay office in Washington. The calcium-phosphorous rare earth elements present suggest that this particle has a different source Fig. 1.20 shows the SEM/EDS spectrum. It is typical of natural thorium monazite minerals.

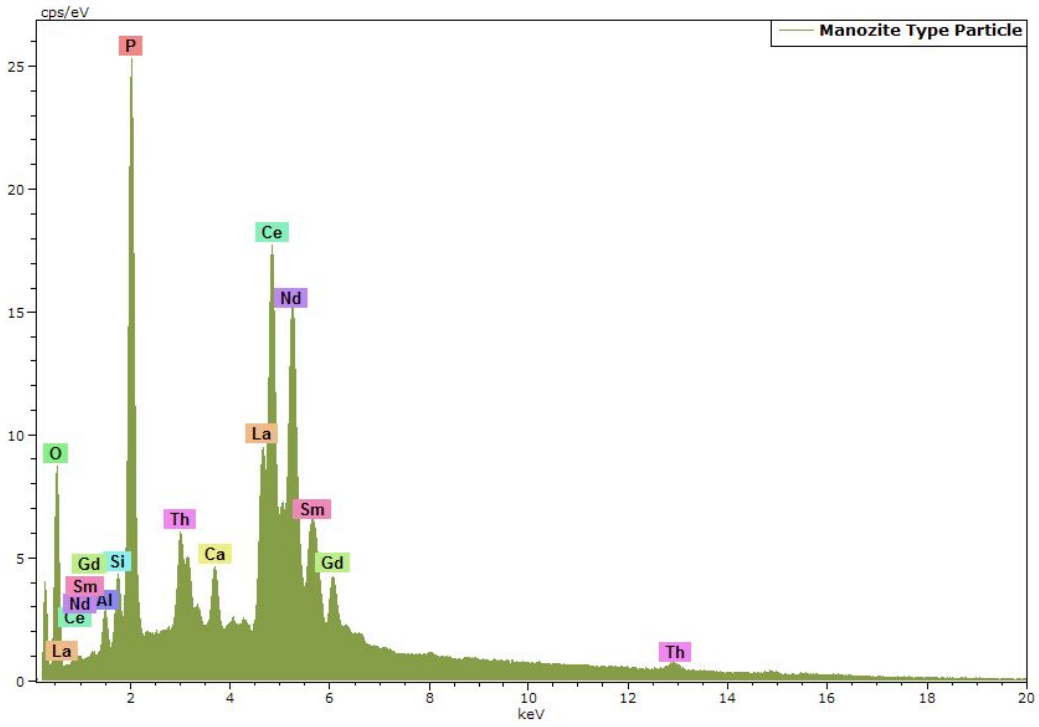

Fig. 1.20 Above: SEM/EDS sprectrum for a monazite mineral particle

It is important to note that the natural and Hanford-sourced dust particles would had strongly similar NaI-gamma spectra. The source of the thorium at each location would not be distinguishable by gamma spectroscopy alone. By analyzing the individual dust particles carrying the radioactive contaminant; natural thorium and processed thorium metal are readily distinguished. The microanalytical evidence demonstrates that the dusts in the worker's home contained industrial thorium contamination similar to the thorium metal found at the Hanford tank farms, as opposed to naturally-occurring thorium.

Isotopes vs. source: The isotopic ratios of radioactive elements in dust samples are an important source of information regarding the source of radioactively-contaminated dust particles. For example, uranium from natural mineral deposits will contain specific ratios of fissile ^{235}U vs. fissionable ^{238}U. If the 235:238 ratio is higher than the natural ratio, the material is called enriched, and will likely be of industrial origin. Using the 235:238 ratio, natural vs. industrial uranium in environmental samples could be distinguished. SEM/EDS analyses do not distinguish isotopes of a given element. Isotopic ratios were therefore undetermined in analyses of individual dust particles in this research. This is important to note for elements such as cesium which have stable natural isotopes, and also have common radioactive isotopes related to industrial nuclear processes. Cesium is an excellent example where confusion is possible when relying on SEM/EDS analysis alone. Two cesium isotopes, 134 and 137 are major radioactive fission products related to the Fukushima nuclear accidents, but stable cesium is a natural trace element in soils.

In a small number of cases, an individual dust particle has sufficient activity to be isotopically described using a gamma photon multichannel analyzer. A high activity radioactively-hot dust particle from Nagoya, Japan had enough activity to perform a gamma photon-based isotopic analysis from a single 10 micron particle. (See Section 2.8 for details.)

1.6 Dust inhalation and ingestion

The dose received from an inhaled dust particle partly depends on the nature of the contaminant. A chemical contaminant may impact the body at a specific site. For example, a particle of caustic material may cause a lesion at the site where the particle first encounters tissue. (29, ATSDR) A dust particle composed of an insoluble material like asbestos may cause a permanent injury to tissues, but only at the final location where it comes to rest. (30, ATSDR) Dusts contaminated with soluble compounds, such as

fluorinated alcohols, may become trapped, then distribute the contaminate throughout the body as the compound dissolves.

For dusts containing radioactive materials, all of these same processes occur. In addition, there is the action at a distance that occurs when radioactive decay occurs. The release of alpha particles, beta particles, gamma photons and other forms of nuclear energy adds a layer of complexity on top of those caused by the chemical and physical behavior of inhaled dusts. To calculate the potential biological impact of the inhaled dose of radioactively-contaminated dusts, the absorbed dose of radioactive energy must be also be described.

Calculating the risk of biological harm from hot particle inhalation means performing a straightforward, but lengthy, bookkeeping task. The physical parameters of dust intake must be calculated: dust concentration in the environment, rate of intake, probability of dust retention in the body, target organ or tissue. The chemical behavior must be known: solubility of radioactive material, rate of dissolution, size effects, biological half life, particle surface charges - if any. The quality, range, radioactive half-life and intensity of radioactive flux must be calculated. All three types of dose variability help determine if absorbed radiation dose from hot particles is a whole body dose, an organ dose, or perhaps a dose to a tissue within an organ.

None of these variables are necessarily unknown. Many physical and biological properties of radioactive isotopes can be looked up in the plentiful tabulated data available from US national laboratory and government agency websites such as NIST's ASTAR database. (24, NIST) One could guess that for actual population exposure events, these critical variables typically remain uncalculated. This level of data collection is a daunting bookkeeping challenge, even though the data itself is straightforward. Instead average exposures have been used to calculate population risks. Regulations and

standards are based on average exposure, and not on the statistical description of a population of hot particles in the environment.

For exposure scenarios where people are exposed to radioactive dusts, the true dose will not be known if the hot particles themselves are not studied. Without knowing some simple facts about the distribution of hot particles, dosage may be miscalculated. Knowing basic statistics of the probability of encountering hot particles of a given size activity distribution would greatly increase the predictive value of environmental risk assessment.

Without a statistical understanding of hot particles in radioactively-contaminated dusts, we are left with average exposure data. Average exposure data can be collected by simple detection equipment that provides scalar results. After the Fukushima accidents for instance, residents of a community may be told that their average exposure is "x" microSieverts per year, causing a risk of "y" percent for a given impact. In some cases, the probability of exposure to high bioavailability, high specific activity dust particles may be significant in the human environment. If these particles are present, but not monitored or measured, then some individuals in a community may unknowingly have substantially higher exposures than others. This remains true even though any given cohort is assigned the same "average" exposure.

The higher dose individuals may experience a biological impact from their hot particle exposures. This impact may be greater than the impact expected from the average dose alone. If this is true then we have failed to adequately estimate exposure for all members of the cohort. In effect, we have underestimated risk to the hot particle-exposed portion of the population. (See Section 2.8 for an example calculation)

Investigators could also falsely assume that these biological impacts from hot particles were the result of receiving the average radiation dose. The average dose ignores high

activity hot particles. This calculated average is smaller than the true average dose that people actually received. This would yield misleadingly high incidence data about the biological impact for a given average radiation dose. The true dose causing a biological impact would have been higher than the calculated average dose, because the true doses include the unmonitored exposures to hot particles.

Lacking environmental hot particle data, we risk overestimating the biological effectiveness of low dose radiation for future exposures. At the same time, we under-anticipate the potential biological harm to the radiologically-impacted population impacted by the current (underestimated) exposures.

The strength of standard models for estimating biological effectiveness per Sv of exposure is not changed by the presence of high activity hot particles. An investigator simply is required to do more data collection when hot particles are present. The full complexity of potential doses must be measured if the models are to accurately predict biological effects incidence rates. (See an example in Sec. 2.8 Nagoya, Japan sample)

The complexity of the data gathering that is needed can make hot particle dose difficult to calculate compared to homogeneous external radiation fields. Whether there is or is not any kind of difference in the biological effect of a given absorbed dose from hot particles or homogeneous external radiation is outside of the scope of this research.

Investigators studying environmental radiation releases should routinely consider whether receptors have a significant probability of exposure to high activity hot particles. If so, then accurate dose calculation requires including the portion of exposure that may be due to hot particles. Failing that, one is simply entering bad data into an already complex model.

Section 1 references

(1) George, A.C. et al, (1991) Abstract: *Indoor radon progeny aerosol size measurements in urban, suburban, and rural regions*, Aerosol Science and Technology, v 15, n 3, Oct, p 170-178

(2) Friedlander, S.K., (2000) Smoke, Dust, and Haze, Fundamentals of Aerosol Dynamics, 2nd Ed., Oxford University Press

(3) Cizdziel, J. V., (a) Hodge, V. F.,(b) (2000) *Attics as archives for house infiltrating pollutants: trace elements and pesticides in attic dust and soil from southern Nevada and Utah*, *Microchemical Journal* 64 2000 85 92, (a) Environmental Science and Health Program, University of Nevada Reno, Reno, NV 89557-0187, USA, (b) Department of Chemistry, University of Nevada Las Vegas, 4505 Maryland Pkwy, Las Vegas, NV 89154-4003

(4) Lewis, Robert G., (1999) *Distribution of Pesticides and Polycyclic Aromatic Hydrocarbons in House Dust as a Function of Particle Size*, Environmental Health *Perspectives V 107, No. 9, Sept.*

(5) US Environmental Protection Agency, Indoor Air Quality Program, 2014

(6) P. E. Rasmussen, *Canadian Journal of Analytical Sciences and Spectroscopy*, *V 49, No. 3, (2004*)

(7) Eisenbud, M., and Harley, J., (1953) *Radioactive Dust from Nuclear Detonations*, *Science, New Series, Vol. 117, No. 3033, Feb. 13, pp. 141-147*

(8) Zannetti, P., Air Pollution Modeling, Ch. 10, Dry Deposition, citing Sehmel 1980, (1990)

(9) Shleien, B., Glavin, T.P., and Friend, A.G. (1965) Particle size fraction of airborne gamma-emitting radionuclides by graded filters. *Science* 147, 290

(10) Shatkin, Jo Anne, (2008) Nanotechnology, Health and Environmental Risks, CRC Press, ISBN-13: 978-1-4200-5363-0

(11) NZ Ministry for the Environment, *Good practice guide for assessing and managing the environmental effects of dust emissions*, ISBN 0-478-24038-4, 2001

(12) Environmental characterisation of particulate-associated radioactivity deposited close to the Sellafield works, Ellis Induro Evans, Doctoral Thesis, Imperial College of Science, Medicine & Technology, October 1997

(13) Birmili, W., et al, (2008) *A case of extreme particulate matter concentrations over Central Europe caused by dust emitted over the southern Ukraine*, Atmos. Chem. Phys., 8, (2008) 997-1016

(14) Eisenbud, M., (1963) Environmental Radioactivity, McGraw-Hill

(15) Broda, R., (1987) Gamma Spectroscopy Analysis of Hot Particles from the Chernobyl *Fallout, Acta Physica Polonica, B18 (10) pp. 935 – 950*

(16) Lang, S., Servomaa, K., Kosma, V.-M., and Rytomaa, T. (1995) Biokinetics of nuclear fuel compounds and biological effects of nonuniform radiation. *Environ. Health Perspect.* 103, 920.

(17) Lioy, P.J., Freeman, N.C.G., and Millette, J.R. (2002) Dust: A metric for use in residential and building exposure assessment and source characterization, *Environ. Health Perspect.* 10, 969.

(18) Rasmussen PE, (2004) Can metal concentrations in indoor dust be predicted from soil geochemistry?, *Canadian Journal of Analytical Sciences and Spectroscopy*. *49:3*

(19) Sajo-Bohus, L., Palfalvi, J., and Greaves, E.D. (1998) *Hot particle spectrum determination by track image analysis, Radiat. Phys. Chem.* 51, 467.

(20) Dordevic, Dragana, et al., (2004) *Contribution of dust transport and resuspension to particulate matter levels in the Mediterranean atmosphere*, Atmospheric Environment 38 (2004) 3637–3645

(21) Castronova, et al., (2000) *Silicosis and Coal Workers' Pneumoconiosis,* Env. Health Perspectives, 108 (2000) 4 675-684

(22) Gerber, Michele, (2007) On the Home Front: The Cold War Legacy of the Hanford Nuclear Site, Third Edition, Univ. of Nebraska Press

(23) IAEA, (1992) Safety Series INSAG-7, The Chernobyl Accident, Vienna

(24) NIST ASTAR online database, http://physics.nist.gov/PhysRefData/Star/Text/ASTAR.html, accessed 1/31/15

(25) Chan TL, Lee PS, Hering WE., (1981) Deposition and clearance of inhaled diesel exhaust particles in the respiratory tract of Fischer rats., J Appl Toxicol. 1981 Apr;1(2): 77-82.

(26) ICRP 72 as cited by the European Atomic Energy Community, (2014) *Polonium-210: Factfile*

(27) Roesch, W.C., (1977) *Microdosimetry of Internal Sources,* Radiation Research, 70 (3) 494-510

(28) Zaider, M., (1988) On the Application of Microdosimetry to Radiobiology, Radiation Research, 113 (1) 15-24

(29) Agency for Toxic Substances and Disease Registry, (2015) Sodium Hydroxide Fact Sheet, http://www.atsdr.cdc.gov/MHMI/mmg178.pdf

(30) Agency for Toxic Substances and Disease Registry, (2015) Asbestos Fact Sheet, http://www.atsdr.cdc.gov/toxfaqs/tfacts61.pdf

(31) Shinonaga, T., et al., (2008) Isotopic analysis of single uranium and plutonium particles by chemical treatment and mass spectroscopy, Spetrochemica Acta part B 63 (2008) 1324-1328

(32) Kaltofen, M. P. J., (2009), Microanalysis of Heterogeneous Radiation in Particulate Matter as an Aid to Nuclear Source Identification, A Thesis Submitted to the Faculty of the Worcester Polytechnic Institute in partial fulfillment of the requirements for the Degree of Master of Science in Environmental Engineering

(33) MIT Energy Initiative (2011), *The Future of the Nuclear Fuel Cycle*, report, http://mitei.mit.edu/publications/reports-studies/future-nuclear-fuel-cycle

(34) US Dept. of Transportation, Federal Highway Administration, Fly Ash Facts for Highway Engineers, url accessed 2015, https://www.fhwa.dot.gov/pavement/recycling/fach01.cfm

(35) Author field samples and microanalytical data

(36) National Institutes of Health http://www.ncbi.nlm.nih.gov/pmc/articles/PMC2270238/

(37) US Environmental Protection Agency http://www2.epa.gov/region8/rocky-flats-plant-usdoe

(38) SEPA UK http://www.sepa.org.uk/radioactive_substances/publications/dounreay_reports.aspx

(39) CIA http://www.foia.cia.gov/sites/default/files/document_conversions/89801/DOC_0000498481.pdf

Section 2: Analyses of Japanese surface soils and dusts after the Fukushima accident

Introduction and accident timeline

: The March 11, 2011 Great East Japan earthquake and ensuing tsunami resulted in the loss of 15,889 lives, with 2,601 still missing in 2014. Ninety percent of these deaths were from drowning. (Japan National Police Agency 2014 tracking data) The earthquake and tsunami also caused catastrophic damage to four of the six nuclear power units at the Fukushima Daiichi Station. Radiological materials escaped from the reactor units at the power plant site via air borne plumes of contaminated gases, aerosols and particles, and by contaminated wastewaters. (1, Nature; 2, Nature) Airborne dusts can transport radioactive materials as trace contamination in homogenous collections of particles, or as isolated individual particles containing high concentrations of radioisotopes. (3, Schleien; 4, Adachi) Contaminated environmental dusts can accumulate in indoor spaces, potentially causing radiation exposures to humans via inhalation, dermal contact, and ingestion. (5, Rasmussen)

The earthquake epicenter was offshore, measuring magnitude 9.0 at sea, and magnitude 7.0 onshore at the plant site. Units 1, 2 and 3 were operating at their rated outputs. The units' power ratings were 460 MW, 460 MW, and 784 MW, respectively. Units 4, 5 and 6 were shutdown for routine inspections. These units were rated 784 MW, 784 MW, and 1,100 MW respectively. All are boiling water reactors, BWRs, and all have at least 30 years of service. Unit 3 began using a modest amount of mixed oxide fuel, MOX, in 2010. In unit 3's fuel, some ^{235}U that makes up about 5 % of the fuel is replaced by ^{239}Pu. (28, TEPCO)

At the time of the earthquake, the three operating reactors went into automatic shutdown, with all control blades fully inserted. Offsite power failed. Onsite diesel generators and battery sources came online to provide controls and active cooling to units 1, 2, and 3,

and to the spent fuel storage pool located above unit 4. Saltwater circulation pumps continued to exhaust residual reactor heat loads to the ocean. (Seven miles to the south, the four BWRs at Fukushima Dai-Ini also went into automatic shutdown, but at Dai-Ini, offsite power was maintained.)

Once shutdown, the three operating units at Daiichi became subcritical, and neutron fluxes plummeted ($K<<1$). Unspontaneous fission stopped. The fission products remaining in the sealed fuel elements reactors are themselves radioactive, and continued to release beta particles, antineutrinos, and radioactive decay heat. The remaining unburned fuels continued to release alpha particles and an occasional spontaneous neutron. Fission products and unburned fuels release enough heat that spent fuel assemblies must be actively water cooled for three to five years after shutdown and fuel assembly removal.

The earthquake generated an historically large tsunami. A single emergency diesel generator, EDG, unit survived at unit 6. This EDG was able to provide enough power to actively cool units 5 and 6, dissipating their residual heat to seawater, and achieving cold shutdown for these units. None of the backup power or seawater circulation systems at units 1, 2, 3, or 4 survived the combined earthquake and tsunami. (28, TEPCO)

With the loss of offsite power and backup AC power sources, limited cooling power was available using residual core heat controlled by battery powered controls. Japanese regulations require eight hours of battery protection, twice the amount of battery availability required at US power stations. Station staff were unable to procure, scavenge, or transport sufficient batteries to maintain emergency core cooling controls. Cores overheated, water levels dropped exposing fuel assemblies, and core temperatures reached 1200 degrees C.

At 1200 degrees C water in contact with Zircalloy fuel cladding disassociates, forming hydrogen gas. The accumulated hydrogen ultimately detonated. The high temperatures also caused zirconium fuel cladding to swell and crack, releasing the fuel, neutron activation products and light and heavy fission products.

A high temperature airborne plume of contaminants escaped from the damaged containments of the fuel cladding, pressure vessel, and containment structure. The plume consisted of aerosolized nuclear fuel particles, fission products, structural materials, and reactivity control materials. Radioactive components of the plume included fission products ^{131}I, ^{134}Cs and ^{137}Cs; neutron activation products ^{60}Co, ^{10}Be, ^{239}Pu and ^{241}Pu; and fuels ^{239}Pu, ^{235}U, ^{238}U, as well as stable isotopes of Fe and Zr. (30, Shultis)

Additional isotopes are produced as the original parent isotopes decay. One key decay product is ^{241}Am, which forms from the beta decay of ^{241}Pu. The ^{241}Pu is formed from the successive absorption of neutrons by ^{238}U in the reactor core.

$$^{238}U \xrightarrow[+n]{} {}^{239}U \xrightarrow[-e^-]{} {}^{239}Np \xrightarrow[-e^-]{} {}^{239}Pu \xrightarrow[+n]{} {}^{240}Pu \xrightarrow[+n]{} {}^{241}Pu \xrightarrow[-e^-]{} {}^{241}Am$$

Fig. 3.1 Above: Formation of ^{241}Am from ^{238}U

While fission products generally decay by beta particle emission, the higher z fuels and fuel decay products, ^{238}U, ^{239}Pu, ^{241}Am, and ^{235}U, are alpha emitters. The neutron activation products include a wide range of isotopes, including tritium, ^{10}Be (formed from ^{10}B) and ^{60}Co. Although ^{60}Co decays by beta emission, the resulting ^{60}Ni-m isotope is metastable, and releases gamma photons at 1.17 and 1.33 MeV.

In a pyrolitic environment, portions of the damaged fuel assemblies are sufficiently hot to become vaporized. As the plume of vaporized core material cooled in the ambient atmosphere, the fuel and nonfuels such as structural materials condensed into ultrafine respirable particles.

The alpha emitters associated with fuels and the beta emitters associated with fission products were adsorbed onto microscopic aerosolized particles and condensation products. The particles were small enough in size, so that their settling velocities are negligible compared to air velocities. These can travel long distances until the particles aggregate and settle, are adsorbed by surfaces of larger particles, or are washed out of the atmosphere by precipitation.

Alpha and beta emissions are charged particles. They are ionizing but not penetrating. Air, building shells, and even clothing and skin provide sufficient protection from external exposure to these forms of radiation in the environment. Internal exposure, however, in the form of ingested or inhaled dusts containing fuel or fission product particles, does present a significant potential human health hazard. For example, a plutonium particle that would result in inconsequential external exposure causes tissue death and has tumorigenic potential in nearby cells that survive the alpha bombardment. (29, Coggle)

The specific activity of an individual particle can be significantly higher than that of the surrounding particles in a dust sample. (6, Lang) These high activity particles, called hot particles, can be isolated and analyzed by scanning electron microscopy / energy-dispersive X-ray analysis. (SEM/EDS) Hot particle environments are found in nuclear power plants, and in nuclear fuel fabrication and reprocessing facilities. (7, Sajo-Bohus)

The fission fragments, ^{134}Cs and ^{137}Cs are among the most commonly found nuclear contaminants found throughout Northern Japan. (4, Adachi) Fission products are the fragments remaining after ^{235}U or ^{239}Pu in nuclear fuels absorb a neutron, become unstable, and split. The fissioning nucleus (A = 235 or greater) splits into a heavy fragment and a light fragment. The higher atomic number fragments cluster about A = 137 and include xenon, cesium, barium, lanthanum, cerium, samarium, europium and promethium. The lighter fragments cluster about A = 95 and include strontium, yttrium,

zirconium, and ruthenium. These fragments are predominantly beta particle emitters. (8, Hochel) The dispersion of radioactively contaminated particles from the Fukushima accidents has the potential to introduce particles enriched in these fission fragments into the environment. Given the large number of fallout particles distributed in the outdoor environment in parts of northern Japan, indoor dusts inevitably have become contaminated with varying amounts of radioactive fallout particles. (9, Cizdziel)

The calculation of the doses received from hot particles is well-described within existing exposure models. The actual calculations however, require exhaustive information about the number and composition of hot particles in the human environment. Realistically, such calculations are rarely done. More typically, exposure data is reported as averages of larger environmental data sets or as modeled doses. In the Phase 2 BEIR VII report on *Health Risks from Exposure to Low Levels of Ionizing Radiation*, the linear no threshhold (LNT) model is still the gold standard of exposure/effects models. Proper calculation of an individual's hot particle exposure is a matter of gathering accurate exposure data for input to the gold standard model. (12, Evans) Given the wide variability in hot particle sizes and activities, some individuals may experience a hot particle dose that is significantly higher or lower than the dose calculated by using averaged environmental data. Calculated exposures to members of a group using averaged data may understate exposure to the subgroup that is exposed to high activity particles. If this unaddressed group experiences excess cancer incidence, researchers might wrongly assert that the relatively low averaged doses were the cause, when in fact it was the much higher, but unrecorded, hot particle doses that had the biological effects.

Thus the objectives of this research on Japanese dust samples was to determine if environmental hot particles were present, were provably from the Fukushima Daiichi release, and could potentially deliver a significant radiation dose to humans if they were inhaled.

Methodology

Samples of house dusts, car engine filters, HVAC filters, and street dusts were collected and shipped to the author for analysis. Samples of environmental airborne fine particulate matter were collected using moderate volume air pumps (drawing 20 liters per minute) and preassembled filter cartridges. Sampling stations were set up in Tsubuka, Ibaraki Prefecture and Tokyo in Japan; Seattle, WA; San Francisco, CA; Aspen, CO; Natick, MA; and Hawaii. (see Fig. 2.1) Filter cartridges with drawn air volumes on the order of 60 cubic meters were shipped and analyzed after a 24-hour holding period. This holding period reduced the effects of natural radon in air. Analysis proceeded by beta and alpha counting, gamma spectrometry, autoradiography, and SEM/EDS analysis of individual particles. Of these analyses, only gamma spectrometry was performed on the WPI campus, primarily on the sealed air filter cartridges. The sampling program produced a minimum volume of solid radioactive wastes (less than 0.5 liters total).

Sampling objective: The goal of this project was to support or disprove the hypothesis that dust particles contaminated by hot particles from the Fukushima radiation releases could be identified in Japan and in the United States, and that the environmental fate and transport of these particles could be related to the hot particles' physical characteristics.

Sampling strategy: Sampling strategies may be judgment-based, random, stratified and/or systematic. Respective examples include sampling from areas stained by an oil spill, Monte Carlo-based methods for selecting numerical coordinates for sampling, sampling of specific materials to reduce variation and sampling on a specific grid spacing. (US EPA 1992) In this study, sampling media were specifically selected to increase the probability of collecting fine particles that could be inhaled or ingested, and that would

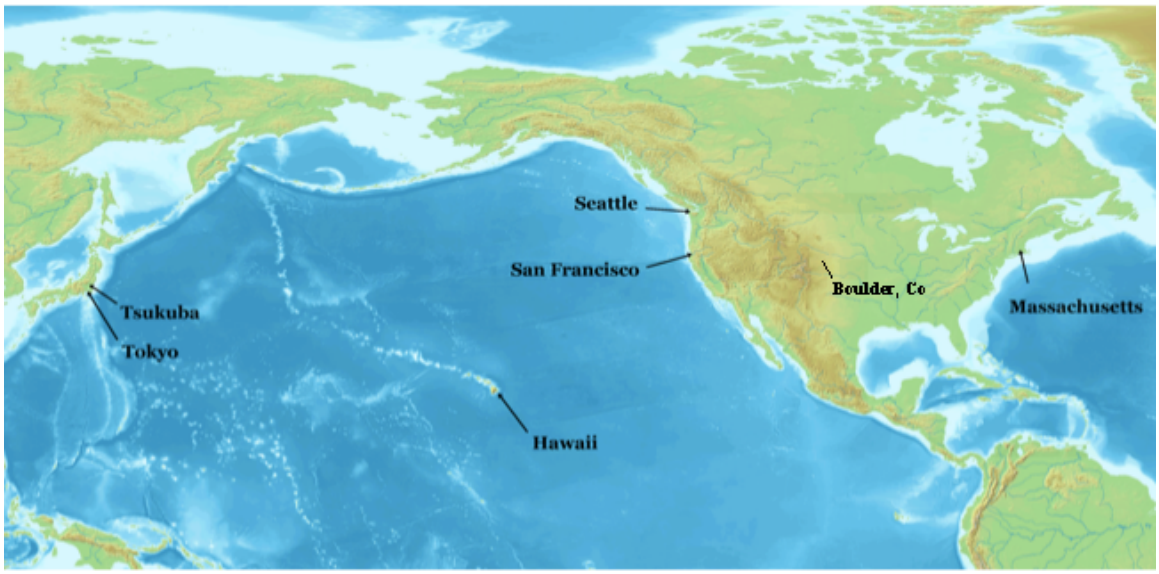

also be more likely to contain radioactively hot particles. The overall sample design was a stratified judgment-based method.

Fig. 2.1 Above: Air Sampling Stations

In three cases wind directions played a key role in choosing sampling locations. Local winds and critically-timed rainouts during key releases from Fukushima caused fallout to deposit to the northwest of the accident site. Days later, southwesterly winds and rains deposited fallout in somewhat lower concentrations in the Greater Tokyo area. (See Fig. 2.3) Prevailing global winds brought radioactive gases and dusts to the US and Canadian west coasts. These areas were therefore targeted for sampling of dusts, sediments, and soils. (See Fig. 3.7)

This study used samples submitted by volunteers, and there were limited controls on the volunteers' methods used to select samples. Volunteers provided quantitative air filters, vacuum cleaner bags and filters, HVAC system filters, vehicle air filters, dusts, surface soils, and wipe samples from inhabited structures. These samples were selected to meet the two primary sampling criteria for likely presence of fine particulates, and potential for human exposure. (ASTM D5438-00 2007) Volunteers were provided standardized equipment by the author for air samples. The remaining samples were collected using

standard personal protective gear and sample containers. There were no other additional controls, save for safety instructions and requirements.

Fig. 2.2 Above: Dust from a failed fuel rod on a 1 cm grid (13, NRC NUREG)

The figure above illustrates part of the rationale for the judgment-based sampling strategy that optimized hot particle collection rates. A loss-of-coolant accident simulation produced a dark-colored fine sand-like fuel fragment, of which 31% were 125 microns or smaller in size. The rupture and fragmentation occurred at 728 Deg. C. (13, US NRC) This study considered that some of these particles would have been transported to sample collection sites significant distances from the Fukushima accident location.

See following page, Fig. 2.3: Map of fallout impacts prepared by Safecast. Highest radiation measurements are marked in yellow. Used by permission, copyright 2014. (33, Safecast)

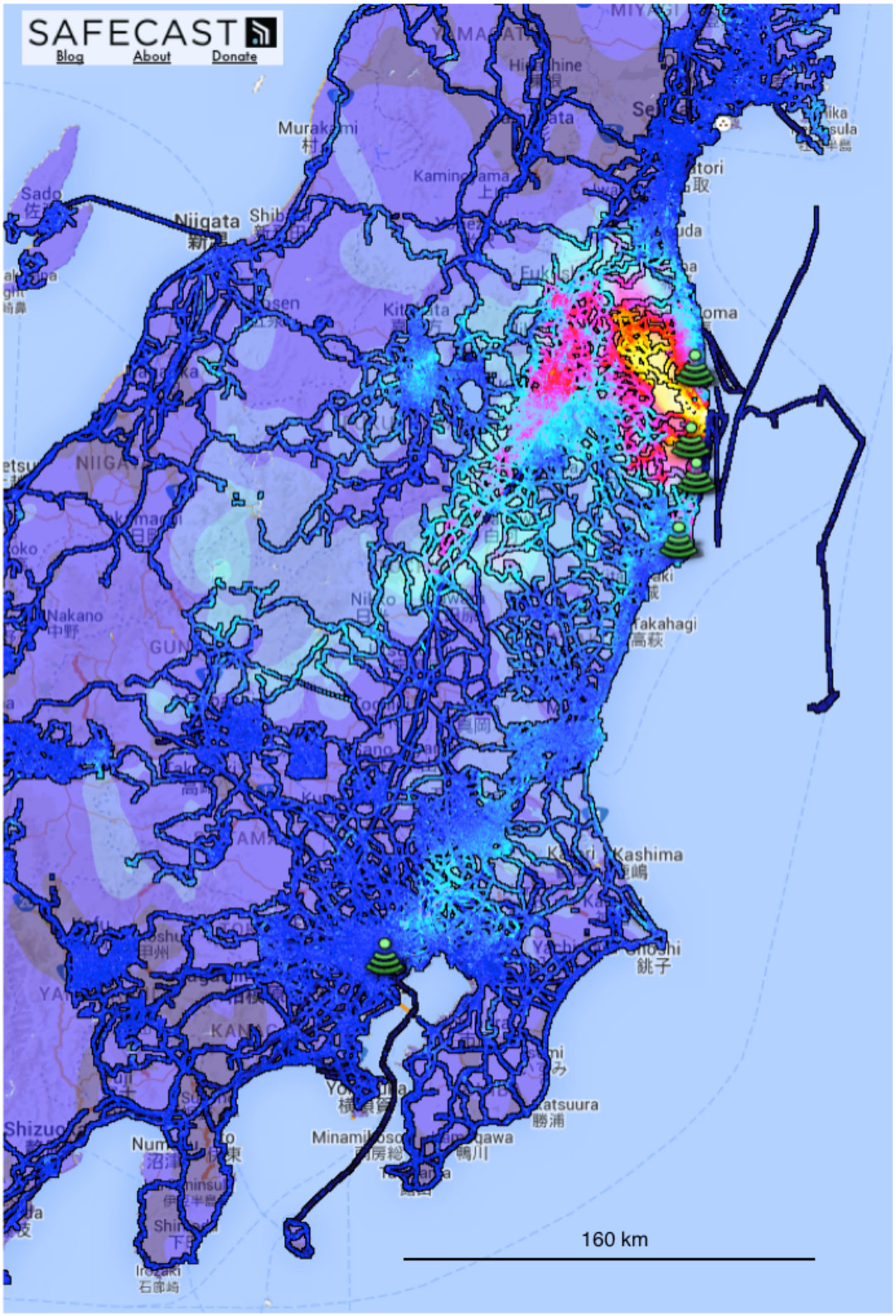

Fig 2.3 Above: Safecast map showing results of ambient radiation surveys

Safecast is a volunteer scientific organization based in Japan, with a mission that includes collecting crowdsourced data and environmental samples related to radioactive contamination from Fukushima. The organization also assembles standardized networked geolocation-enabled radiation measurement devices for use by its members and others. Some of the testing devices constructed by Safecast are shown in Fig. 2.4.

Fig. 2.4 Above: GPS-enabled, networked bGeigie test gear, (27, Safecast)

A map of sampled locations is on the following page. (See Fig. 2.5) Note that the sampling locus roughly followed the high fallout locus around the Fukushima Daiichi nuclear power plant, with additional sampling sites around Tokyo. The sampling objective of this study was to capture a sufficiently-large number of hot particles for microanalysis. The sample sites corresponded to a judgment-based sampling plan, and were not necessarily designed to be geographically representative. A total of 118 soil, dust, or clothing samples from Japan were accepted and analyzed, of which 85 were dusts or accumulations of surface soils and sediments.

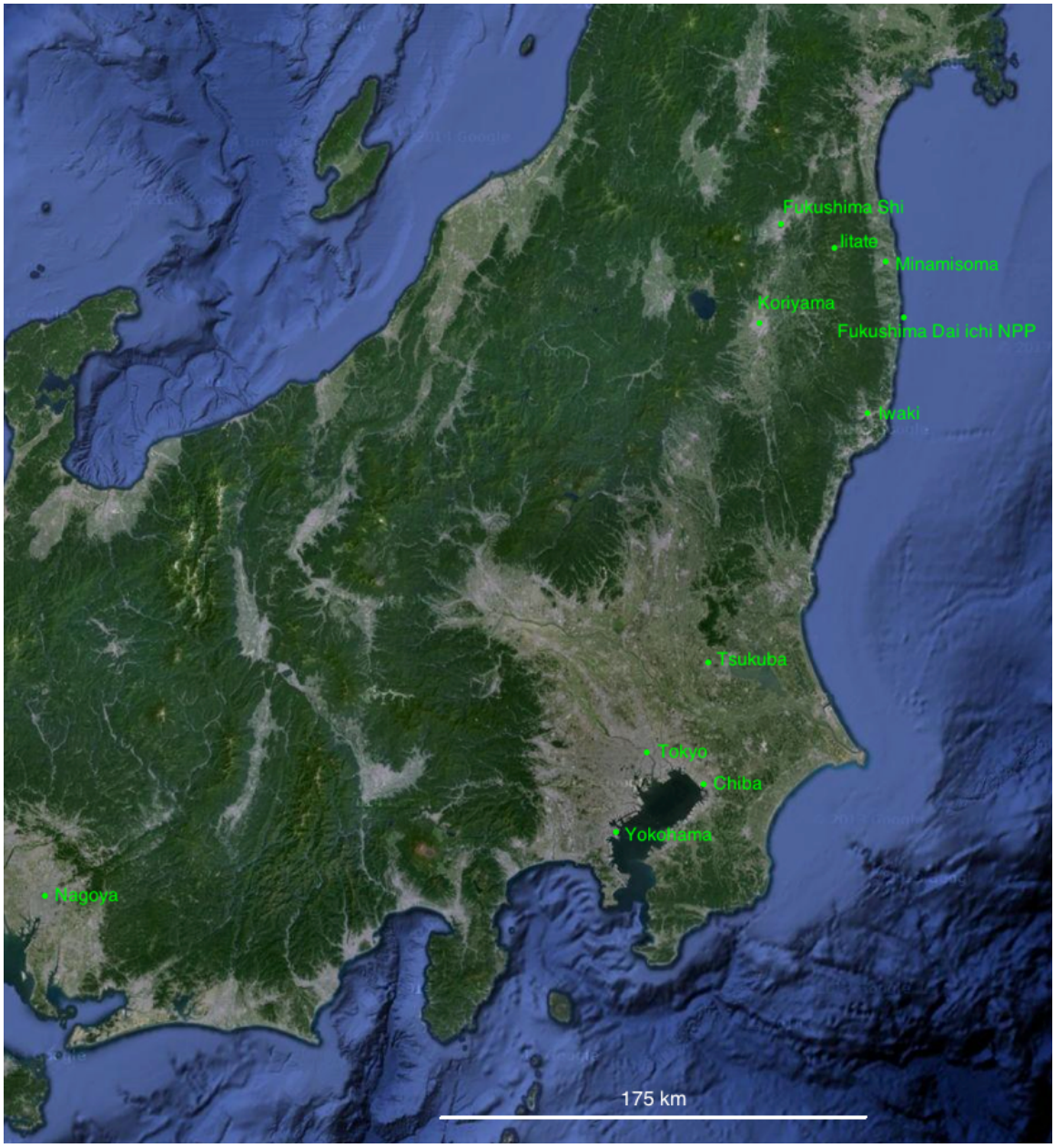

Fig. 2.5 Above: Dust, soil and air sample locations for this study in Northern Japan. (34, Google Earth)

Sampling Safety

The incorporation of safe procedures is the critical beginning to any field sampling plan. The key safety features of these procedures were embedded throughout the methodology, and were repeated in the safe sampling instructions. (See: *Appendix A - Safety: Sampling Instructions for Volunteer Samplers in Japan,* for additional information about sampling procedures actually employed for this research.)

It is important to note that during these studies, minor cultural differences between the United States and Japan became apparent. One key difference that was observed was with the difficulty in maintaining compliance with respiratory protection advisories. We were unable to provide a sufficient number of high-quality filtering respirators to all of the parties operating in Japan. There were multiple expressions of reluctance by volunteers to openly wear respirators that were substantially more effective than those generally available to the public. It was beyond the scope of this study to fully discuss the full range of motivations for respirator noncompliance, but it is worth noting that this occurred during the course of the study. This was a good demonstration of the need for researchers to be aware of potential differences between the researcher's personal experiences, and the experiences of others.

Transporting samples safely between Japan and the United States required proper sample prescreening, packing, and labeling. Soil and dust sample masses were adjusted downward. No attempt was made to shield samples. In some cases, using lead or similar shielding can worsen potential radiation exposure by creating X-rays from the scatter of energetic beta particles. Instead, small (1 to 10 gram) samples were packed with crumpled newspaper in oversize boxes. This geometry allowed small samples with elevated specific activities to be packed in such a way that there was no detectable radiation above background on the outside edge of packing boxes. Reduced sample sizes also allowed for reduced sample disposal costs. For the life of this research project, the

total volume of waste dust, soil and contaminated packing materials collected and requiring disposal was approximately one half liter.

No live plants or seeds were accepted. Sieving removed essentially all live plant materials or seeds. The only serious difficulty in sample transport came from a sample that was shipped from California to this project without prior contact or communication. A drinking water filter cartridge was shipped, and water leaked from the sample and dampened the packing box. As a result, this researcher had multiple urgent conversations with an inspector from the United States Postal Service (USPS), some of which were conducted after normal business hours by cell phone. The USPS analyzed the contents of the package by GC/MS and cleared the material for delivery. After this incident, all volunteer samplers were informed that no wet or water samples of any kind would be accepted for this study under any circumstances.

When collecting samples, care was taken not to lose fine materials that were more likely to retain contaminants. (14, Lioy) All samples were double bagged in polyethylene Ziplock® bags, with identifying information attached. Sample and data tracking was done using a Microsoft Excel® spreadsheet.

Samples were collected primarily from areas known to be impacted by fallout from the reactor accidents. A surface contamination map was prepared by the crowd-sourced data gathering organization, Safecast. Safecast provided contacts in Japan, encouraged public discussions and sharing of test data, and also hand-delivered samples to the author for analyses.

Air sampling station & filter set up: An Allegro sampling pump drawing 10 to 25 LPM or equivalent was used to draw air samples through sealed polycarbonate filter assemblies. The sampling period was as close as was practical to 48 hours per filter. Given that quantities of analytes captured were assumed to be very low for US sites, flow rates for

US stations were maximized for a given pump set up. Start and end time, date, and flow rates were recorded in a bound sampling note book and transferred to sample tracking sheets and a chain of custody. The air filter assemblies contained a support pad and a 0.45 micron pore size membrane filter.

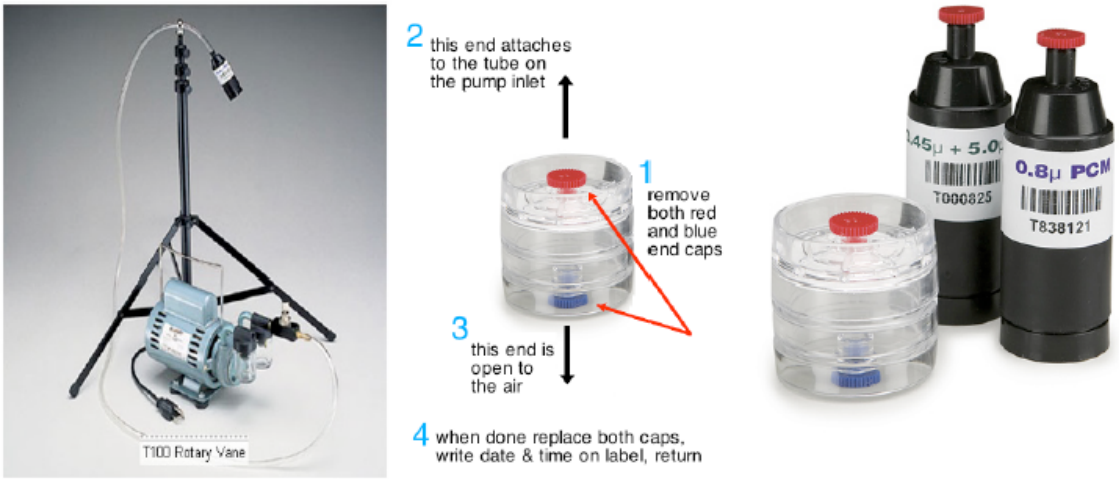

Fig. 2.6 Above: L to R, Air sampling set-up, sealed air sampling cartridges, 37 mm and 25 mm cartridges.

The samples were collected at different rates in order to reduce the possibility of having to store, transport, handle, or dispose of more radioactive materials that exceeded the exempt quantity. (See NRC Regulations section, on the amounts of radioactive material that can be handled without triggering the need for additional permitting.) The two Gillian/MSA-type pumps sent to Japan collected from 1 to 3 LPM or about 5.7 m^3 per filter +/- 20%. Those used in the USA, where lower concentrations were anticipated, collected 15 to 800 LPM using Allegro rotary vane pumps and a commercial HEPA vacuum from Lab Safety Supply, Inc. The higher sampling rates for these (presumed) lower exposure-stations provided large air sample sizes. Total air sample volume was 60 m^3 per filter, +/- 5%. These higher sample volumes increased the probability of collecting any hot particles.

Sample recruiting: Social media played an important role in getting samples from Japan and other distant sites. Facebook (www.facebook.com) and blogspot (googleblog.blogspot.com) made it possible to communicate verbally with volunteers without incurring telephone costs. Initial contacts were set up via Skype (www.skype.com/en) so that the author could assemble any sampling equipment on camera while the volunteer in Japan assembled their own gear. Scheduling Skype sessions was important, as Tokyo Standard Time is +13 hours Eastern Standard Time. Instructional video was produced for volunteers via youtube. (www.youtube.com)

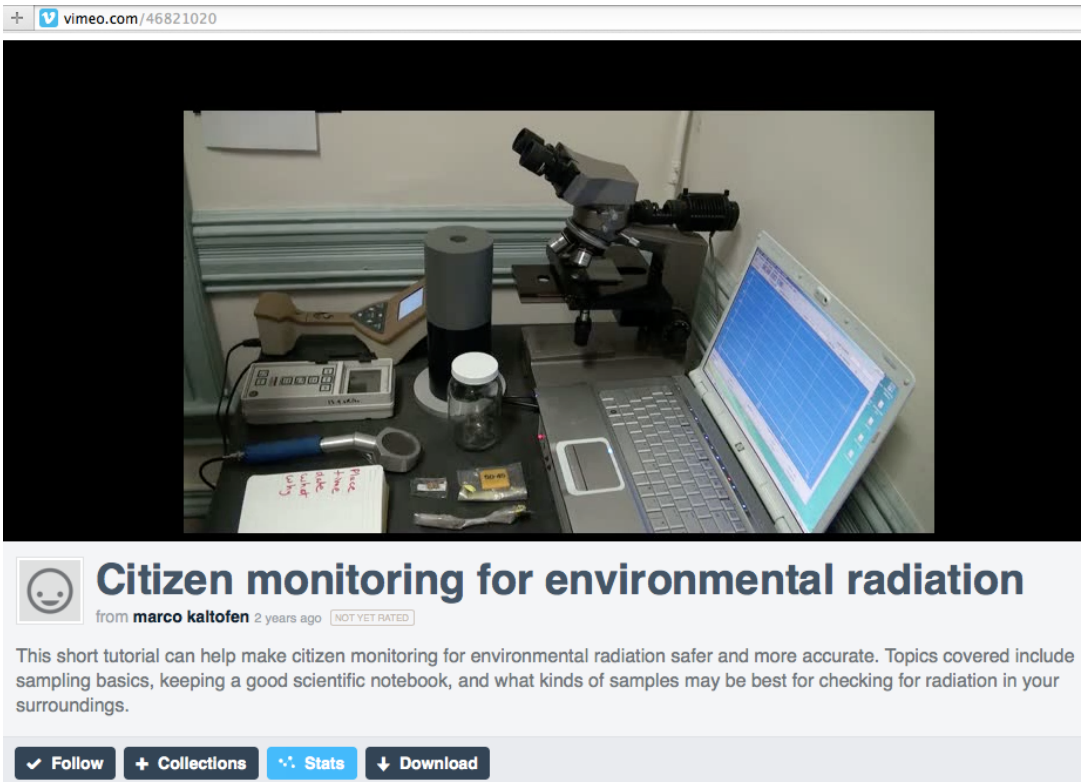

Fig. 2.7 Above: Sampling video screenshot

A radiation sampling procedure and safety video was produced for this study. The video is at https://www.youtube.com/watch?v=KsXaKpEdc4E, and is repeated at multiple addresses, including on Vimeo (www.vimeo.com). The Vimeo version of the video had 8,338 views as of January 30, 2015. The url is http://vimeo.com/50406479.

From time to time preliminary results were reported to the sampling volunteers via youtube. This had both advantages and disadvantages. These videos were open to the public, and this resulted in increased numbers of volunteers. The disadvantage, and this was a significant issue, is that preliminary data release is never truly private in social media. Any errors in preliminary work will be propagated on the internet. Likewise, preliminary data may be misinterpreted. For example, when preliminary data was separated from its context, there was confusion about whether results were blank corrected, or uncorrected. For low level radiation, the difference between corrected and uncorrected data may be significant as a percentage of the actual result. Based upon this experience, preliminary data was released in .tiff image format (tagged image file format), a format which produces a raster image that cannot be directly cut and pasted into text or data format. This reduced the odds of individual data becoming separated during distribution on social media.

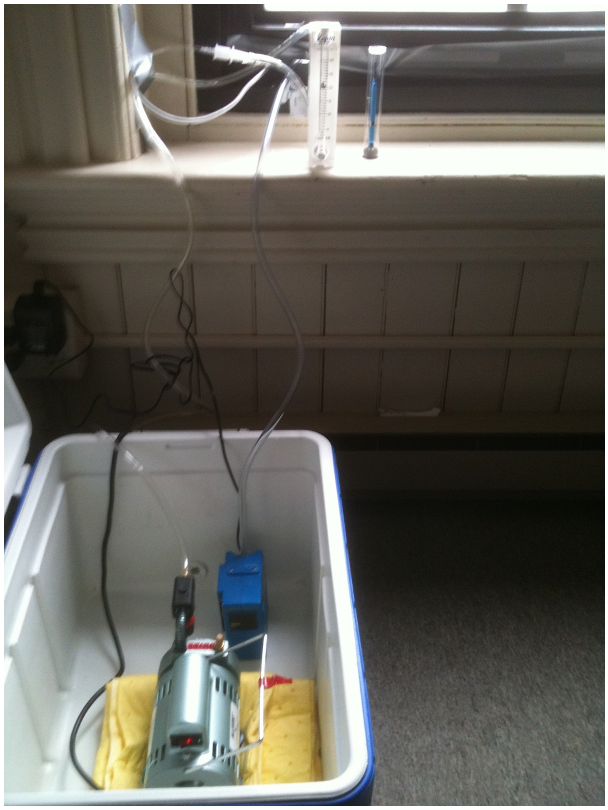

Fig. 2.8 Right: Air sampling set up showing high volume Allegro pump (20 LPM) and low volume Gilson pump (2 LPM). Valving and sample inlets are on the sill. The pumps were boxed for noise reduction.

Dusts: Following sample collection, the dust samples were double wrapped in low density polyethylene single track Ziploc® bags purchased from S.C. Johnson & Sons or equivalent suppliers. Shipping from Japan was by Nippon Post.

Sample preparation: Bulk dust and street dust/soil samples were air dried at ambient temperatures prior to analyses. Dust samples containing macroscopic objects and excessive pet hair were sieved to pass a 150 micron brass ASTM #100 screen. Due to the small size of high activity samples, no sieving was done on samples exhibiting more than 1 to 10 Bq g^{-1} total activity. Soil samples were not sieved. Sample sieves were water and Alconox® washed, triple rinsed with purified water (Thermo Scientific Barnstead® RO model D12651 in line with a Thermo Fisher NANOpure Ultrapure® Water System Model D11971) and air dried prior to reuse.

Automobile engine filters were cut from their frames so that they would be small enough to be analyzed whole. Following gamma spectral analyses, vacuum cleaner bag dusts were removed from their original packaging and weighed to record the mass of dust in the sample. Large vacuum bag dust samples were subsampled as needed to complete the quantitative analyses. Sample results for all bulk dust samples were reported on a Bq per gram basis.

Appliance and vehicle air filters were generally too large to fit within the shielded cavity of the gamma detector's sample chamber. Dust had to be mechanically removed from filtering media, unless the filter media could be removed from its frames to allow the entire sample to be contained within the shielded cavities of the gamma spectral detectors. The masses of dusts captured by air filters varied. The amount of dust on each filter was expected to vary based on capture efficiency, the volume of air filtered and on the concentration of dust per unit volume of air. Filter samples were generally accompanied by a usage log or description of origin. Vehicle filters varied in usage from nearly new to as much as 55,000 logged kilometers of use. Blank filters were new, dust-

free and in their original packaging. Results for vehicle or home air filter samples were reported as gamma-Bq per gram of dust removed from each filter. Eight samples with detectable activity but with insufficient mass to remove from the filter media were assigned a weight of 1.0 g. This unavoidably introduced a low bias to eight of the samples. For the filters with less than 1.0 gram of removable dust, the final results were normalized to 1.0 grams mass for reporting specific activity. While a total of twenty-three filters had less than 1.0 grams of removable dust, sixteen of these filters did not have detectable radioactivity above background levels. Activities were reported as nondetectable for these sixteen samples, and no specific activities were calculated.

Alpha and beta counting, total counts: All incoming samples, prior to unpacking, were also screened using a hand held ^{63}Ni-standardized Victoreen counter with a pancake type detector. No sample shipments produced packaging readings above 20 uR/hr. Samples were screened for total alpha and beta counts on a DPM basis using a Ludlum Model 3030 counter. Count periods were 60 minutes each. Air filter samples collected locally were held until after a 24 hour holding period to reduce the influence of local radon accumulations. The air filter assembly must be opened for alpha and beta analyses. No other preparation of the air filter sample is required. Once received, all sample cassettes must be handled using disposal gloves to prevent contamination. After recording the count results, the sample filters are immediately returned to their respective cassettes. The count results are recorded in a log book, in the sample tracking form, and, using a marker, on the cassette housing.

Screening of samples by hand held detectors occasionally found dusts which exhibited heterogeneous distributions of activity. These samples were divided in half, sequentially if necessary, to determine if any one half screened at a higher count level than the other. Samples with this behavior were presumed to contain one or more high activity hot particles, and were analyzed separately by gamma spectrometry and beta counting, but were reported as one sample.

Gamma spectrometry: Gamma photon analyses used WPI Physics Department-owned Ortech® NaI and Canberra® GeLi detectors. An Ortech® NaI well detector was also used. The well detector geometric efficiency was assumed to be 100%, while the Ortech® and Canberra® devices assumed a 50% geometric efficiency. Count efficiency @ 662 keV was 30%. Filter cartridges remained sealed, and the integrity of each seal was ensured with evidence tape. The entire assembly fit into the gamma spectrometer wells. Analyses proceeded by use of the MAESTRO® software package. After gamma photon results were reviewed, higher activity assemblies were selected for autoradiographic analyses.

Autoradiography-SEM/EDS**:** Autoradiographs were exposed in a light-free box approximately 12x18x24 inches in size. Autoradiography is the last step prior to selecting samples for SEM/EDS analysis. SEM work was done at Microvision Laboratories, a licensed commercial facility. Samples analyzed offsite were disposed of by the commercial laboratory. If samples were analyzed nondestructively, the remaining samples were maintained at WPI for storage, pending final disposal.

Autoradiographs provide important information on the number, intensity, and exact filter pad location of radioactively-hot particles. The filter pads which have positive gamma spectrometry or alpha/beta count results are mounted in a single layer onto double sided adhesive paper sheets. These sheets with dusts were then attached to 3 mm thick copper plates. Vehicle and HVAC air filters were prepared by cutting the filter media from their frames, and mounting the filter media on 3 mm thick copper plates. A sheet of blue-sensitive X-ray film was sandwiched with the mounted filters, and exposed in a dark photographer's box for seven days. After exposure, the films were developed in a commercial darkroom, using the Kodak® D76 process. Each autoradiograph included a predetermined blank area and a control area containing a known amount of fine carnotite dust, a naturally occurring uranium-containing mineral. The positive carnotite control

provided a check for the wet chemical X-ray film development process. The autoradiographs used MidSci® classic blue autoradiography film BX with a 72 hour exposure and D76 processing. See Appendix C for a full frame example of a positive autoradiograph.

The mounted filter assembly was transported to Microvision Laboratories of N. Billerica, MA. Areas of filters which caused exposures to the Xray film were removed from the mounts in a fume hood, and analyzed by SEM/EDS with a LEO/Brucher SEM/EDS system, using a lithium drifted silicon semiconductor X-ray detector. After SEM/EDS analysis, some samples were returned to WPI for storage and proper disposal.

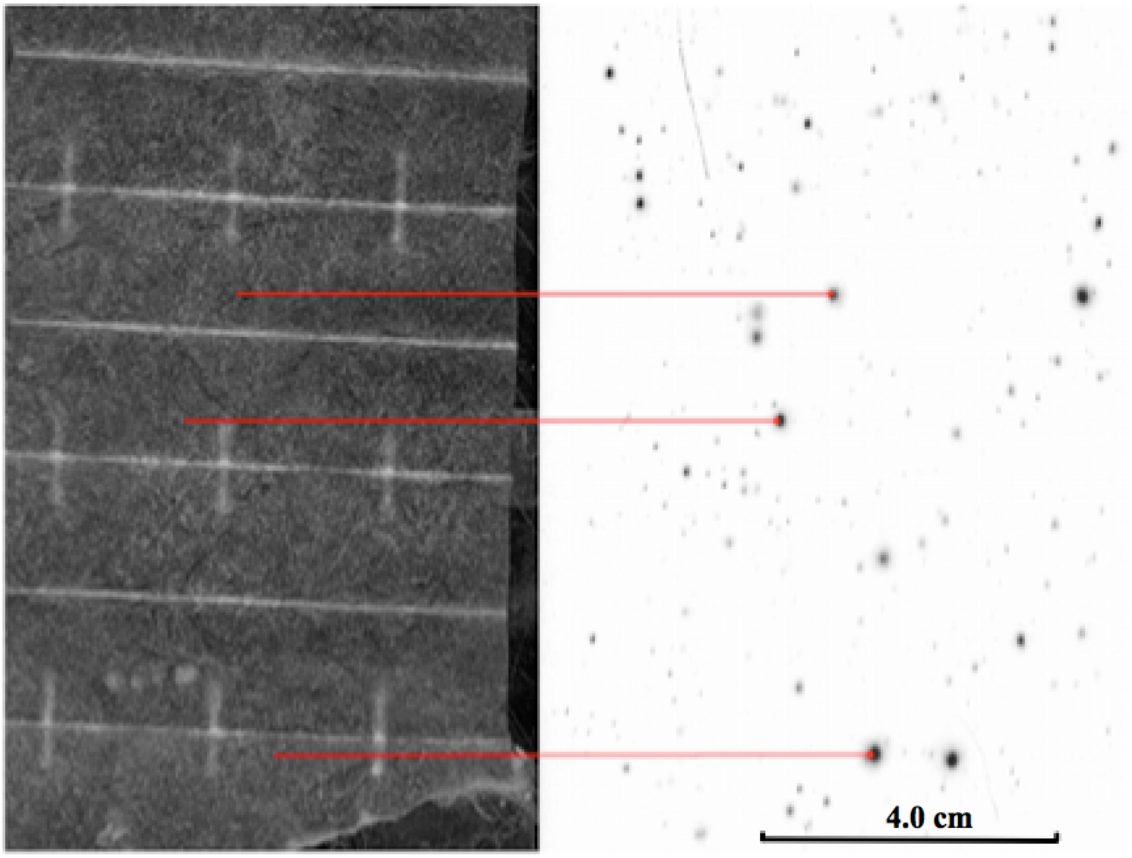

Fig. 2.9 Above: Tokyo vehicle air filter image (Left) and 7 day exposure autoradiograph (Right) Corresponding auto exposed points on the X-ray film are connected by red lines.

Disposal: To facilitate sample storage and disposal, minimum sample volumes were collected so that only the quantity actually needed for analysis was on hand. This analytical work was generally nondestructive, so arrangements for sample disposal were necessary. One function of the sample tracking spreadsheet was to identify samples which were radiologically-hazardous or which contained hazardous constituents. Samples loaned from other researchers were also logged in using this form, until the time of their final return. This form was also used to ensure that the project remained well below the exempt isotope quantities. Early samples had detectable ^{131}I. This does not represent a disposal issue, as this isotope has now fully decayed away. (see below, NRC Regulations)

NRC Regulations: § 30.18, (a) (e) Exempt quantities.

(a) Except as provided in paragraphs (c) through (e) of this section, any person is exempt from the requirements for a license set forth in section 81 of the Act and from the regulations in parts 30 through 34, 36, and 39 of this section to the extent that such person receives, possesses, uses, transfers, owns, or acquires byproduct material in individual quantities, each of which does not exceed the applicable quantity set forth in § 30.71, Schedule B.

(e) No person may, for purposes of producing an increased radiation level, combine quantities of byproduct material covered by this exemption so that the aggregate quantity exceeds the limits set forth in § 30.71, Schedule B, except for byproduct material combined within a device placed in use before May 3, 1999, or as otherwise permitted by the regulations in this part. This NRC exemption schedule is at URL http://www.nrc.gov/reading-rm/doc-collections/cfr/part030/part030-0071.html

The isotopes under study, and the respective schedule B, sec. 30.71 exempt quantity limits are radioiodine (^{131}I - 1,000 nCi) and radiocesium (137Cs - 10,000 nCi, 134Cs - 1,000 nCi).

This project resulted in the collection of air filtering media, soils and dusts requiring disposal. The total volume was below 0.5 liters. The total activity was well below the exempt quantities. In addition, a number of standard materials were analyzed to standardize the gamma spectrometers. These standards were already resident at WPI. No additional radioactive standard materials were purchased for this study. The primary standard material used to quantify samples from Japan was an Eckert & Ziegler Isotope Products multi nuclide standard source, dated Sept. 12, 2011, with 40.12 nCi of ^{137}Cs.

Review of preparation steps of the microanalytical procedure: Microanalysis is a set of analytical techniques designed to collect, separate, analyze, and speciate radionuclides in hot particles. Dusts, air filters, and fine surface soils or street dusts were collected using biased sample selection. Dust samples were sieved to pass a 150 micron screen if necessary. Samples were prescreened by total, alpha or beta counting, or by all three methods. Heterogeneous samples were split and the higher activity samples proceeded to final analyses. After analysis by gamma spectrometry, high activity samples were autoradiographed. Autoradiography was the last step to select samples for SEM/EDS analysis, which was done off campus at a licensed commercial facility. Blank, duplicate (10 percent rate per batch) and certified radiological standards were employed following good laboratory practices.

SEM/EDS analyses: During micrographic scanning, electron photomicrographs and EDS spectra of high z particles in dusts were reviewed by employing a Robinson® detector. This detector brightens the image of high z particles. All particles were mounted as a monolayer on a 25 mm OD Ted Pella, Inc., PELCO® tape tab-covered aluminum SEM stub. If necessary to improve particle conductivity, the samples were carbon or gold coated prior to SEM/EDS analysis. The coated and dust-covered SEM posts were scanned in a LEO/Brucher SEM/EDS system. The electron beam current was 0.60 nAmperes, accelerated at a voltage of < 0.5 to 60 keV. Secondary electrons ejected by

surface atoms were detected for imaging. Backscattered electrons were detected and provided imaging contrast determined by the atomic number of the nuclei with which it interacts. Characteristic X-rays are emitted by ions in excited states created by interaction with the electron beam. These characteristic X-rays were detected by the lithium drifted silicon semiconductor X-ray detector.

SEM/EDS does not distinguish between stable and unstable radioactive nuclei of a given element. Some elements are necessarily radioactive, such as polonium, uranium, thorium, and americium. Other elements such as cesium have both stable and radioactive isotopes. Given this limitation, suspect hot particles were analyzed by gamma spectrometry along with the SEM/EDS analyses. Some isotopes are primarily beta emitters, and are not amenable to gamma spectrometry due to the low abundance of their gamma emissions. For example, ^{90}Sr decays to ^{90}Y, a nearly pure beta emitter. Only SEM/EDS data was available for strontium and yttrium; therefore no activities or exposure rates are discussed in this study for nuclides of these two elements.

Archived sample materials are being held for additional testing pending acquisition of additional funding. These are the filter hot spots detected by autoradiography which have not yet been tested by SEM/EDS. The purpose of this future testing is to develop a statistically-valid data describing the geographic spread of radioactively-hot particles.

Results

Section 2.1: Atypically Radioactive Particles in Japanese House and Street Dusts

Eighty-five post-Fukushima accident dust samples were collected from northern Japan and analyzed. Of these, twenty-five were HVAC filter samples, twenty-four were automobile air filters, six were street dusts (accumulated surface soils) and thirty were vacuum cleaner bag or other dust samples. Samples were also screened for the presence of radioactively-hot particles. These were defined as individual dust particles with

significantly greater specific activity than the remaining bulk sample. The median total gamma activity in the eighty-five dust samples was 2.5 Bq g^{-1} +/- 1.6 Bq g^{-1}. The mean total gamma activity was 71.3 Bq g^{-1} with (sigma) = 335 Bq g^{-1}. Dusts could not be quantitatively removed from HVAC filters. As the removable fraction of material was in all cases less than 0.5 to 0.7 g, the specific activities for these samples were calculated at an assumed mass of 1.0 grams. This had the effect of lowering the specific activities of these samples by a modest amount. No corrections were made to data for decay. Activities at the time of release were generally higher at their time of origin and release.

The mean specific activity exceeded the median by a large margin due to the positive skew introduced by five out of the eighty-five samples that had atypically high activities. These high values also led to the relatively high relative standard deviation in the sample set, with the standard deviation exceeding the mean by a factor of 4.7 times.

One vacuum bag received from a home in Nagoya, Japan, yielded subsamples with no detectable radioactivity above background, despite a sizable amount of activity for the bag as a whole. This result was consistent with the presence of heterogeneously distributed radioactive contamination in the sample. By successive division and reanalysis, a single 1 cm by 2 cm glass microscope slide was prepared, with three microscopic dust particles mounted via double sided adhesive tape. This slide had 310 Bq of (efficiency-uncorrected gamma) activity, while the remainder of the dust sample was nondetect for activity above background count levels. The mass of the subsample was below the lowest detectable differential mass of the slide and the slide plus sample. The apparent mass was calculated by volume and reported composition. (See sec. 2.8) The slide containing high activity dust particles from Nagoya was further analyzed by SEM/EDS. The slide contained two microscopic radioactively-hot particles, while the entire remainder of this dust sample showed essentially no detectable activity above background. The two hot particles isolated from this individual house dust sample

accounted for all of the excess activity in the sample. This was the most extreme example of heterogeneity in the sample set.

The highest bulk sample specific activity from the eighty five sample set was 2.8 kBq g^{-1} +/- 53 Bq g^{-1}. The radioactively-hot particles from Nagoya were 9.0 and 8.5 microns in their longest dimensions, as measured by scanning electron microscopy (SEM). Sodium iodide gamma spectrometry of the two particles identified ^{226}Ra, ^{134}Cs, and ^{137}Cs as the major detectable gamma photon emitters. SEM analysis of the two hot particles found that these were aggregates of finer particles. X-ray microanalysis of the aggregates mapped varying concentrations of tellurium up to 48.0 %, cesium up to 15.6 %, rubidium up to 1.22 %, polonium up to 1.19 %, and dysprosium up to 0.18 %, as well as trace amounts of tin, lead, nickel, iron, and chromium. The combined specific activity of these particles was 5.2 Peta Bq kg^{-1}. Using the National Cancer Institute's RADRAT risk calculator, the excess lifetime lethal lung cancer risk for a two-year-old male child was 0.50 +/- 0.30 per 1000. This is a relatively higher risk case. The calculator gives a lower risk value for adults. (See sec. 2.8 for details) The specific activities of the complete sample set are tabulated below.

Table 2.1 Japanese Dust Sample Activities by Range

Specific activity	Number of samples
>1 Bq g^{-1}	23
1 to 10 Bq g^{-1}	35
>10 to 100 Bq g^{-1}	21
>100 to 1000 Bq g^{-1}	3
>1000 to 10000 Bq g^{-1}	2
>10000 to 100000 Bq g^{-1}	0
>100000 Bq g^{-1}	1

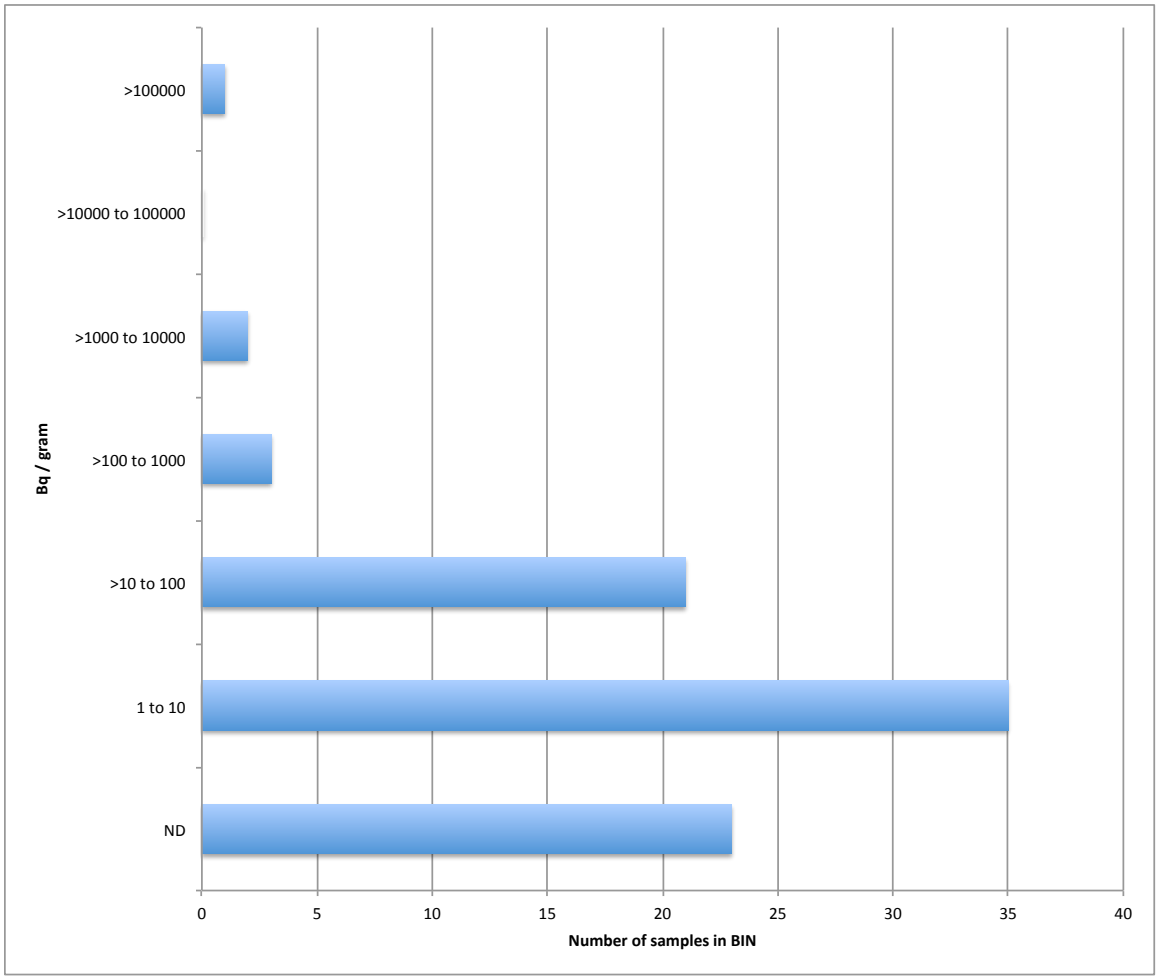

Fig. 2.10 Above: Dust Sample Activities in Bq g^{-1} by range

Five of eighty-five dust samples had activities two or more orders above the median. Twenty-seven dust samples exceeded 10 Bq g^{-1}.

Eighty-five samples in total
Median dust specific activity 2.5 Bq g^{-1} +/- 1.6 Bq g^{-1}
Mean dust specific activity 71 Bq g^{-1}, RSD = 335 %

Specific activities are by sodium iodide gamma well detector or equivalent, with appropriate geometric or counting efficiency normalization. Results are standardized against a known activity of ^{137}Cs calibrated in June 2011. Tabulated sample data are uncorrected for ^{134}Cs and ^{131}I decay.

Table 2.2 Japanese dust samples with highest specific activities

Nagoya single dust particle	+Specific activity 5.2 PBq kg^{-1}
Namie "Black Sand" street dust	Specific activity 1.50 MBq kg^{-1}
Iitate street dust/sediment	Specific activity 1.34 MBq kg^{-1}
Fukushima City car filter dust #J5	*Specific activity 0.169 MBg kg^{-1}
Tokyo apartment dust #5D	Specific activity 0.167 MBg kg^{-1}
Minamisoma street dust:	#Specific activity 0.089 MBq kg^{-1}
Tokyo apartment dust #3D	Specific activity 0.085 MBg kg^{-1}
Tokyo hotel balcony dust	Specific activity 0.081 MBg kg^{-1}
Tokyo car filter dust #J11	*Specific activity 0.059 MBg kg^{-1}
Tokyo street soil # 2	Specific activity 0.044 MBg kg^{-1}
Tokyo apartment dust #M1	*Specific activity 0.037 MBg kg^{-1}

The study dust samples with the highest specific activities are presented above, in descending order. These are substantially higher than the median dust specific activity of 2.5 Bq g^{-1} with a counting error of 1.6 Bq g^{-1}. "Street dusts" are outdoor accumulations of soil, dust and/or sediment without soil structure.

* Sample weight not quantitatively obtained. Assumed mass of 1.0 gram.
# Initially at > 0.1 MBg kg^{-1}, upon later retest sample had decayed to 0.089 MBq kg^{-1}.
+ Sample weight calculated from isolated micro-particle volume and composition

Results of Japanese air filter samples in Bq/filter

Fifty-five of eighty-five Japanese dust samples were air filter samples collected from homes and automobiles. These filters were all in use for some time during 2011. All filters were still in service on or after March 11, 2011, the date of the initial releases from the Fukushima Daiichi reactors. Filters were collected until July 2011. The entire air filter sample, or a known percentage of the sample, was analyzed by gamma spectrometry, using a fixed geometry. The total activity in Bq was calculated for each sample. All data were corrected for background counts and for geometry. No further correction was made for counting efficiency for samples standardized against a known quantity of ^{137}Cs.

As with the soil and dust samples, there was a wide variation in the results for the air filter samples. The data are presented logarithmically in the histogram in Figure 2.11. (Below) Samples were counted for 30 minutes each, with error rates approximated by the square root of the count rate. Total Bq per sample ranged from non detectable (less than 0.1 Bq per sample) to 2,792 Bq per sample. The standard deviation of the entire set of fifty-five samples is 384 Bq per sample vs. a mean of 76 Bq per sample. Without the three highest values of the set (2792, 628 and 327 Bq/sample) the standard deviation was 16.7 Bq per sample, with a mean of 8.3 Bq per sample.

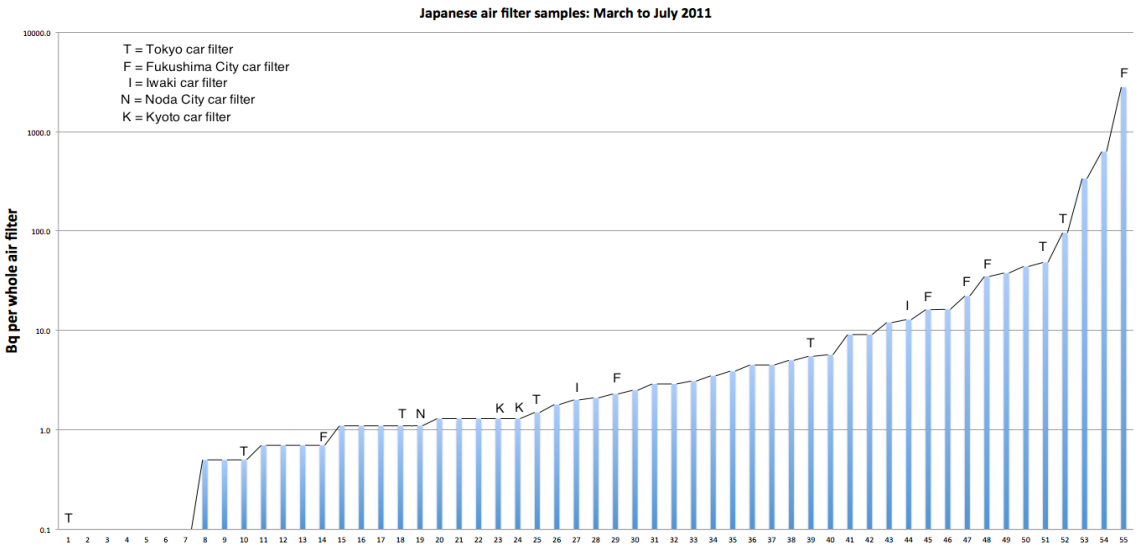

Fig. 2.11 Above: Log Bq/filter for Japan air samples collected 3/2011 to 7/2011

The primary radioactive isotopes detected were ^{134}Cs and ^{137}Cs. Radioactive ^{131}I had decayed by the time these air filters were analyzed.

The letter-labeled samples are automobile air filters. The remaining samples were collected from residential air filtering units in the greater Tokyo area. Based on available usage records for a limited number of samples, total volumetric air flows ranged from a few hundred cubic meters to no more than 5,000 cubic meters.

The analytical objective of the air filter sample collection was to collect a large number of radioactively-hot dust particles. A secondary objective was to produce a semiquantitative evaluation of the potential for airborne radioactive dust contamination. Given the potential inaccuracy of usage logs, particularly for unmetered equipment, no additional attempt was made to produce a quantitative examination of Bq per volume of air filtered.

An additional thirty-two US automobile air filter samples were collected and analyzed in the same fashion. The mean activity per US filter was 0.36 Bq per filter with a standard deviation of 0.26 Bq per filter. Almost all US filter activity was accounted for by naturally occurring nuclides of U, Th and K and their daughters.

Forty-five of the fifty-five Japanese air filter samples had a total activity greater than those of the US filters. The two sample sets were statistically different. The mean US filter activity was 0.36 Bq. One of the thirty-two US automobile filters had detectable radiocesium. In Japan, the mean activity was 76. Bq and 88 % of filters had detectable radiocesium. At the mean count rate, the error bars for the Japanese measurements are +/- 8.7 Bq. The mean US activity per vehicle air filter is plotted (Figure 2.12) on a log scale versus the activities of the Japanese air filter sample set on the following page.

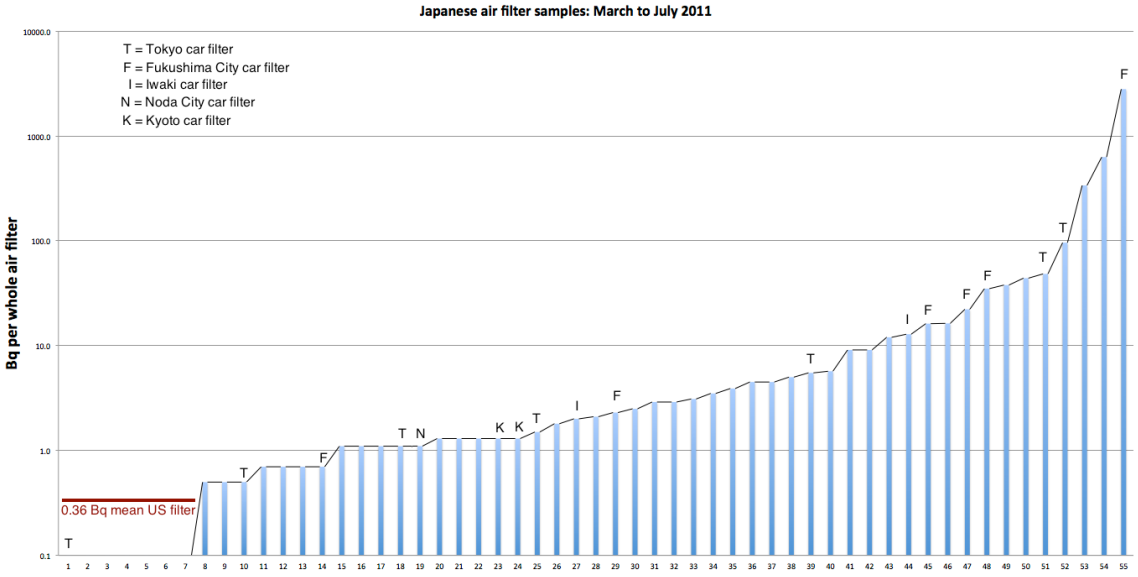

Fig. 2.12 Above: Total activity of Japanese vehicle air filters versus the mean total activity of thirty two US vehicle air filters.

Japan mean activity = 76.0 Bq +/- 8.7 Bq, n = 55
USA mean activity = 0.36 Bq +/- 0.1 Bq, n = 32

The mean of Japanese samples is more than 200 times greater than the mean of the US samples. This difference between the two sets of data was more than three standard deviations. Counting statistics alone understate the variation between the two sets of samples, given that the activity in the US filters was from naturally occurring progeny of ^{232}Th and ^{238}U. The activity in the Japan filters was primarily from ^{134}Cs and ^{137}Cs. The detection limit for combined ^{134}Cs and ^{137}Cs was 0.1 Bq per sample. While these isotopes were ubiquitous in the study area in Northern Japan, they were not detected in US air filter samples. Had the naturally occurring isotopes been subtracted from these results, the difference between the two sets would have been larger than 200 times.

It is important to note that the study area in Japan was deliberately selected, so that the probability of collecting hot particles would be significant. This study includes only three samples collected south of Tokyo, Japan. The remainder of the section describes results from the study area in Northern Japan in more detail. The full list of Japanese samples is in Appendix B.

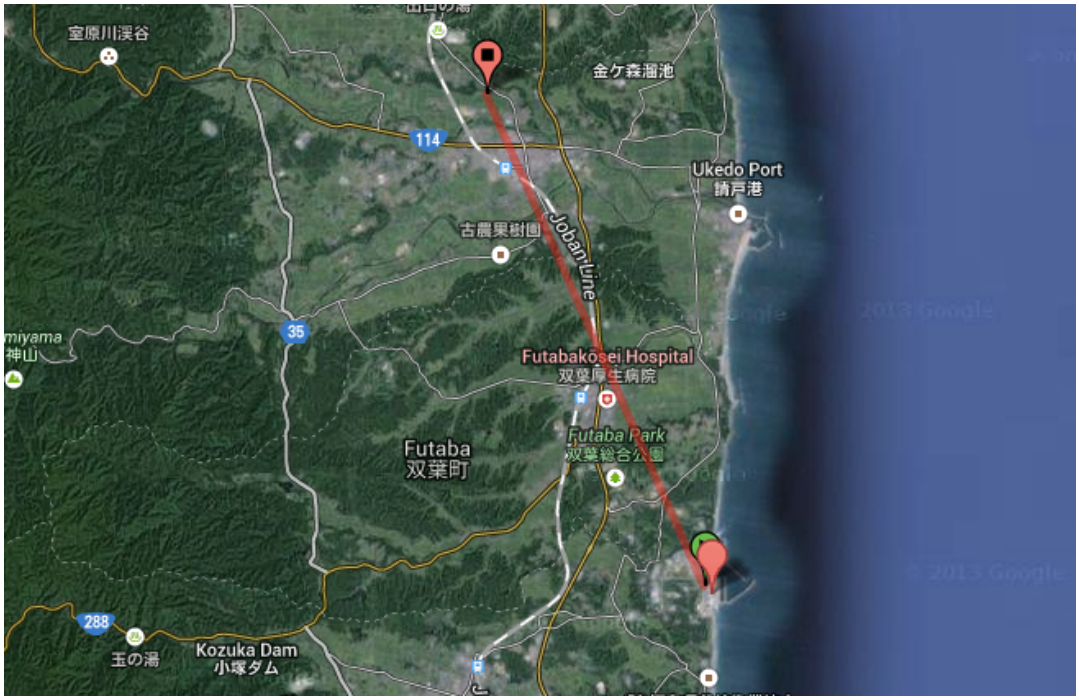

Section 2.2:

Namie, Japan
Distance from Fukushima Daiichi: 10.00 km

Namie, Japan, is on the Northern boundary of the 10 kilometer full exclusion zone around the Fukushima Daiichi plants. Sample collection and transport from Namie and from other areas in Japan was facilitated by local volunteers reached via social media, the Fairewinds Energy Education Foundation, and Safecast.

Safecast and other organizations reported the presence of unusually radioactive deposits of black sandy materials after the reactor accidents. While activity levels varied widely, in general the black sand registered activities one to three orders of magnitude higher than the activity levels in surrounding soils and dusts. In the general media, reports were made about this unusually hot material, causing public concern. (24, blog) These reports created some confusion, as there are nonradioactive minerals that have the same appearance. There are also naturally radioactive minerals that have the same appearance

as Japanese "Black Sand," and that go by the same colloquial name. Of these, the mineral monazite is the most common. The nation of India is known to have areas with sedimentary deposits of the calcium-phosphate-based thorium and uranium monazites. (23, Nair) While the Indian black monazite sand may look like the black sands found in Japan, the Japanese version is distinguished by its high radiocesium content.

A 300 mg sample of street dust was received from a location about 10 km from the Fukushima-Daiichi accident site. The street is in Namie-machi, Futaba-gun, Fukushima Prefecture. This is in the restricted zone, close to but just outside of the exclusion zone. The dust sample was analyzed by Scanning Electron Microscopy with Energy Dispersive X-ray analysis and by sodium iodide gamma spectrometry. An autoradiograph was prepared from the sample using blue-sensitive X-ray film. The sample contained 1,500 Bq g^{-1} of combined ^{134}Cs + ^{137}Cs as well as 0.3 Bq g^{-1} of ^{60}Co. The sample was uniformly radioactive when analyzed by autoradiography. Analysis by SEM/EDS found widely scattered particles of suspected fission products among larger aggregates of mineral matter.

In Japan, however, anthropogenic Black Sand would be expected to contain significant levels of ^{134}Cs and ^{137}Cs. These two fission products are overwhelmingly the most common environmental radioisotopes found in the wake of the Fukushima releases. Japanese Black Sand can be distinguished from natural monazite sands using sodium iodide spectrometry. Their spectra would be distinguished by the strong peak for ^{137}Cs decay at 662 keV in the case of Japanese Black Sand, vs. the characteristic X-rays and low energy gamma peaks related to the decay of ^{232}Th and ^{238}U progeny in monazites. On the following page are two sodium iodide gamma spectra with identical energy (x axis) scales. One is for the Namie Black Sand. The other is a Ganges Valley, India, sediment known to contain thorium/uranium monazite "black sands." The clear radiocesium (661 and 795 keV) versus uranium/thorium progeny energy lines are clearly visible, making it possible to distinguish these two distinct but similarly-named materials.

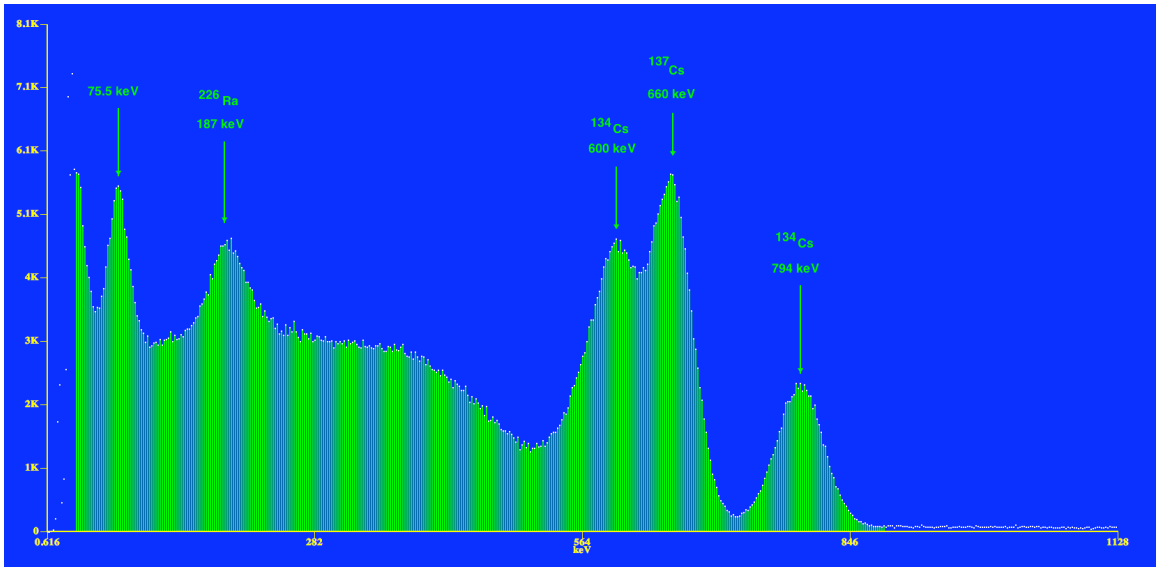

Fig. 2.13 Above: NaI gamma spectrum of Namie street dust with "Black Sand," showing radiocesium peaks, Compton bands, and X-ray peaks. The peak marked ^{226}Ra was absent in higher resolution scans and is likely due to Compton scatter. (DPM = CPM/0.30)

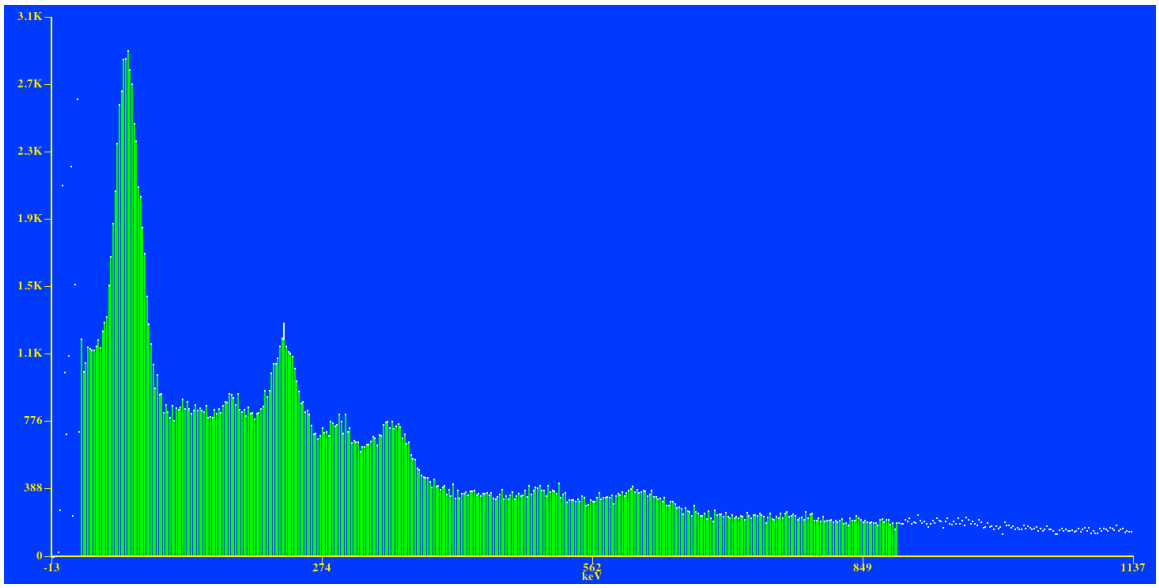

Fig. 2.14 Above: NaI gamma spectrum of Ganges Valley, India, monazite sands showing uranium and thorium low energy and X-ray peaks. (DPM = CPM/0.30)

Namie, Japan, Black Sand sample: A portion of the Namie dust sample was analyzed by SEM/EDS, which does not distinguish between stable and unstable (radioactive) nuclei of a given element. For certain elements, including uranium, thorium, and plutonium, the known isotopes are radioactive. For other elements, including lead, yttrium, and many rare earths, the known isotopes are both radioactive and stable. For elements with both stable and radioactive forms, gamma spectrometry provides confirmation of the presence of radioactive isotopes in bulk particulate samples. In this analysis, initial gamma spectrometry analyses were performed with an Amptek® CdTe gamma detector and MCA, scanning the range from 10 to 2060 keV, and equipped with a copper/lead multilayer shield and an Ortech® 2 inch NaI gamma detector and lead shield.

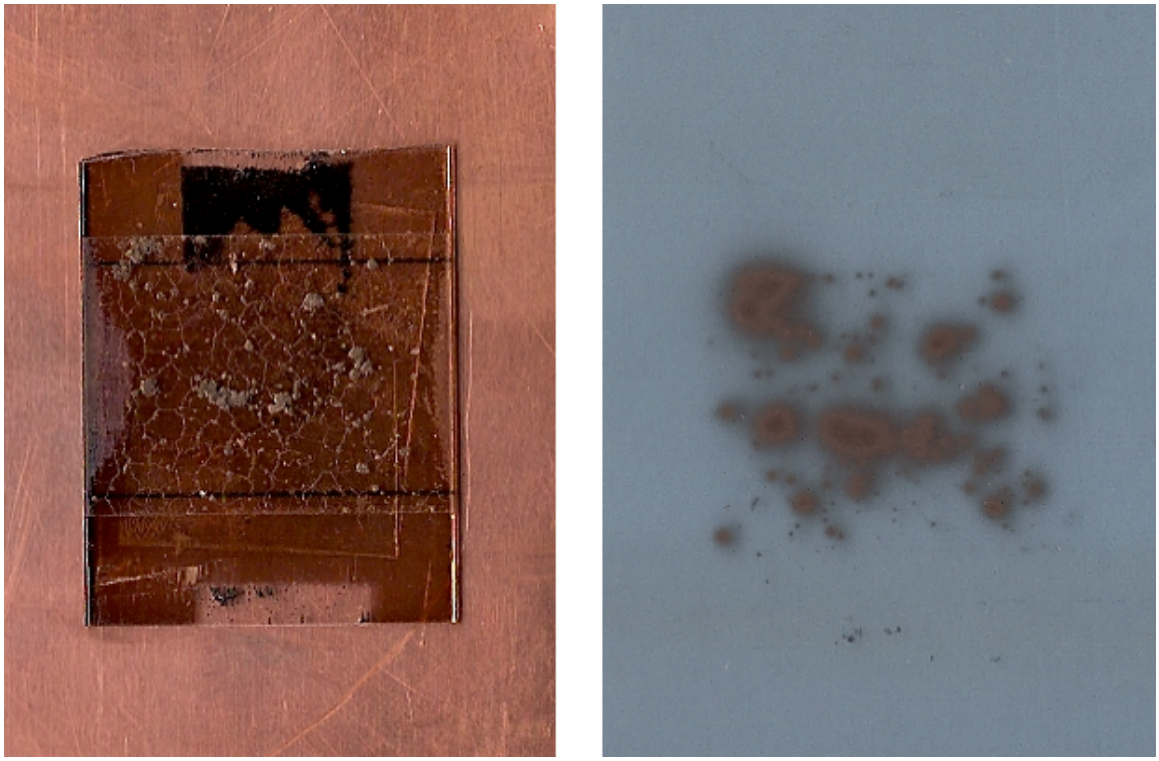

Fig. 2.15 Above: Digital image of slide and autoradiograph of Namie dust sample X-ray film autoradiograph (right) and same scale true color scan (left)

The sodium iodide (NaI) spectrometers has sufficient sensitivity to detect the low level activities often found in environmental samples. The NaI detector's efficiency curve and energy resolution are sufficient to detect low levels of the environmentally significant isotopes including ^{241}Am, ^{134}Cs, ^{137}Cs, and ^{60}Co. Plutonium isotopes are not distinguishable by NaI and were analyzed using CdTe or GeLi gamma spectrometry. For the samples from Japan described in this section, no plutonium isotopes were detected above 0.1 Bq per sample.

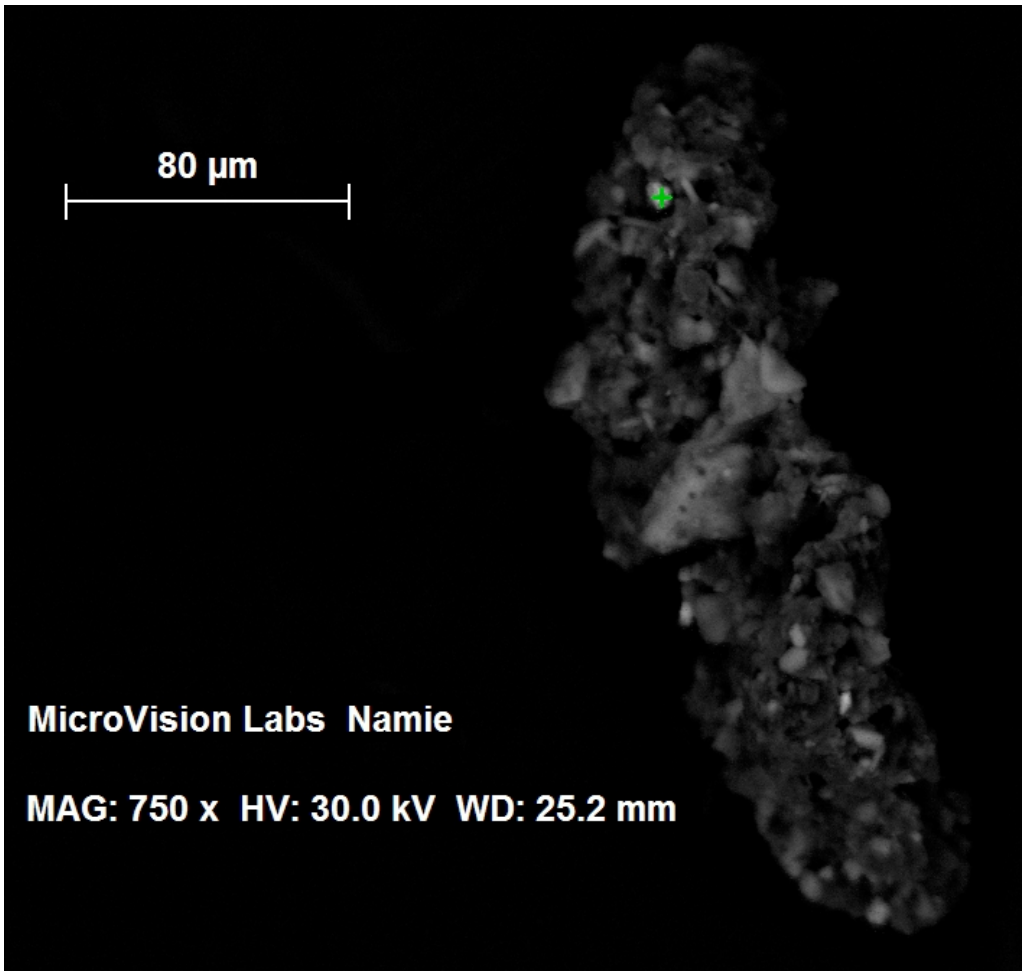

Fig. 2.16 Above: Scanning Electron Micrograph w/ Robinson® Detector image of a lead particle imbedded in a larger aggregate particle in the Namie sample.

Figure 2.17 shows the percent elemental composition of a lead particle embedded in a larger aggregate particle Figure 2.16. The origin of this particle is uncertain; however both lead and titanium are commonly found in street marking paint. Additional particles also contained lead and chromium, both of which are also components of lead chromate traffic marking paints.

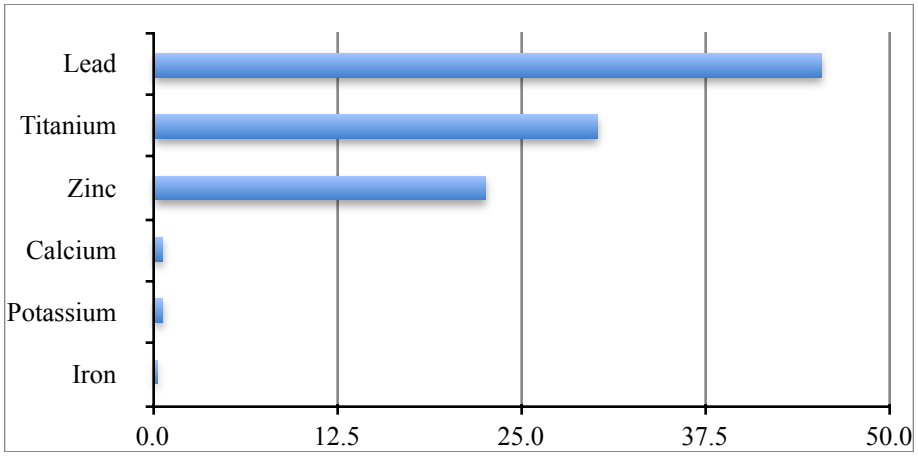

Fig. 2.17 Above: Percent composition for aggregate particle in Fig. 2.16

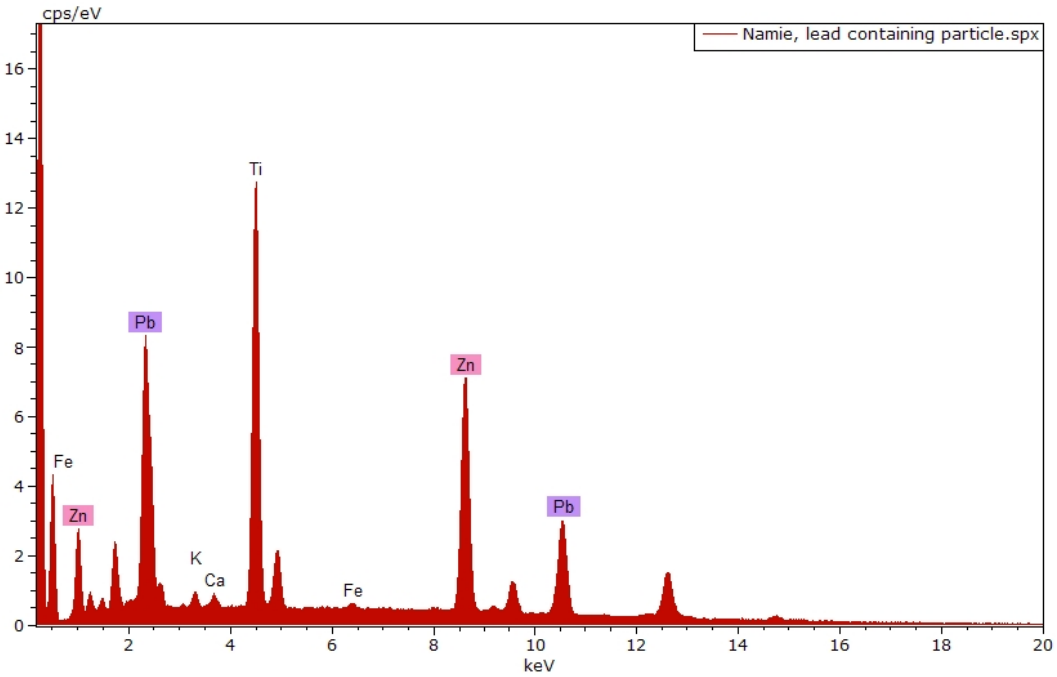

Fig. 2.18 Above: SEM/EDS spectrum for the same particle.
(See cps to mass data in Appendix E)

The Robinson® Detector image in Figure 2.19 shows high Z elements in a larger aggregate. The calcium-phosphorous rare earth composition in the highlighted subparticle is consistent with monazites. Nevertheless, the majority of radioactivity in the aggregate as a whole is due to ^{134}Cs and ^{137}Cs. NaI gamma spectrometry was used to identify the isotopes responsible for the aggregate's activity.

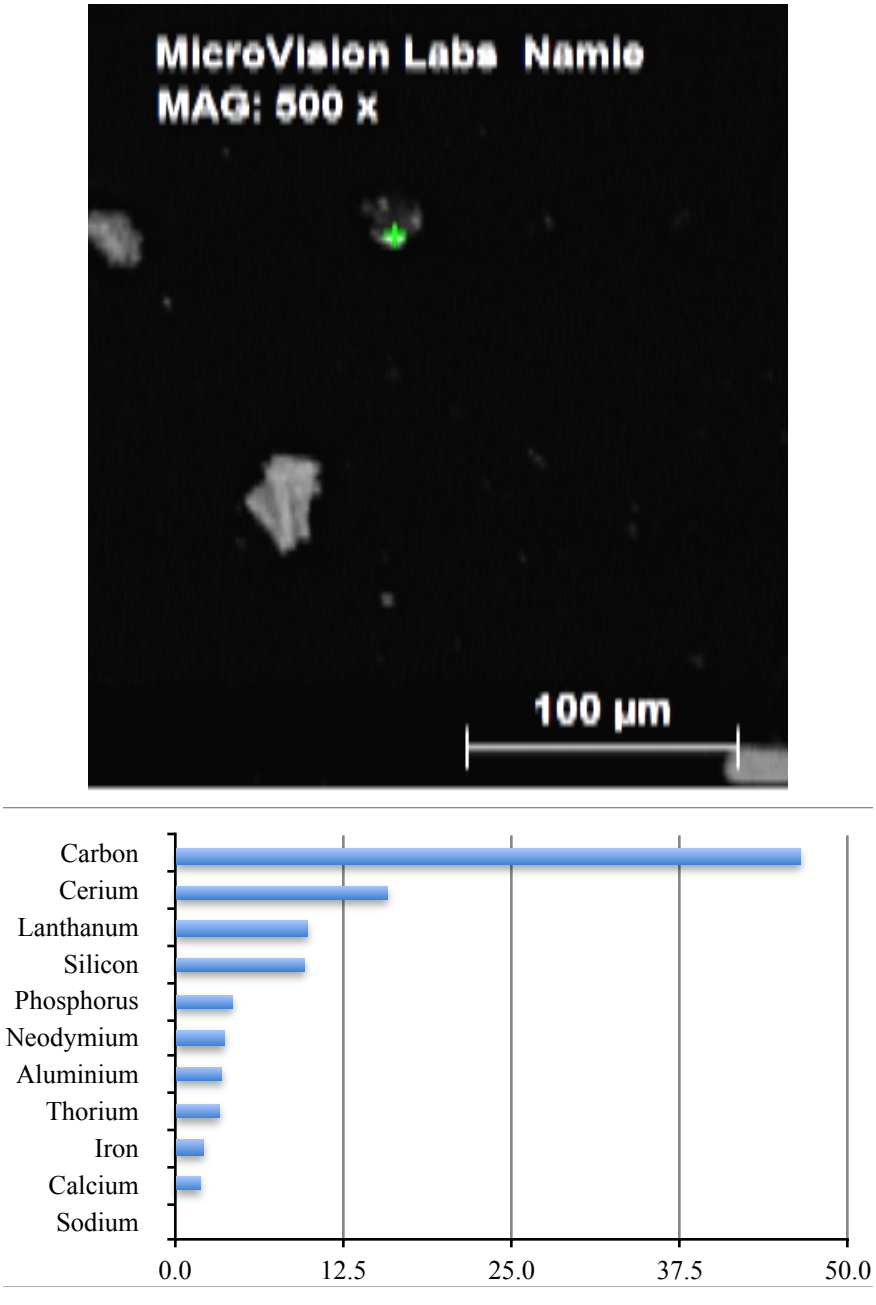

Fig. 2.19 Above: Elemental composition of a thorium particle embedded in an aggregate

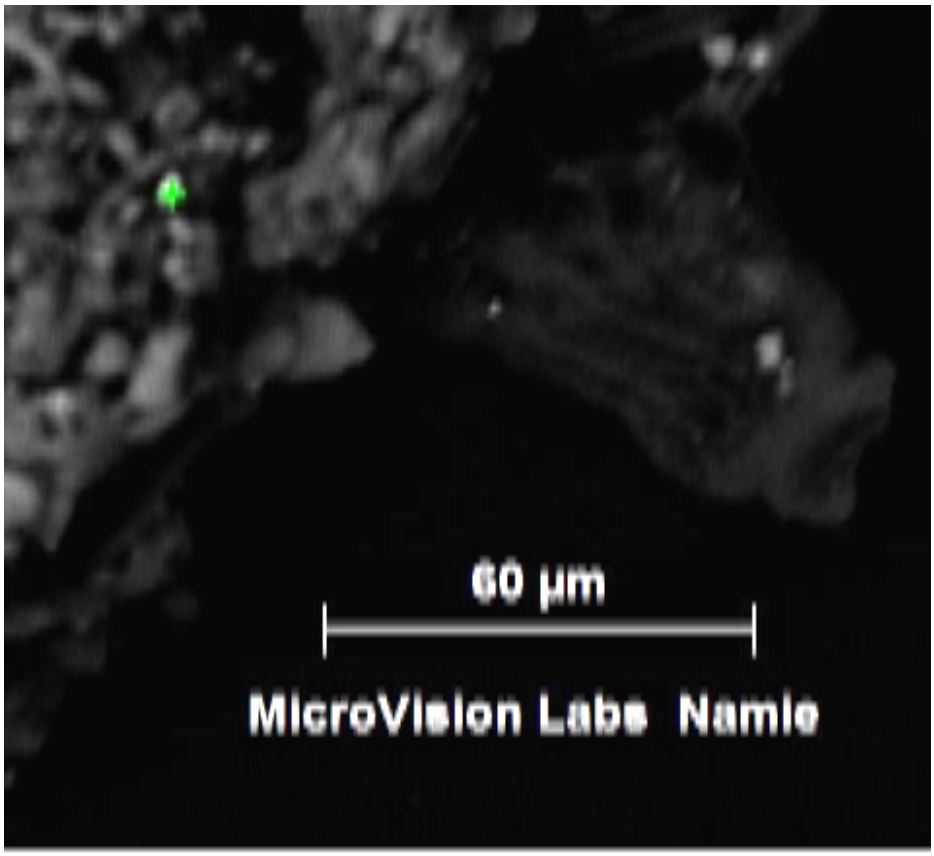

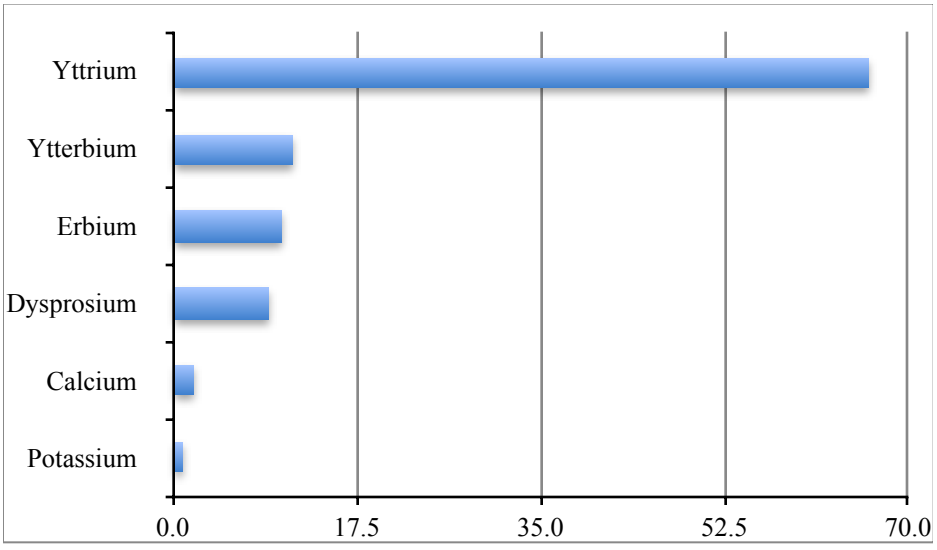

Fig. 2.20 Above: Scanning Electron Micrograph w/ Robinson® Detector image of a yttrium-lanthanide particle embedded in a larger aggregate; with a chart showing percent elemental composition of the particle.

Namie, Japan, Results and Discussion

This analysis focused on fission products that are released from damaged nuclear fuels. The most common fission products found in radioactively-contaminated dusts from Fukushima Prefecture include ^{134}Cs and ^{137}Cs. Nuclear reactors tend to produce both heavy (atomic weight 125 to 155) and light (atomic weight 80 to 110) byproducts. These include light radioactive isotopes of the elements yttrium and silver, plus the heavier isotopes tin, antimony, cesium, cerium, neodymium, and lanthanum. All of these were detected in this dust sample by SEM/EDS, in the form of tiny particles on the order of 10 microns in size. Examples of the SEM/EDS-detected particles in the small (100 milligram) dust sample included thorium-containing rare earth particles, lead titanate, and yttrium lanthanide particles. These were in the 2 micron to 10 micron size range.

The sample of street dust was also analyzed by sodium iodide gamma spectrometry. (See Figure 1) An autoradiograph was prepared from the sample. Gamma spectroscopy detected 153 Bq total of radioactive cesium (^{134}Cs + ^{137}Cs) and uranium daughter isotopes in the 100 milligram sample. This is equivalent to 1530 Bq, per gram or 1.5 MBq per kg. ^{60}Co was present at 0.3 Bq per gram.

The dust sample had numerous particles containing mostly lead, yttrium, various rare earths, and thorium. Some of these lead and rare earth particles were in the respirable size range, measuring only 1 or 2 microns in size.

This dust was collected just a few hundred feet outside the exclusion zone around Fukushima Daiichi. Occasionally observers have reported small deposits of windblown black sediment that measures higher than normal for radioactive forms of cesium and other radioisotopes. This is the first time we have examined a sample that was clearly distinct from surrounding soils and dusts, by virtue of its high radioactivity. The sample appeared to have the highest ^{226}Ra levels of the approximately 200 dust and soil samples

analyzed in this study. The result was based only on sodium iodide gamma spectroscopy. SEM/EDS did not confirm the presence of radium. Alternatively, the 188 keV gamma peak may be due to Compton scatter.

This analysis is a limited one, since the subject is a single (and small) dust sample. This sample is not representative of the Namie region as a whole. This data demonstrates that isolated street dusts can reach radiation levels well in excess of their general surroundings.

There is insufficient data in this single sample to explain why a small amount of street sediment or dust was so contaminated with radioactive substances compared to surrounding materials. Clearly some environmental mechanism has allowed this more radioactive material to remain segregated, rather than dispersing into the soils or being washed away by rains. This analysis suggests that at least some small localized radioactive hot spots can persist, despite the passage of months and years since the Great East Japan earthquake and the subsequent radiation releases.

The author gratefully acknowledges the efforts of Mr. Jun Ohnishi, who provided the sample for this analysis.

Section 2.3:

Minamisoma
Distance from Fukushima Daiichi: 25 km

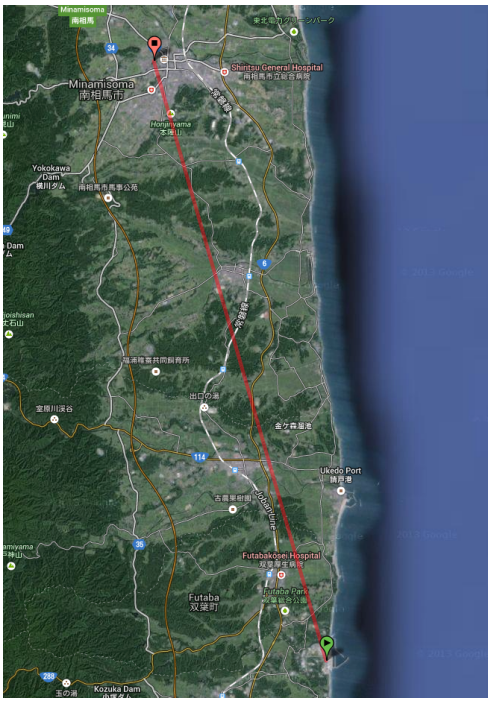

Fig. 2.21 Above: (L) Approximate sample locus (R)
Safecast photo showing Minamisoma sample in the field.

A sample of unusually high specific activity was received from Mr. Azby Brown at Safecast. The sample consisted of street dust and/or surface water runoff sediment from a road side in Minamisoma, Japan. (36, Safecast) The 2.37 g sample was collected on September 4, 2013 by Safecast on Japan Route 120, at latitude 37.5197 and longitude 140.9786. The ambient air dose at 1 m altitude was measured at 0.33 μSv/hr. The laboratory measurement of the material found a gamma specific activity of 0.089 MBq kg^{-1}. This material was the second example of "Black Sand" a.k.a. "black substance" received for this study. Like the Namie sample discussed in Section 2.2, ^{134}Cs and ^{137}Cs were the primary radioactive isotopes quantified by gamma spectroscopy.

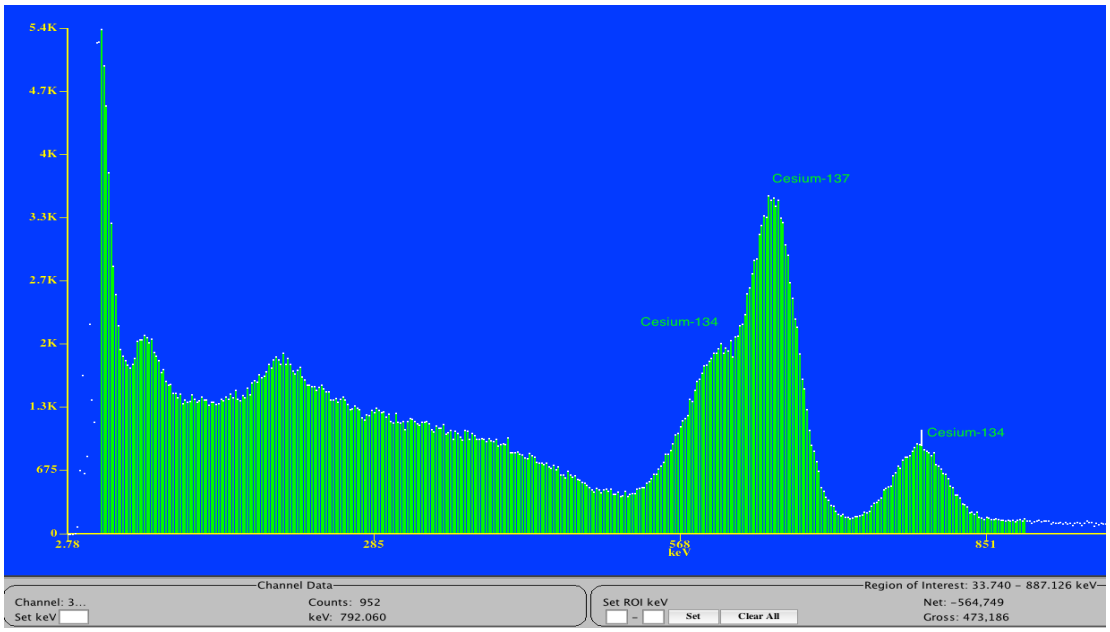

Fig. 2.22 Above: NaI well-type gamma detector spectrum, Minamisoma sample, (DPM = CPM/0.30)

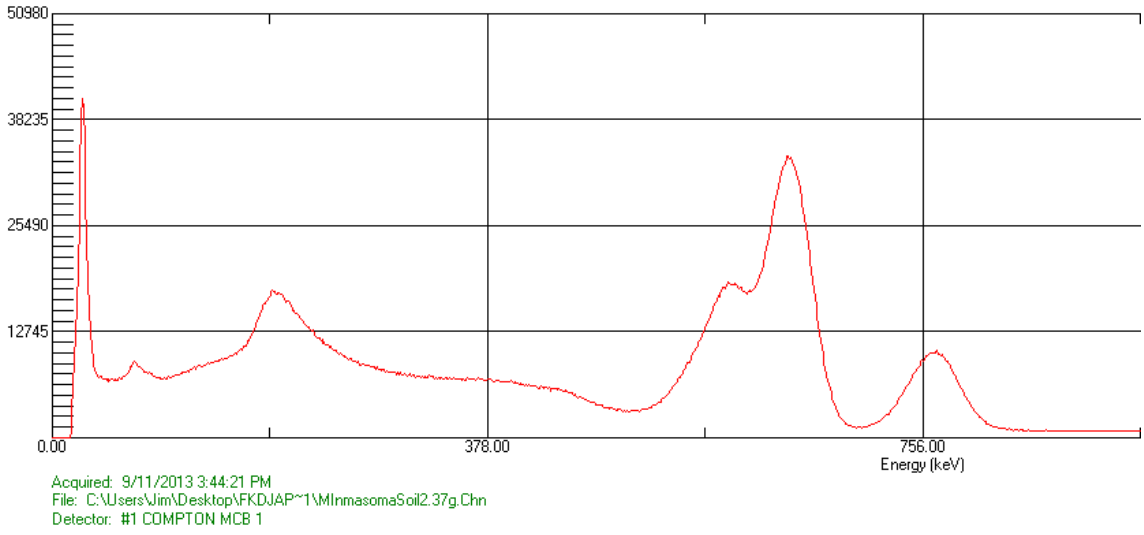

Fig. 2.23 Above: Same sample with its gamma spectrum from a 2 inch NaI flat disk detector. The low energy bands show a somewhat different Compton scatter while radiocesium is essentially unchanged. This is further evidence that radio cesium isotopes are the primary source of radioactivity in the sample.

Section 2.4:

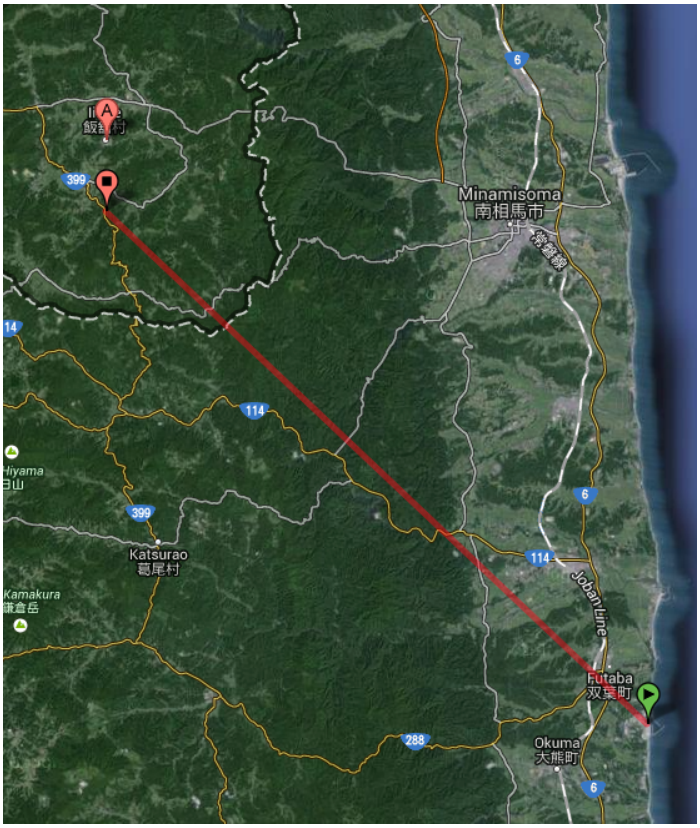

Iitate

Distance from Fukushima
Daiichi: 36 km

This surface soil of unusually high specific activity was provided by Safecast. It was collected on September 4, 2013. The collection site was at latitude 37.6250 and longitude 140.7413. This is Rte 399, in a parking lot on mountain road, at the barricade to the exclusion zone. The sample donor measured the ambient air dose at 1 meter above ground surface as 1196 CPM (3.62 µSv/hr) using a *bGeigie* networked geolocating survey meter. The sample appeared to be a wind or waterborne surficial soil material. This Iitate sample had a specific activity of 1.34 MBq kg^{-1} when measured in the laboratory using sodium iodide gamma spectroscopy. This is the third highest specific activity among those in the overall sample set, and is another example high activity material known in Japan as "Black Sand". The sample run is logged by Safecast at: https://api.safecast.org/en-US/bgeigie_imports/12583

Given that the sample collection date is about 2.5 years after the initial release, more than 50 % of the ^{134}Cs (half life 2.06 years) that would have been in the material at the time of release has decayed away. Other isotopes have even shorter half lives, such as ^{131}I, with a half life of 8.02 days.

The two gamma spectra below illustrate this difference. The Iitate sample measured in 2013 is the topmost of the two spectra below. A similar soil sample collected a few kilometers south of Iitate and measured in April 2011 is at the bottom. The central energy peak at 661 keV for ^{137}Cs is dominant in the 2013 spectrum, while the ^{134}Cs and ^{137}Cs peaks are nearly at a 1:1 ratio in the 2011 measurement. As previously stated, no attempt is made to decay-correct data in this report. Actual dates of all measurements are given in Appendix B.

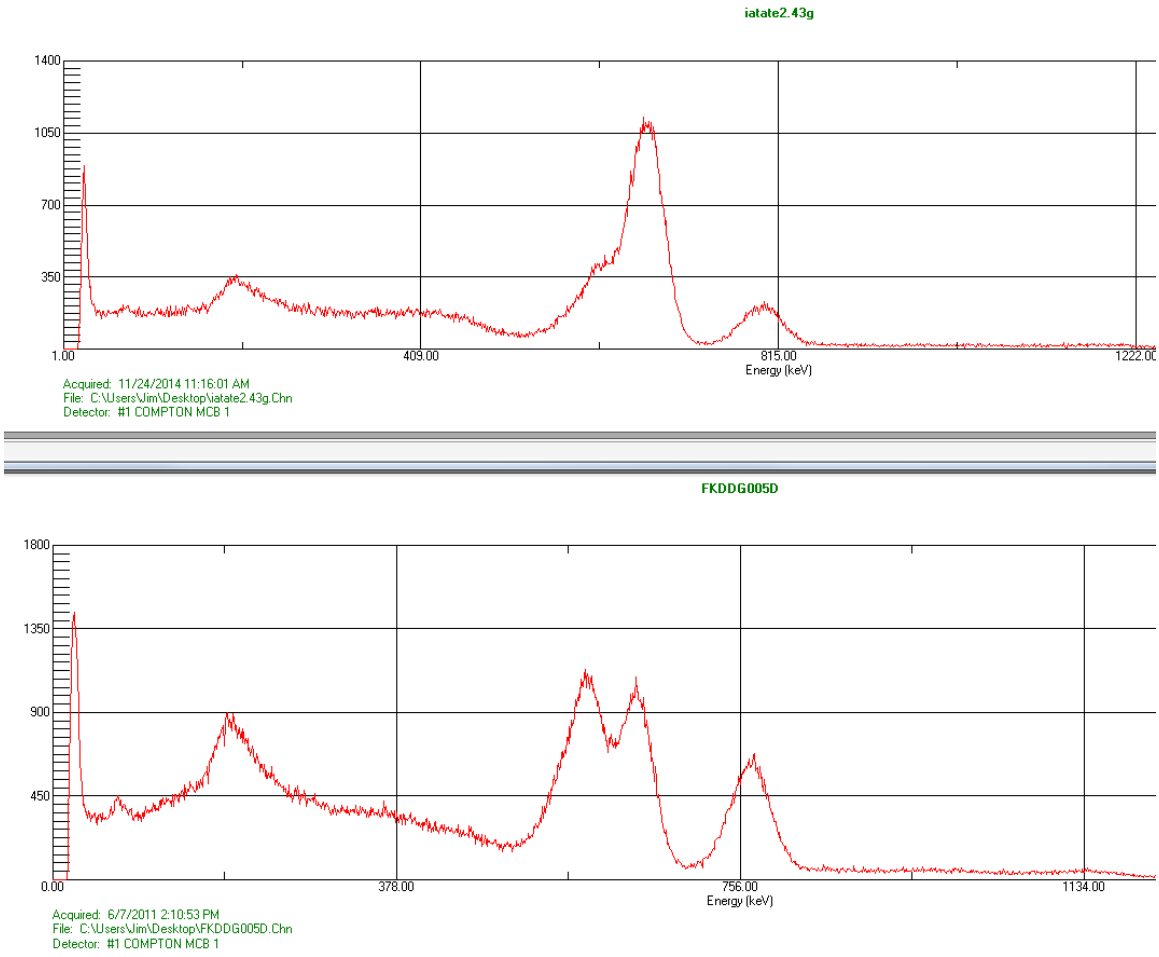

Fig 2.24 Above: Apparent decay of ^{134}Cs in Iitate sample compared to an April 2011 soil sample of similar type. While differential distribution of cesium isotopes is certainly possible, these spectra show cesium isotope ratios typical of the entire study sample set. The cesium isotope ratios are predominantly a function of the passage of time since 3/11/11, rather than of geographic distribution within Northern Japan.

Section 2.5:

Koriyama, Fukushima Prefecture
Distance from Fukushima Daiichi: 61 km

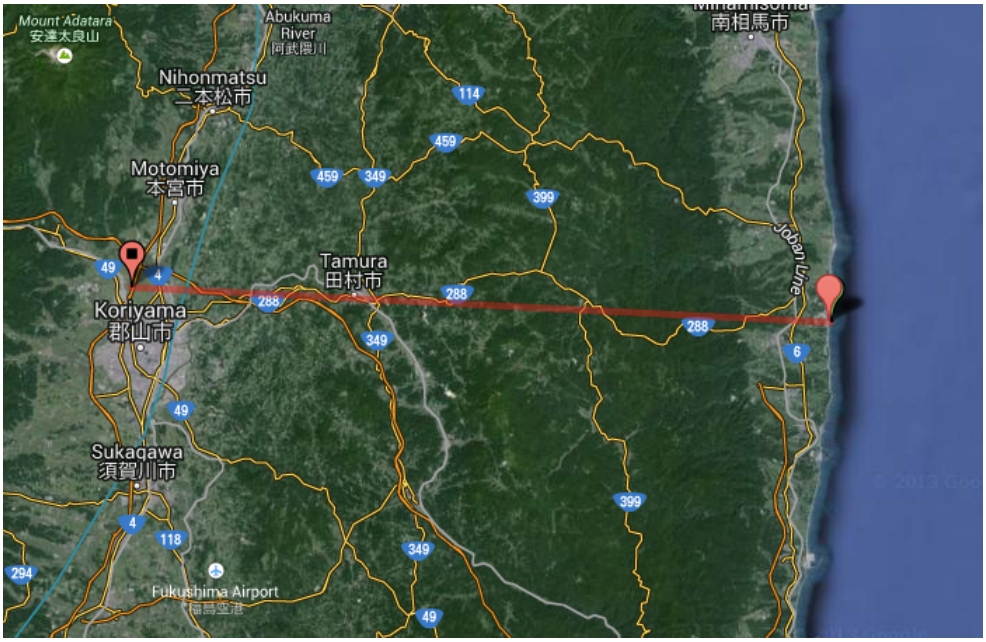

Childrens' shoes can pick up soil and dusts from the areas where the children walk, play, or study. A set of shoes were collected from parent volunteers in the US and Japan, and the shoes were examined for the presence of gamma emitting nuclides. Eighteen childrens' shoes were collected; six from Koriyama, Fukushima Prefecture, Japan, two from Tokyo, Japan, and eight from Worcester, MA, USA. Japanese sample donors self-report that, upon removal, shoes are commonly left outside of living spaces, and that it is common to leave one's shoes outside of the living space of the home.

Shoes were first wanded with a Victoreen alpha, beta, gamma counter with a pancake-type scintilator probe. Surface activity levels at the laces were noted in a one hour integrated count. Activities are reported as uR/hr. against a ^{63}Ni standard.

The shoes were then prepared for sodium iodide gamma spectral analysis by separating the toe, sole, laces and uppers. Each component was analyzed separately due to detector

volume limitations. Results were reported as total ^{134}Cs and ^{137}Cs activity for the combined shoe subsamples. The mean total radiocesium activity for the Japanese shoes was 1.18 nCi per shoe with a standard deviation of 0.79 nCi per shoe. The shoes worn in Tokyo had total activities of 0.2 and 0.39 nCi. The eight USA shoes analyzed in an identical fashion had no detectable radiocesium, with a detection limit of 0.01 nCi per shoe. The results of the initial survey probe testing of childrens' shoes are below.

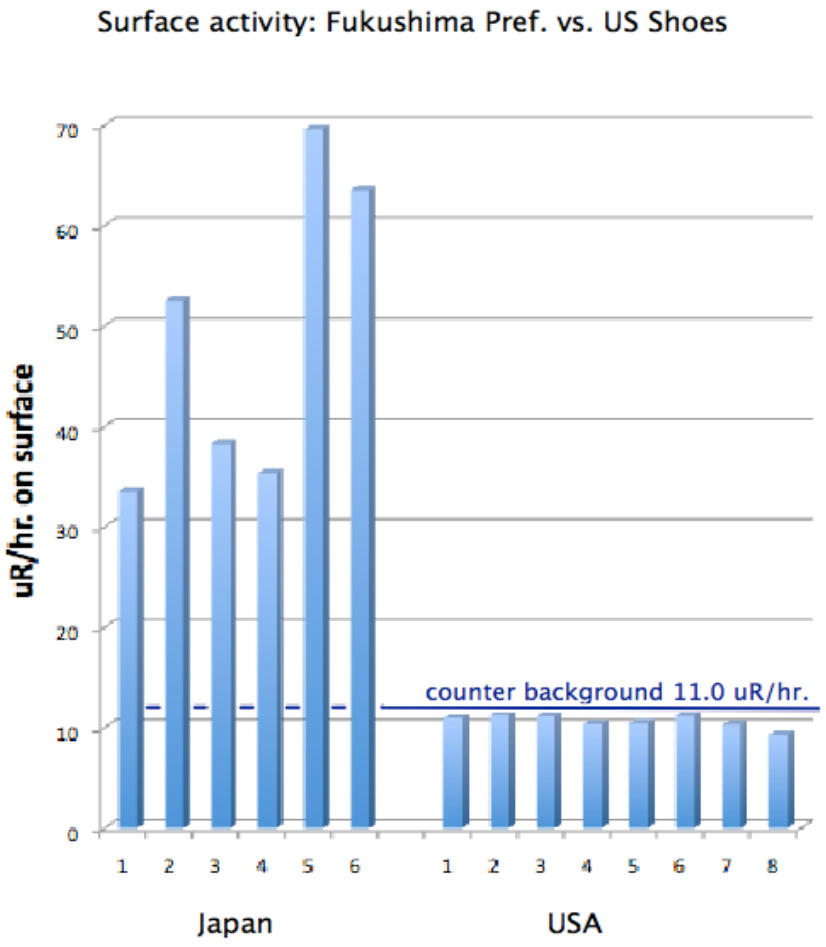

Fig. 2.25 Above: Total activity data in
Fukushima Prefecture vs. US child shoes

In addition, gamma spectral testing of a May 12, 2012 bulk house dust sample from a shoe sample-donor home in Koriyama found 1.12 Bq g^{-1} of ^{134}Cs and 1.23 Bq g^{-1} of ^{137}Cs, both at +/- 0.34 Bq g^{-1}. No other contaminant isotopes were identified in the dust.

Section 2.6:

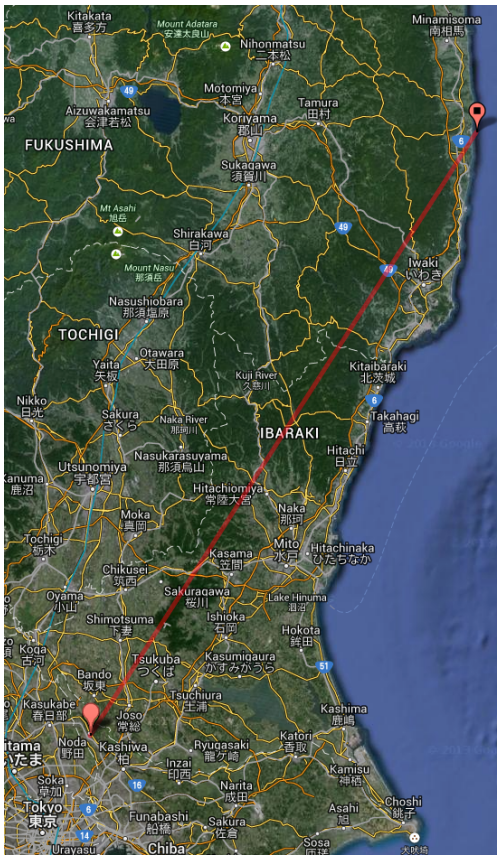

Noda City
Distance from Fukushima Daiichi 197 km

Three air filters were received from Noda City. These were a home air filter and two automobile engine filters. One vehicle was used primarily within Noda City, and the second was used to drive between Noda City and Tokyo. These samples cover the period between June and midSeptember 2011. The mean radiocesium content was 7.9 Bq per filter +/1 2.6 Bq per filter.

An autoradiograph was prepared from one quarter of the automobile engine air filter media and exposed for seven days to X-ray film. On development a single positive response was found in the autoradiograph. The portion of the original filter media corresponding to the autoradiographically-positive location was removed from the remaining autoradigraphically-negative portion and was analyzed by sodium iodide gamma spectroscopy. The subsample contained 36.9 +/- 6.1 pCi ^{134}Cs and 32.9 +/- 5.7 pCi ^{137}Cs. This is equivalent to 1.37 +/- 0.23 Bq ^{134}Cs and 1.22 +/- 0.21 Bq ^{137}Cs. No other contaminant radioisotopes were detected in the autoradiographed sample. The autoradigraphically-positive subsample was archived for future SEM/EDS testing. (See autoradiograph on the following page.)

Twelve similar house air filters were also received from a single address in Noda City between June 29, 2011, and Feb. 1, 2013. These results are on the second page following.

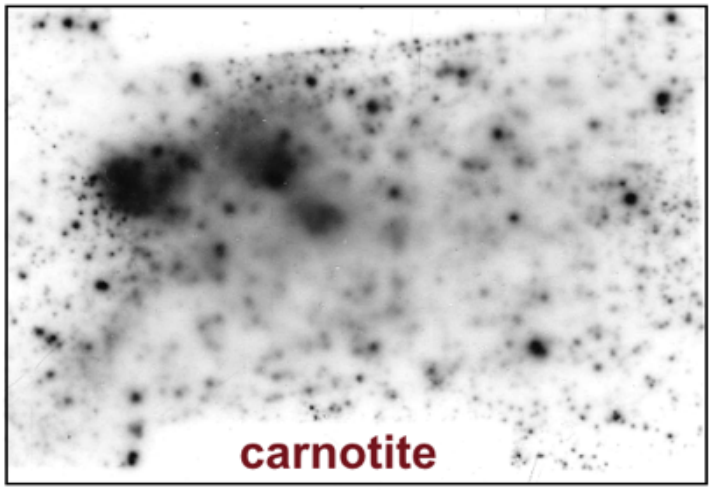

width = 10 cm

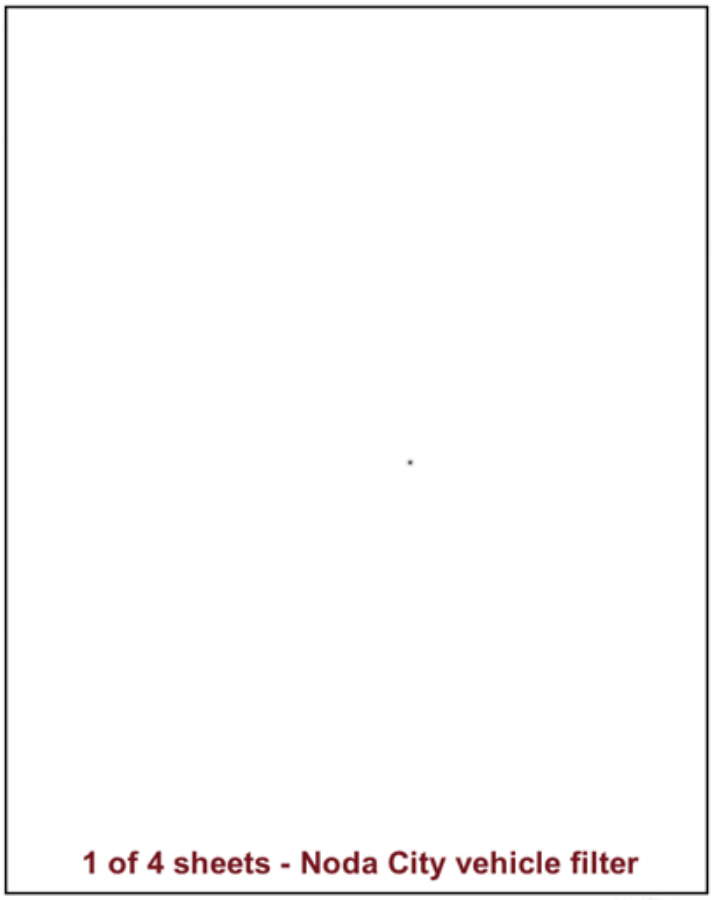

Noda City, Japan ~200 km distant car air filter used for 2 mos. @ 600 M^3/mo.

Cesium-137 32.9 pCi

Cesium-134 36.9 pCi

No other radioactive isotopes detected

Fig. 2.26 Above: Autoradiograph of Noda City car air filter (bottom) vs. control sample of carnotite dust. The Noda City filter was autoradiographically negative.

The data plotted below are for a set of twelve similar house air filters were received from a single address in Noda City between June 29, 2011, and Feb. 1, 2013. These are reported in kBq per m^2 of filter material. Note that these samples were found to contain ^{60}Co. This isotope was detected in less than 10% of samples from Northern Japan. The maximum values among this set are for the June 2011 samples. Each filter was used for approximately one month prior to ship to this study.

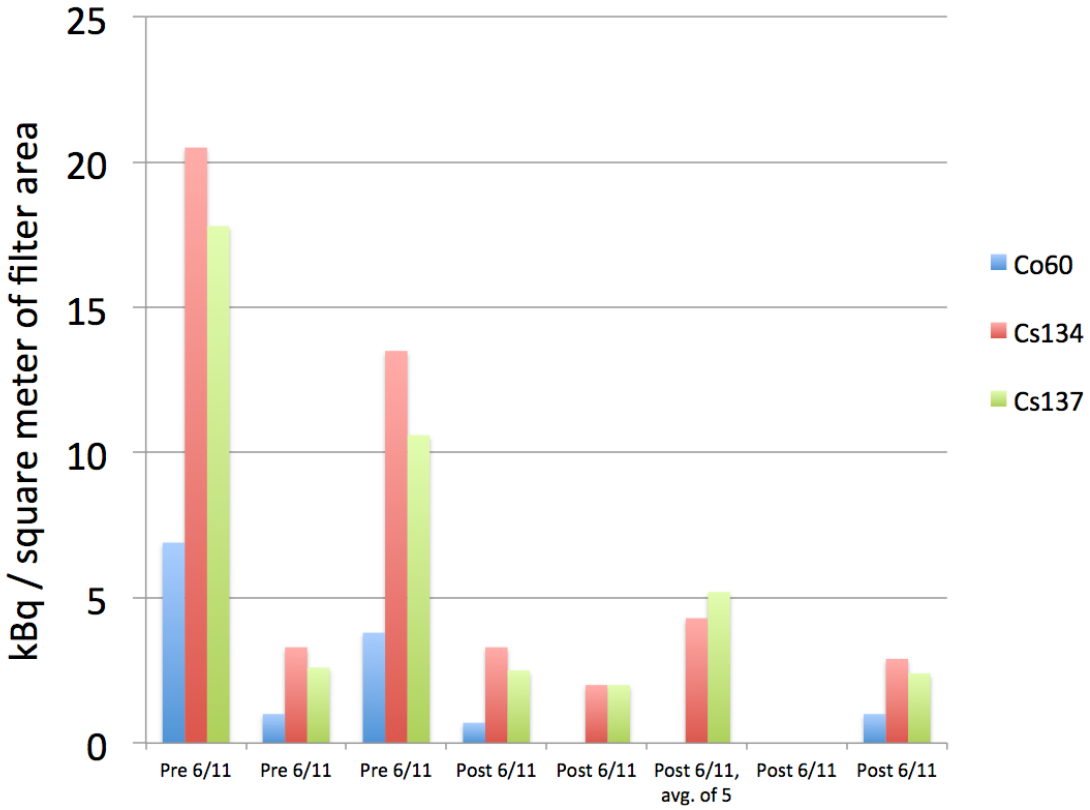

Pre June 2011 mean = 26.7 kBq/m^2, SD = 19
Post June 2011 mean = 7.1 kBq/m^2, SD = 4.5

Fig. 2.27 Above: Time trend in air filter sample activity
Data based on NaI gamma spectroscopy

Section 2.7 :

Tokyo, Japan
Distance from Fukushima Daiichi: 162 to 223 km

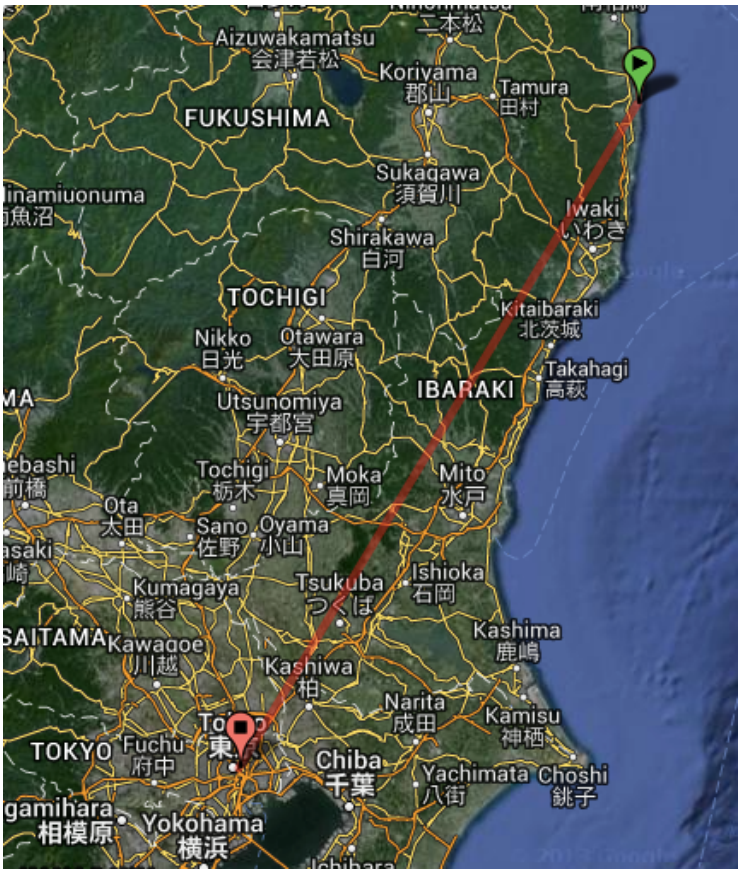

Most of the samples received during the first weeks after the Great Northern Japanese Earthquake and the ensuing Tsunami came from the Greater Tokyo area. The importance of these early data are two-fold. First of all, sample donors were able to receive critical information about the state of potential radiological contamination in their area. Dust hygiene has been an important part of public health concerns. Dusts containing lead paint particles, Hanta virus, asbestos, dust mite feces, or nonradioactive industrial toxins have presented exposure hazards to the public at innumerable locations. Early data about detections of radiologically contaminated dusts allowed sample donors to make hygiene changes designed to reduce potential dust exposure, and by extension, exposure to radiologic hazards. EPA has routinely engaged families to reduce dust intake by removing shoes, using door mats, hand washing, and other methods. These may appear to be trivial changes, but they can help reduce dust exposures. (See http://www2.epa.gov/lead/protect-your-family) The second item of importance is that early samples still retained significant quantities of the critical fission product isotope ^{131}I. This nuclide has a short 8.02 day half life. All ^{131}I-positive samples were received for this study in early April 2011, less than four half lives after the original accidents at Fukushima Daiichi.

Below: Nippon Post Express shipping label and an early dust wipe sample from Ibaraki Prefecture, just north of Tokyo, Japan. This sample collected on April 5, 2011 had a combined ^{131}I, ^{134}Cs and ^{137}Cs activity of 12.6 Bq.

Fig. 2.28 Above: Wipe sample and original mailer

This sample (pictured above) was analyzed on April 11, 2011. At the time of analysis, three to four half lives of ^{131}I had passed since the release date, meaning that the ^{131}I content of the dust had been diminished by eight to sixteen times from its original level. The majority of samples tested for this study were tested substantially later than these Tokyo samples. Any ^{131}I present would have essentially decayed away prior to any analyses. This indicates that potentially, most of the results given for this study are underestimates of the original short term radiological exposures received in Japan. The wipe sample had insufficient mass to compute specific activity accurately. For an assumed 100 mg mass, the approximate specific activity estimate is 0.12 MBq kg^{-1}.

On the following page is a companion dust sample from the same home in Ibaraki. It was tested on April 11, 2011. The gamma spectrum for this dust sample has a strong peak for ^{131}I at a gamma photon energy of 364.5 keV. This is at accident start plus 31 days, almost

four half lives of ^{131}I from initial commencement of the release. There is still a markedly high level of ^{134}Cs compared to ^{137}Cs. This ratio shrinks in the 2013 samples, due to the disparity in radio cesium half lives. (See sec. 2.5 for comparison results.)

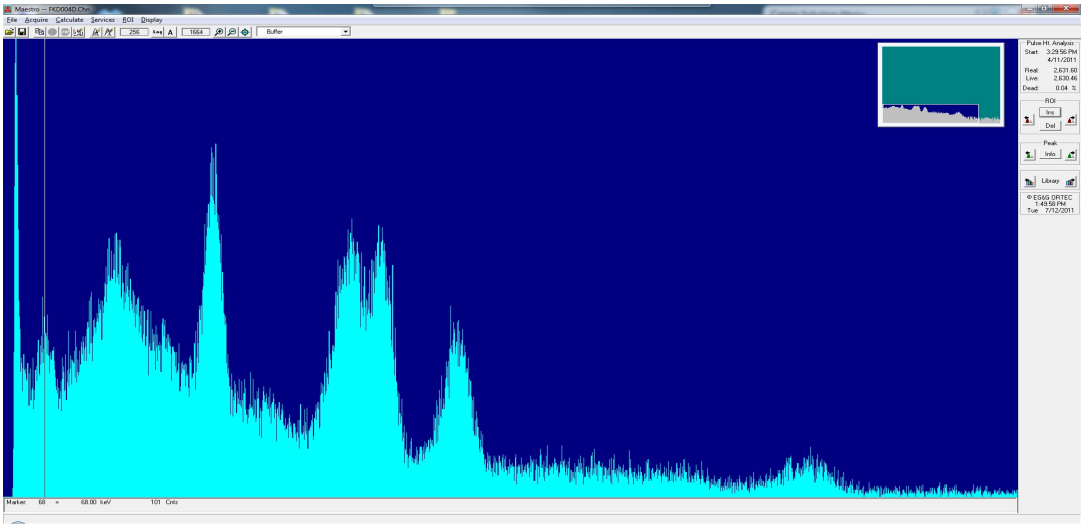

Fig. 2.29 Above: NaI gamme spectrum for house dust in Ibaraki Pref. (dpm = cpm/0.15)

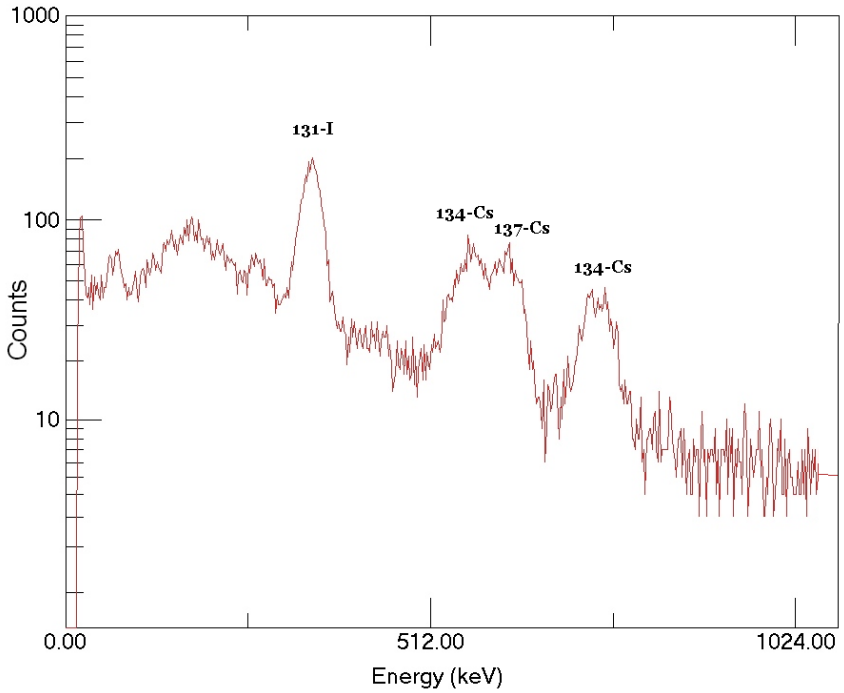

Fig. 2.30 Above: Tsukuba (Greater Tokyo) surface soil sample (top 1 cm) collected 5 April 2011 and analyzed 11 April 2011, (dpm = cpm/0.15)

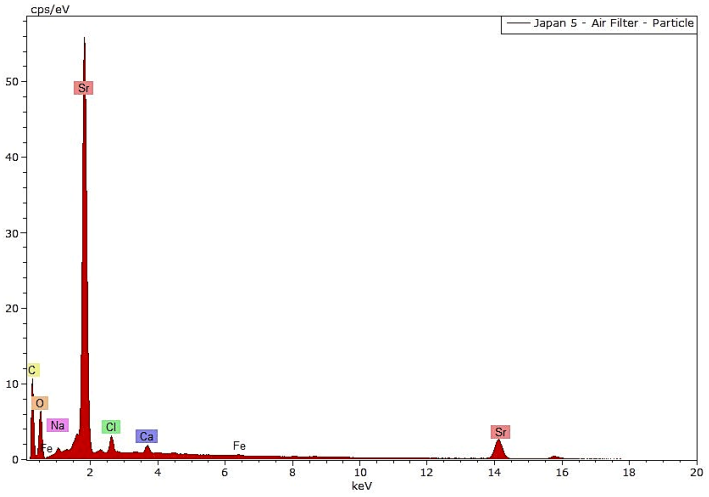

Fig. 2.31 Left: SEM-EDS spectra and photomicrograph of a dust particle collected from a Greater Tokyo vehicle air filter, 4/5/2011. This particle is almost entirely strontium. The activity of the particle, if any, is in determinant because stable and unstable nuclei with the same z can not be distinguished by this method.

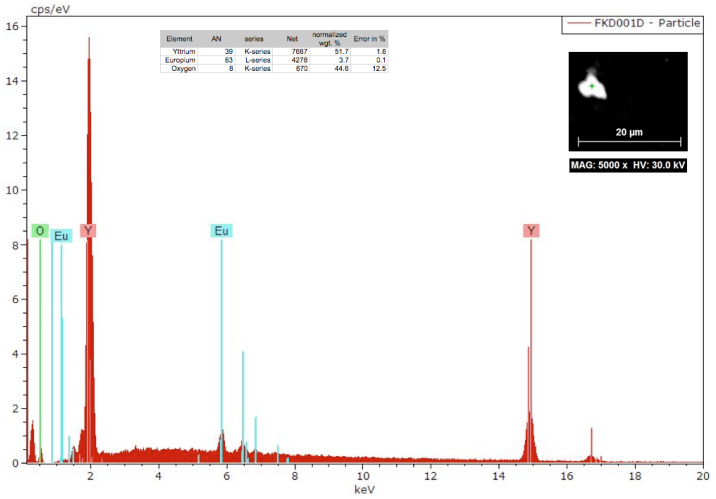

Fig. 2.32 Left: This spectrum from an Ibaraki Pref. home contained yttrium and europium. Eu and Y are common fission products. ^{90}Y is the decay daughter of ^{90}Sr. If ^{90}Sr were present, one would also expect to find yttrium.

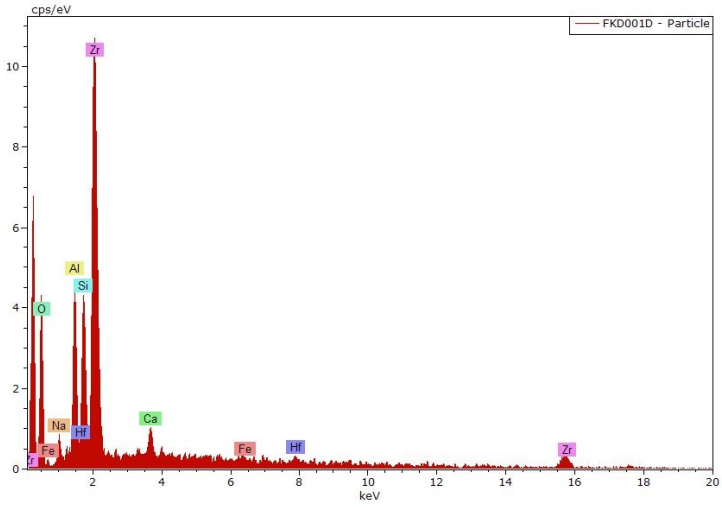

Fig. 2.33 Left: This particle from the Ibaraki Pref. house dust sample seen in the above middle example also contained Zirconium. Zr is an important component of nuclear fuel assemblies, but also has many nonnuclear uses. CPS to mass data for this set of spectra are in Appendix E.

Two scaled photomicrographs of the Ibaraki Pref. particle from which the two preceding spectra were taken are shown below. The green cross hatch mark in the upper SEM photomicrograph shows a location on the particle that contained lead and americium. The transuranic element americium does not have a stable isotope.

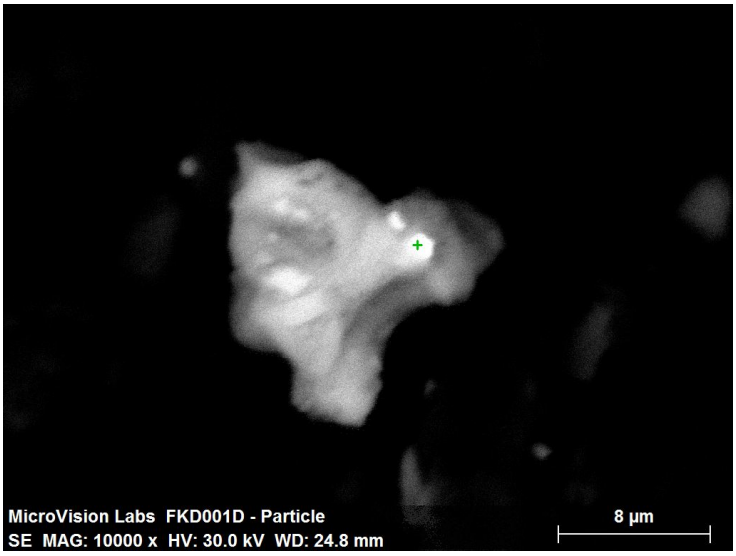

Fig. 2.34 Above: 2011 photomicrograph of Am-containing dust particle

Fig. 2.35 Right: Showing the specific location that corresponds to the detections for Eu and Y, respectively the *potential* fission product and *potential* decay product of ^{90}Sr. This is a lower magnification view of the same particle shown above. Given the presence of americium in this particle, a necessarily radioactive element, this particle is definitively a radioactively hot particle. The conclusion is based on both indirect and direct evidence. (See cps to mass data, Appendix E)

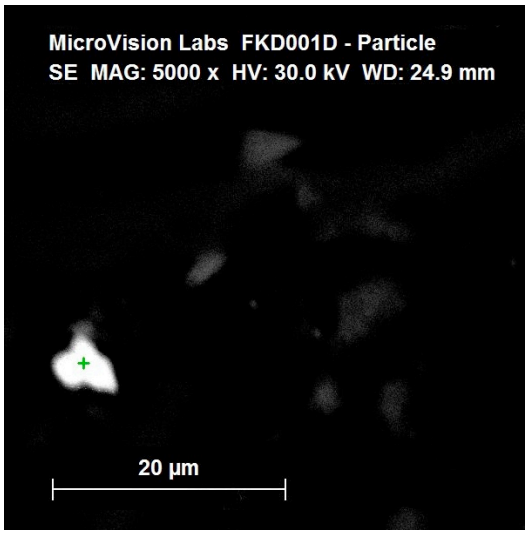

Below are two additional sets of SEM/EDS spectra and scaled photomicrographs. These detail further detections of particles with Zr, rare earths and Y, as well as thorium and rare earths. These data are from dusts removed from an automobile air filter. Based on both the SEM/EDS and gamma spectrometry data, dusts from Greater Tokyo were found to contain the radioactive contaminants ^{241}Am, ^{134}Cs, ^{137}Cs, ^{131}I, and thorium; along with indirect evidence of potentially radioactive contaminants, ^{90}Y, ^{90}Sr, and Eu. Rare earths and zirconium of unknown stability were also detected by SEM/EDS. The specific activity for the Greater Tokyo house dust as of April 11, 2011 was 0.12 MBq kg^{-1}.

Fig. 2.36 Right: SEM/EDS photomicrographs for Tokyo vehicle air filter dust particle.

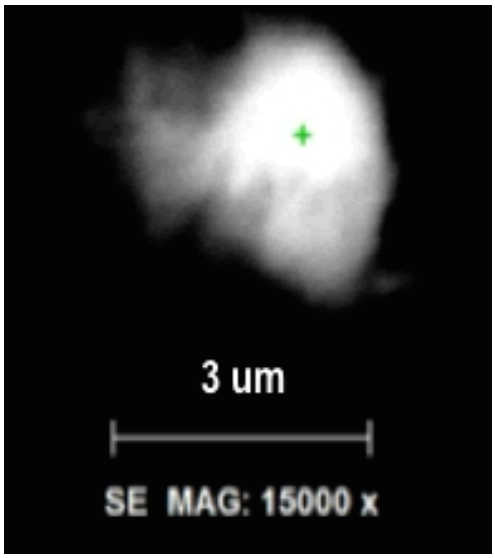

Fig. 2.37 Below: Corresponding SEM/EDS spectrum. (Additional data in Appendix E)

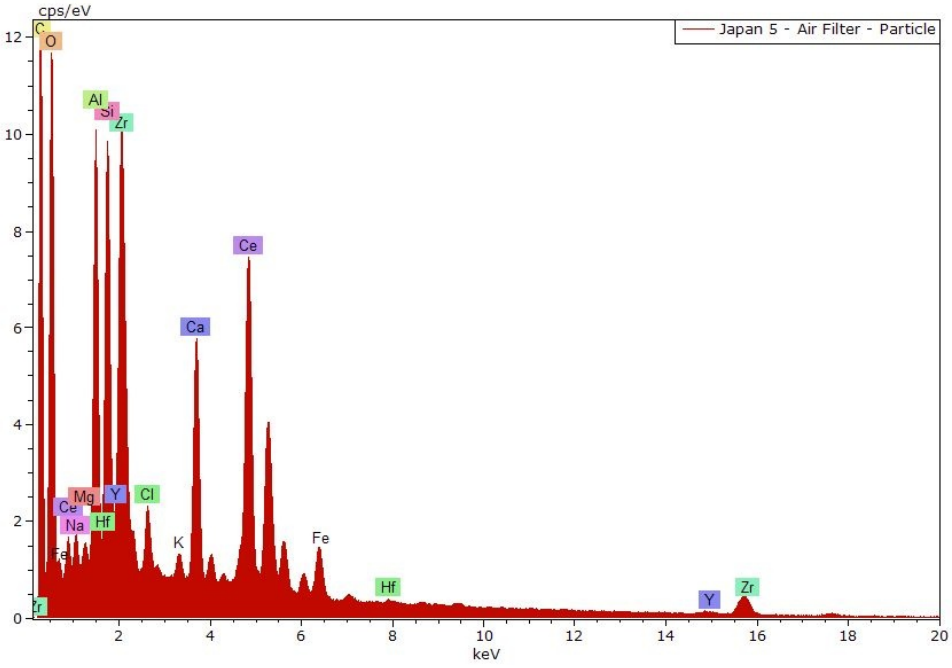

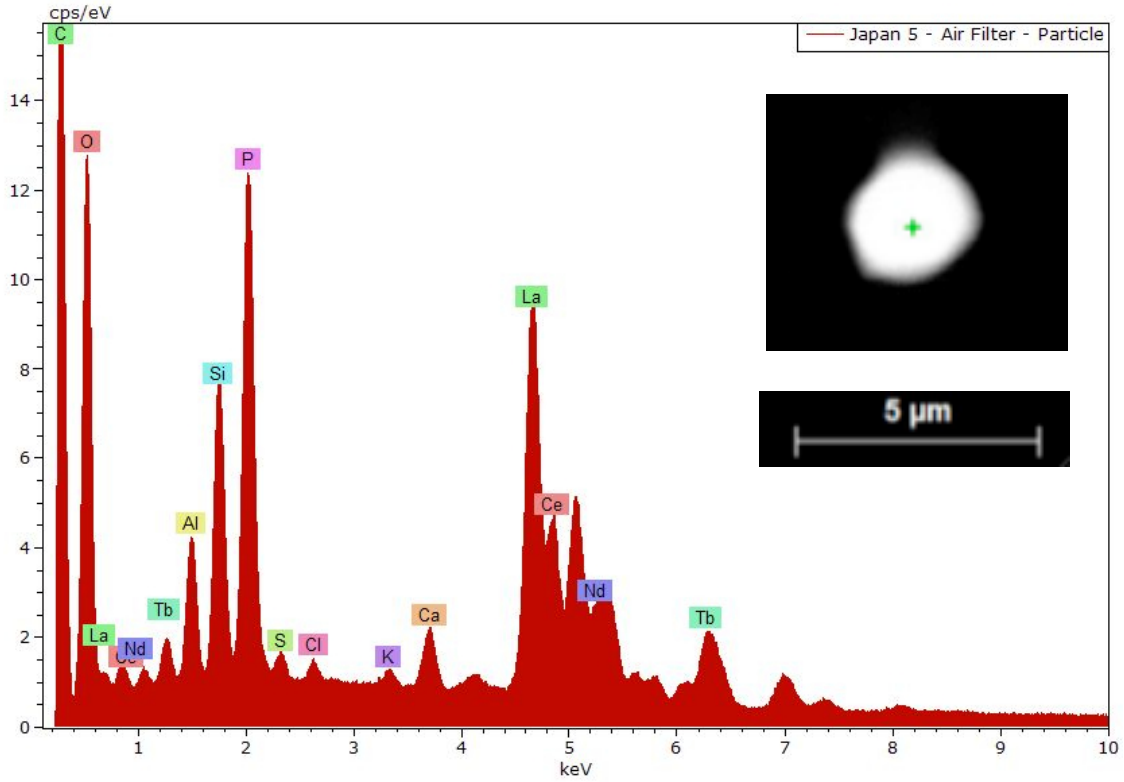

Fig. 2.38 Above: SEM/EDS spectrum and photomicrograph for Tokyo vehicle air filter dust

Table 2.3 Below: cps to mass data corresponding to spectra above in Fig. 2.38

Element	AN	series	Net	[wt.-%]	[norm. wt.-%]	[norm. at.-%]	Error in %
Carbon	6	K-series	121520	15.06775	12.12662761	21.833799	8.780553
Aluminium	13	K-series	42389	3.155715	2.539741036	2.03559388	0.18921
Silicon	14	K-series	89207	5.108086	4.111021858	3.16545439	0.253296
Phosphorus	15	K-series	152952	7.983804	6.42541932	4.48617262	0.346736
Sulfur	16	K-series	9893	0.455022	0.36620503	0.24697213	0.042867
Chlorine	17	K-series	6029	0.255975	0.206010373	0.12566323	0.034757
Potassium	19	K-series	4015	0.150805	0.121368525	0.06713	0.030589
Calcium	20	K-series	18871	0.771696	0.621065846	0.33511976	0.048639
Lanthanum	57	L-series	264591	17.48721	14.07382119	2.19109406	0.565671
Cerium	58	L-series	118707	8.009875	6.446401364	0.99491424	0.408857
Neodymium	60	L-series	8283	0.593245	0.477447806	0.07158279	0.305698
Terbium	65	L-series	66617	6.63878	5.342934478	0.72703487	0.197212
Oxygen	8	K-series	127112	58.57547	47.14193556	63.719469	6.539724
			Sum:	124.2534	100	100	

The final Tsukuba sample arrived separately three days after the previous sample set. This analysis of this soil sample was delayed three days more than the prior samples. Despite this minor delay, the peak height ratio between the 364.5 keV peak for short-lived ^{131}I and the 662 keV peak for ^{137}Cs were the highest of any samples received for this study. These data show that soils and dusts at this site more than 162 km from the accident had substantial amounts of adsorbed ^{131}I near the time of the accident. This is in line with estimates that the ^{131}I release was an order of magnitude greater than the ^{137}Cs release (26, Hirose). The soil activity measured as beta decay was 5 +/- 2.3 kBq kg^{-1}.

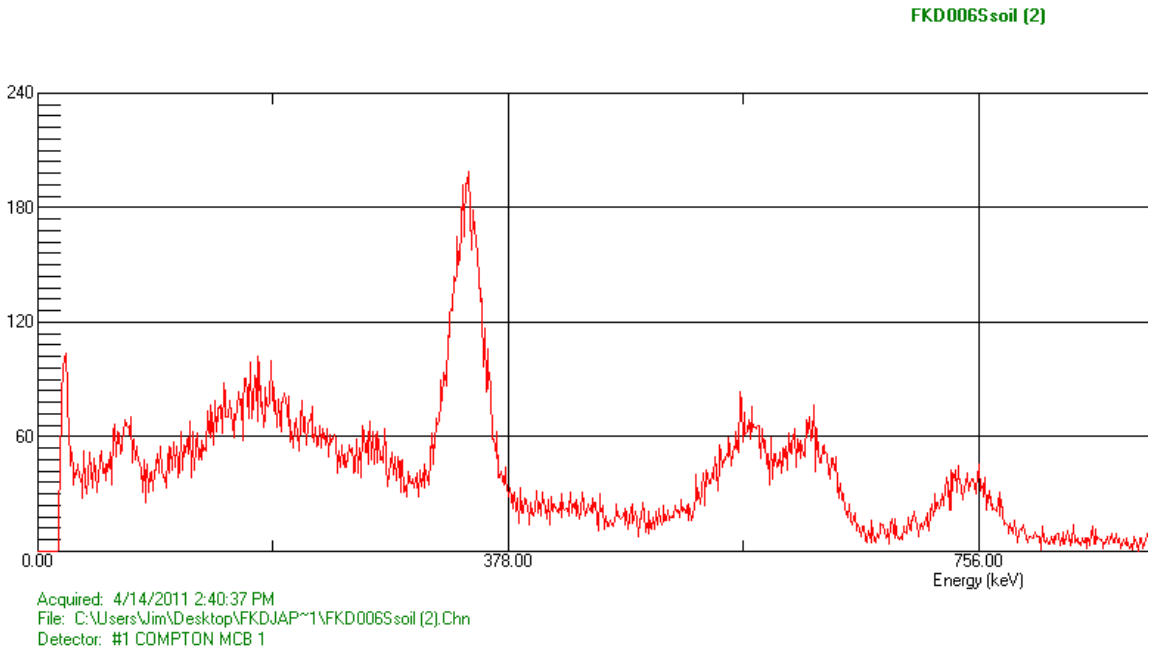

Fig. 2.39 Above: Tsukuba soil sample showing ^{131}I peak (DPM = CPM/0.15)

A second set of five Tokyo dust wipe samples was collected on April 18, 2011. Four were from the roof top of a commercial structure., and one was from the balcony of a residential building. These samples were hand delivered to the author in Cambridge, MA. This set also included a trip blank. The trip blank measured 0.6 Bq for a blank wipe using gamma spectrometry. The mean activity of these five samples was 70.2 +/- 8.4 Bq per wipe. None of these had sufficient mass to yield an accurate weight.

Motor vehicle engine air filters process large volumes of air. In Japan private vehicles average 65 liters of gasoline use per month. (15, Schipper) This fuel requires approximately 638 cubic meters of air for complete combustion. This is about 30 cubic meters per day, which is in the same order of magnitude as a working adult tidal air volume of 10 to 20 cubic meters per day. It was hypothesized that engine air filters in routine use and first installed prior to March 11, 2011 would provide an approximation of the amount of radioactive dusts present in ambient air for each driving region. Sixteen vehicle air filters were collected during May 2011 from drivers in Fukushima City and Tokyo, Japan, and from Seattle, WA, USA. Given the limited information available on the specific driving history related to each filter, the study was designed to determine the relative availability of hot particles in different regions. The surface contamination of the filter media was directly measured using a using a ^{63}Ni-standardized pancake probe and counter. Subsamples of each were autoradiographed, and individual particles were analyzed by SEM/EDS. Total activity results are in Table 2.4.

Table 2.4 Below: Total activity from automotive air filters

Tokyo, Japan filters averaged 20.6 uR/hour with a relative standard deviation (RSD) of 7.5 % and n = 7.

Fukushima City filters averaged 199 uR/hour with an RSD of 11.5 % and n = 6.

Seattle, WA, USA-based filters averaged 11.2 uR/hour with n = 9.

Three blank automotive filters averaged 11.3 uR/hour.

The Tokyo and Fukushima City vehicle filters were heavily loaded with dust particles capable of darkening X-ray film (autoradiographically positive). Autoradiographs from Seattle, WA filters and blanks were negative. In the US filters, any radioisotopes present were related to uranium, thorium, or ^{40}K, all of which are primordial nuclides. The Japanese filters contained ^{134}Cs and ^{137}Cs as the dominant nuclides, along with lesser amounts of ^{60}Co and ^{40}K.

Section 2.8 : Isolation of an atypically hot particle with calculation of dose and risk

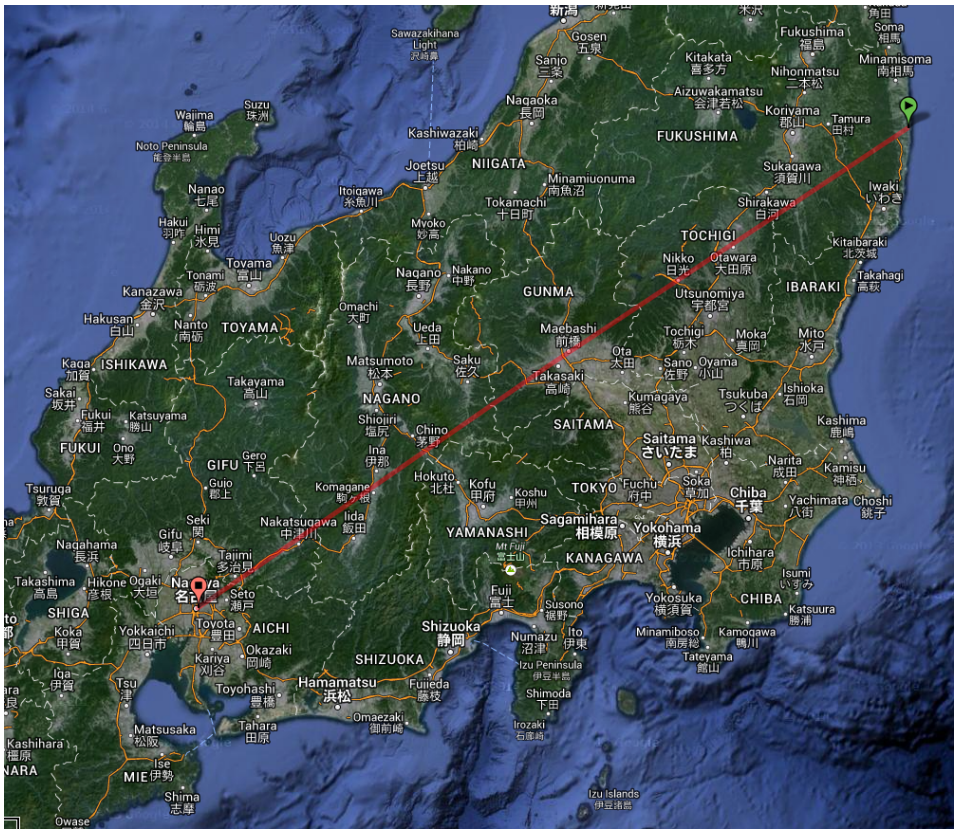

Nagoya, Japan

Distance from Fukushima
Daiichi: 433 km

Two vacuum cleaner bags were received from a home in Nagoya, Japan. Both had approximately 300 grams of house dust. Both bags were tested in their entirety, as they

were small enough to fit into the test well of the NaI detector. The bags were screened by gamma spectroscopy prior to any sample preparation or sieving. One of the vacuum bags was non detect for radioactivity above the instrument background. The second sample had a strong response greater than > 60 gCPS above instrument background. The standard procedure for high activity samples involves sequential division and rescreening of the samples. After one sequential division, both subsamples were found to be non detect for radioactive contamination. Wanding of the aluminum sample preparation tray and razor cutter identified a hot particle attached to the razor. This was removed with a double sided mounting tape for an SEM/EDS slide, photographed, and retested using the NaI gamma detector. The slide yielded a count of 162.1 gCPS above instrument background (nongeometry corrected). The sample was counted on a two-channel alpha beta counter (Ludlum Model 3030). The mounted slide was carbon-coated and analyzed by SEM/EDS. After the SEM analyses were completed, a final gamma count rate was determined by a long count on an NaI well detector.

The Fig. 2.40 shows the images of the particle on a standard bioslide. Optical and SEM images at moderate and high magnification are on the following pages, in Figs. 4.41, 4.42 and 4.43.

Fig. 2.40 Above: standard bioslide with dust particles at lower left, with 0.9 cm scale.

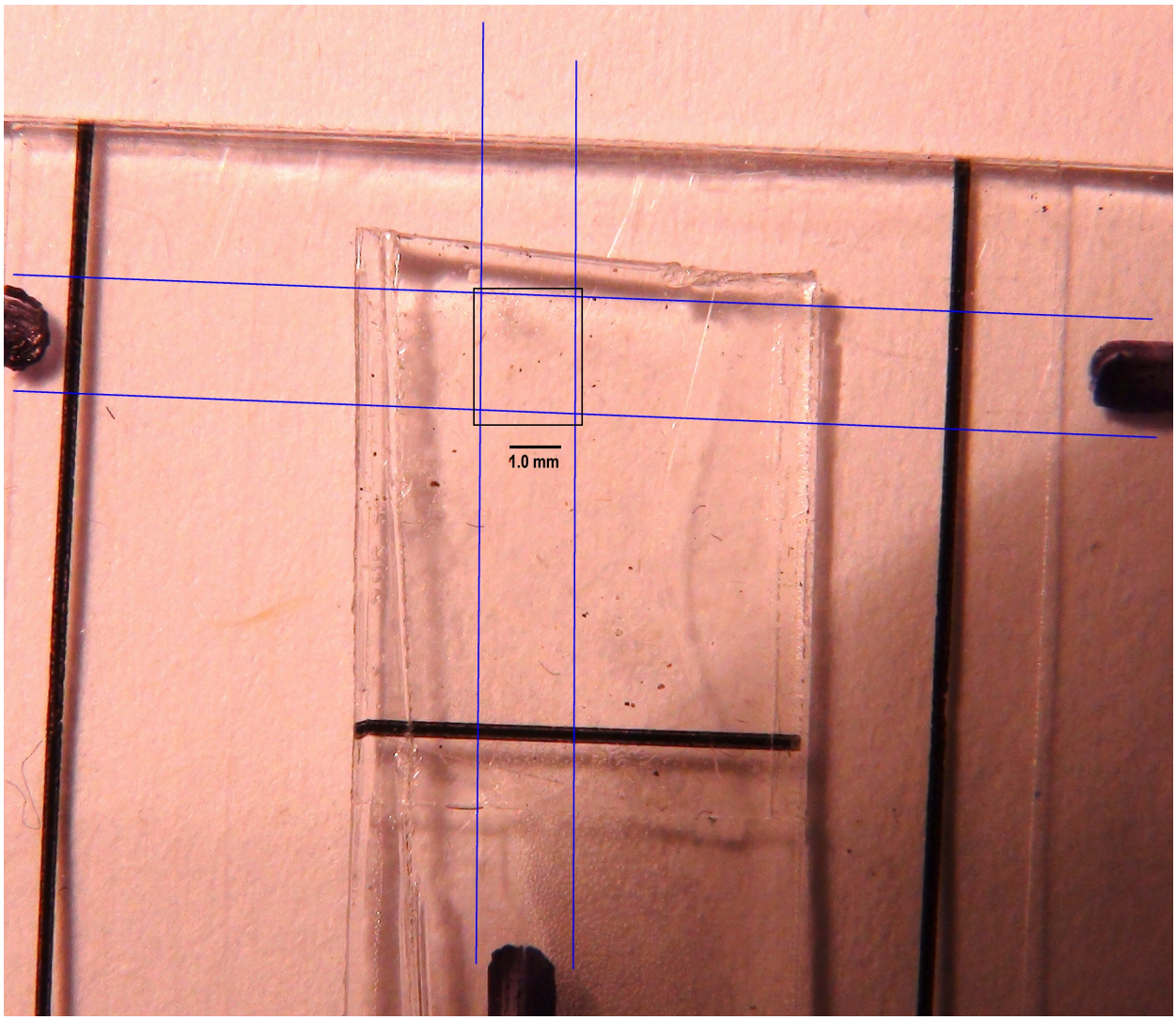

Fig. 2.41 Above: Magnified image of dust particles mounted on a biotape slide. Note 1.0 mm scale.

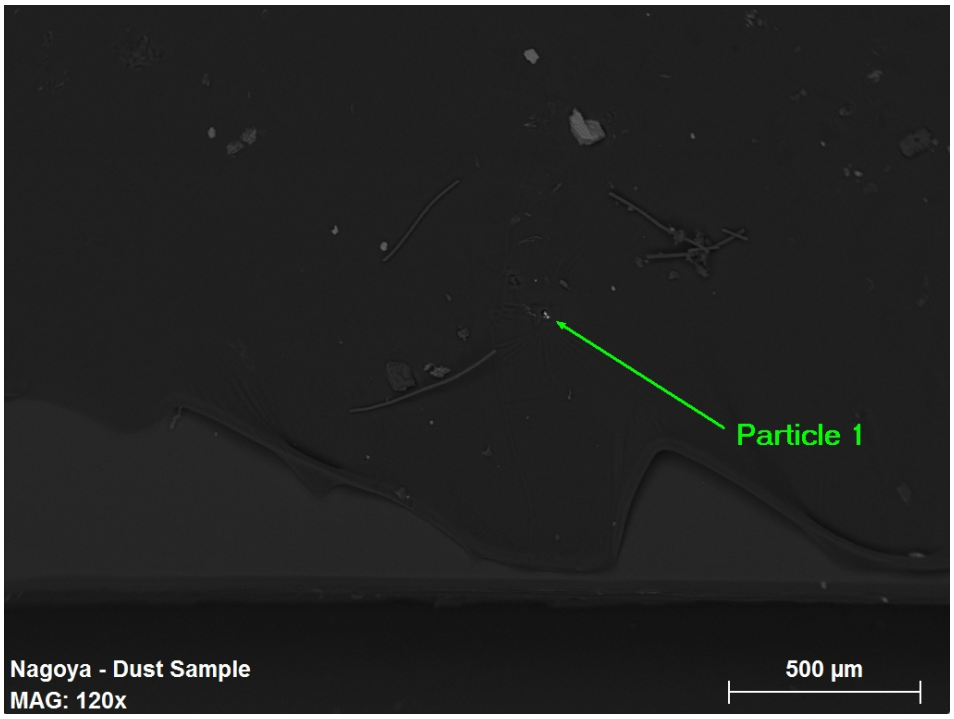

Fig. 2.42 Above: SEM image of hot particle, magnification 120 X.

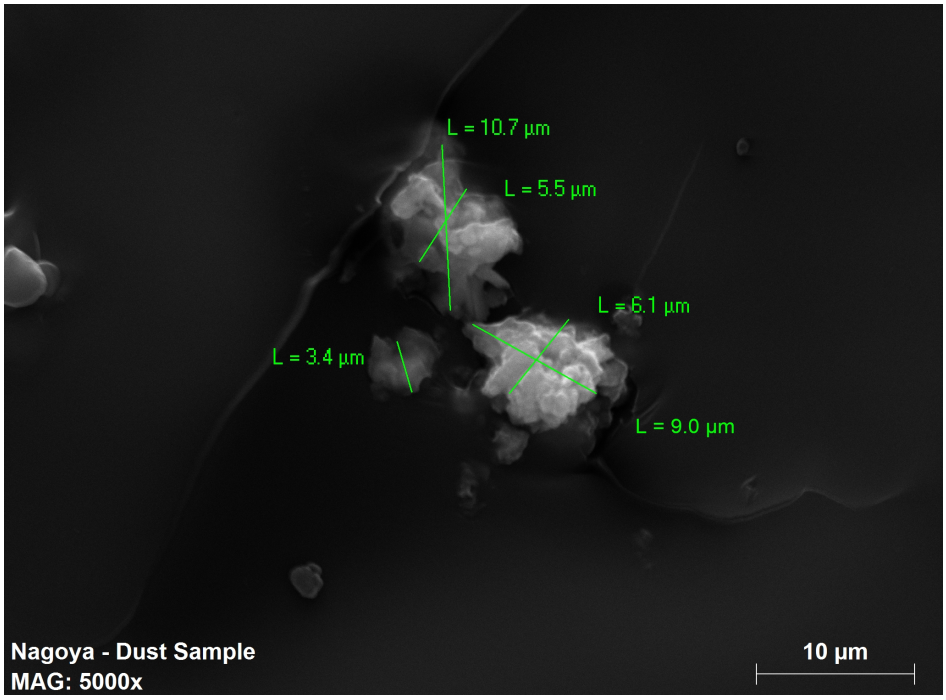

Fig. 2.43 Above: SEM image of hot particle, magnification 5000 X.

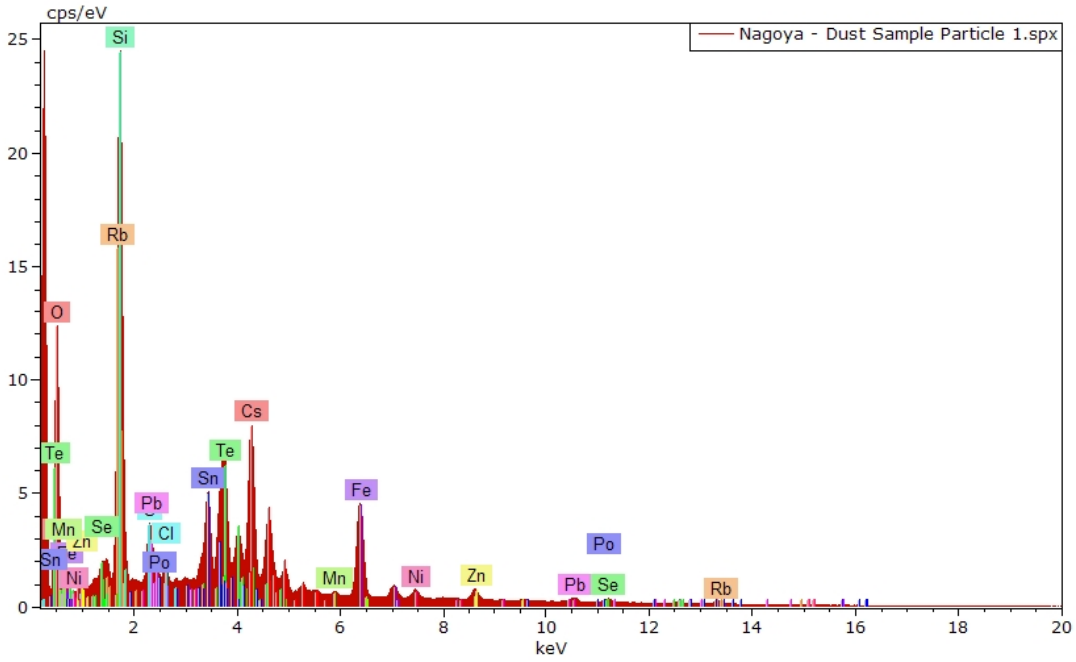

Fig. 2.44 Above: SEM/EDS spectrum showing area of hot particle with Cs, Te, Rb, Po, Dy, along with metals Ni, Fe, Pb, Cr, Zn, and Sn.

Table 2.5 Below: CPS to mass conversion data for spectrum shown above, analysis date December 18, 2013

Element	AN	series	[wt.%]	[norm. wt.%]	[norm. at.%]	Error in wt.% (1 Sigma)	K fact.	Z corr.	A corr.	F corr.
Oxygen	8	K-series	39.8211	39.8211	74.3619	2.1072	1	3.5621	0.0815	1.0004
Tellurium	52	L-series	16.7339	16.7339	3.9182	0.4911	1	0.0175	0.7545	1.0000
Cesium	55	L-series	15.6023	15.6023	3.5074	0.4576	1	0.0126	0.7601	1.0000
Silicon	14	K-series	10.5460	10.5460	11.2188	0.4828	1	0.3088	0.2902	1.0002
Iron	26	K-series	5.5500	5.5500	2.9692	0.1722	1	0.0120	0.8232	1.0009
Tin	50	L-series	3.6612	3.6612	0.9215	0.1307	1	0.0227	0.7117	1.0071
Lead	82	L-series	2.3785	2.3785	0.3430	0.0846	1	0.0007	0.9706	1.0011
Zinc	30	K-series	1.3434	1.3434	0.6138	0.0591	1	0.0049	0.9130	1.0000
Rubidium	37	K-series	1.2237	1.2237	0.4278	0.0556	1	0.0009	0.9871	1.0000
Sulfur	16	K-series	0.7973	0.7973	0.7429	0.0552	1	0.1638	0.4298	1.0002
Selenium	34	K-series	0.7215	0.7215	0.2730	0.0431	1	0.0019	0.9658	1.0000
Polonium	84	L-series	0.6118	0.6118	0.0875	0.0403	1	0.0006	0.9778	1.0000
Nickel	28	K-series	0.5317	0.5317	0.2707	0.0387	1	0.0079	0.8695	1.0026
Chlorine	17	K-series	0.2837	0.2837	0.2391	0.0350	1	0.1175	0.5063	1.0000
Manganese	25	K-series	0.1936	0.1936	0.1053	0.0303	1	0.0147	0.7845	1.0000
		Sum:	100	100	100					

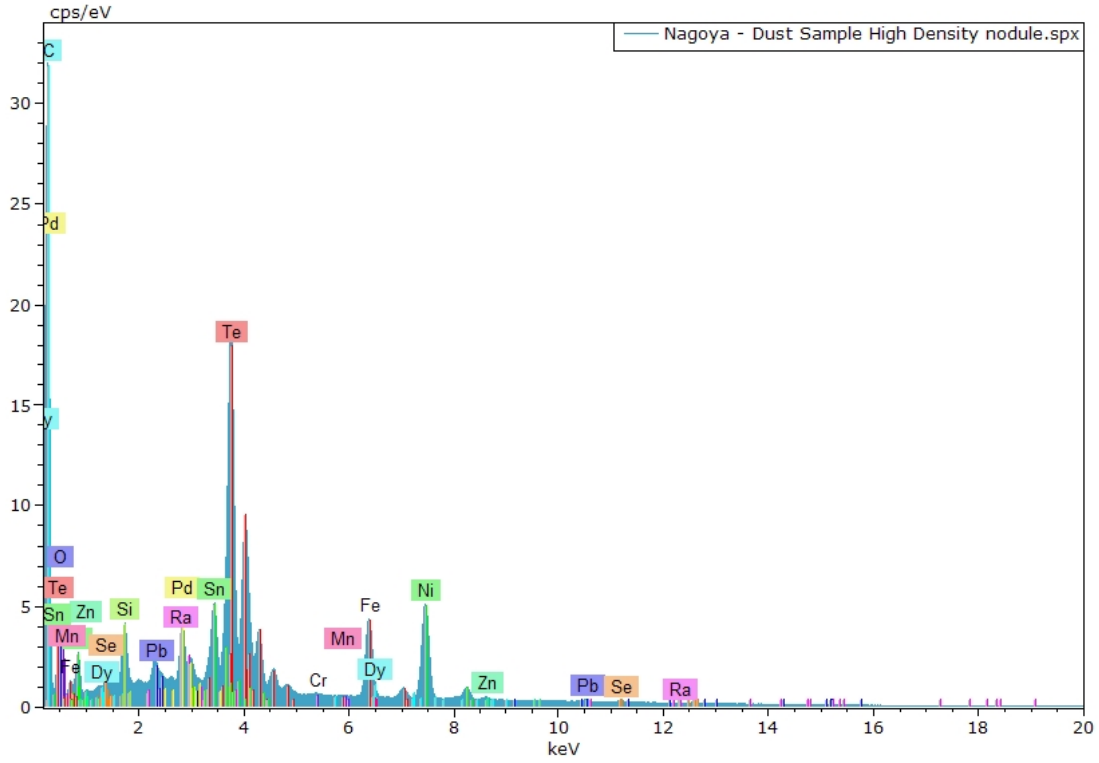

Fig. 2.45 Above: SEM/EDS spectrum showing area of hot particle with Te, Ra, Dy, along with metals and other elements.

Table 2.6 Below: CPS to mass conversion data for spectrum shown above, analysis date December 18, 2013

Element	AN	series	[wt.%]	[norm. wt.%]	[norm. at.%]	Error in wt.% (1 Sigma)	K fact.	Z corr.	A corr.	F corr.
Tellurium	52	L-series	48.0378	48.0378	17.9999	1.4231	1	0.0193	0.7020	1.0000
Oxygen	8	K-series	12.0514	12.0514	36.0140	0.6488	1	3.9053	0.0936	1.0007
Nickel	28	K-series	9.3505	9.3505	7.6170	0.2725	1	0.0087	0.8262	1.0004
Tin	50	L-series	6.3113	6.3113	2.5420	0.2153	1	0.0250	0.6629	1.0000
Palladium	46	L-series	5.9454	5.9454	2.6711	0.2211	1	0.0447	0.5699	1.0106
Iron	26	K-series	5.8357	5.8357	4.9961	0.1862	1	0.0132	0.7653	1.0121
Carbon	6	K-series	5.4094	5.4094	21.5334	0.3131	1	12.6038	0.0595	1.0003
Silicon	14	K-series	3.1420	3.1420	5.3489	0.1676	1	0.3386	0.2425	1.0000
Lead	82	L-series	1.7953	1.7953	0.4143	0.0701	1	0.0008	0.9462	1.0000
Polonium	84	L-series	1.1904	1.1904	0.2723	0.0549	1	0.0007	0.9573	1.0000
Zinc	30	K-series	0.2991	0.2991	0.2187	0.0328	1	0.0054	0.8635	1.0000
Selenium	34	K-series	0.2987	0.2987	0.1809	0.0325	1	0.0021	0.9402	1.0000
Dysprosium	66	L-series	0.1813	0.1813	0.0533	0.0299	1	0.0042	0.7966	1.0001
Chromium	24	K-series	0.1226	0.1226	0.1127	0.0287	1	0.0207	0.6656	1.0059
Manganese	25	K-series	0.0290	0.0290	0.0253	0.0258	1	0.0162	0.7191	1.0000
		Sum:	100	100	100					

The Nagoya dust sample measured 324 Bq/sample as gamma and 285 Bq/sample as beta. In calculating a dose, the measured activity must be converted to the actual energy emitted by the dust particle. Based upon the NaI gamma spectral results, ^{137}Cs, and to a lesser extent, ^{134}Cs, were responsible for the largest part of the activity of this particle. Although the NaI spectrum for the particle had a major peak at 188 keV, the peak was apparently due to Compton scatter. Reanalysis using a CdTe gamma detector did not indicate 226Ra was responsible for a significant portion of the particle's activity.

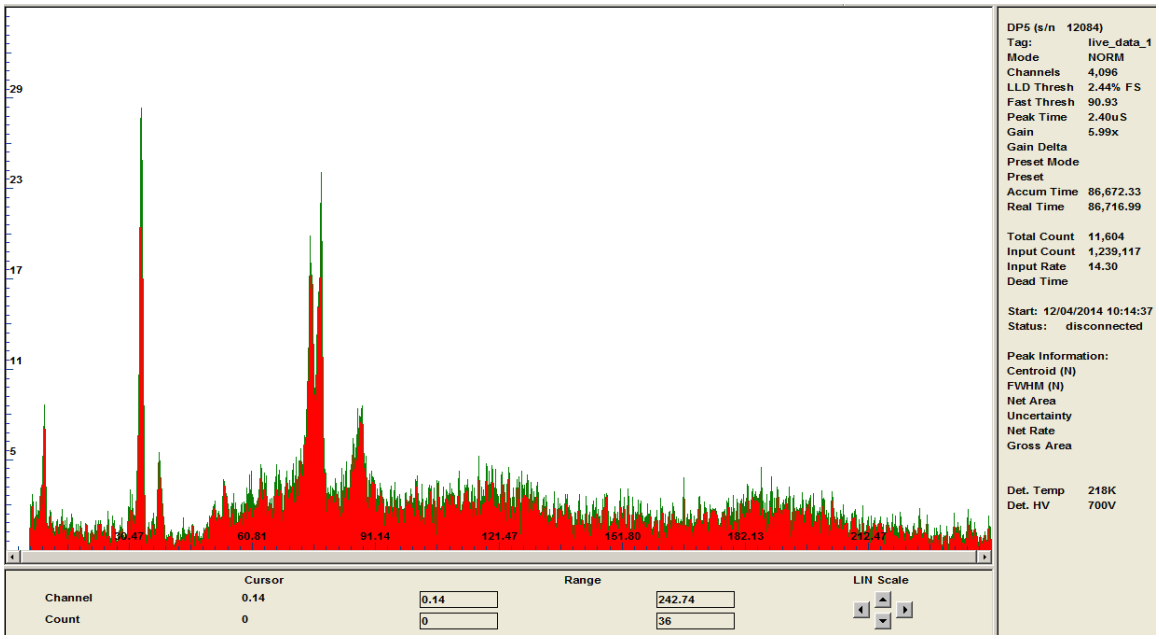

Fig. 2.46 Above: CdTe low energy gamma spectrum of Nagoya hot particle, showing much smaller gamma peak at 188 keV than the NaI spectrum. This is evidence that the apparent 188 keV NaI detector peak is due to Compton scatter.

The decay modes of ^{137}Cs are detailed below.

For each decay:

Beta: 5.6 % @ 352 keV, 94.4 % @ 154 keV (mean energies)

Gamma photons: 85.1 % @ 661.7 keV

X-rays: 5.8 % @ ~ 32 keV

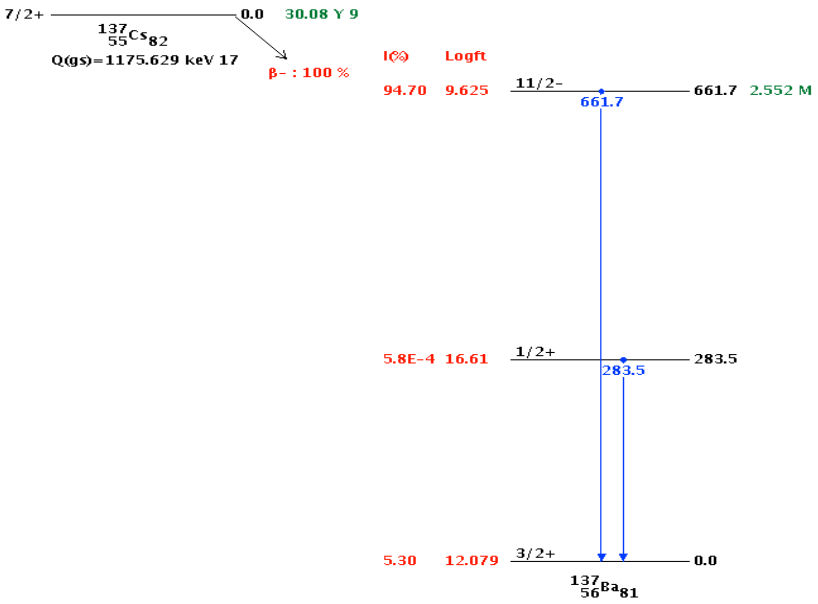

Fig. 2.47 Above: ^{137}Cs decay scheme from IAEA Chart of Nuclides

The total energy dissipation is normalized to the 661.7 keV ^{137}Cs gamma photon. This approximation is reasonable given that ^{137}Cs is the source of the majority portion of the sample's gamma and activity. The mean beta energies of ^{137}Cs beta decay are 154 keV (94.4%) and 352 keV (5.6%). The human lung accounts for 12% of the whole body dose. Using geometry corrected count rates, his yields:

Energy emitted in organ per unit time = (activity) * (mean energy per decay)

E = 285*(0.944 * 154 keV + 0.056 * 352 keV) + 0.12 * 0.851 * 324 * 661.7 keV

E = 47 MeV + 21.9 MeV = 68.9 MeV = 1.1 EE-11 J/s

The detection efficiency against a certified standard of ^{137}Cs sample was 30 %.

1.1 EE-11 J/s / 0.29 = 3.6 EE-11 J/s

Given the size of this particle, a conservative exposure scenario assumes that it produces a committed effective dose, requiring the use of a 50 year time frame in calculating the dose. Empirical SEM/EDS data does not give sufficient certainty that this particle has such a long human body-lifetime. For this reason, both an annualized and a committed dose (long term dose from internalized radioactive material) are calculated here.

The annual dose at this energy dissipation rate is 1.15 EE-3 J/yr. (1.15 mGy).
The committed dose adjusted for ^{137}Cs and ^{134}Cs decay is 0.028 J.

The quality factors for both beta and gamma radiation are both 1, so there is no weighting factor adjustment. The total alpha activity for this sample is not significant compared to the beta and gamma activity, and is neglected in these calculations. The target organ is presumed to be the human lung, which has a typical mass of 0.88 kg. (NIH data, 2014) This gives a committed lung dose of 0.03 Sv. Using the SEM/EDS and standardized count data, the specific activity is:

Table 2.7 Below: Physical data on Nagoya particle and dose result

Particle density = 4.2 g cm^{-3}
Particle volume = 933 um^3
Mass = 3.9 nanograms
Measured (corrected) activity = 2.03 kBq
Specific activity = 2.03 kBq / 3.9 ng = 5.2 x 10^{15} Bq kg^{-1}
5.2 x 10^{15} Bq kg^{-1} = 5.2 PBq kg^{-1}
Lung dose = 1.15 mGy yr^{-1}

This particle potentially could have included some amount of ^{131}I, but given the passage of time, ^{131}I could not be measured. Any activity from this isotope is ignored in these calculations as it makes no long term contribution to dose. As with other samples in this study, ^{134}Cs has not been retrospectively decay-corrected.

Section 2.8.1 Calculating excess cancer risk

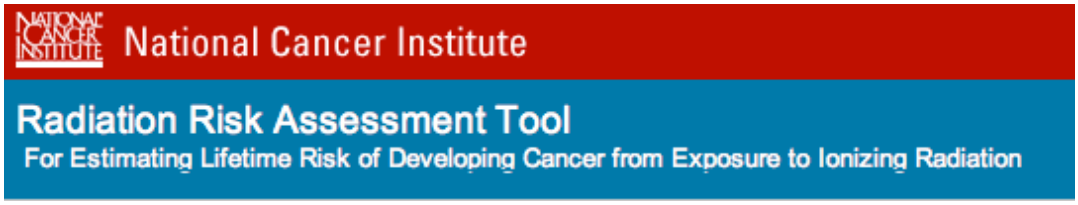

Risk calculations for this particle use the previously calculated 1.15 mGy annual dose. Excess cancer risk was calculated using RADRAT, the National Cancer Institute Radiation Risk Assessment Tool. (ref. https://irep.nci.nih.gov/radrat/model/inputs/) For a male child, age 2 years when initially exposed in 2011, with a lung exposure of 1.15 mGy per year depending on growth and isotopic decay, the mean excess lifetime cancer risk is 4 per 100,000 per year of exposure. The lower and upper bound of the risk estimate is 2 to 8 per 100,000 per year of exposure. For a committed dose the lifetime excess cancer rate is approximately 0.5 per 1,000; (0.2 to 1.0 per 1,000; lower and upper bound). An ingestion dose could be similarly calculated, however it is less likely that this would become a committed dose. This would result in a smaller risk.

The distance between the hot particle sample site and Fukushima Daiichi is approximately 433 km. The hot particle is small enough to be transported by the atmosphere alone, but it also could have been partly or wholly transported on clothing or a vehicle. It would require further study and mapping of more particles such as this one to confidently determine a mode of particle transport.

After completing the analysis of the hot particle in the vacuum cleaner dust from Nagoya, two additional vacuum cleaner bags were received from the same home. These were non detect for radioactivity above background. Except for the very high activity particle, no other contamination was detected in dust from this home. For the entire sample set analyzed during this study, this hot particle event represented the most extreme example

of heterogeneous radiation detected against an inert background. The annual dose based on average activity data is zero. The dose based on inhalation of this hot particle is a lung dose of 1.15 mGy yr^{-1}. If risks to this household had been calculated solely on the average level of potential exposure from dusts, then this would have ignored the potentially significant hot particle radiation exposure.

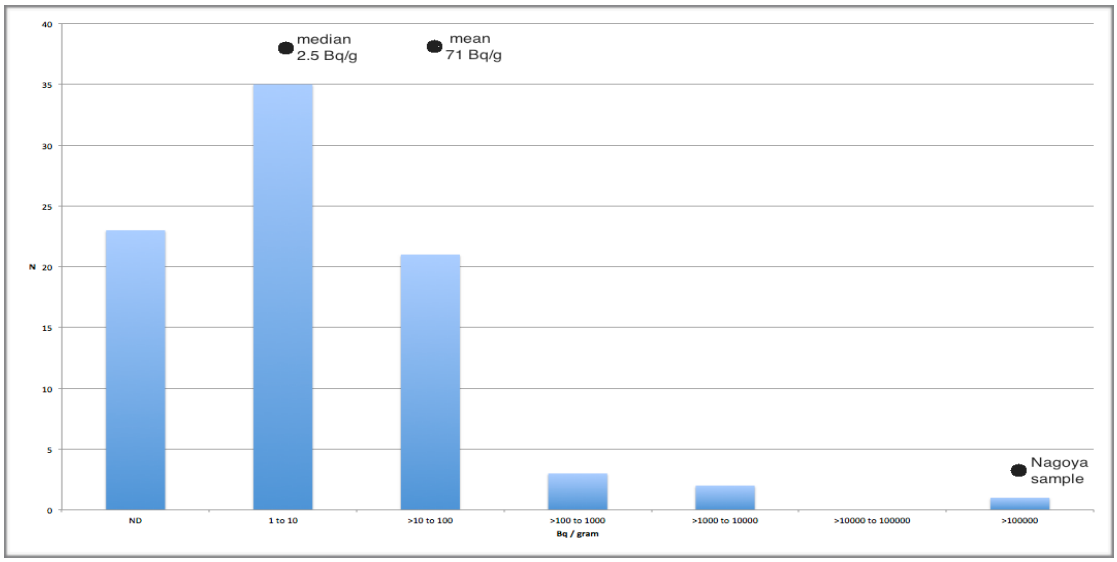

Fig. 2.48 Above: median and mean dust activity levels vs. activity histogram

By way of example, assume the Nagoya particle caused an excess cancer. (It did not, and it is unlikely to do so, but this is for argument's sake.) It would be highly misleading to state that the cancer was caused by dusts with a mean specific activity of 71 Bq g^{-1}, or by dusts with median specific activity of 2.5 Bq g^{-1}. Our (presumed) cancer was in fact caused by dust with a much higher specific activity. The error can work in the other direction as well. One can only state that dusts with a low mean specific activity *are unlikely to* cause a cancer, if there is enough data to rule out any significant probability of exposure to atypically hot particles.

The United States Environmental Protection Agency (http://www.epa.gov/ncea/efh/pdfs/efh-chapter05.pdf) provides guidance for human exposure to inhaled and ingested dusts. The US adult dust ingestion rate is assumed to be 30 mg d^{-1}, while the US adult dust

inhalation rate is 0.48 mg d^{-1}. Twenty-seven Japanese dust samples in this study set had specific activities greater than 10 kBq kg^{-1}. This specific activity level in dust corresponds to a daily intake of 0.348 Bq d^{-1} of radiologically-contaminated house dust. This value is only representative of the actual households sampled, and only for the time periods sampled. The value of 0.348 Bq d^{-1} is not representative of Japanese homes generally, nor is it necessarily representative of homes in Fukushima Prefecture. Japanese dust intake rates may be different from the calculated US rates. The value of this radioactive particulate intake rate is that it can be used to calculate the specific excess risk to the occupants of a home, and this excess risk number can be very different from the average value calculated for a population. At the median dust specific activity 2.5 kBq kg^{-1} +/- 1.6 Bq kg^{-1}, the intake rate is 0.087 Bq d^{-1} +/- 0.056 Bq d^{-1}.

Section 2 Conclusions

Radioactively-hot particles in the respirable size range (< 10 um) were routinely detected in dusts from Northern Japan, with one atypically hot particle collected 433 km from the release site. No hot particles larger than 20 um were isolated from Japanese dust samples. One hot particle was identified in a dust sample from Nagoya that had a specific activity of 5.2 x 10^{15} Bq/kg (5.2 PBq) yielding a lung dose of 1.15 mGy yr^{-1}. If no other tissues are significantly exposed, this is also the approximate effective dose. (22, Bolch)

The relatively small size (<20 um) of these hot particles means that these particles can potentially become airborne and travel long distances (>400 km) from the point of release. (31, Friedlander) The dust samples analyzed in this study were intentionally selected for analysis because of the assumption that hot particles from the reactor accident could and would be transported in the atmosphere. The presence of several hundred autoradiographically positive hot particles in dust samples from Japan appears to bear out this assumption.

Although the hot particles detected in this study were universally small enough to travel as airborne dusts; surface water transport, sediment erosion and resuspension, and some degree of facilitated transport by human activities like truck traffic are also possible explanations for the appearance of any given hot particle at a sample site.

The mean activity for the dust sample set was significantly higher than the median activity due to five of eighty-five atypically radioactive dust samples, with specific activities > 0.1 MBq kg^{-1}. (See Fig. 2.49 below)

Fig. 2.49 Above: Sample locus in Japan showing sites where the highest specific activity indoor and street dusts were found. (35, Google Earth)

Twenty-seven dust samples had specific activities greater than 10 kBq kg^{-1}. These samples contained fission products, primarily ^{134}Cs and ^{137}Cs, but isolated samples contained the activation product ^{60}Co, and fuel-related isotopes such as ^{226}Ra (a uranium daughter) ^{241}Am and polonium.

Thorium (always unstable) and strontium (has both stable and unstable isotopes) were also detected in radioactive particles, but these were not necessarily from Fukushima Daiichi.

Twelve dust samples tested were collected in late March and early April 2011. These samples from Tsukuba and other parts of Greater Tokyo initially had more ^{131}I than ^{137}Cs. The radioactive iodine was lost to decay for all samples tested after April 14, 2011. The specific activities, doses, and excess cancer risks in this research do not include the contribution from this potentially significant but necessarily unmeasured source of radiation dose.

Some individuals may actually receive a dose that is skewed higher than the mean dose calculated from average environmental data, due to inhalation or ingestion of hot particles in dusts. Exposure to radioactive contaminants in Northern Japan can be described as an average exposure, plus an additional probability of exposure to a distribution of inhalable or ingestable hot particles found in dusts. This distribution includes a limited number of dust particles of unusually high activity.

Autoradiography identified hundreds of candidate hot particles in dust samples, primarily in automobile air filter samples. These were too numerous to fully explore via SEM/EDS and these represent an archive of potential future data. Characterizing a sufficient number of these archived hot particles could provide enough detail on their geographic,

size, and activity distributions, that it might be possible to calculate potential hot particle-based internal radiation doses for larger number of residents of Northern Japan.

Section 2. References

(1) *Nature* 472, 145-146 (2011)

(2) *Nature* 471, 555-556 (2011)

(3) Shleien, B., et al, (1965) *Particle Size Fraction of Airborne Gamma-Emitting Radionuclides by Graded Filters*, Science Vol. 147 p. 290

(4) Adachi, K., Kajino, M., Zaizen, Y. & Igarashi, Y. Emission of spherical cesium-bearing particles from an early stage of the Fukushima nuclear accident.
Sci. Rep. 3, 2554; DOI:10.1038/srep02554 (2013)

(5) P. E. Rasmussen, *Canadian J. of Analytical Sci. and Spectroscopy V 49, No. 3, (2004*)

(6) Lang, S., Servomaa, K., Kosma, V.-M., Rytomaa, T., (1995) *Biokinetics of Nuclear Fuel Compounds and Biological Effects of Nonuniform Radiation*, Environmental Health Perspectives, Vol. 103, No. 10. Oct., pp. 920-934.

(7) Sajo-Bohus, L., Palfalvi, J., Greaves, E.D., (1998) Hot Particle Spectrum Determination by Track Image Analysis, Rad. Phys. Chem., V 51, No 4-6, pp 467-468

(8) Hochel, R.C., Characterization of Mixed Beta/Gamma Surface Contamination Using Passive Radiation Measurements, WSRC-MS-2000-00331, Westinghouse Savannah River Company, Aiken, SC 29808, URL accessed 11/22/13, http://sti.srs.gov/fulltext/tr2000331/tr2000331.html

(9) Cizdziel, J. V., Hodge, V. F., (2000) Attics as archives for house infiltrating pollutants: trace elements and pesticides in attic dust and soil from southern Nevada and Utah, Microchemical Journal 64 2000 85 92

(10) M.P.J. Kaltofen, J. Bergendahl, (2010) Microanalysis of Workplace Dusts from the Mixed Waste Tank Farm of the Hanford Nuclear Reservation, Env. Eng. Sci. 27, 2, 2010

(11) Aya Sakaguchi, Peter Steier, Yoshio Takahashi, and Masayoshi Yamamoto, Isotopic compositions of 236U and Pu isotopes in “Black Substances” collected from roadsides in Fukushima Prefecture: fallout from the Fukushima Daiichi NPP accident, Env. Sci. & Tech., DOI: 10.1021/es405294s, (2014)

(12) Environmental characterisation of particulate-associated radioactivity deposited close to the Sellafield works, Ellis Induro Evans, Doctoral Thesis, Imperial College of Science, Medicine & Technology, October 1997

(13) J. P. Ackerman, T. R. Johnson, Argonne National Laboratory, (1993)

(14) Lioy, Paul J., (2002) Dust: A Metric for Use in Residential and Building Exposure Assessment and Source Characterization, Environmental Health Perspectives

(15) L. Schipper, Behavior, Energy & Climate Change, Wash. DC. Nov. (2009)

(16) Health Risks from Exposure to Low Levels of Ionizing Radiation BEIR VII PHASE 2, Com. to Assess Health Risks from Exposure to Low Levels of Ionizing Radiation, Board on Radiation Effects Research Division on Earth and Life Studies, (2006)

(17) NUREG 2121, Fuel Fragmentation, Relocation, and Dispersal During the Loss-of-Coolant Accident, US NRC, March 2012, pp 44-45

(18) Sakaguchi, A., Steier, P., Takahashi, Y., and Yamamoto, M., (2014) Isotopic compositions of 236U and Pu isotopes in “Black Substances” collected from roadsides in Fukushima Prefecture: fallout from the Fukushima Daiichi Nuclear Power Plant accident. *Environmental Science & Tech*., 10.1021/es405294s

(19) ASTM International, (2007) Standard Practice for Collection of Floor Dust for Chemical Analysis, ASTM D 5438-00

(20) US Environmental Protection Agency, (1992) Preparation of Soil Sampling Protocols: Sampling Techniques and Strategies, ORD, EPA/600/R-92/128

(21) J. Diaz Leon, D. A. Jaffe, J. Kaspar, A. Knecht, , M. L. Miller, R. G. H. Robertson, and A. G. Schubert, Arrival time and magnitude of airborne fission products from the Fukushima, Japan, reactor incident as measured in Seattle, WA, USA,

(22) Bolch, W.E., et al., (2009) MIRD Pamphlet No. 21: A Generalized Schema for Radiopharmaceutical Dosimetry—Standardization of Nomenclature, J. Nuclear Medicine, 50 (3) 477-484

(23) Nair, R.R. (2009), Abstract: *Background radiation and cancer incidence in Kerala, India-Karanagappally cohort study*, Health Phys. 2009 Jan;96(1):55-66. doi: 10.1097/01.HP.0000327646.54923.11.

(24) Blog: http://fukushima-diary.com/tag/black-substance/, accessed 2/22/2015

(25) HPS, Health Physics Society, (2010) *Environmental Radiation Fact sheet*, http://hps.org/documents/environmental_radiation_fact_sheet.pdf

(26) Hirose, K., et al., (2013) *Dispersion of Fukushima radionuclides in the global atmosphere and the ocean*, App. Radiation and Isotopes, 81 383-392

(27) Safecast, (2014) used by permission, presentation to IAEA Vienna meeting, Feb. 17 - 21, http://www-pub.iaea.org/iaeameetings/cn224p/Session6/Brown.pdf

(28) Fukushima Nuclear accident Investigation Committee, (2012) *Fukushima Nuclear Accident Analysis Report*, Tokyo Electric Power Company, Inc.

(29) Coggle, J.E., et al., (1986) *Radiation Effects in the Lung*, Environmental Health Perspectives, Dec; 70: 261–291

(30) Shultis and Faw, Fundamentals of Nuclear Science and Engineering, Second Edition, ISBN:978-1-4200-5135-3, www.crcpress.com

(31) Friedlander, S.K., (2000) Smoke, Dust, and Haze, Fundamentals of Aerosol Dynamics, 2nd Ed., Oxford University Press

(32) Nature (2011) vol. 471, p417-419

(33) Safecast (2015) http://blog.safecast.org/maps/

(34) Goggle Earth map, accessed 3/2015, url: https://www.google.com/maps/place/Tokyo,+Japan/@36.1272075,139.5400999,516548m/data=!3m1!1e3!4m2!3m1!1s0x605d1b87f02e57e7:0x2e01618b22571b89

(35) Goggle Earth map, accessed 3/2015, url: https://www.google.com/maps/place/Tokyo,+Japan/@36.2025983,138.8095091,8z/data=!4m2!3m1!1s0x605d1b87f02e57e7:0x2e01618b22571b89

(36) Safecast (2013) https://api.safecast.org/en-US/bgeigie_imports/12568

(37) Kaltofen, M. P. J., (2014) *Follow-up of the Fukushima Dai-ichi Disaster: High Radioactivity Particles in Japanese House Dusts*, American Public Health Association 139th Annual Meeting and Exposition, November 17, 2014, URL: https://https://apha.confex.com/apha/142am/webprogram/Paper315702.html

Section 3: USA and Canada house dust detections

Traces of Fukushima accident-related radioactive
contaminants found in the US and Canada western coast

Distance from Fukushima Daiichi: 7546 km

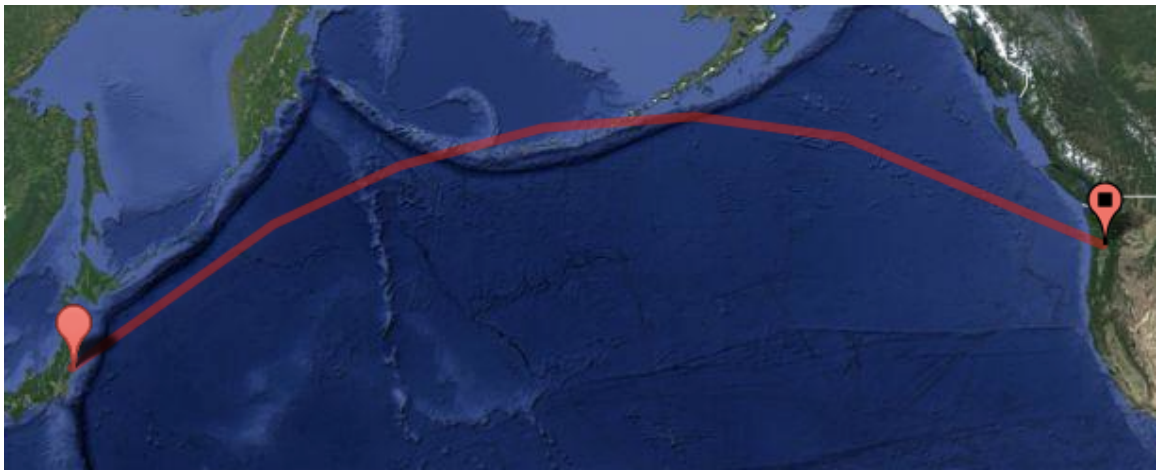

3.1 US and Canada Data

Introduction: An airborne plume of radioactive contaminants from the Fukushima Daiichi reactor accidents spread over Northern Japan. A diluted portion of this airborne plume reached the US and Canada. (8, USGS) Radioactive materials were released from the Fukushima Daiichi reactors after three reactors and a spent fuel pool catastrophically overheated, and at least two reactor structures detonated. (1, TEPCO)

The spent fuel assemblies at Fukushima Daiichi had an inventory of 134 MegaCuries of ^{137}Cs at the time of the accident, with much of this inventory in the spent fuel storage pools. Fresh fuel assemblies do not contain fission products, so these would not contribute to the cesium inventory. One percent or more of the cesium inventory was assumed lost to the airborne plume. (1, TEPCO)

The 1986 Chernobyl release aerosolized 1.5 MCi of ^{137}Cs, out of a total release of 270

MCi for all isotopes. (Am J Public Health. 2007 September; 97(9): 1595–1600.) This is about the same amount of ^{137}Cs as the Bravo test shot. When looking at radionuclide release totals, Bravo, Chernobyl, and Fukushima are fairly comparable events. While the total dispersed radioisotope quantities were similar in scale for Bravo, Chernobyl, and Fukushima Daiichi, but the population exposure patterns were very different. The exposures in Japan are lower, longer term doses, rather than acute doses received by those residing near the Bravo test site and Chernobyl.

The highest detected US exposures to Fukushima radionuclides were substantially less than those associated with more significant US radiation releases, such as the 1979 Church Rock Uranium Mine tailings pond dam collapse, which released 46 Ci of alpha emitters, or the 1986 Oklahoma Sequoyah Fuels Corporation release of 3 curies of uranium hexafluoride gas. (23, Brugge) The Church Rock accident was the largest release of radioactive material to the US public to date. This New Mexico release discharged more than three times the number of curies as the officially-stated 13 curies released at Three Mile Island. The Church Rock release, which impacted mostly low income, rural Native American Indians, is little known outside of the health physics community. These domestic exposures were higher in magnitude for the affected US residents, even though the distant Fukushima release was larger than the Three Mile Island, Church Rock, or Sequoyah Fuels releases.

In 2000, the Centers for Disease Control estimated that the 1954 record-breaking Bravo thermonuclear weapon test yielded about 100,000 Ci of ^{137}Cs per megaton detonated. The 1954 Bravo shot (~15 Megatons) released ~1.5 million curies of ^{137}Cs. A ten megaton H-Bomb would yield roughly as much ^{137}Cs as Fukushima Daiichi's total release to the environment. (13, Alvarez)

Measurement of Fukushima-related radioactivity in Japan or the US first requires that contaminants be distinguished from the radioactive background and these historic major

radiation release events. Background levels vary widely as a function of local sources of natural or industrial radiation, and altitude. Human exposure to background radiation also varies depending on diet, age, occupation, or medical care history.

Background radiation is sometimes described using examples, such as ^{40}K found naturally in bananas or exposure to cosmic radiation on an airline flight. Cosmogenic radiation, for instance, causes exposures in people traveling in airliners above the shielding provided by the atmosphere. These background exposures are qualitatively different from internal inhalation exposure to radioactive particles that emit alpha or beta particles. For example, insoluble inhaled radioactive dust particles may concentrate their activity on a single target organ, with the rest of the body shielded from any direct effects. This is particularly true for high LET short range radiation such as alpha particles. (25, HPS) External radiation fields, on the other hand, can expose the entire body uniformly. The biological effects of these internal vs. external doses are not necessarily identical, even if the amount of energy absorbed (effective dose) is the same. This does not equate to an assumption that the energy absorbed from an internal dose is more biologically effective than the external dose. Instead, internal vs. external exposures expose different tissues, at different rates, with potentially different biological results.

Primordial nuclides in inhaled or ingested dusts are another source of background exposure. This portion of this research ignores gross ^{238}U, ^{40}K, and ^{232}Th activities in attempting to detect traces of Japanese accident releases. The primordial nuclides were the dominant source of radioactivity in US and Canadian environmental samples, but are unrelated to events in Japan. Only four out of the 234 US and Canadian samples had detectable radiocesium, an isotope potentially from the events in Japan, while primordial nuclides were essentially ubiquitous in the sample set.

This assessment of residues from Fukushima's releases to the Western Hemisphere was aided by the existence of isotopes that are, on a practical level, unique to reactor

operations. Some of these isotopes also have modest half-lives, allowing researchers to rule out some other historic radiation releases. For example, ^{137}Cs (half life 30 yrs.) from nuclear test detonations of the 1950s and 1960 remains in the environment. The fission product isotope, ^{134}Cs, has a two year half life. The ^{134}Cs from bomb tests and from Chernobyl has essentially decayed away. Finding both ^{134}Cs and ^{137}Cs in an environmental sample was evidence of impact from the Fukushima release, while finding only ^{137}Cs, was not sufficient evidence.

Methods: Quantitative environmental data is used in this research to describe radiological impacts on US and Japanese dusts and soils. Additional data from the US Geological Survey and US Environmental Protection Agency sources are used to confirm data in this study. Data for this report was generated from environmental samples tested by NaI and GeLi gamma spectrometry at WPI's Dept. of Physics, by a commercial laboratory, and by CdTe X-ray spectroscopy.

Samples of indoor and outdoor dusts and soils were collected from throughout northern Japan and from the US, especially in the western US. The purpose of this sampling and testing was to compare relative Japan and US radioactive contamination levels, and to determine the size, composition, and morphology of dust particles with high radioactive contaminant levels, e.g., "hot particles." (see list of US/Canada samples in Appendix F)

A total of 234 US and Canadian environmental samples were collected and measured at WPI's Nuclear Materials Lab. These included samples of home air filters and vehicle engine intake filters, soils, and samples of dust from vacuum cleaner bags. Air samples were collected using 37 mm quantitative air filters and metered sampling pumps at known flow rates. Air sampling stations were set up in Massachusetts, Seattle, Aspen, CO, San Francisco, Hawaii, and Tokyo. An additional set of 85 Japanese samples are described in section 2, along with a detailed description of the full testing methodology.

Specific isotopes were measured that relate to likely sources within the failed reactors. These include nonprimordial isotopes such as ^{134}Cs, which is a high-yield fission product with a modest decay constant, ^{60}Co, which is a neutron activation product, and ^{241}Am, which is a component of spent or partially-burned nuclear fuels. These isotopes, along with the environmental setting of the samples, distinguish Fukushima contaminants from naturally occurring or industrial isotopes present prior to the arrival of the accident residues. These data on environmental samples provide insight into the limits to the size of the impact area of an IAEA level seven nuclear release. The objective of this study was to determine if hot particles or contaminated dusts related to the Fukushima Daiichi accidents could be detected at very long distances from the release site. These data also reveal that the exposures to US and Canadian populations were orders of magnitude lower than those experienced in Japan. Nevertheless, based on these data, some localized Western US exposures were higher than the overall US average exposure to radionuclides originating in Japan.

Results and discussion:

The detection of ^{241}Am was confirmed in this research for a limited number of dust samples from the greater Tokyo area, and in dust from one site in Sendai, Miyagi Prefecture, 100 km north of Fukushima. There were no detections of ^{241}Am or ^{239}Pu in any of the US samples tested at WPI. The only isotopes potentially related to Fukushima found in the US and Canadian samples were ^{134}Cs and ^{137}Cs.

By comparison, in northern Japan, researchers sampled offsite soil samples, finding many of the same elements found by SEM-EDS in dusts in Japanese homes for this study. These soils were collected along an axis running southeasterly 150 miles from Fukushima to Tokyo. Soils were found to contain the fission products: ^{131}I, ^{134}Cs, ^{137}Cs, ^{110m}Ag, ^{132}Te, ^{140}Ba, ^{140}La, ^{91}Sr, ^{91}Y, ^{95}Zr, and ^{95}Nb. (12, Shozugawa)

Offsite testing by Japanese agencies also found the neutron activation products ^{239}Np, ^{241}Am, ^{59}Fe and (rarely) ^{239}Pu. The original nuclear fuels ^{238}U, ^{235}U, and ^{239}Pu were found at the highest concentrations onsite at the Fukushima Daiichi complex itself. Recall that Unit Three is a MOX fueled reactor, so ^{239}Pu is potentially both a fuel material and a neutron activation product.

US air samples

Some US locations experienced a short term increase in airborne hot particles related to the passage of the plume of dust particles from Fukushima. (20, Diaz Leon) A total of seventy-one quantitative air filters from Massachusetts and Seattle, WA were analyzed. The Massachusetts filters showed a short term doubling of total beta counts per filter for the month of April 2011, @ 40 +/- 6 DPM, compared to later samples collected in May 2011 through December of 2011, @ 20 +/- 2 DPM. Each filter sampled 57.6 +/- 3 m^3 of air. For the entire set of filters, the beta DPM results were:

Table 3.1 Below: Beta DPM per filter

Seattle, WA	24.4 +/- 3.0
Natick, MA	32.2 +/- 6.9
Aspen, CO	21.7 +/- 3.7
Honolulu, HI	23.2 +/- 1.7
San Francisco, CA	25.6 +/- 2.9

Net alpha counts per filter for the month of April 2011 in Massachusetts were at 3 +/- 2 DPM compared to nondetect (0 +/- 1 DPM) for later samples collected in May 2011 through December of 2011. These results are presented below. Counts were done on Ludlum Model 3030 2-channel alpha beta counter. The counter is unable to distinguish between the various beta or alpha emitting isotopes, so these data provide only indirect evidence of the potential impact of radioactive contaminants related to Fukushima.

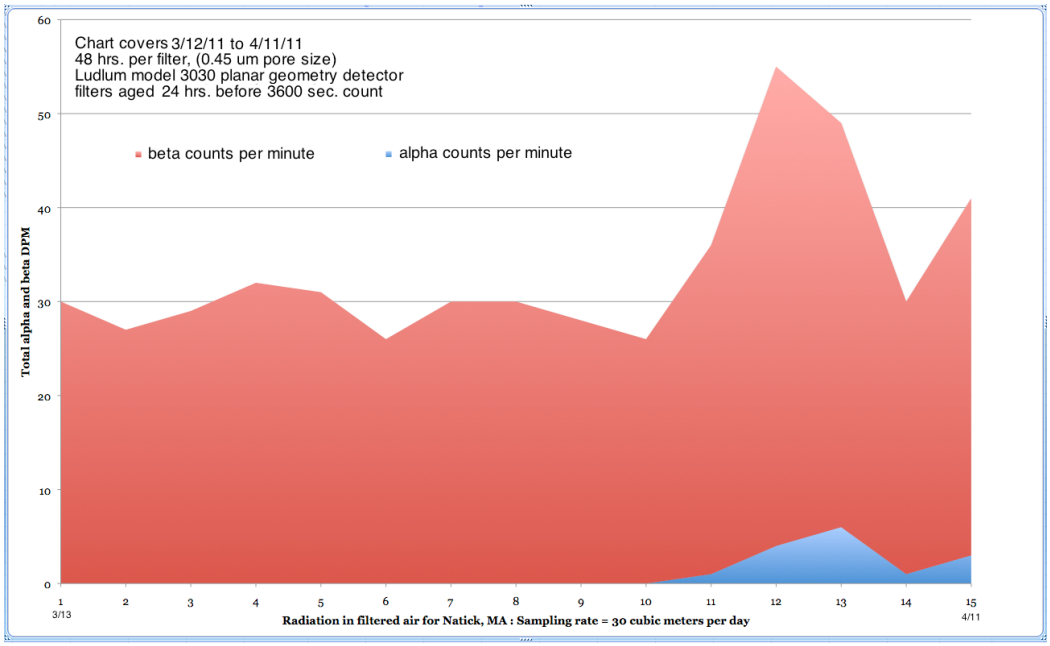

Fig. 3.2 Above: Total alpha and beta count data for quantitative air filters

The Seattle, WA filters collected during mid-April 2011 were autoradiographically positive. (See following page: Seven day autoradiographs on X-ray sensitive films of 37 mm air filter discs each exposed to 60 m^3 of air in Seattle, WA) The air filters from Seattle for this two week period in April 2011 were the only autoradiographically positive filters from the Western Hemisphere for the study period. While this is consistent with a potential increase in airborne radioactive particle concentration, the same effect could occur due to increased atmospheric dust concentrations such as that caused by higher average wind speeds. Autoradiography does not distinguish between industrial versus primordial nuclides. For this reason, it is not possible to determine the concentration of industrial hot particles in each filter (in effect, the HP concentration in each 60 m^3 air sample) without more extensive SEM/EDS analyses.

In total, thirty-seven filters were collected from Seattle, WA; six from Hawaii; thirty-four from Massachusetts; twenty-nine from Colorado; and eleven from San Francisco, CA. As noted, only the subset of the Seattle filters shown on the following page produced positive autoradiographs.

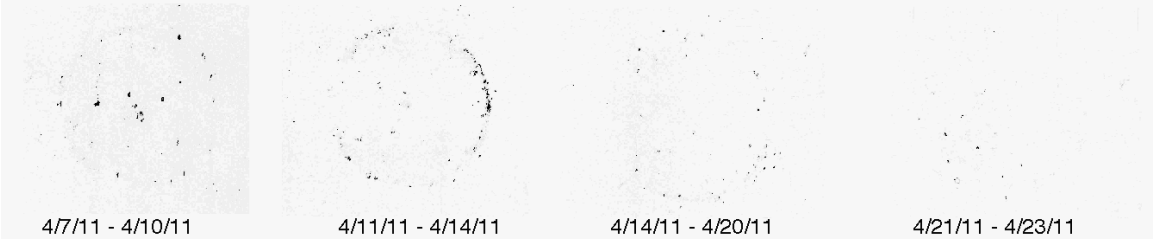

Fig. 3.3 Above: Seven day autoradiographs on X-ray sensitive films of 37 mm air filter discs each exposed to 60 m^3 of air in Seattle, WA

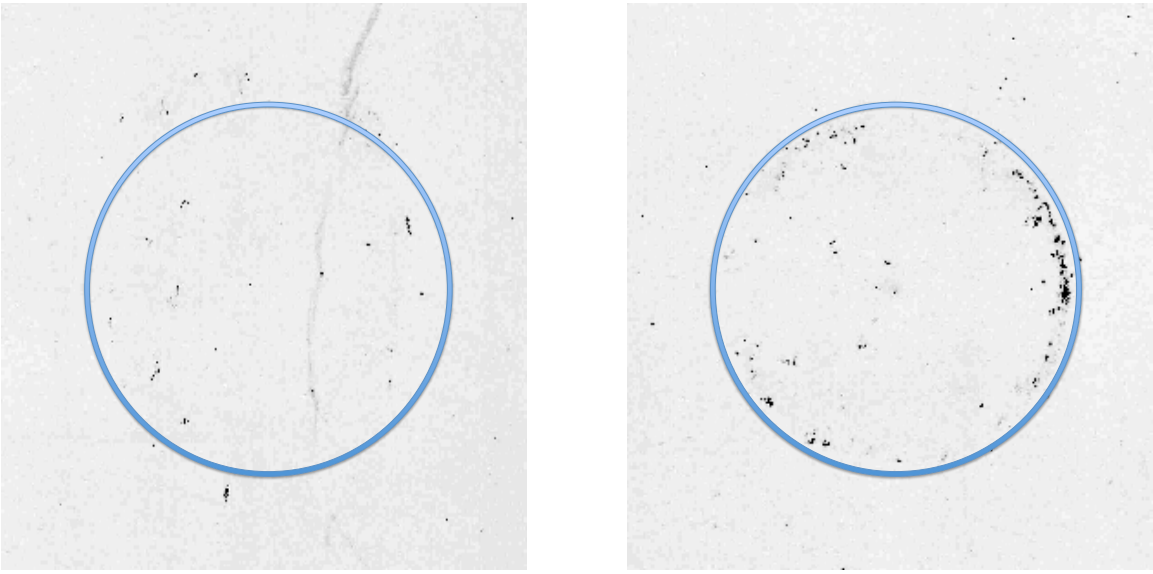

Fig. 3.4 Above: Autoradiographs of quantitative 35 mm air filters

Left: March 28 to April 1, 2011 Right: April 11 to April 14, 2011

SEM/EDS analyses were performed on two of the Natick, MA, air filters. These were the March 13, 2011, filter (essentially a pre-impact filter in this hemisphere, with beta DPM = 7.0 +/- 3.0) and the April 7, 2011, filter (beta DPM 37 +/- 3.0). No high Z particles were found using the SEM Robinson® detector for the March filter.

The April filter had a large number of particles containing zirconium, indium, or both. While neither element is explicitly radioactive, nor is their use restricted to nuclear reactors, they are used in reactor cores. Two of the elemental analyses for these particles are shown below. With one exception, the indium-containing particles also contained up to 3% zirconium. The exception was a particle of 99.9 % pure indium. Both metals are commonly found in nuclear reactors. Zirconium is used in the cladding of fuel assemblies because of its heat resistance and small neutron absorption cross section. Zirconium particles were commonly found in the SEM/EDS analyses of dusts from Fukushima City. Indium is a neutron absorbing material. Indium is normally alloyed with silver and cadmium in reactor control materials, but these elements were not detected in indium-containing particles for any sample.

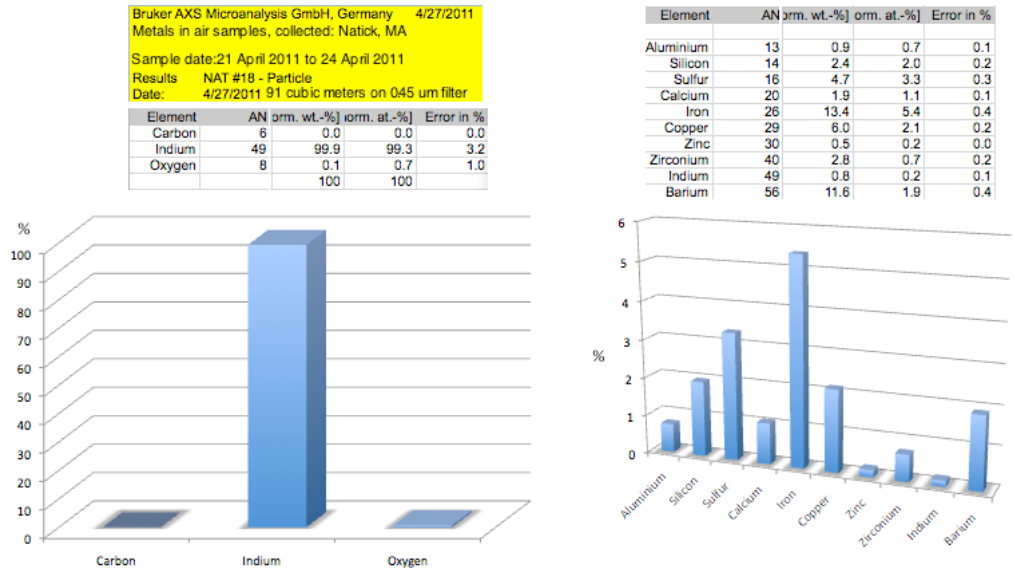

Fig. 3.5 Above: SEM/EDS data for indium-containing Massachusetts dust particles

Thirty-two US car engine filters and twenty Japanese car and truck engine filters were tested by gamma spectrometry at WPI. All of the Japanese vehicle engine filters contained ^{134}Cs, and ^{137}Cs at levels between 2.3 Bq/filter to 550 Bq/filter. Three car filter samples from the Fukushima area also contained a neutron activation product, ^{60}Co, at levels of about 1 Bq/filter.

Of the US filters, one filter from Seattle, WA, contained 0.04 Bq/filter of combined ^{134}Cs and ^{137}Cs. The remaining US filters did emit detectable radioactivity, often well in excess of 0.04 Bq/filter, but the radioactivity was in the form of primordial nuclides such as uranium and thorium daughters. Except for the one Seattle filter, radiocesium was not detected in any other US car filter samples.

These inferential data, and the explicit result for radiocesium in the Seattle car filter, indicate the potential for impacts from Japanese radiocontaminants in the US. The air filter samples collected in the US generally did not show significant impacts that were positively identified as related to Fukushima. Due to funding constraints, only three US air filters were fully analyzed by SEM/EDS. Analyzing a greater number of samples by this sensitive method may provide more certainly about the level of radiological impact in the US. Nevertheless, the data make clear that the number of hot particles in US and Canadian samples was low compared to Japan. Japanese dust samples were necessarily small, to prevent generating radiological wastes. On the other hand, US samples remained close to the limit of detectability for the gamma spectroscopy methods used.

The sampling method employed also was designed to detect hot particles. Radiological contaminants originating in Japan were clearly detected in the US by government observers. These studies used methods that sampled gases and precipitation for radioisotopes related to the accident. These methods were designed to detect trace contaminants in environmental media, rather than a small number of higher-activity particles.

The Pacific Northwest National Laboratory of Richland, WA, monitored three isotopes of xenon, ^{133}Xe, ^{131m}Xe and ^{133m}Xe, during the same time period. Short-lived xenon fission products are often used as indicators of anthropogenic nuclear activity. Xenon isotopes are routinely tested in air as part of efforts to assure compliance with the comprehensive nuclear test ban treaty. (19, PNNL) The laboratory documented a 100,000 times increase of gaseous radioxenon in ambient air during March 2011. The number of Bq of Xe per cubic meter of air moved from 1.0 EE-4 on March 6 to 6.0 EE+2 on March 19. The failure of the Fukushima reactors began on March 11, 2011.

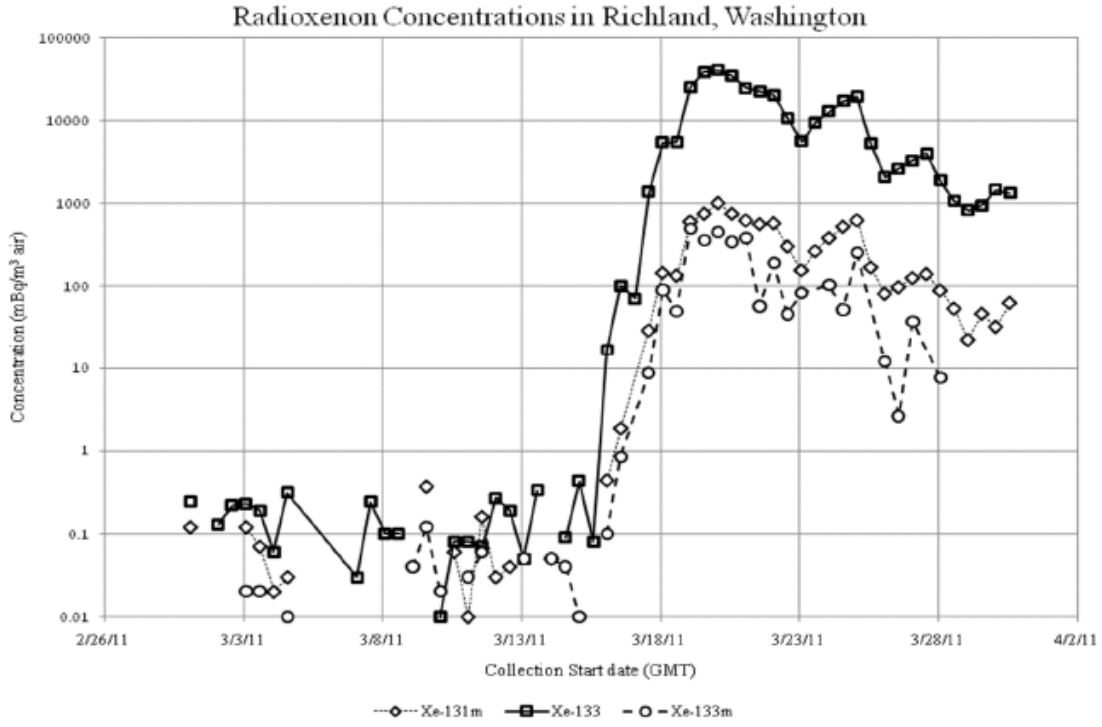

Fig. 3.6 Above: US Dept. of Energy data, 2011 (19, PNNL)

Soil and dust samples

A total of seventy-eight soil and six dust samples were collected in the US and Canada along with the air filters already described. The most contaminated of the US soil samples contained 0.30 +/- 0.10 Bq/g of ^{134}Cs and ^{137}Cs and the median US sample result

was a non detect at a limit of less than 0.03 Bq/g. Three US soil samples had 0.04 Bq/g of combined ^{134}Cs and ^{137}Cs. The remaining seventy-four US soil samples were nondetect for radiocesium. In Greater Tokyo more than 90% of the WPI-tested soil samples were between 0.4 and 11 Bq/g for combined ^{134}Cs and ^{137}Cs. The most contaminated soil sample was found in the Portland, OR, suburbs. A duplicate of the Portland sample was analyzed by a commercial Laboratory (General Electric Walter Miltz Lab./PACE Analytics) with a result of 0.41 +/- 0.12 total ^{134}Cs and ^{137}Cs.

The 0.30 Bq/g result was a WPI-tested soil sample from a farm in Portland, OR. The remaining positive soil samples came from other parts of Portland and from Boulder, CO. A 2012 USGS Fukushima fallout study also detected “hot spots” in these two cities, along with another hot spot near San Francisco. (8, USGS)

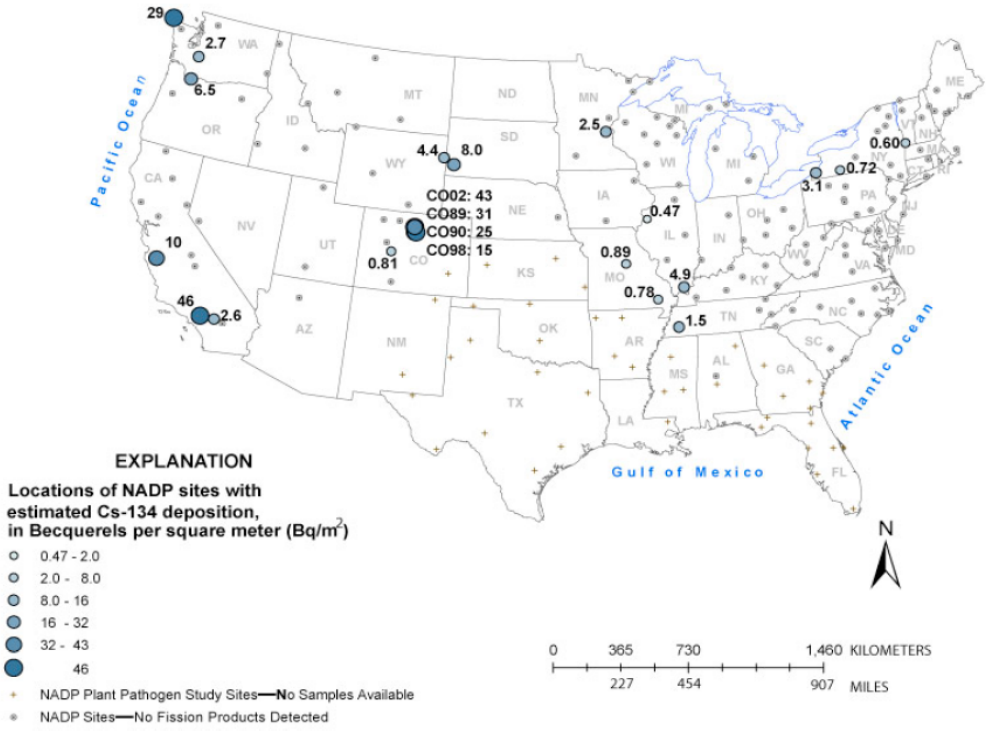

Fig. 3.7 Above, ^{134}Cs deposition in the US, USGS data March 15 to April 5, 2011

Section 3 Conclusions

Sampling locations studied in this research were partially chosen for their accessibility, and not due to any specific predictive model. Environmental samples were selected that would be more likely to contain any radioactively-hot particles. These data do not tell us how many remaining soil hot spots may have existed in the US, nor do they address radioactive cesium or radioactive iodine in atmospheric gases or in precipitation.

Massachusetts air particulate samples using quantitative 0.45 micron filters had beta count rates at about twice the background rate during portions of March and April 2011. Alpha count results were also elevated, but remained within a few counts per minute of background. Seattle, WA air particulate samples did not have elevated count rates, but did have the only US autoradiographically-positive results, while San Francisco, Massachusetts, Colorado, and Hawaii samples were autoradiographically-negative.

Two samples were selected from the Massachusetts filter set, one with and one without elevated beta count rates. The higher count rate sample had suspect but not definitively-radioactive particles that were potentially related to nuclear reactor materials.

West Coast automobile engine filters had detectable ^{134}Cs and ^{137}Cs in one sample out of thirty-two collected. Similarly, soil samples had detectable ^{134}Cs and ^{137}Cs in four out of seventy-four samples, with a maximum of 0.30 +/- 0.10 Bq/g of ^{134}Cs and ^{137}Cs in soil.

This data set shows that most US samples studied were below detectable limits for particulate matter carrying Fukushima-related radio-contaminants. There were a limited number of samples indicating both direct and indirect evidence of the presence of hot particles in particulate matter.

Section 3 References

(1) Fukushima Nuclear accident Investigation Committee, (2012) *Fukushima Nuclear Accident Analysis Report*, Tokyo Electric Power Company, Inc.

(2) United States Code of Federal Regulations, (2012) 40 CFR 141.66(d)

(3) Shleien, B., (1965) et al, *Particle Size Fraction of Airborne Gamma-Emitting Radionuclides by Graded Filters*, Science, Vol. 147 p. 290

(3) Eisenbud, M., and Harley, J., (1953) *Radioactive Dust from Nuclear Detonations*, Science, New Series, Vol. 117, No. 3033, Feb. 13, pp. 141-147

(4) Kaltofen, M. P. J., (2010) *Microanalysis of Workplace Dusts from the Mixed Waste Tank Farm of the Hanford Nuclear Reservation*, J. of Envir. Eng. Sci., February 2010

(5) Cizdziel, J. V., Hodge, V. F., (2000) Attics as archives for house infiltrating pollutants: trace elements and pesticides in attic dust and soil from southern Nevada and Utah, Microchemical Journal 64 2000 85 92

(6) Kathren, R. L., (1998) *NORM Sources and Their Origins*, Appl. Radiat. Isot., 49 (3) 149-168

(7) Lioy, (2003) *The historical record of air pollution as defined by attic dust, Atmospheric Environment*, 37, 2379 – 2389

(8) US Geological Survey, (2011) *Fission Products in National Atmospheric Deposition Program—Wet Deposition Samples Prior to and Following the Fukushima Daiichi Nuclear Power Plant Incident*, March 8, [2012] – April 5, [2012]

(9) United States Environmental Protection Agency, (2011) RadNet database, *Japanese Nuclear Emergency Radiation Monitoring Archive*, March – June 2011, URL: http:// www.epa.gov/japan2011/index.html

(10) Kaltofen, M. P. J., (2011) *Radiation Exposure to the Population of Japan After the Earthquake*, American Public Health Association 139th Annual Meeting and Exposition, Oct. 31, 2011, URL: https://apha.confex.com/apha/139am/webprogram/Paper254015.html

(11) AREVA, (2012) *The Fukushima Dai Ichi Incident* – Dr. Matthias Braun, PEPA4-G, AREVA–NP GmbH, October 5, 2012

(12) Safecast.org, (2012) crowd sourced environmental radiation monitoring dataset. Downloaded 12 October 2012. URL: http://blog.safecast.org/measurements.csv

(13) Bob Alvarez, (2010) The Legacy of Nuclear Weapons testing, Institute for Policy Studies, May 20, 2010 URL: http://www.ips-dc.org/reports/testimony_the_legacy_of_nuclear_weapons_testing

(14) Science, News 26/10/2012: V338 n. 6106 pp. 480-482

(15) D. Madigan, *Pacific bluefin tuna transport Fukushima-derived radionuclides from Japan to California*, Pro. Nat. Acad. Sci., 27 May, 2012

(16) Nature, *Ocean still suffering from Fukushima fallout*, 14 Nov. 2012

(17) Shozugawa, K., (2012) *Deposition of fission and activation products after the Fukushima Daiichi nuclear power plant accident*, Envir. Pollution, 163 (2012) 243-247

(18) Nature, *Fukushima fish still hot*, 26 Oct. 2012, Nature News blog

(19) T.W. Bower, et al., (2011) *Elevated radioxenon detected remotely following the Fukushima nuclear accident*, J. Environmental Radioactivity, 102 (2011) 681-687, as cited by Pacific Northwest National Laboratory, US Dept. of Energy

(20) Diaz Leon, J., et al., (2011) *Arrival time and magnitude of airborne fission products from the Fukushima, Japan, reactor incident as measured in Seattle, WA, USA*, J. Env. Rad., 102 (2011) 1032-1038

(21) Sohtome, Tadahiro, et al., Radiological impact of TEPCO's Fukushima Daiichi Nuclear Power Plant accident on invertebrates in the coastal benthic food web, J. Env. Rad., 138 (2014) 106-115

(22) Smith, John, et al., (2014) Arrival of the Fukushima radioactivity plume in North American continental waters, PNAS, www.pnas.org/cgi/doi/10.1073/pnas.1412814112

(23) Brugge, D. et al., *The Sequoyah Corporation Fuels Release and the Church Rock Spill: Unpublicized Nuclear Releases in American Indian Communities*, Am J Public Health. 2007 September; 97(9): 1595–1600. doi: 10.2105/AJPH.2006.103044 http://www.ncbi.nlm.nih.gov/pmc/articles/PMC1963288/

(24) Coggle, J.E., et al., (1986) *Radiation Effects in the Lung*, Environmental Health Perspectives, Dec; 70: 261–291

(25) HPS, Health Physics Society, (2010) *Environmental Radiation Fact sheet*, http://hps.org/documents/environmental_radiation_fact_sheet.pdf

(26) Shultis and Faw, Fundamentals of Nuclear Science and Engineering, Second Edition, ISBN:978-1-4200-5135-3, www.crcpress.com

Section 4: Perfluorinated compounds in house dusts

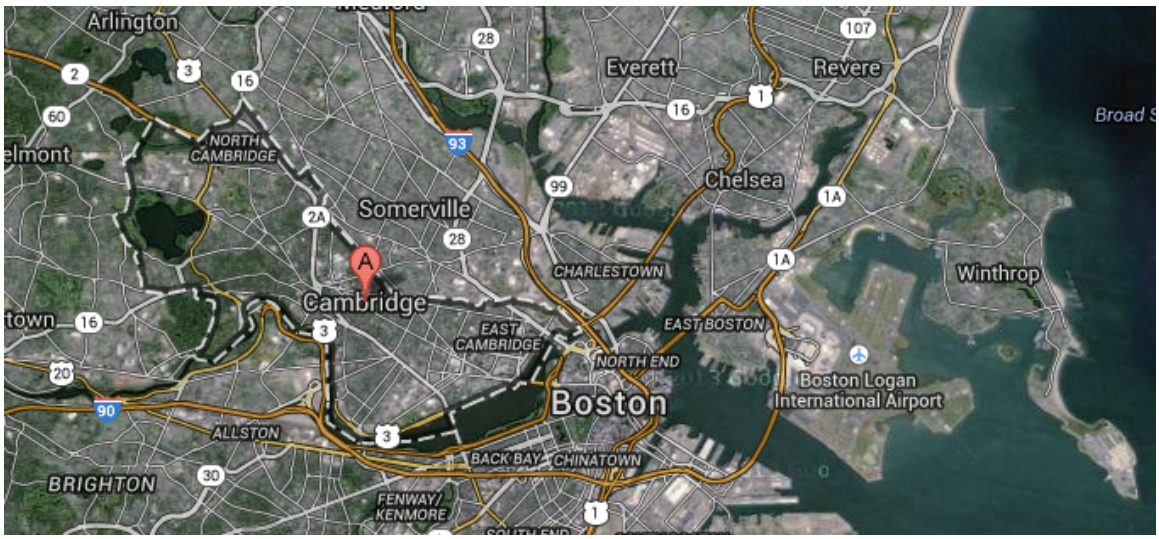

4.1 Introduction

This study sampled and measured the concentration of perfluorinated compounds (PFCs) in indoors dusts collected from residences. Samples were from three cohorts with known household income levels. Testing was by GC-ECD. This instrument is a widely available analytical tool. One objective of the study was to see if this instrument could produce usable data for perfluorinated compounds in dusts. A second objective was to examine data for significant concentration differences based on household income. Twenty-five vacuum cleaner bag dust samples were collected from households in Cambridge, MA. Results were compared to eleven similarly collected house dust samples from middle income homes in Washington State (n = 6) and low income homes in Alabama (n =5).

House dusts may contain chemical or radiological contaminants or both. Contaminated dusts represent a means of transporting contaminated materials over a distance, and also a potential route of exposure due to dust ingestion or inhalation. Calculating the dosage of contaminant intake is an important step in assessing the risk of potential biological effects. The US Environmental Protection Agency (26, EPA) provides the following

guidance for human exposure to inhaled and ingested dusts. Based on the 2011 EPA data, the adult dust daily ingestion and inhalation rates are:

Adult dust ingestion rate: 30 mg/day
Adult dust inhalation rate: 0.48 mg/day

Mass inhalation rates assume twelve cubic meters per day of air exchange, based on 9/2011 US EPA exposure factors data. The dust inhalation rate uses an average measured house dust concentration of 40 ug/m^3 for airborne indoor dusts less than 10 microns in size. This results in daily a dust intake rate for adults of 0.35 mg d^{-1}. (WHO 1989 data, as cited by 22, Butte) At this intake rate, indoor dust is a significant vector of human exposure to any chemical and radiological contaminants. These dust-borne contaminants may be from environmental or industrial sources. (1, Lioy; 3, Lewis; 4, Kato) Consumer products commonly contribute to chemical contamination in the indoor environment, including consumer goods that contain perfluoroalkyl and polyfluoroalkyl compounds. (4, Kato; 5, Huber)

Study Area: In Cambridge, MA, high technology, education and other services are the major drivers of the economy. Population density is heavily urbanized. Housing is mixed multi and single family homes. Overall, household income is above the national average. The dominant geographical feature is the Boston Basin. For this study, samples of house dusts were collected from self-identified high income and low income households within Cambridge.

Previous studies of breast cancer incidence rates have found positive correlations between household income, potential consumer chemical exposure, and breast cancer incidence. (17, Brody-Ozonoff) The Newton Breast Cancer Study found that higher income households were nearly twice as likely to use professional lawn care services and/ or home termite treatments than were lower income households.

Samples of household dust were collected from homes with (2013) household incomes at or below 50% of the reported City of Cambridge median household income, and from homes with reported incomes above 120% of the same median. Income guidelines are based on 2013 data provided by the City of Cambridge, MA. Incomes were adjusted for household size. The low income households report incomes below $47,200 per year for a family of four, and the higher income households report income greater than $113,280 per year for a family of four.

Table 4.1 Below: 2013 Cambridge, MA income guidelines in dollars

	below 50% of household median	above 120% of household median
1 person	< 26,440	> 79,320
2 persons	< 37,800	> 90,720
3 persons	< 42,500	> 102,000
4 persons	< 47,200	> 113,280
5 persons	< 51,000	> 122,400

Perfluorooctanoic acid (PFOA), perfluorooctane sulfonate (PFOS), Perfluorononanoic acid (PFNA), fluorotelomer alcohols (FTOH), and N-ethylperfluoro-1-octanesulfonamide (N-EtFOSA-M, FMC Corporation's branded pesticide, Sulfluramid®) are the most commonly encountered or measured perfluorinated compounds in both outdoor and indoor environments. (5, Huber; 6, Murakami; 7, Jogsten) These perfluoroalkyl compounds are amphiphilic, with functionalities that are soluble in both polar (aqueous) and nonpolar (lipid) solvents.

This set of perfluorinated compounds is used in coatings, textiles, pesticides and other consumer and industrial products. PFOS is no longer manufactured in the US, but can be imported in existing products. PFOS was part of the Scotchguard® stain repellent formulation, manufactured by the 3M Company. PFOA is used in the manufacture of

fluoropolymers such as Teflon® polymer manufactured by the DuPont Company. When heated, Teflon® polymers may degrade into PFOA. (13, US EPA)

Perfluorooctanoic acid (PFOA) and **perfluorooctane sulfonate (**PFOS) are stable, and are resistant to abiotic and biotic degradation in the environment. They have been detected in surface waters, sediments, WWTP effluents, and sewage sludge. PFOS is bioaccumulative in fish and fish-eating birds. (13, US EPA) PFOA, and to a lesser extent, PFOS, have been implicated in human and animal health damage. Perfluorinated compounds, including PFOA, have been implicated in the causation of obesity in women, reduced human birth weight, degraded semen quality in men, and increased human serum cholesterol levels. (8, Halldorsson; 9, Nelson; 10, Nordstrom; 11, Washino) Both PFOA and PFOS are among the 109 chemicals on the US EPA's revised second screening list of chemicals for tier 1 screening as part of EPA's endocrine disruptor screening program. (27, US EPA)

Sulfluramid® (N-EtFOSA) is an insecticidal compound and was previously registered for indoor use in roach and ant baits. According to US EPA product cancellation order EPAHQOPP 2007 1082 FRL 8364-2, all sales of products containing Sulfluramid® were scheduled to end in the United States on December 31, 2013. The reason for the cancellation was the compound's demonstrated reproductive toxicity. According to an August 23, 2001, *New York Times* article, one manufacturer of Sulfluramid®-containing consumer products was fined $950,000, by the state of New York for illegal distribution of roach baits that could cause irreversible reproductive and developmental damage. Sulfluramid® has been replaced in some formulations by the fluorinated aromatic amide, Hexaflumuron®.

Fluorotelomer Alcohols: "FTOHs are typically used as precursor compounds in the production of fluorinated polymers used in paper and carpet treatments and have similar applications as those of PFOS-based products." (18, Kissa; 19, Maras; 20, Ellis) The 8:2

vs. 10:2 and so on naming convention comes from the relative number of fluorinated versus hydrogenated carbons in the compound. The fluorotelomer alcohols 6:2 FTOH (perfluorooctanol) and 8:2 FTOH (perfluorodecanol) are estrogenic, upregulating estrogen-responsive genes. FTOHs biodegrade to perfluorocarboxylic acids. (20, Ellis) Analysis of purified FTOH standard materials has shown that linear perfluorinated alcohols are actually mixtures of linear and branched FTOH isomers. (19, Maras) FTOH and N-EtFOSA are more volatile than either PFOA or PFOS. N-EtFOSA is one of the most commonly detected volatile perfluorinated compounds in house dusts. (4, Kato) FTOH is a chemical precursor to PFOA and PFNA. FTOH can degrade in the atmosphere to a range of perfluorinated carboxylic acids. (20, Ellis)

PFOA, PFNA and PFOS data from existing studies may not be comparable, as methodologies are not optimized, nor have all of the data and methods been validated. (12, EPA) In particular, PFOS does not derivatize quantitatively. PFOS also exists in isomeric forms as a mixture of linear PFOS (L-PFOS) and as branched chain PFOS. (16, Letcher) While most investigators use LC-MS to quantify perfluorinated compounds, this equipment is not as common in laboratories as are GC-ECD units. Developing a reliable GC-ECD method for detecting PFCs in house dust was an important goal of this research.

4.2 Methods

This study determined the concentration of perfluorinated compounds (PFCs) in indoor dusts in two cohorts with varying income levels, using GC-ECD, a widely available analytical tool. The two study groups have different household incomes, but are both within the same community. Samples were collected from vacuum cleaners in private homes. Methanol (Sigma Aldrich LC-MS Ultra Chromasolv® grade) extracts of dust samples were analyzed for nonvolatile PFCs by first derivatizing the nonvolatile PFOS, PFOA and PFNA to more volatile isobutyl esters. Analysis then proceeded by GC-ECD. Inherently volatile perfluorinated sulfonamides and fluorotelomer alcohols were extracted

and run directly without derivatization.

Dust samples were sieved to separate the fraction passing 150 microns prior to analysis. Size separation helps ensure a consistent sample between households that is less dependent on the capture efficiency of the vacuum cleaner, and less biased by coarse materials that are not dust. In samples collected to assist in method development, this coarse matter has included paper clips, food items, medications, tacks and nails, pet foods, insects, nail clippings, textile remnants, wood chips, paper and similar materials which do not pass a # 100 ASTM standard sieve.

Sampling details: Samples consisted of the contents of whole vacuum cleaner bags or entire bagless vacuum cleaner contents. In a fume hood 5.00 g of the <150 um dust fraction passing a #100 ASTM sieve was removed for analysis.

Sample Collection: Cambridge residents were initially contacted via a local custodial trades union, which provided local names and addresses of individuals potentially willing to donate a dust sample. Various Cambridge community-based nonprofit organizations provided additional leads. All leads were emailed as a first contact. Residents willing to participate in the study were visited, and a dust sample was collected on the same day. While many residents offered to make introductions to neighbors and friends, none of these were followed up, as issues related to confidentiality could not be resolved. Instead, residents, if they chose, forwarded the initial study request email, and residents could decide independently if they wished to participate. No compensation of any kind was offered for participation in this study.

Cleaning: Sieves and glassware were cleaned with Alconox® or equivalent, followed by a DI water and then a methanol (Sigma Aldrich LC-MS Ultra Chromasolv® grade) rinse.

Sample Preparation: Sample documentation included the age and gender of residents, the

style of home (condo, apartment, single family house, townhouse), adult occupations, vacuum cleaner type and address. Samples and addresses were not cross referenced anywhere other than the sample log, which is kept in a secure location.

The entire vacuum bag was collected, or for bagless vacuum cleaners, a brush was used to place the entire contents of the bagless cleaner into a gallon-sized Ziplock® plastic bag. Bags were tagged with the appropriate study sample ID number. An example of the sample log sheet is appended to the end of this section. (See Appendix D)

Contents were weighed to three decimal places at the WPI Water Quality Laboratory. Fines were separated using a # 100 ASTM standard brass sieve. Hair passing the sieve was removed from the < 150 micron passed fraction using tweezers.

The 5.00 gram sample of fine dusts were placed in a tared 40 ml Teflon®-sealed glass jar and the gross filled weights were recorded. Samples were stored in a lab freezer until extracted. Between uses, each sieve was washed with Alconox® solution, rinsed with tap water, then with purified water (Thermo Scientific Barnstead® RO model D12651 in line with a Thermo Fisher NANOpure Ultrapure® Water System Model D11971) and Ultra® grade methanol, sequentially. A water rinsate blank was tested along with samples PFCs for this study.

Extraction Method Summary

1) Extract a 5.00 +/- grams fine (< 150 um) dust sample with 10 ml ultrapure methanol (Sigma Aldrich LC-MS Ultra Chromasolv® grade) in a 40 ml VOA vial.
2) 1 minute manual shaking, 10 minutes sonication, 30 minutes standing.
3) Pipette out solvent to a pre-cleaned 2 ml autosampler vial with a Pasteur pipette. Filter solvent through a glass fiber filter in the Pasteur pipette as needed to reduce turbidity. Fill vials completely. (approx. 2 ml)

4) Evaporate vials at room temperature to 1 ml mark.

5) Analyze raw extract for volatile PFCs.

6) If possible (meaning if analysis is completed on the same day) recover remaining extract for derivatization and analysis of PFOA, PFNA and PFOS.

7) Using a Pasteur pipette, derivatize according to the procedure.

8) Analyze extract immediately after derivatization as PFOS derivatives are not stable.

Blanks: Blank solutions were produced by extracting empty VOA vials selected at random, and derivatized as appropriate.

Standards: External standards were supplied by Sigma Aldrich, prepared in (Sigma Aldrich LC-MS Ultra Chromasolv® grade) methanol. MPFOS, PFOA and PFOS are the catalogue numbers for external standards from the same source, 50 ug/ml in 1.2 ml vials. Standards were run as calibration curves, with matrix addition spikes as quality control runs. Standards underwent derivatization for PFOA, PFNA and PFOS, and were run unaltered for FTOH and N-EtFOSA. Trifluoroacetate (TFA) was used as an internal standard, added directly to dust samples immediately prior to extractions.

Comparison samples: The eleven samples from middle income homes in Washington State and low income homes in Alabama had been archived in a laboratory freezer. These were originally collected from a study of house dust metals content. These had been stored sealed in plastic Ziplock® bags in their original vacuum cleaner bags. Aliquots from these samples were prepared at the same time and in the same fashion as the Cambridge, MA samples.

Target Analytes

Perfluorooctanesulfonate, PFOS, $C_8F_{17}SO_3^-$
MW: 538 (Potassium salt) CAS: 2795-39-3
MP: > 400 deg. C BP: NA
Fish bioconcentration factor: 1000 to 4000
VP (20 deg. C): 0.00033 Pa
Solubility in water 680 ppm at STP
pKa 3.3

Fig. 4.1 Below: PFOS (14, EFSA)

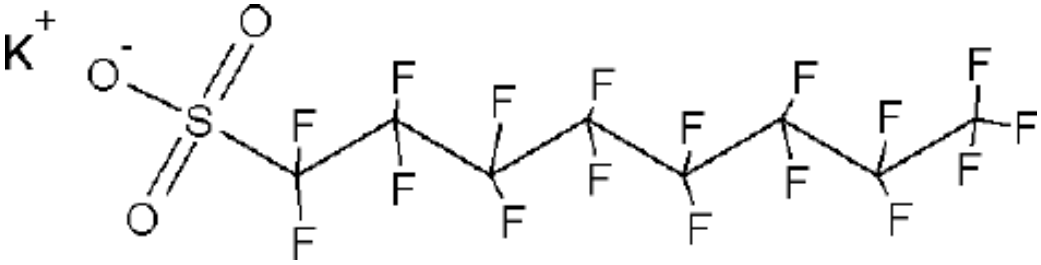

Perfluorooctanoate, PFOA, $C_7F_{15}COO^-$
MW: 413
MP: 55.2 deg. C BP: 188 deg. C
VP (25 deg. C): 4.1 Pa
Solubility in water 13,000 ppm at STP
pKa 2.5
Acid form structure

Fig. 4.2 Below: PFOA (14, EFSA; 25, Nielsen)

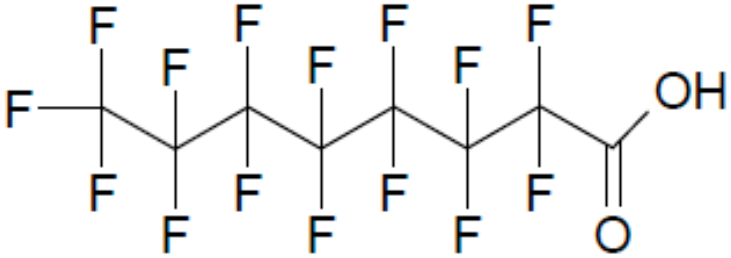

Perfluorononanoate, PFNA, $C_8F_{17}COO^-$
***N*-Succinimidyl 4,4,5,5,6,6,7,7,8,8,9,9,9-tridecafluorononanoate**

MW: 463
MP: 59-62 deg. C BP: 218 deg. C

Fig. 4.3 Right: PFNA

perfluoroundecanoate Sigma Aldrich # 73028-5mg
***N*-Succinimidyl 4,4,5,5,6,6,7,7,8,8,9,9,10,10,11,11,11-heptadecafluoroundecanoate**

Fig. 4.4 Below: PFDA

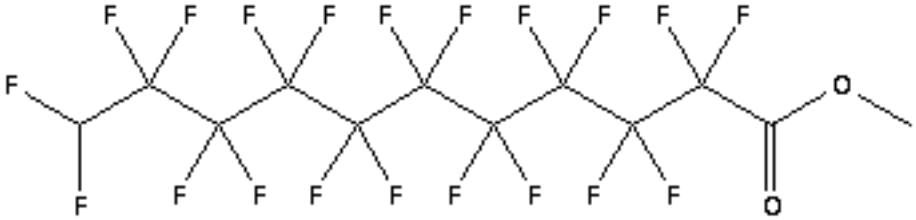

8:2 Fluorotelomer alcohol, 8:2 FTOH

1H, 1H, 2H, 2H-Perfluorodecanol

MW: 464.1

Fig. 4.5 Right: FTOH

6:2 Fluorotelomer alcohol, 6:2 FTOH

1H, 1H, 2H, 2H-Perfluorooctanol

MW: 364.1

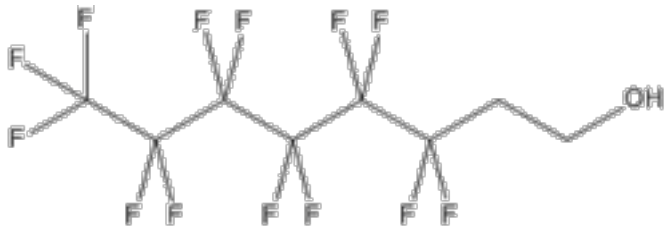

Fig. 4.6 Right: FTOH

N-ethylperfluoro-1-octanesulfonamide, N-EtFOSA, $C_{10}H_8F_{17}NO_2S$

MW: 527.2, CAS: 4151-50-2

Fig. 4.7 Below: Et-FOS

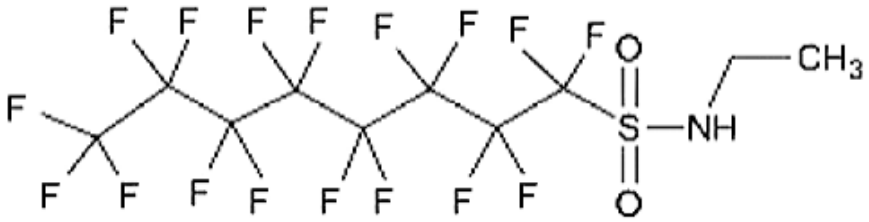

Perfluor-1-octanesulfonamide, a major metabolite of N-EtFOSA.

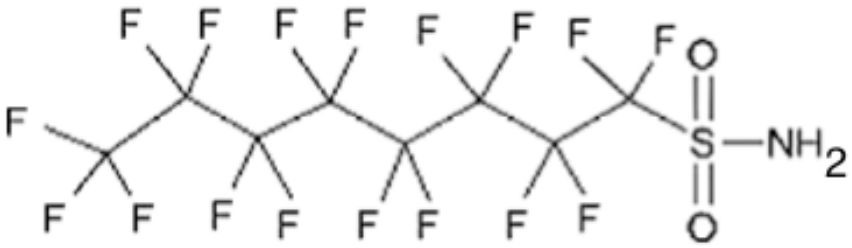

Fig. 4.8 Above: Hydrolysis product of Et-FOSA

Melt point, boiling point , molecular weight and solubility data is by Sigma Aldrich, Inc. (28, Sigma) unless stated.

Derivatization: The PFOA, PFNA, PFDA, PFUA and PFOS molecules are highly polar, and are poorly mobilized during gas chromatography. Boiling points of PFOA isomers cluster around 190 deg. C. Derivatization of per fluorinated carboxylic acid and per fluorinated sulfates form isobutyl ester analogues that are less polar and more volatile than the precursors. Adapting the procedure by Dufkova et al, pyridine-catalyzed esterification with isobutyl chloroformate was used to form the isobutyl esters of the per fluorinated carboxylic acids and sulfates. (2, Dufkova) The net reaction for PFOA is below. The reaction forms a reactive intermediate which decarboxylates, as shown.

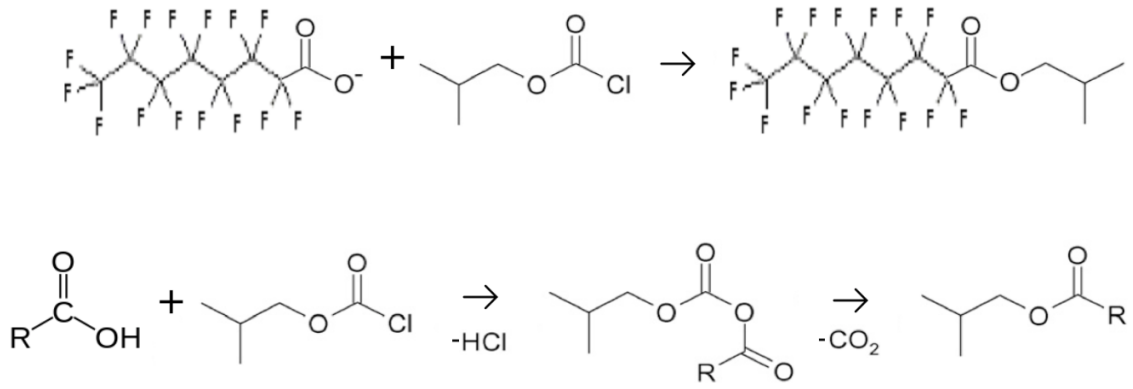

Fig. 4.9 Above: Derivatization scheme for PFOA (2, Dufkova)

Derivatization was done in 2 ml autosampler vials with 1.0 ml methanol extract. The ACS-certified reagents added were 50 uL isobutyl alcohol, 25 uL pyridine and 50 uL isobutyl chloroformate. (IBCF). Vials were then sonicated for ten minutes. PFOS derivatized nonquantitatively using the isobutyl ester method. A parallel derivatization procedure was adopted using 50 uL tetrabutyl ammonium hydroxide added directly to each vial with 1 ml of sonicated dust methanol extract. Fluorotelomer alcohols and perfluorosulfonamides are less polar than perfluoricarbozylic acids. These are sufficiently volatile for GC separation, and were underivatized.

GC-ECD conditions:

GC-ECD analyses used an Agilent® 6890 gas chromatograph and a 30 meter 0.25 mm ID, 0.25 um film thickness Restek® SIL column with splitless injection and ^{63}Ni electron capture detection. The GC oven temperature program was ramped to a high temperature (290 ◦C) to reduce analyze carry over between runs. Multiple blanks were run in succession to ensure a full return to a clean baseline between runs. Individual response factors were also very sensitive to changes in GC conditions. An Agilent® 7683 automatic liquid sampler was used for sample injection.

Initial oven temp. 50 ◦C
Inlet temp. 175 ◦C
Back detector temp. 250 ◦C
Carrier gas: N_2 at 0.44 mL min−1
On injection, hold oven at 50 ◦C for 1 min.
Ramp at 5 ◦C/min. to 90 ◦C
Ramp at 10 ◦C/min. to 220 ◦C
Hold for 3 min. at 220 ◦C
Ramp at 15 ◦C/min. to 250 ◦C
Hold for 2 min. at 250 ◦C
Ramp at 10 ◦C /min. to 290 ◦C
Fan on, cool down to 50 ◦C

A DB-5 second column test for Sulfluramid® was performed separately to confirm the retention times for this compound.

4.3 Results:

Example chromatograms for individual standard solutions are shown below. The GC-ECD chromatograms of derivatized PFOA, fluorotelomer alcohol, mixture of 6:2, 8:2 and 10:2 FTOHs; n-ethyl perfluoro-1-octane sulfonamide (Sulfluramid®), and trifluoroacetic acid are shown below. These volatile PFCs are underivatized.

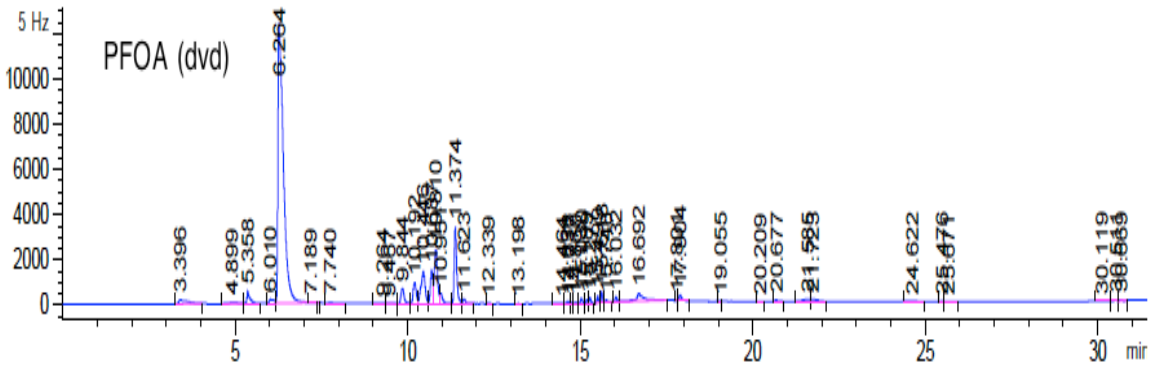

Fig. 4.10 Above: GC-ECD chromatogram: 20 ug/ul of derivatized PFOA, showing the derivatized PFOA at RT = 6.264 min., and the solvent peak at RT = 3.396 min.

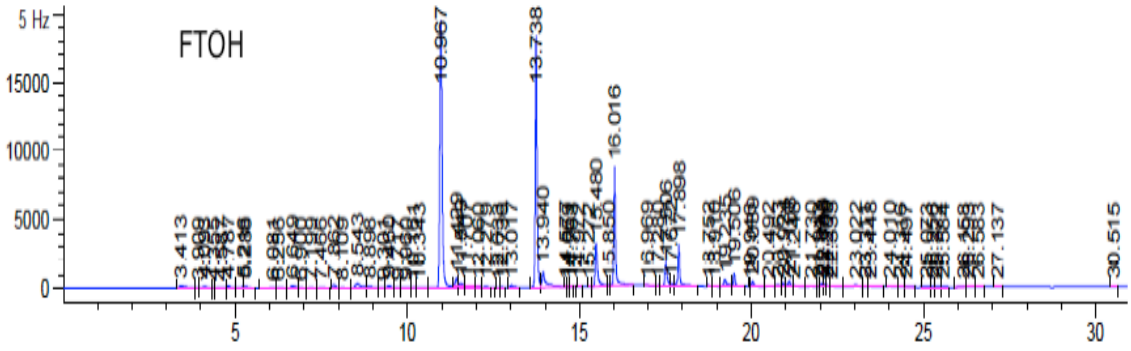

Fig. 4.11 Above: GC-ECD Chromatogram: 4 ug/ul underivatized (volatile) FTOH mixture showing the primary peaks of the mixture at RT = 10.967, 13.738 and 16.010 min.

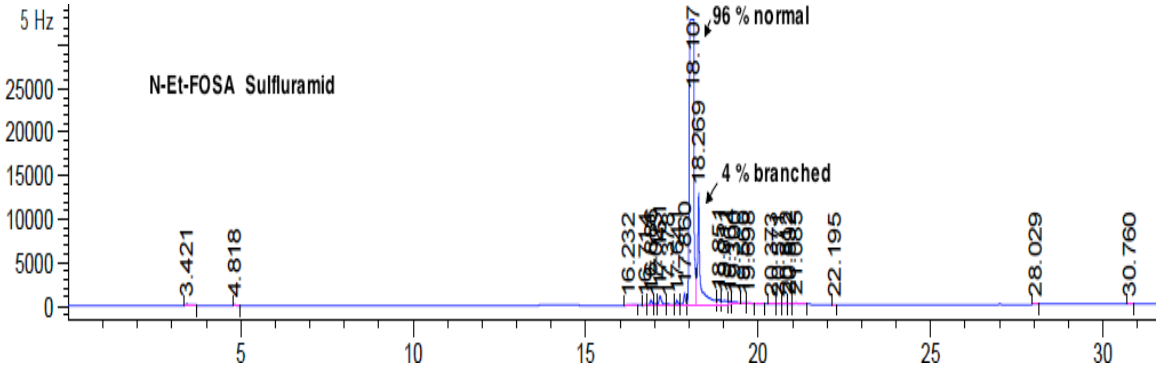

Fig. 4.12 Above: GC-ECD Chromatogram: 1.5 ug/ul underivatized Sulfluramid®, showing the parent peak for Sulfuramid® at RT = 18.107 min. and a branched isomer of Sulfluramid® at RT = 18.269 min.

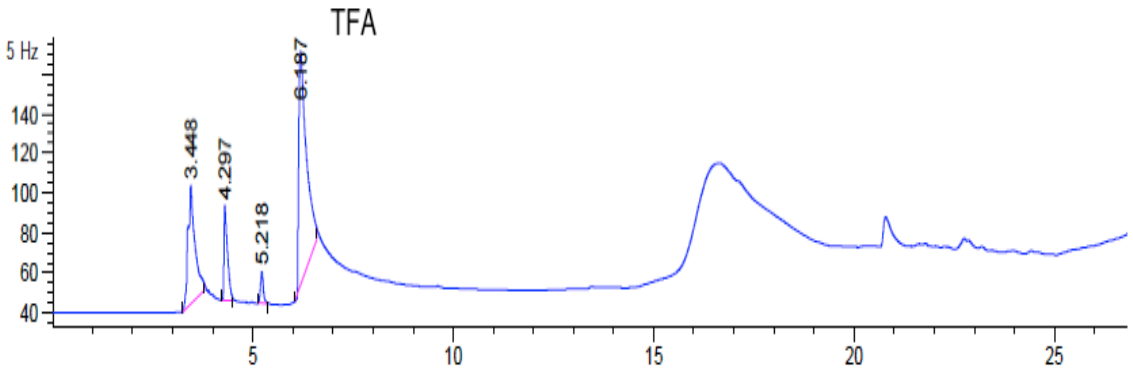

Fig. 4.13 Above: GC-ECD Chromatogram: 20 mg / ml Trifluoroacetic acid (TFA) showing the TFA peak at RT = 6.187 min. TFA was originally proposed a quality control check on volatilization of derivatized PFOA, however its retention time was too close to that for derivatized PFOA (6.264 min.) to be usable. The two peaks overlapped under these chromatographic conditions. In addition, the TFA response factor was very low and displayed multiple higher boiling peaks.

This page and the following page shows the aggregated mean results of the analyses of the twenty-five Cambridge, MA, samples by household income, and a comparison set of eleven samples from middle income homes in Washington State and low income homes in Alabama.

Table 4.2a Below: Results of GC-ECD Analyses, part 1 of 2

Primary Analyte	PFOA	PFNA	PFDA	PFUA	6:2 FTOH	8:2 FTOH	FTOH
Synonym	PF8A	PF9A	PF10A	PF11A	perfluoro octanol	perfluoro decanol	Flurotelomer alcohol mix
fluorinated alcohol degradation product or isomer of primary analyte							isomer of FTOH mix
Units - Dry wgt. concentrations, PPM	mg/kg in dust	mg/kg in dust	mg/kg in dust	mg/kg in dust	mg/kg in dust	mg/kg in dust	mg/kg in dust
Column 1 Retention Time (minutes)	6.276	8.401	11.972	14.149	8.569	18.634	11.594
Mean upper income Cambridge home	**<0.002**	**<0.015**	**<0.010**	**<0.25**	**0.621**	**0.009**	**0.136**
SD (n=16)					1.21	0.027	0.441
Mean lower to middle Cambridge home	**0.0045**	**<0.015**	**<0.010**	**<0.25**	**0.336**	**<0.005**	**0.151**
SD (n=9)	0.0091				0.763		0.252
Mean lower to middle income home, outside of Cambridge	**0.0006**	**<0.015**	**<0.010**	**<0.25**	**< 0.027**	**<0.005**	**< 0.005**
SD (n=11)	0.0024						

Table 4.2b Below: Results of GC-ECD Analyses, part 2 of 2

Primary Analyte	FTOH	FTOH	FTOH	Et-FOSA	Et-FOSA	FTOH	FTOH
Synonym	Flurotelomer alcohol mix	Flurotelomer alcohol mix	Flurotelomer alcohol mix	sulfluramid	isomer of sulfluramid		
fluorinated alcohol degradation product or isomer of primary analyte	isomer of FTOH mix	isomer of FTOH mix	isomer of FTOH mix			isomer of Et-FOSA and FTOH	isomer of Et-FOSA and FTOH
Units - Dry wgt. concentrations, PPM	mg/kg in dust	mg/kg in dust	mg/kg in dust	mg/kg in dust	mg/kg in dust	mg/kg in dust	mg/kg in dust
Column 1 Retention Time (minutes)	16.025	16.73	17.898	18.025	25.535	18.806	9.948
Mean upper income Cambridge home	**0.0526**	**0.0639**	**0.003**	**15.4**	**0.166**	**0.251**	**0.120**
SD (n=16)	0.0201	0.0606	0.012	33.6	0.213	0.573	0.245
Mean lower to middle Cambridge home	**0.0306**	**0.0479**	**<0.001**	**12.5**	**0.050**	**0.004**	**0.185**
SD (n=9)	0.0113	0.0500		9.5	0.052	0.012	0.41
Mean lower to middle income home, outside of Cambridge	**0.0225**	**0.0172**	**0.0047**	**1.52**	**0.048**	**0.006**	**0.773**
SD (n=11)	0.0079	0.0224	0.0128	3.75	0.070	0.017	0.967

These data are also shown graphically on the following page as mean data for each PFC compound, divided by income group. Given the high variability in the samples, the mean concentrations for the different income levels did not differ by two or more standard deviations. Sulfluramid® (Et-FOSA) was significantly lower for the low to middle income Washington households than for either the affluent or non-affluent group in Cambridge, MA. The difference was more than two standard deviations. Note that the tables on the following page are logarithmic.

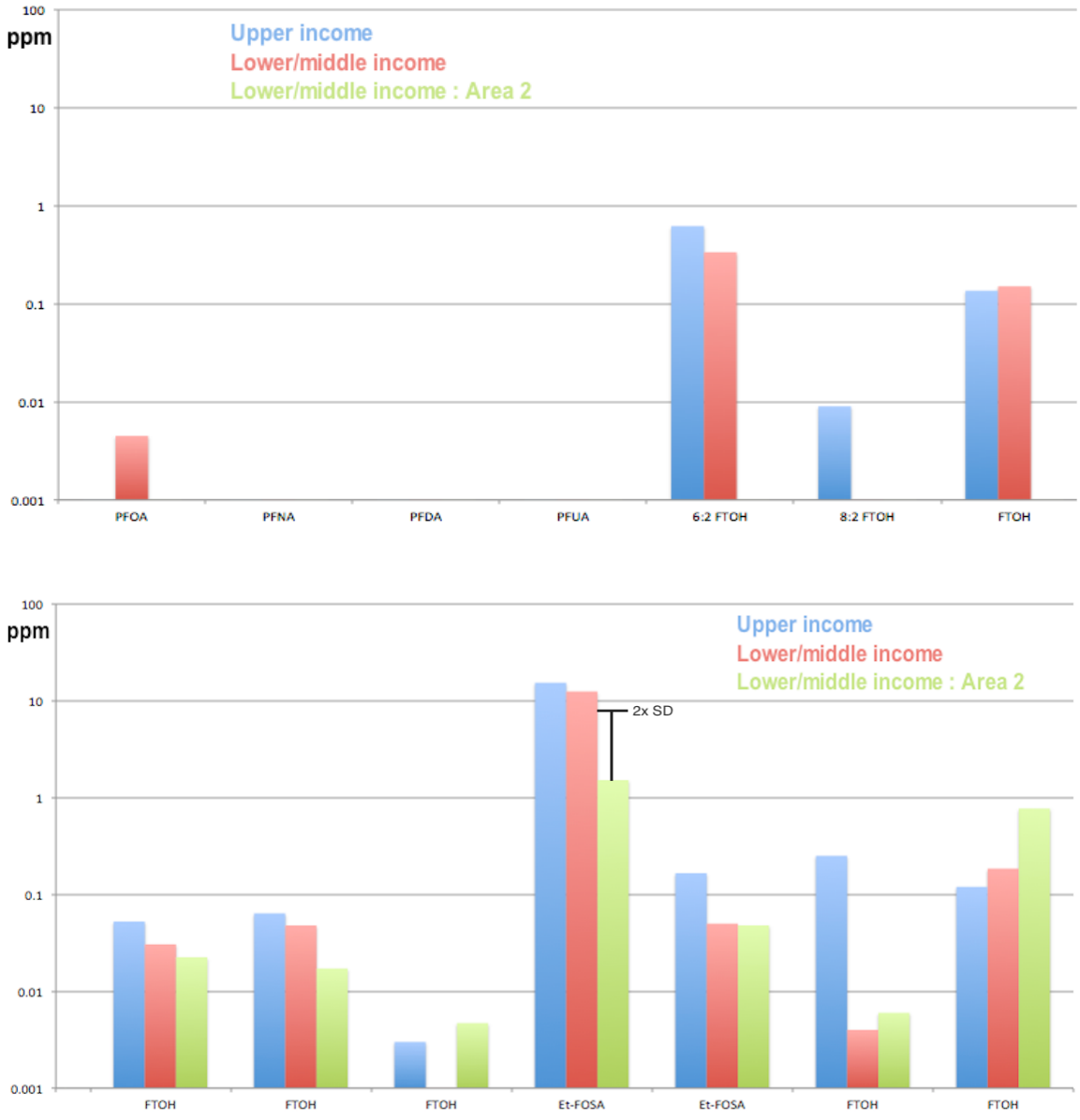

Fig. 4.14 Above: Mean PFC results in dust (mg kg^{-1}) by compound and income bracket

The distribution of total PFCs in the dust samples as a whole followed a Gaussian curve. The graphs on the following page show the total GC-ECD peak areas for each sample. Peak areas were graphed instead of concentrations due to chromatographic overlaps. Et-FOSA and FTOH compounds are isomeric mixtures. Certain isomers of both types of PFCs had identical retention times (RTs) and could not be separated. They may, in fact,

have been identical compounds as well, but this was not determined analytically. These overlapping RTs are noted in the two data tables, "Results of GC-ECD Analyses." Graphing by peak area circumvented this difficulty, so long as total PFCs rather than individual PFCs were being related.

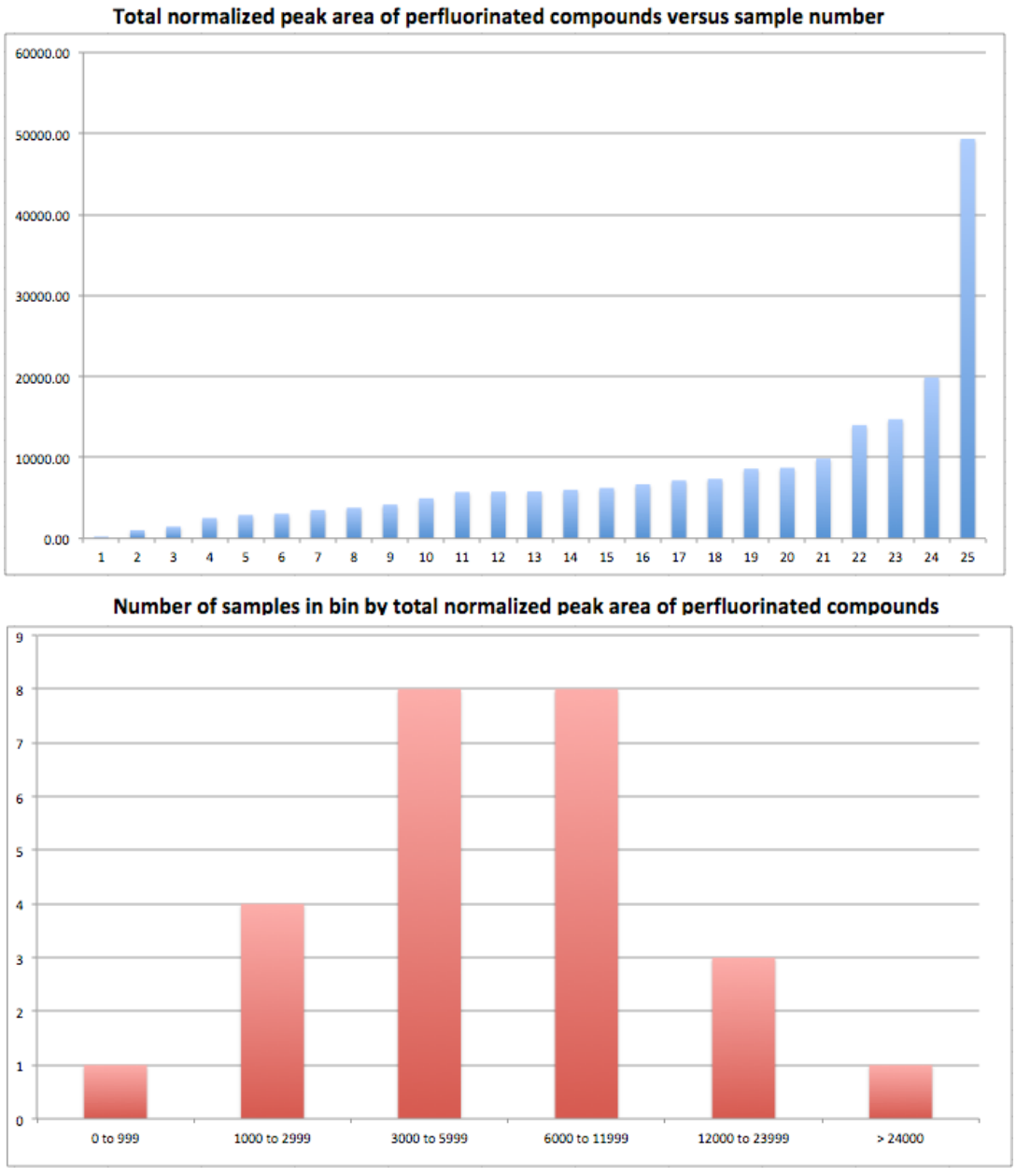

Fig. 4.15 Above: Histograms of GC-ECD Results for 25 dust samples

Discussion

The PFOS derivatization method was not successful. After repeated attempts, no stable volatile perfluorinated compound amenable to the GC-ECD technique could be reproducibly measured. An alternate TBAH (Tetrabutyl ammonium hydroxide) derivatization was attempted. This did produce a small reproducible peak at RT 28.91 minutes, but this peak also appeared in the derivatization method blank. (See below)

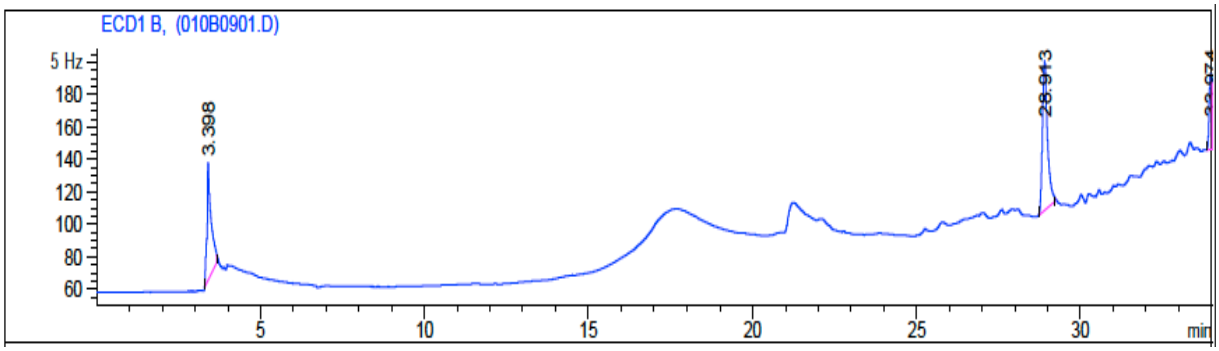

Fig. 4.16 Above: Method blank, TBAH derivatization of PFOS, showing solvent peak at RT = 3.398 min. and TBAS reagent peak at 28.913 min.

PFNA, PFDA, and PFUA were successfully derivatized and analyzed by GC-ECD, but were not detected above the limits of detection for this sample set. These limits were, respectively, 0.015, 0.010 and 0.25 mg kg^{-1}. The limit for PFUA was an order of magnitude higher than for any other perfluorocarbozylic acid tested.

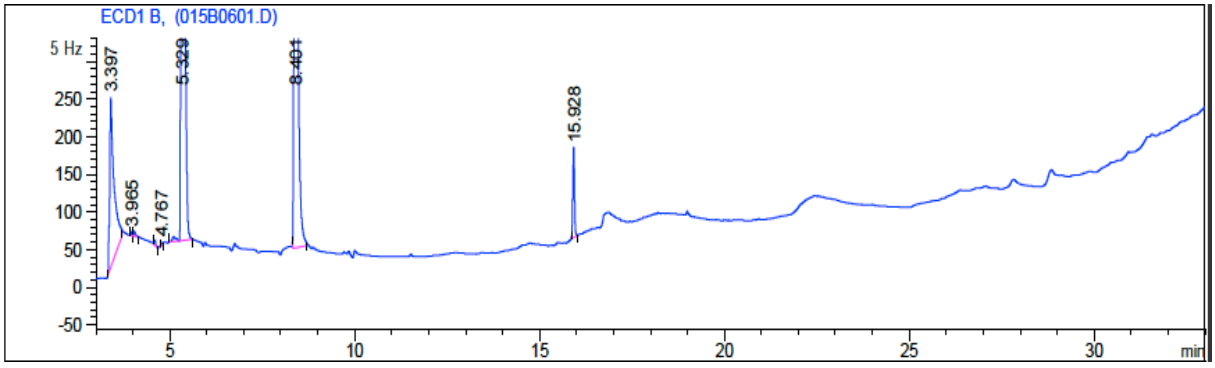

Fig. 4.17 Above: 12.6 mg ml^{-1} of isobutyl ester of PFNA showing analyze peak at RT = 8.401 min.

PFOA was successfully derivatized and was found above the detection limit (2x SD) of 0.002 mg kg^{-1} in the sample sets. The detector response factor for the isobutyl ester of PFOA was two orders of magnitude lower than for the volatile perfluorinated alcohols, which implies a relatively poor yield to the chemical derivatization reaction. No standardized isobutyl ester of PFOA was commercially available as a comparison material, thus it is unproven whether this low response factor was related to the nature of the derivatized product, or if it was due to poor chemical yield in the derivatization process itself. The result of this low response factor was that the detection limit for PFOA was in the low parts per billion range, rather than in the sub parts per billion range reported with electrospray LC-MS methods. The GC-ECD chromatogram showing this RF disparity is below. The RF increased as sonication time during derivatization was extended, implying that chemical yield was at issue.

When the volume of the injection was increased from 1 uL to 8 uL (two injections of 4 uL each), the response factor increased.

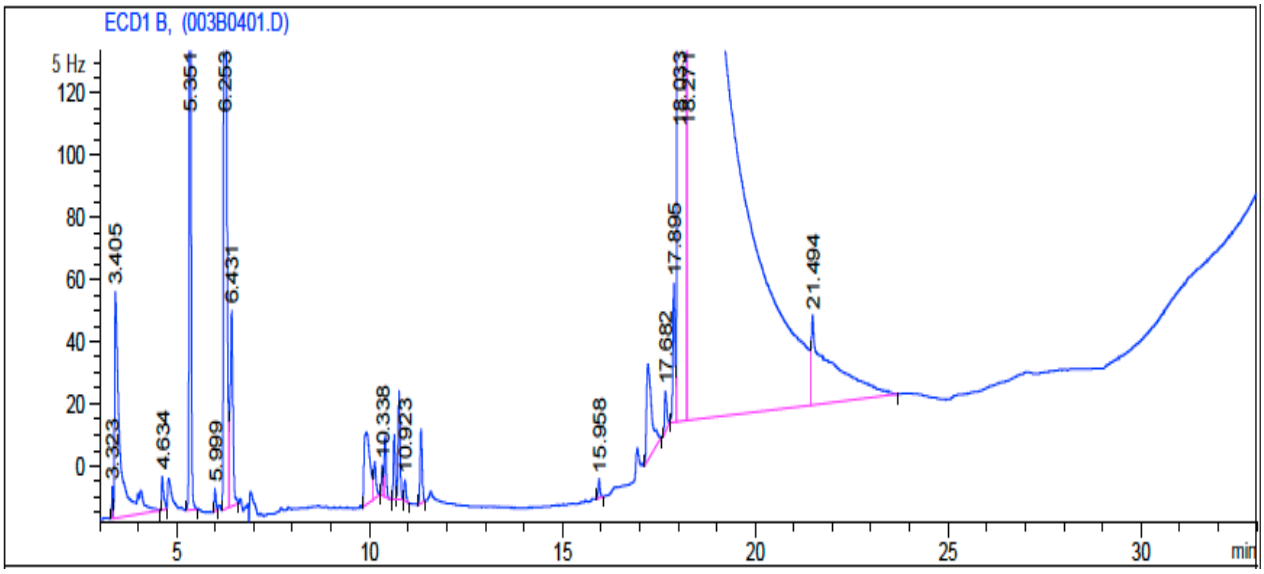

Fig. 4.18 Above: i uL injection of 1 mg ml^{-1} of IB ester of PFOA (6.26 min.) and Et-FOSA (18.21 min.)

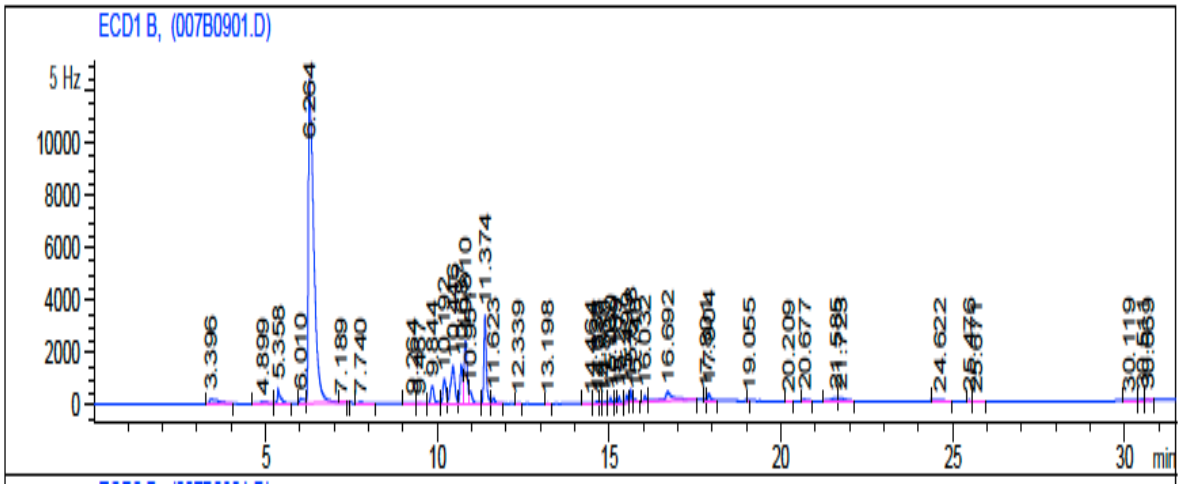

Fig. 4.19 Above: GC-ECD chromatogram, PFOA, 1 mg ml^{-1} with 2x4 uL injections with IB ester of PFOA at RT = 6.264 min.

The variability among samples for Et-FOSA and FTOHs was large. (See Table 4.2a and Table 4.2b) The variabilities between replicates of the same sample, on the other hand, for Et-FOSA and FTOHs were low. The relative standard deviation between replicates of the same sample was generally less than 1% for identical conditions. All thirty-six dust samples contained detectable concentrations of perfluorinated compounds in the form of Et-FOSA, and/or FTOHs of various fluorinated chain lengths. Relative standard deviations were calculated from the base peak for each compound. This was necessary because FTOH mixtures, different numbered FTOHs (e.g. 6:2 FTOH), and Et-FOSA had minor peaks with identical retention times. These may or may not have been the same isomer or impurity compound. These minor peaks were absent in method blanks.

Given the high number of non detects for the derivatized PFCs, the relative standard deviations between dust samples is not meaningful. Only two of thirty-six samples had detectable PFOA, and only three of thirty-six samples had detectable PFDA (Perfluorodecanoic acid). The remaining derivatized PFCs went undetected in the full sample set. The relative standard deviation among replicates for derivatized PFCs was on

the order of 25% to 30%, even for identical conditions. Higher relative deviations were found when replicates for polar nonvolatile PFCs came from different derivatization batches.

US EPA dust inhalation and ingestion guidance was discussed in Section 2.8 (http://www.epa.gov/ncea/efh/pdfs/efh-chapter05.pdf). In this guidance, the US adult dust ingestion rate is assumed to be 30 mg d^{-1}, while the US adult dust inhalation rate is 0.48 mg d^{-1}. The mean Sulfluramid® concentration all Cambridge, MA, households was 14.0 ug g^{-1} (SD = 21.0 ug g^{-1}). This gives a daily Sulfluramid® intake value of 0.43 ug d^{-1} (SD = 0.64 ug d^{-1}).

4.4 Conclusions

This study of house dusts found that all thirty-six dust samples analyzed contained measurable volatile perfluorinated alcohol and/or amide contaminants. These perfluroinated compounds (PFCs) were detected using by gas chromatography with electron capture detection (GC-ECD). This instrumentation is common in academic and commercial laboratories.

One compound, the deregistered pesticide Sulfluramid®, was found in greatest abundance, and it also was found at the highest concentrations in homes with the greatest household income levels. Polar, less volatile, perfluorinated compounds were found in only five of thirty-six dust samples tested. The detection limits for these compounds (PFOA, PFOS, PFNA, PFDA and PFUA) were elevated by an order of magnitude or more compared to volatile PFCs. PFOS was not detectable by this method. The universal prevalence of anthropogenic perfluorinated compounds in house dusts studied for this research is a potential health hazard. This study reinforces the existing evidence that house dusts represent a significant source of contaminant exposure to the public.

Further research involving GC-ECD techniques for polar perfluorinated compounds would benefit from improvements to the derivatization method. The yield of isobutyl esters of perfluorocarboxylic acids is too low by this method to provide fully usable detection limits. Method improvements could focus on the rigor of the derivatization process, the recovery of ester derivative from the dust matirx, or increases in the precision of polar PFC analyses. Making these changes would allow more labs to perform meaningful PFOA and PFOS analyses.

Section 4 Acknowledgments**:** The author gratefully acknowledges the more than two dozen households in Cambridge, MA, that provided samples for these analyses.

Section 4 References

(1) Lioy, Paul J., (2002) Dust: A Metric for Use in Residential and Building Exposure Assessment and Source Characterization, Environmental Health Perspectives

(2) Dufkova, Veronika et al, A fast derivatization procedure for gas chromatographic analysis of perfluorinated organic acids, Journal of Chromatography A, 1216 (2009) 8659–8664

(3) Lewis, Robert G., (1999) Distribution of Pesticides and Polycyclic Aromatic Hydrocarbons in House Dust as a Function of Particle Size, *Environmental Health Perspectives,* 107 (9) 721-726

(4) Kato, Kayoko, (2009) Perfluoroalkyl chemicals in house dust, *Environmental Research*, 109 518 – 523

(5) Huber, Sandra, (2011) Per- and polyfluorinated compounds in house dust and indoor air from northern Norway – A pilot study, *Chemosphere*, 84 1686 – 1693

(6) Murakami, Michio et al, (2008) Perfluorinated surfactants (PFSs) in size-fractionated street dust in Tokyo, *Chemosphere* 73 1172-1177

(7) Jogsten, Ericson, et al, (2012) Per- and polyfluorinated compounds (PFCs) in house dust and indoor air in Catalonia, Spain: Implications for human exposure, *Environment International*, 39 172-180

(8) Halldorsson, Thorhallur I., et al, (2012) Prenatal Exposure to Perfluorooctanoate and Risk of Overweight at 20 Years of Age: A Prospective Cohort Study, *Environmental Health Perspectives*, 120 (5) 668-673

(9) Nelson, Jessica W., et al, (2010) Exposure to Polyfluoroalkyl Chemicals and Cholesterol, Body Weight, and Insulin Resistance in the General U.S. Population, *Environmental Health Perspectives*, 118 (2) 197-202

(10) Nordstrom Joensen, U., et al, (2009) Do Perfluoroalkyl Compounds Impair Human Semen Quality?, *Environmental Health Perspectives*, 117 (6) 923-927

(11) Washino, N., et al, (2009) Correlations between Prenatal Exposure to Perfluorinated Chemicals and Reduced Fetal Growth, *Environmental Health Perspectives*, 117 (4) 660-667

(12) Overview of the Analysis of Perfluorinated Acids, (2012) http://www.epa.gov/oppt/pfoa/pubs/Analytical%20Methods-Reagen_finalrev1.pdf

(13) US EPA, (2014) Emerging Contaminants –Perfluorooctane Sulfonate (PFOS) and Perfluorooctanoic Acid (PFOA) http://www2.epa.gov/sites/production/files/2014-04/documents/factsheet_contaminant_pfos_pfoa_march2014.pdf

(14) European Food Safety Authority, EFSA, Perfluorooctane sulfonate (PFOS) perfluorooctanoic acid (PFOA) and their salts, Scientific Opinion of the Panel on Contaminants in the Food chain, (Question No EFSA-Q-2004-163) Adopted on 21 February 2008

(15) Powley CR, George SW, Ryan TW, Buck RC., (2005) Matrix effect-free analytical methods for determination of perfluorinated carboxylic acids in environmental matrixes, Anal Chem. Oct 1;77(19):6353-8.

(16) Letcher, R. J., et al., (2009) Analytical Challenges and Environmental Relevance of Branched and Linear Isomers of Perfluorooctane Sulfonate and Related Fluorinated Compounds in Biota Examples of Fluorinated Surfactants Reported in (Biotic and Abiotic) Environmental Compartments, Presentation by Environment Canada,

(17) Brody, J., Ozonoff, D., et al., (1996) Newton Breast Cancer Study, Silent Spring Institute, John Snow Institute

(18) Kissa, E. *Fluorinated Surfactants, Synthesis, Properties, Applications*; Marcel Dekker: New York, 1994; Vol. 50. as cited in Mary Joyce A. Dinglasan, *Fluorotelomer Alcohol Biodegradation Yields Poly- and Perfluorinated Acids*, Environ. Sci. Technol. 2004, 38, 2857-2864

(19) Maras, M., *Estrogen-Like Properties of Fluorotelomer Alcohols as Revealed by MCF-7 Breast Cancer Cell Proliferation*, Environmental Health Perspectives, 2006, 114, 100 - 105

(20) Ellis, D. et al, *Degradation of Fluorotelomer Alcohols: A Likely Atmospheric Source of Perfluorinated Carboxylic Acids*, Environ. Sci. Technol. 2004, 38, 3316-3321

(21) National Institute of Environ. Health Sciences, Perfluorinated Chemicals, PFCs, https://www.niehs.nih.gov/health/materials/perflourinated_chemicals_508.pdf

(22) W. Butte and B. Heinzow, (2002) Reviews of Environmental Contamination and Toxicology, vol. 175, p. 6, G.W.Ware, editor, Springer, ISBN 0-387-95446-6)

(23) SSI resource, (2014) *Silent Spring Institute Guide to Cohort Studies for Environmental Breast Cancer Research*, http://www.silentspring.org/sites/default/files/CohortStudiesTable.pdf

(24) Schaider, L., et al., (2011) *Emerging Contaminants in Cape Cod Private Drinking Water Wells*, Silent Spring Institute

(25) Nielsen, Claus Jorgen, (2012) PFOA Isomers, Salts and Precursors, Literature and evaluation of phusico-chemical properties, Univ. Oslo, Dept. of Chemistry

(26) US EPA, (2011) Exposure Factors handbook, Ch. 5, Soil and Dust ingestion, site accessed 7/2012, url: http://www.epa.gov/ncea/efh/pdfs/efh-chapter05.pdf

(27) US EPA, (2014) url: http://www.epa.gov/endo/pubs/prioritysetting/revlist2.htm)

(28) Sigma Aldrich, Inc., (2012) http://www.sigmaaldrich.com/catalog/product/aldrich/171468?lang=en&region=US

Summary

Fine particulate matter in dusts conveys radioactive material over large distances in a form that results in human exposure to excess radioactivity and to toxic chemical contamination. Once transported by air, particulate matter contributes to soil and indoor dust contamination. For the soil and dust samples in this study, this contamination exists as uniformly contaminated material and as radioactively-hot particles. These hot particles transported radioactive materials in the form of isolated individual particles containing high concentrations of radioisotopes. These were both natural (such as monazites and uranium mineral particles) and industrial (such as particles containing fission products, nuclear fuels and/or neutron activation products).

The specific activity of some individual particles was significantly higher than that of the surrounding particles in Japanese dust samples collected after the Fukushima Daiichi accidents. High activity radioactively-hot particles were isolated and analyzed for this research. On a case by case basis, hot particles can contribute to human radiation dose over and above that expected from average environmental conditions alone.

Industrial radioactive contamination was ubiquitous in the Northern Japan environmental sample set. Relative variability among dust samples from Japan was very high, due to the nonuniformity in how contaminants were distributed in environmental materials. Five of eighty-five dust samples contained unusually high specific activities that were at least two orders of magnitude above the median dust specific activity 2.5 Bq g^{-1} +/- 1.6 Bq g^{-1}, and likewise an order of magnitude above the mean dust specific activity 71 Bq g^{-1}, RSD = 335%. These unusually high activity levels are representative only of the specific collection locations at the specific time of sampling, and are not representative of average, likely or typical Japanese radiation exposures. In addition, hundreds of additional radioactively-hot particles were detected in the Japanese sample set that could not be fully analyzed. These samples were retained and are the potential objects of future

research. Most of the activity detected in Japanese samples came from ^{134}Cs and ^{137}Cs, and for samples collected and analyzed immediately after the Fukushima accidents, ^{131}I.

For environmental samples collected in Canada and the United States after the Fukushima accidents, isolated samples definitively contaminated with industrial radioactivity from Fukushima were identified. Any hot particles inferentially identified in the US and Canada were two orders of magnitude fewer and of lower activity than hot particles that were routinely found in Japan. Japanese vehicle engine filters contained ^{134}Cs and ^{137}Cs at levels between 2.3 Bq/filter to 550 Bq/filter. Only one of the US filters, from Seattle, WA, contained 0.04 Bq/filter of combined ^{134}Cs and ^{137}Cs. The most contaminated of the US soil samples contained 0.30 +/- 0.10 Bq g^{-1} of ^{134}Cs and ^{137}Cs and the median US soil sample result was non detect at a limit of less than 0.03 Bq g^{-1}. Most of the activity detected in US and Canadian samples was related to the presence of the naturally occurring radioactive substances thorium, uranium and ^{40}K.

Additional testing of US samples also found perfluorinated toxic or cancer-causing chemical contaminants in house dusts. These exotic compounds were detected using GC-ECD instrumentation that is common in academic and commercial laboratories. Relatively volatile perfluorinated compounds were most often detected. One compound, the deregistered pesticide Sulfluramid®, was found in greatest abundance, and it also was found at the highest concentrations in homes with the greatest household income levels.

Household dusts were shown to contribute to human toxic and radioactive contaminant exposure. For Japanese households, the data showed that hot particles transported radioactive contaminants from the Fukushima Daiichi site to homes as much as 400 km distant. Accurate assessment of biological health effects from low level radiation exposure requires that any hot particle exposures be included. Likewise, accurate human dose or radiation risk assessments require that the probability and magnitude of hot particle exposure be evaluated.

Future research directions

There are two important goals in further research on assessing the contribution of dusts to human exposure to contaminants. One goal is to automate the process of identifying, isolating, and analyzing hot particles. This would allow a larger number of hot particles to be characterized. With further data, it may become possible to draw conclusions about the size distribution among hot particles. This may provide insight into how hot particles form and how they are distributed in the environment. This would also give better data on the statistical probability of human exposure to hot particles of a given activity.

A second goal is to increase the percentage of archived and newly acquired samples from Hanford, Los Alamos and Northern Japan; that have been fully explored for potential hot particle contamination. Fully characterizing a sufficient number of archived or new dust samples could provide details on the geographic, size, and activity distributions of hot particles. Knowing these distributions, it would be possible to calculate likely ranges of hot particle-based internal radiation doses for larger numbers of impacted residents.

Appendices

A: Sampling instruction sheet

B: Japanese samples received

C: Full frame autoradiograph example

D: Vacuum cleaner log sheet for perfluorinated compounds study

E: SEM/EDS cps to mass conversion data

F: US and Canadian sample list

G: Sample collection acknowledgments

Appendix A - Safety: Sampling Instructions for Volunteer Samplers in Japan

Things to know before you sample:

Avoid working alone.

Remember that radioactive dusts can be inhaled, ingested, or can be retained on clothing and shoes. You can walk away from external radiation, but radioactive dust may result in lifelong exposures!

Do not use tobacco, eat, or drink while sampling. This reduces the chances of ingesting radioactive dusts.

When sampling, wear long sleeved shirts, trousers, and shoes that cover your feet – no sandals.

Use disposable gloves while sampling to reduce cross contamination between samples, and to reduce your exposure to dusts.

Do not bring contaminated samples, used masks and gloves, or dusty clothing into clean environments. Bag your dusty used gear before entering your vehicle or home.

High quality disposable P95 dust masks are recommended for general sampling. See photo below. Old military type masks may be unreliable, or may become contaminated by repeat use.

Bring a jug of water to clean off any dirt or dust on yourself or on your tools. Keep clean – change your gloves when they become soiled or contaminated.

Radioactive particulate filtering masks are expensive, but provide even better protection. Using these in high risk zones requires training beyond the scope of this sampling guide. The outside of these masks must be cleaned after use and before storage. These masks should be stored in air tight bags. See photo below

The cheap dust mask pictured below is not very effective. It may be better than nothing, but it is less effective than the masks pictured above.

Consider changing your clothing and shoes when sampling is completed. Keep these possibly contaminated materials segregated from other household items and clothing.

Wearing protective gear can make you more likely to suffer heat stroke. Take frequent breaks, and decontaminate sufficiently so that you can find a clean place to drink lots of water.

Make sure that all potentially hazardous samples are labeled. Take smaller samples if materials have high count rates.

Wash hands or better yet, shower, after leaving the field.

The instructions for collecting samples are as follows:

Samples should be collected in sealed plastic bags.

Use double bagging to prevent escape of contaminated material.

For soils, the preferred sample weight is about 30 grams. The sample does not need to be weighed. It is important for us that samples not be too large, or they

will become expensive to discard properly. If the sample has a high CPM, then collect a smaller sample.

Automobile and truck engine air filters are a very important sample. If these are collected please take the following steps:

Write down the make, model, and year of the vehicle.

Write down how long the filter was in use, (if you know) and the city where the vehicle is normally used or stored.

Note if the filter is a cabin filter or an engine filter.

These filters may potentially be quite radioactive. Bag these carefully. Using packing material like newspaper to keep the sample in the center of any shipping box or container.

If any one sample is much hotter than the rest, it may contaminate those other samples. Collect a smaller sample for high activity materials to reduce this potential problem.

Please label all bags, in fact, label everything. Even though you know what something is, your sample may be retested many months or even years after it is collected.

Please include a list of samples sent, and note the time, place, and date that samples are collected.

The person collecting the samples should sign their name to the list of samples. A sample worksheet for signatures and sample indexing can be found on the final page of this guide.

Please include a name and email address, so that we can share the test results with you. Samples should be addressed to:

Marco Kaltofen, PE (Civil, Mass.)
Boston Chemical Data Corp.
2 Summer Street, Suite 14
Natick, MA USA 01760
Tel. 508 651 1661, email: Kaltofen@wpi.edu

Out of respect for the many people who are involved in delivering packages, please do not send large amounts of highly radioactive material. Samples should

be small enough and well packaged, so that radiation counters (if you have one) do not show much radiation through the sealed package.

Using personal radiation monitors

To make the best use of your new monitoring device, it would be helpful to follow some of these steps.

MEASURE Consistently. Choose a medium, technique or location and measure the same way consistently over time.

KEEP good records. The idea is that someone should be able to reproduce exactly what you did just by reading your notes. Sign and date your data. Use a high quality notebook with numbered pages. Sign and date your entries.

Take multiple measurements. If measurements are made in triplicate, you can calculate your standard deviations. This makes your data much more usable to others.

Collecting enough data to be meaningful means having enough sample volume to have detections in ranges that are within your instruments' sensitivity. We use a 20 LPM air sampler through a 37 mm filter pad to collect 60 to 90 cubic meter air samples, using a 0.45 micron pore size filter. Samples are counted for 1 hr. just after pulling the filter, then again 24 hours after collection to allow natural radon and uranium daughters to decay.

Other scientists are finding that the top 1 cm of dry soils is the best trap for fallout particles on open areas. Be sure to test an identical known area each time, for example, sample using a 10 cm by 10 cm square.
Samples should be dry. Use dry wipes as water can affect the size and shape of the particles which we are trying to capture and analyze. Wear a suitable dust mask (see page 1) to avoid inhaling radioactive dust while you sample.

Use the form below to record the samples you have collected.

Shipping soils to the United States

Soils may not be shipped to the United States without following US Agriculture Department rules.

Samples that can be sent to us include:

Any processed materials such as fill materials which are free from plants, plant parts, or seeds. This would include fill brought in for school yards or construction projects, as long as it was purely mineral matter.

Any sediment, mud or rock from the ocean.

Freshwater mud or peat so long as it is free of plant parts or seeds.

Geologic samples or drill cores, so long as it is free of organic material

We can accept seaweed collected from the oceans if it is fully dried and dead.

Things we can not accept include:

Soil, particularly unprocessed soil or soil containing plant parts or seeds.

Living plants or seeds.

Farm soils are not acceptable unless they have been sieved and had organic material and seeds removed. (Keep and ship the fraction that passes the sieve, and discard or return the fraction that is coarse and contains all of the seeds and plant parts.)

Be aware that sieving is a potentially hazardous processing step for highly contaminated soils, as you may distribute breathable dusts.

Your shipping papers should note which of the allowed materials above apply, such as:

"Geologic sample with no plants or seeds" or "Ocean sediment" or "Processed material free of plant parts and seeds"

Please do not send more than 30 grams of any material, so that we do not exceed our storage permits. Please send even less than this if the sample is "hot".

And there is one last important instruction; no wet samples or water samples of any kind can be accepted. ***Any water samples received will not be analyzed. These will be refused and returned to you unopened.***

Appendix B - Complete list of samples from Japan

sample description	date run	sample or usage date	matrix
filter blank	6/7/12		filter
filter blank	6/7/12		filter
filter blank	8/6/12		filter
filter blank	8/6/12		filter
filter blank	6/15/12		filter
filter blank	8/7/12		filter
filter blank	7/30/12		filter
filter blank	8/18/12		filter
filter blank	8/20/12		filter
Jp. trip blank M0	8/3/12	sampled 4/18/2011	wipe
Control: Cs137	7/22/12		solid
Tokyo house dust 1	8/1/12	5/25/2011 wipe	bulk dust
Ibaraki outside rail wipe 4/5/11	8/2/11		wipe
Ibaraki outside bannister wipe	8/3/12		wipe
Ibaraki cabinet dust "bunny"	8/1/12	3/23/11	bulk dust
Ibaraki floor dust "bunny"	8/1/12		bulk dust
Ibaraki dust wipe <10 cm sq.	8/1/12		wipe
Ibaraki dust mask	8/2/12	4/4/11 - 4/5/11	filter
Tokyo 001 rooftop wipe	7/24/12	sampled 4/18/2011	wipe
Tokyo 003 rooftop wipe	8/1/12	sampled 4/18/2011	wipe

sample description	date run	sample or usage date	matrix
Tokyo Garage 004 rooftop wood chip	8/3/12	sampled 4/18/2011	solid
Tokyo Garage 005 rooftop wipe	7/24/12	sampled 4/18/2011	wipe
Tokyo dust Minato-ku, Mita 1 veranda	7/24/12	sampled 4/18/2011	wipe
Tokyo dust mask 6/24/11	7/27/12		bulk dust
Ogawa cho Shinchi village Fukushima	7/1/12	6/26/12 9-1 7-6	bulk dust
Souma City Fukushima Pref.	7/1/12	6/26/12 5-6	bulk dust
Sugimi aza Shinchi village Fukushima	7/1/12	6/26/2012 1-4	bulk dust
House dust Koriyama	5/12/12		bulk dust
House dust Koriyama	5/15/12		bulk dust
Fukushima City house dust	6/18/12		bulk dust
Tokyo upstairs house filter	7/25/12	jun11/11 to jan10/12	filter
Tokyo upstairs house filter	7/26/12	to 6/11/11	filter
Tokyo front house	8/6/12	jun11/11 to jan10/12	filter
Tokyo front house	7/26/12	to 6/11/11	filter
Tokyo back house	7/28/12	jun11/11 to jan10/12	filter
Tokyo back house	8/5/12	to 6/11/11	filter
Azumino City	7/13/13	31-May-11	filter
Noda City house	7/27/12	7/20/11 - 9/15/11	filter
Japan 18 R. prefilter Chiba	7/17/12		filter
Japan 18 R. Chiba	7/17/12		filter
Japan 19 R. filter	7/17/12		filter
Jp 20 Chiba S.E.	8/7/12	19-Jun-11	filter

sample description	date run	sample or usage date	sample or usage date
Japan 21 Chiba S.E. Filter	8/7/12	19-Jun-11	filter
Japan 22 Chiba S.E.	8/2/12		filter
Japan 23 Chiba S.E.	7/3/12		filter
Japan Chiba S.E. Filter gym	6/29/12	5/28/12- 6/11/12	filter
Japan Chiba S.E. Filter tatame	6/29/12	5/28/12- 6/11/12	filter
Japan Chiba S.E. Filter entry	6/29/12	5/28/12- 6/11/12	filter
Japan Chiba S.E. Filter living room	6/29/12	5/28/12- 6/11/12	filter
Japan Chiba S.E. Filter master bedroom	6/29/12	5/28/12- 6/11/12	filter
Japan Chiba S.E. Filter gym	8/6/12	jan102012 - jan232012	filter
Jp Chiba S.E. Filter tatame	7/24/12	jan102012 - jan232012	filter
Japan Chiba S.E. Filter entry	8/6/12	jan102012 - jan232012	filter
Chiba S.E. Filter living room	8/6/12	jan102012 - jan232012	filter
Japan Chiba S.E. Filter master bedroom	7/24/12	jan102012 - jan232012	filter
Japan Chiba S.E. Filter entry	12/17/12	Oct to Dec.4, 2012	filter
Jp Chiba S.E. Filter garden	12/17/12	Oct to Dec.4, 2012	filter
Japan Chiba S.E. Filter gym	12/17/12	Oct to Dec.4, 2012	filter
Jp Chiba S.E. Filter 2nd floor	12/17/12	Oct to Dec.4, 2012	filter
Japan, Miyagi vac bag dust, Izumi Chuo, Sendai, Miyagi	8/13/12	to August 2, 2012	bulk dust
Fukushima Car filter FKD011	11/2/11		filter
Tokyo Car filter FKD005D	11/2/11		filter
Iwaki Car filter	11/2/11		filter
Japan 5 Tokyo engine filter	8/6/12		filter

sample description	date run	sample or usage date	matrix
Tokyo quant filter 3	6/7/12	apr24/11 to apr27/11	filter
Tokyo quant filter 4	6/15/12	5/4/11-5/6/11	filter
Tokyo quant filter 5	6/5/12	may7/11 to may9/11	filter
Nagoya dust particle	11/13/14		slide
Tokyo black sand # 1			dust/sediment
Tokyo black sand # 2			dust/sediment
Tokyo black sand # 3			dust/sediment
Iitate mineral sample 14a			dust/sediment
Minamisoma sediment sample 39c			dust/sediment
Nagoya dust w/o particle 1			bulk dust
Nagoya dust 2			bulk dust
Nagoya dust 3	2/4/15		bulk dust
Fukuoka City, JP soil 0.80 g			soil
sediment tokyo hotel drainage opp. US Embassy	8/2/12		dust/sediment
Soil Sapporo 5-14 2-17 Miyanomori Chouh-ko NaI-Lud	8/1/12		soil

sample description	date run	sample or usage date	matrix
Soil Gunma Pref.	8/1/12		soil
Ibaraki-Tsukuba apt. soil	8/1/12		soil
surface Tokyo soil 1 - Shibuya district	3/7/12		soil
surface Tokyo soil 2 - Kamakura	3/7/12		soil
surface Tokyo soil 3 - Chiyoda-Ku playground	3/7/12		soil
surface Tokyo soil 4 - Chiyoda-Ku	3/7/12		soil
surface Tokyo soil 5 - Hibiya park	3/7/12		soil
Shoe Japan Koriyama A1	8/22/12		solid
Shoe Japan B1	8/8/12		solid
Shoe Japan C1	8/9/12		solid
Shoe Tokyo D1	8/8/12		solid
Shoe Japan A2	8/22/12		solid
Shoe Japan B2	8/8/12		solid
Shoe Japan C2	8/9/12		solid
Shoe Tokyo D2	8/8/12		solid

sample description	date run	sample or usage date	matrix
Japan 9: Tokyo vehicle air filter	8/9/12		filter
Japan 15 fukushima cabin	8/9/12		filter
Japan 10: Tokyo vehicle air filter	8/8/12		filter
Japan 26 Saporo Hokkaido car	8/8/12	Dec. 2010 to Sept. 18, 2011	filter
Japan 8 tokyo engine filter	8/3/12		filter
Japan 7 Tokyo engine filter	8/10/12		filter
Fukushima 30 engine	8/10/12	sep. 2010 to June 17, 2011	filter
Fukushima 13 engine	8/1/12		filter
Japan 17 Iwaki cabin filter	7/3/12		filter
Fukushima 14 engine	7/19/12		filter
car filter toyota Fukushima C. Izumi dis. 24	7/17/12	Feb 2009 to 6/20/11	filter
Japan 28 car filter Noda City	7/17/12		filter
Japan 29 car filter Noda City to Tokyo use	7/17/12		filter
Otsu City Shiga Pref., JP 4 yr old engine 55,000 km	7/1/13	to June 1, 2013	filter
Otsu City Shiga Pref., JP 4yr old cabin 55K km	7/1/13	to June 1, 2013	filter
Tokyo quant 1	6/7/12		37 mm filter
Tokyo quant 2	6/7/12	4/18/11-4/20/11	37 mm filter
Fukushima 12 engine	5/23/12		filter
Saitama cabin filter 16	5/13/12		filter

Appendix C

Raw autoradiograph example: 8.5” x 11” Fukushima City car filter # 11

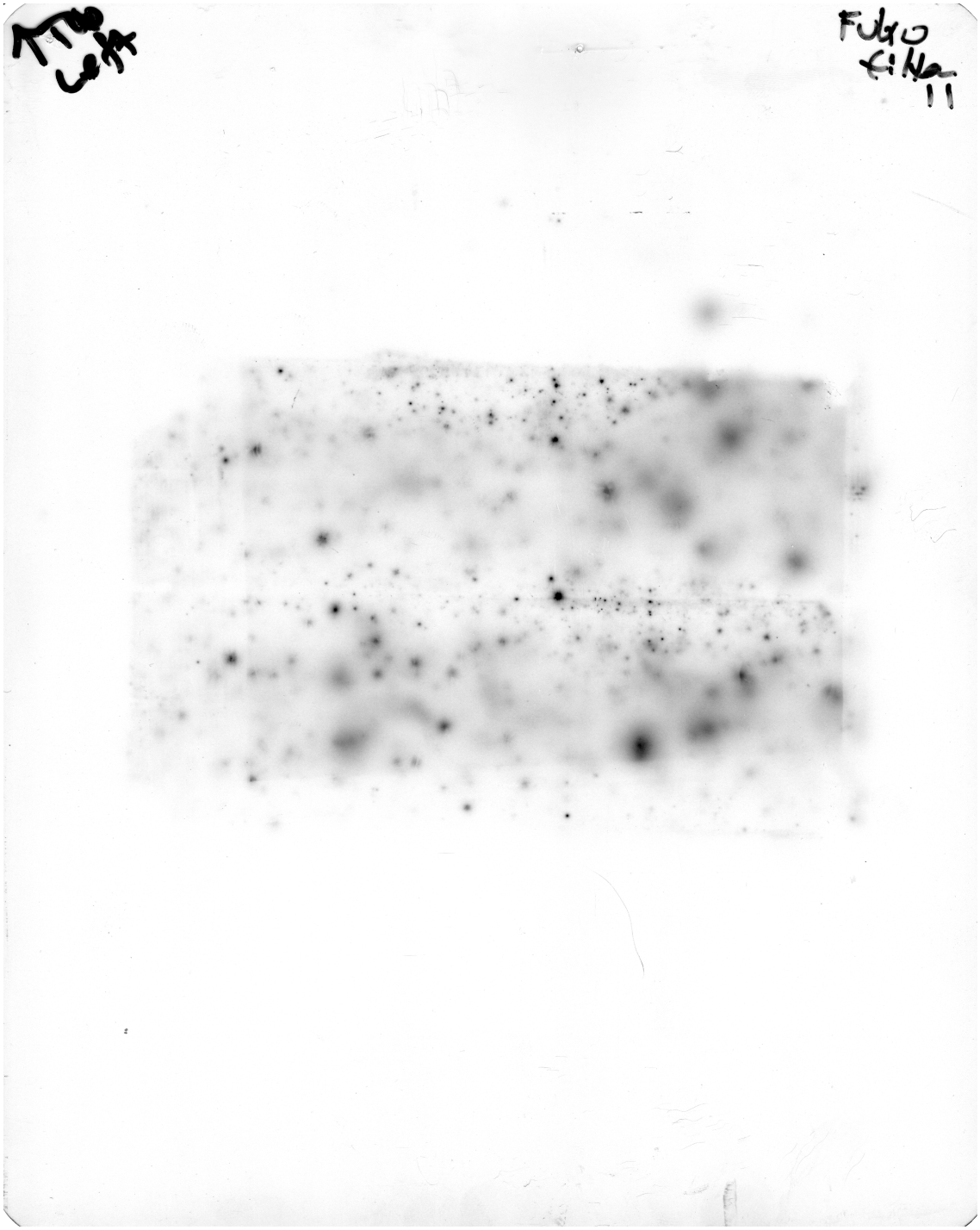

Appendix D:

Vacuum bag or dust sample log sheet

Collect entire vacuum bag or place entire contents of bagless vacuums into a gallon size ziplock bag. If there is no vacuum cleaner, consider taking appliance filter dusts. Please collect as much dust as you can, at least 3 to 4 ounces.

Samples will be tested for chemical contaminants such as perfluorooctanoic acid and perfluorooctonoate, and possibly additional chemical compounds. Test results may take many months to produce. The aggregate results of this study will be published in the scientific literature, but individual names or results will not be published. This test is designed to improve our knowledge of chemicals in the home. This test can not provide any personal medical information or diagnosis.

Address (number and street) _____
Zip code: _____ Date sampled: _____
What is your occupation? _____
What is your spouse, partner or roommate's occupation(s)? _____
List number of adults and children in home: Adults_____ Children_____
When was your home built? _____
How long have you had this vacuum cleaner? _____
Does your vacuum cleaner use a bag? _____
What make and model is your vacuum cleaner? _____
Is this home a freestanding house, triple
decker, duplex, apartment, or condo? _____

If you wish to learn more about the results
of your test please include your email address:_____

Thank you for your participation in this study.

Marco Kaltofen, MS, PE (Civil, Mass.) kaltofen@wpi.edu
Dept. of Civil and Environmental Engineering
Kaven Hall, Worcester Polytechnic Institute
Worcester, MA 01609

Appendix E

SEM/EDS: CPS data converted to weight percent in particle

Sample HR0218P, p 17 (Hanford workplace dust)

Element	AN	series	Net	[wt.-%]	[norm. wt.-%]	[norm. at.-%]	Error in %
Copper	29	K-series	712	2.459538	2.448173948	8.39458264	0.140497
Thorium	90	L-series	5435	98.00464	97.55182605	91.6054174	2.89047
			Sum:	100.4642	100	100	

Sample MMU002D, p 21 (Uranium mine offices, Wellpinit, WA, indoor dust)

Element	AN	series	Net	[wt.-%]	[norm. wt.-%]	[norm. at.-%]	Error in %
Carbon	6	K-series	95683	7.8643	7.864457531	17.7433271	4.432643
Magnesium	12	K-series	17925	2.17358	2.173623803	2.42345081	0.15315
Aluminium	13	K-series	38924	3.322142	3.322208014	3.33661073	0.193304
Silicon	14	K-series	85352	5.614824	5.614936523	5.41761507	0.276028
Calcium	20	K-series	26645	1.668346	1.668379661	1.12806545	0.078701
Iron	26	K-series	11646	1.093386	1.0934083	0.53055202	0.054767
Copper	29	K-series	6079	0.745617	0.745631517	0.31796659	0.046048
Niobium	41	K-series	6434	8.94763	8.947808939	2.60985587	0.433368
Uranium	92	L-series	38762	31.4228	31.4234281	3.57741352	0.930196
Oxygen	8	K-series	119977	37.14537	37.14611761	62.9151429	13.34865
			Sum:	99.998	100	100	

Sample 006D, p 30 (Thorium particle in Hanford worker house dust)

Element	AN	series	Net	[wt.-%]	[norm. wt.-%]	[norm. at.-%]	Error in %
Carbon	6	K-series	18753	10.48008	9.28371742	14.8028878	1.379126
Aluminium	13	K-series	10845	1.38075	1.223129069	0.86817896	0.097096
Silicon	14	K-series	69345	6.708186	5.942405606	4.05213433	0.325439
Iron	26	K-series	4247	0.480136	0.425325923	0.14585647	0.039592
Copper	29	K-series	1783	0.262968	0.23294871	0.07020625	0.034327
Lead	82	L-series	5959	2.231186	1.976482115	0.18268666	0.143368
Thorium	90	L-series	19636	17.19889	15.2355346	1.25748293	0.608998
Oxygen	8	K-series	50804	74.1445	65.68045656	78.6205665	8.75525
			Sum:	112.8867	100	100	

Namie high activity sample, p 71

Element	AN	series	[wt.%]	[norm. wt.%]	[norm. at.%]	(1 Sigma)
Lead	82	L-series	42.62761	45.39547454	17.6898163	1.084518
Titanium	22	K-series	28.36661	30.20849301	50.9419345	0.807795
Zinc	30	K-series	21.21292	22.59030138	27.894026	0.549196
Calcium	20	K-series	0.703447	0.749122503	1.5092018	0.051453
Potassium	19	K-series	0.663188	0.706249512	1.45848108	0.050868
Iron	26	K-series	0.328997	0.350359055	0.50654031	0.038184
		Sum:	93.90277	100	100	

Sample Japan 5, Tokyo automobile filter dust, top of p 88

Element	AN	series	Net	[wt.-%]	[norm. wt.-%]	[norm. at.-%]	Error in %
Carbon	6	K-series	40620	6.912519	6.912657571	18.4698061	4.666505
Sodium	11	K-series	3705	0.7912	0.791215382	1.10447669	0.083548
Chlorine	17	K-series	17975	2.127999	2.128041748	1.92631491	0.100917
Calcium	20	K-series	9926	1.089889	1.089911158	0.87273324	0.059517
Iron	26	K-series	3029	0.468802	0.468811293	0.26939819	0.040097
Strontium	38	K-series	46126	61.22097	61.22219078	22.4234316	1.589059
Oxygen	8	K-series	35636	27.38662	27.38717206	54.9338393	10.27928
			Sum:	99.998	100	100	

Sample FKD001D, middle of p 88 (Ibaraki dust, Y and Eu in Ibaraki dust particle)

Element	AN	series	Net	normalized wgt. %	Error in %
Yttrium	39	K-series	7687	51.7	1.6
Europium	63	L-series	4278	3.7	0.1
Oxygen	8	K-series	670	44.6	12.5

Sample FKD001D, bottom of p 88 (Ibaraki dust, zirconium in Ibaraki dust particle)

Element	AN	series	Net	[wt.-%]	[norm. wt.-%]	[norm. at.-%]	Error in %
Sodium	11	K-series	180	1.920413	1.685971261	1.56348937	0.265525
Aluminium	13	K-series	1425	5.940178	5.215008201	4.12066828	0.400547
Silicon	14	K-series	1157	4.226223	3.710290926	2.81647044	0.316965
Calcium	20	K-series	396	1.194451	1.0486337	0.55782396	0.100671
Iron	26	K-series	187	0.777071	0.682207183	0.26043289	0.087862
Zirconium	40	K-series	419	23.7011	20.80769882	4.86288876	1.410926
Hafnium	72	L-series	438	3.062367	2.688517119	0.3211281	0.197448
Oxygen	8	K-series	1202	73.08363	64.16167279	85.4970982	15.76545
			Sum:	113.9054	100	100	

Sample Japan 5, Tokyo automobile filter dust, p 90

Element	AN	series	Net	[wt.-%]	[norm. wt.-%]	[norm. at.-%]	Error in %
Carbon	6	K-series	48645	0.015934	0.015058859	0.06151999	0.159184
Sodium	11	K-series	7601	3.535762	3.341497456	7.13197585	0.286912
Magnesium	12	K-series	8092	2.459708	2.324564383	4.69298655	0.230506
Aluminium	13	K-series	65404	14.96519	14.14295686	25.7203479	0.779367
Silicon	14	K-series	65072	13.30977	12.5784928	21.9760584	0.663696
Chlorine	17	K-series	21211	3.827288	3.617006218	5.00614351	0.160774
Potassium	19	K-series	9362	1.360296	1.285557834	1.6133816	0.070769
Calcium	20	K-series	50921	7.770854	7.343901893	8.99133505	0.256495
Iron	26	K-series	10555	2.29983	2.173470464	1.90966527	0.097732
Yttrium	39	K-series	1569	2.659193	2.513089164	1.38701344	0.124789
Zirconium	40	K-series	8311	20.56637	19.43640014	10.4546639	0.611363
Cerium	58	L-series	139657	31.60097	29.86472268	10.4583149	0.864298
Hafnium	72	L-series	3446	1.358473	1.28383439	0.35293804	0.067108
Oxygen	8	K-series	69657	0.084066	0.079446861	0.2436556	0.864816
			Sum:	105.8137	100	100	

Appendix F

US and Canadian Sample List

Sample ID, Air filter collection dates, final date run

controls - red granite , NA ,8/6/12
controls - low density tephra , NA ,8/21/12
controls - geothermal effluent scale , NA ,7/13/12
controls - black marine sands , NA ,7/19/12
controls - low density tephra , NA ,7/19/12
controls - high density tephra , NA ,7/31/12
controls - Chernobyl Cs137 check sample , NA ,7/22/12
control soil Bayou Corn, LA 1" , NA ,9/9/12
control soil Bayou Corn, LA 2" , NA ,9/9/12
Shoe A3 US nuclear worker , NA ,8/12/12
Shoe A4 US nuclear worker , NA ,8/12/12
Shoe A5 US child SLC resident , NA ,8/20/12
Shoe A6 US child Mass. Resident , NA ,9/2/12
Shoe A7 US child Mass. Resident , NA ,9/2/12
Shoe A8 US child Mass. Resident , NA ,9/24/12
Shoe A9 US child Mass. Resident , NA ,9/24/12
Shoe A10 US child Mass. Resident , NA ,1/9/13
Shoe A11 US child Mass. Resident , NA ,1/10/13
Shoe A12 US child Mass. Resident , NA ,1/10/13
Shoe A32 US child Mass. Resident , NA ,1/10/13
Shoe BLK blank, NA ,
Seattle quant filter, mar18/11 to mar19/11,7/24/12
Seattle quant filter, mar20/11 to mar21/11,7/23/12
Seattle quant filter, mar22/11 - mar23/11,7/28/12
Seattle quant filter, mar22/11 - mar23/11,7/28/12
Seattle quant filter, mar23/11 to mar24/11,7/24/12
Seattle quant filter, mar26/11 to mar28/11,6/7/12
Seattle quant filter, mar28/11 to apr1/11,6/7/12
Seattle quant filter, apr4/11 to apr6/11,6/7/12
Seattle quant filter, apr7/11 to apr10/11,6/7/12
Seattle quant filter, apr11/11 to apr14/11,6/6/12
Seattle quant filter, apr14/11 to apr20/11,6/6/12
Seattle quant filter, apr21/11 to apr23/11,6/7/12
Seattle quant filter, apr25/11 to apr27/11,6/7/12
Seattle quant filter, apr28/11 to may2/11,6/7/12
Seattle quant filter, may2/11 to may6/11,6/7/12
Seattle quant filter, may6/11 to may9/11,6/8/12
Seattle quant filter, may9/11 to may13/11,6/18/12
Seattle quant filter, may13/11 to may16/11,6/18/12
Seattle quant filter, may17/11 to may20/11,6/4/12
Seattle quant filter, may22/11 to may25/11,7/26/12
Seattle quant filter, may26/11 to may30/11,6/17/12
Seattle quant filter, may30/11 to jun2/11,7/21/12
Seattle quant filter, jun3/11 to jun8/11,6/15/12
Seattle quant filter, jun9/11 to jun12/11,6/30/12
Seattle quant filter, jun13/11 to jun16/11,6/30/12
Seattle quant filter, jun17/11 to jun20/11,6/6/12
Seattle quant filter, jun20/11 to jun23/11,7/21/12

Sample ID, Air filter collection dates, final date run

Seattle quant filter, jun23/11 to jun29/11,7/23/12
Seattle quant filter, jun30/11 to july5/11,7/23/12
Seattle quant filter, july8/11 to july12/11,7/23/12
Seattle quant filter, july14/11 to july19/11,7/23/12
Seattle quant filter, july20/11 to july24/11,7/23/12
Seattle quant filter, aug6/11 to aug11/11,7/23/12
Seattle quant filter, 10/22/11 - 10/26/11,7/27/12
Seattle quant filter, oct28/11 to nov3/11,7/26/12
Seattle quant filter, 11/5/11 - 11/9/11,7/27/12
Seattle quant filter, nov/12/11-nov/17/11,6/20/12
Hawaii quant filter #1, 4/23/11-4/25/11,6/7/12
Hawaii quant filter #2, 4/25/11-4/27/11,6/25/12
Hawaii quant filter #3, 4/27/11 - ,6/19/12
Hawaii quant filter #4, 5/1/11-5/3/11,7/2/12
Hawaii quant filter #5, 5/3/11 - 5/8/11,6/19/12
Hawaii quant filter #6, 5/8/11 - 5/10/11,6/20/12
Hawaii refrigerator dust - microsample, 3-May-11,8/3/12
Natick associated BLK , NA ,7/26/12
Natick quant filter 7 , 3/23/11 - 3/24/11,7/26/12
Natick quant filter 9 , 3/25/11 - 3/28/11,7/26/12
Natick quant filter 11 , 3/30/11 - 3/31/11,7/2/12
Natick quant filter 12 , 3/30/11 - 3/31/11,7/2/12
Natick quant filter 16, 4/6/11 - 4/8/11,8/1/12
Natick quant filter 17, 4/8/11 - 4/11/11,7/1/12
Natick quant filter 18, 4/11/11 - 4/13/11,6/15/12
Natick quant filter 19, to 4/13/12,6/30/12
Natick quant filter 21, 4/13/11 - 4/17/11,7/2/12
Natick quant filter 22, 4/17/2011 - 4/24/11,7/1/02
Natick quant filter 23, 4/24/11 - 5/2/11 ,
Natick quant filter 24, 5/2/11 - 5/9/11,7/2/12
Natick quant filter 25 , 5/10/11 - 5/15/11,6/21/12
Natick quant filter 26, 5/15/11 - 5/22/11,6/21/12
Natick quant filter 27, 5/22/11 - 5/29/11,7/26/12
Natick quant filter 28, 5/29/11 - 6/5/11,7/26/12
Natick quant filter 29 , 6/7/11 - 6/15/11,7/26/12
Natick quant filter , 6/15/11 - 6/23/11,7/25/12
Natick quant filter , 7/6/11 - 7/12/11,6/20/12
Natick quant filter , 7/12/11 - 7/ /11,6/30/12
Natick High Volume air 4/11 , NA ,7/30/12
"Aspen, Colorado Quant filter 1 ",5/24/11 - 5/27/11,7/2/12
"Aspen, Colorado Quant filter 2 ",5/27/11 - 5/30/11,7/2/12
"Aspen, Colorado Quant filter 3 ",5/30/11 - 6/2/11,7/20/11
"Aspen, Colorado Quant filter 4 ",6/14/11 - 6/18/11,7/20/12
"Aspen, Colorado Quant filter 5 ",6/18/11 - 6/21/11,7/20/12
"Aspen, Colorado Quant filter 6 ",6/21/11 - 6/25/11,7/16/12
"Aspen, Colorado Quant filter 7 ",6/25/11 - 6/28/11,7/16/12
"Aspen, Colorado Quant filter 8 ",6/28/11 - 7/2/11,7/20/12
"Aspen, Colorado Quant filter 9 ",8/18/11 - 8/21/11,7/20/11
"Aspen, Colorado Quant filter 10 ",8/21/11 - 8/24/11,7/20/11
"Aspen, Colorado Quant filter 11 ",8/24/11 - 8/27/11,7/20/11
"Aspen, Colorado Quant filter 12 ",9/4/11 - 9/7/11,7/24/12
"Aspen, Colorado Quant filter 13 ",9/7/11 to 9/10/11,7/24/12

Sample ID, Air filter collection dates, final date run

"Aspen, Colorado Quant filter 14 ",9/10/11 to 9/14/11,7/24/12
"Aspen, Colorado Quant filter 15 ",9/14/11 to 9/19/11,7/24/12
"Aspen, Colorado Quant filter 16 ",9/28/11 to 10/1/11,7/24/12
"Aspen, Colorado Quant filter 17   ",10/1/11 to 10/5/11,7/23/12
"Aspen, Colorado Quant filter 18   ",10/21/11 to 10/24/11,7/23/12
"Aspen, Colorado Quant filter 19   ",11/2/11 to 11/5/11,7/23/12
California Quant filter 1, 4/1/11 - 4/3/11,7/19/12
California Quant filter 2, 4/3/11,7/3/12
California Quant filter 3, 4/5/11,7/3/12
California Quant filter 4, 4/9/11,7/18/12
California Quant filter 5, 4/11/11,7/17/12
California Quant filter 6, 4/14/2011 - 4/14/11,7/18/12
California Quant filter 7, 4/17/2011 - 4/22/11,7/18/12
California Quant filter 8, 4/22/11,7/18/12
California Quant filter 9, 5/14/11 - 5/16/11,7/19/12
California Quant filter 10, 5/17/11 - 5/20/11,7/19/12
California Quant filter 11, 5/21-23/2011,7/19/12
"Redmond, WA Microsoft Way soil " , NA ,6/6/12
"Brookings, OR 19507 Ocean view " , NA ,6/6/12
"Daniels, OR soil " , NA ,4/3/12
Oregon 1 soil , NA ,6/20/12
Oregon A soil , NA ,6/19/12
Oregon B soil , NA ,6/19/12
Oregon C soil , NA ,6/19/12
Oregon D soil , NA ,6/19/12
Oregon D soil duplicate , NA ,9/3/12
La Center WA soil # 1 , NA ,6/20/12
La Center WA soil # 2 , NA ,6/20/12
La Center WA soil # 3 , NA ,6/20/12
La Center WA soil # 4 , NA ,6/20/12
La Center WA soil # 5 , NA ,6/20/12
La Center WA soil # 6 , NA ,6/20/12
La Center WA soil # 7 , NA ,6/20/12
La Center WA soil # 8 , NA ,6/20/12
La Center WA soil # 9 , NA ,6/20/12
La Center WA soil # 10 , NA ,6/20/12
J.A. Snoqualmie golf course , NA ,6/8/12
J.A. Soil Farm , NA ,6/8/12
J.A. Soil Farm , NA ,6/14/12
J.A. Soil Farm , NA ,6/14/12
J.A. Soil Farm , NA ,6/14/12
J.A. country club soil , NA ,6/14/12
"J.A. garden soil Sawamish, WA " , NA ,6/9/12
J.A. garden SE 26th way , NA ,6/21/12
"J.A. soil Langley, BC, near 56th " , NA ,6/14/12
" SE 28th Way Sammamish, WA soil " , NA ,5/5/12
"Boulder, CO soil " , NA ,8/10/11
"Boulder, CO soil " , NA ,8/10/11
"Boulder, CO soil " , NA ,8/10/11
"Boulder, CO soil " , NA ,8/10/11
"Boulder, CO soil " , NA ,8/10/11
"Boulder, CO soil " , NA ,8/10/11

Sample ID, Air filter collection dates, final date run

"Boulder, CO soil " , NA ,8/10/11
"Boulder, CO soil " , NA ,8/10/11
"Boulder, CO soil " , NA ,8/10/11
"Boulder, CO soil " , NA ,8/10/11
"Boulder, CO soil " , NA ,8/10/11
"Boulder, CO soil " , NA ,8/10/11
"Boulder, CO soil " , NA ,8/10/11
"Agoura, CA garden soil" , NA ,4/9-14/2012
CA soil sample 4 , NA ,4/9-14/2012
CA soil sample 5 , NA ,4/9-14/2012
CA soil sample 6 , NA ,4/9-14/2012
CA soil sample 7 , NA ,4/9-14/2012
CA soil sample 8 , NA ,4/9-14/2012
CA soil sample 9 , NA ,4/9-14/2012
CA soil sample 10 , NA ,4/9-14/2012
CA soil sample 11 , NA ,4/9-14/2012
CA soil sample 12 , NA ,4/9-14/2012
CA soil sample 13 , NA ,4/9-14/2012
CA soil sample 14 , NA ,4/9-14/2012
CA soil sample 15 , NA ,4/9-14/2012
CA soil sample 16 , NA ,4/9-14/2012
CA soil sample 17 , NA ,4/9-14/2012
CA soil sample 18 , NA ,4/9-14/2012
CA soil sample 19 , NA ,4/9-14/2012
CA soil sample 20 , NA ,4/9-14/2012
CA soil sample 21 , NA ,4/9-14/2012
willow grove organic matt sample , NA ,11/2/11
California sand , NA ,5/22/12
Seattle moss/soil , NA ,4/9/12
Oregon Soil NaI , NA ,6/20/12
"Davis, OR soil " , NA ,8/31/11
"Abbotsford, BC, CAN wipe" , NA ,4/3/12
"Cleveland, OH wipe from car" , NA ,8/1/12
"Cleveland, OH wipe from car",21-Aug-11,8/2/12
CA2 car filter San Diego 8/23/11, 21-Aug-11,8/2/12
D. K. #27 car filter , NA ,7/30/12
"Seattle, WA car engine filter (1) " , NA ,7/27/12
"Seattle, WA car engine filter (2) ",collected 6/6/11,8/3/12
"Seattle, WA car engine filter (3) " , NA ,8/3/12
"Seattle, WA car engine filter (4) ",collected 6/8/11,8/6/12
"Seattle, WA car engine filter (5) ",collected 6/8/11,8/6/12
"Seattle, WA car engine filter (7) ",collected 6/8/11,8/7/12
"Seattle, WA car engine filter (8) " , NA ,8/13/12
"Seattle, WA car engine filter (9) ","collected July 5, 2011",8/20/12
"Portland, OR truck filter ","collected July 5, 2011",8/20/12
"Klamath, OR Dodge truck engine filter " , NA ,5/1/12
"Klamath, OR Dodge truck engine filter ",collected 8/23/11,7/30/12
"Klamath, OR Dodge truck engine filter ",collected 8/23/11,7/30/12
"Klamath, OR Ford truck engine filter ",collected 8/16/11,7/27/12
"Klamath, OR Porche car air filter ",collected 8/16/11,8/2/12
"Klamath, OR Porche car air filter   rerun",collected 8/16/11,8/18/12
"Kirkland, WA (5) car filter ",collected 8/16/11,8/18/12

Sample ID, Air filter collection dates, final date run

"Kirkland, WA (6) car filter ",7/28/11,8/13/12
"Kirkland, WA (7) car filter ",7/28/11,8/11/12
"Kirkland, WA (8) car filter ",7/28/11,8/11/12
"Kirkland, WA (9) car filter ",7/28/11,8/7/12
"Kirkland, WA (10) car filter ",7/28/11,7/28/12
"Kirkland, WA (11) car filter ",7/28/11,5/3/12
"Kirkland, WA (12) car filter ",7/28/11,5/2/12
"Kirkland, WA (13) car filter ",7/28/11,5/2/12
"Kirkland, WA (14) car filter ",7/28/11,7/25/12
"Kirkland, WA (15) car filter ",7/28/11,7/27/12
"Kirkland, WA (16) car filter ",7/28/11,5/7/12
"Kirkland, WA (17) car filter ",7/28/11,5/4/12
"Kirkland, WA (18) car filter ",7/28/11,7/27/12
"Kirkland, WA (19) car filter ",7/28/11,6/4/12
"Kirkland, WA (20) car filter ",7/28/11,9/17/12
Seattle Morgan St. Vac Bag, 7/28/11,9/25/12
Seattle Morgan St. Vac Bag, 1/11 to 10/11,8/21/12
Serendipity downstairs house air filter,1/11 to 10/11,8/22/12
Seattle house filter SEA(6), 10/10 to 2/9/12,8/3/12
J.A. HEPA residue II , NA ,5/2/11
J.A. HEPA residue I , NA ,6/28/12
S.C. filter , NA ,6/28/12
clothing sample , NA ,7/30/12
Washington marine sand sample , NA ,Aug. 2014
Washington marine sand sample , NA ,Aug. 2014
Washington marine sand sample , NA ,Aug. 2014
Washington marine sand sample , NA ,Aug. 2014
Washington marine sand sample , NA ,Aug. 2014
Washington marine sand sample , NA ,Aug. 2014

Appendix G

Sample collection acknowledgments

Fig. G.1 Below: Hanford Nuclear Reservation 300 Area sampling site. All Hanford samples were collected from area homes or from outside the plant perimeter.

Fig. G.2 Below: Hanford Nuclear Reservation K Reactors sampling site
K Area samples came from public waterways in the Columbia R. basin

Fig. G.3 Right: Washington State uranium mine mineral core storage building.

Fig. G.3 Below: Muslyumovo, Chelyabinsk Oblast, Russia, sampling site
Formerly a closed Soviet city near Chelyabinsk-65 and site of the Kyshtym
disaster. This research would not be possible without these unsung hosts.

Fig. G.4 Below: Former Hanford Works 1940's era nuclear worker shuttle bus
Vehicle collectors allowed the author to remove vehicle air filters from
the original engine that saw service during the earliest part of the Cold War.

Glossary

Becquerel - (Bq) SI unit of radioactivity defined as one nuclear decay per second in an amount of radioactive material

Committed dose - long term dose from internalized radioactive material

Dose - amount of radiation energy absorbed by the body or by an object

Dose equivalent - biological damage to living tissue resulting from absorption of a given amount radioactive energy times a quality factor

Effective dose equivalent - the sum of the products of the dose equivalent to the organ or tissue and the weighting factors applicable to each of the body organs or tissues

Fission products - nuclei formed by the fission of heavy elements, plus the nuclei formed by the radioactive decay of fission products

Hot particle - discreet individual particles or aggregates of particulate matter with significantly greater specific activity than surrounding materials

Primordial radionuclide - naturally occurring radioactive isotopes such as ^{40}K and isotopes of uranium and thorium

Quality factor - a factor that represents the differing amounts of biological damage done by different forms of radiation for a given amount of radioactive energy

Robinson® detector - a backscattered electron detector for scanning electron microscopes

Sievert - (Sv) SI unit for dose equivalent equal to 1 Joule per kilogram

Specific activity - radioactivity per unit mass

uR/hr - NonSI unit, microRem per hour, equivalent to 0.01 uSv

Glossary Reference

(1) US Nuclear Regulatory Commission, NRC Library, Basic References Glossary, http://www.nrc.gov/reading-rm/basic-ref/glossary.html, URL accessed 3/21/15